Vers la synthèse directe d'amines chirales via des réactions d'hydroaminométhylation asymétrique catalysées par le rhodium

Joris Langlois

THÈSE

En vue de l'obtention du

DOCTORAT DE L'UNIVERSITÉ DE TOULOUSE

Délivré par :

Institut National Polytechnique de Toulouse (Toulouse INP)

Discipline ou spécialité :

Chimie Organométallique et de Coordination

Présentée et soutenue par :

M. JORIS LANGLOIS

le vendredi 15 décembre 2023

Titre :

Vers la synthèse directe d'amines chirales via des réactions d'hydroaminométhylation asymétrique catalysées par le rhodium

---

Ecole doctorale :

Sciences de la Matière (SDM)

Unité de recherche :

Laboratoire de Chimie de Coordination (LCC)

Directeur(s) de Thèse :

MME MARTINE URRUTIGOÏTY

M. CYRIL GODARD

Rapporteurs :

M. ERIC MONFLIER, UNIVERSITE D'ARTOIS

Membre(s) du jury :

M. VINCENT CESAR, CNRS TOULOUSE, Président

M. CYRIL GODARD, UNIVERSITAT ROVIRA I VIRGILI TARRAGONA, Invité

MME MARTINE URRUTIGOÏTY, TOULOUSE INP, Membre

M. OSCAR PAMIES, UNIVERSITAT ROVIRA I VIRGILI TARRAGONA, Membre

Joris Langlois

Towards The Direct Synthesis Of Chiral Amines Via Asymmetric Rhodium Catalyzed Hydroaminomethylation Reactions

DOCTORAL THESIS

Supervised by

Prof. Cyril Godard

Prof. Martine Urrutigoïty

Departament de Química Física i Inorgánica

UNIVERSITAT ROVIRA i VIRGILI

Université de Toulouse

Tarragona 2023

DEPARTAMENT DE QUÍMICA
FÍSICA i INORGÀNICA
Universitat Rovira i Virgili

C/ Marcel·lí Domingo 1,
Campus Sescelades,
Edifici N4, 2nd floor
43007 Tarragona
Tel. +34 977 55 81 37

Prof. Cyril Godard from the Department of Physical and Inorganic Chemistry at Universitat Rovira I Virgili.

AND

Prof. Martine Urrutigoïty from Laboratoire de Chimie de Coordination at INP-Ensiacet.

We STATE that the present study, entitled "Towards The Direct Synthesis Of Chiral Amines Via Asymmetric Rhodium Catalyzed Hydroaminomethylation Reactions", presented by Joris Langlois to receive the degree of Doctor, and suitable for the International Mention, was carried out under our joint supervision.

Tarragona, November 2nd 2023

Doctoral Thesis Supervisors

Prof. Cyril Godard

Prof. Martine Urrutigoïty

The present Doctoral Thesis was developed within the framework of the European EJD project CCIMC. The project leading to this application has received funding from the European Union's Horizon 2020 research and innovation programme under the Marie Skłodowska-Curie grant agreement No 860322.

The realization of this work was also possible thanks to the financial support from the following research projects:

-Ministerio de Ciencia e Innovación (MICINN) and Agencia Estatal de Investigación (AEI), PID2019-104427RB-I00.

-Ministerio de Ciencia e Innovación (MICINN), Agencia Estatal de Investigación (AEI) y Fondo Europeo de Desarrollo Regional (FEDER), CTQ2016-75016-R.

-AGAUR (Agencia de Gestión de Ayudas Universitarias y de Investigación) from Generalitat de Catalunya, 2017 SGR 1472 and 2021 SGR 00163.

Acknowledgments

My journey in chemistry started in the university of Caen in Normandie where I had the chance to meet professors that shared their passion for chemistry. The first big change in my life was when I joined the European school of chemistry polymers and materials of Strasbourg. Having a multicultural environment made me want to learn more about the Spanish culture and was one of the reasons I looked for this new challenge abroad.

First and foremost, I am deeply thankful to my supervisors, Cyril Godard and Martine Urrutigoïty. I remember the interview when I immediately felt that I had found great people as advisors. Thank you very much to both of you to give me the opportunity to realize this PhD. I am thankful to you Cyril for your mentorship during this journey and for your expertise that helped me become a better scientist.

Martine thank you for being always supportive and positive. I valued our daily meetings where we could speak about chemistry and life in general.

I am grateful to the CCIMC European network for organizing workshops, conferences, and school during those 3 years. Thanks to all the professors involved in this project for the constructive feedbacks and discussions we had. This particular PhD gave me the opportunity to be part of 15 early-stage researchers coming from different horizons. I acknowledge those nice moments we could spend in Toulouse, Leipzig, Barcelona and Bucharest. Special thanks to my friend Agustin who's sharing this chemistry path ever since the engineering school. Paven, I'm really happy to meet you and glad we shared some runs and puns. Pawel, ESR1 the big brother of all of us, it was nice to share some beers with you. Max always loved your energy around with your famous Spanish accent. Sara, the best foosball player I know, thanks for your kindness in all times. Irina to whom I shared some pizzas in Milan and Arese. Of course, thank you Zinnia for your good mood in the lab I really enjoyed sharing that time in Toulouse with you. And to all of you Joel, Anastasiia, Massimo, Chantal,

Wimonsiri, Deepthy and Aswin. Alida, thank you for your friendship and all the help you provide me during these 3 years. I wish you all the best in your future.

I am deeply thankful and grateful for my lab partners in Tarragona. I first started here, knowing a few sentences of Spanish taught by my fantastic roomates in Strasbourg but I learned Castellano in Cataluña donde se parla catala!

Como aspecto general, gracias a todos por su paciencia y cálida bienvenida. Jessica, gracias por enseñarme cómo hacer mi primera columna de argón en el laboratorio y estar dispuesta a ayudar en cualquier momento. Me gusta presumir que dijiste que soy un gran DJ. Gracias, y felicidades a ti Lola por completar tu doctorado, tu profesionalismo siempre ha sido inspirador. Roger, fue un placer conocerte, gracias por incluirme en los planes con tu equipo. Un gran agradecimiento a Sai y Orianne, los dos estudiantes que tuve la oportunidad de supervisar en el laboratorio. Realmente aprecié compartirles mi conocimiento y esta experiencia fue realmente enriquecedora. Valero, estuviste allí el primer día que llegué y aunque ya no estás en la universidad, eres uno de los mejores compañeros que tuve durante este viaje. Recordaré el laboratorio 216 con Mireia y Paula haciendo una columna por la mañana, siendo la primera persona que veo todos los días. Masterchef o la isla de la seducción se mostraba mientras recogíamos fracciones. Oriol estaba cantando desde algún lugar mostrando a algunos estudiantes cómo hacer una columna y cómo reutilizarla 10 veces. Por supuesto, Oriol, gracias por ser un amigo tan agradable, siempre escuchando, servicial y un buen maestro. Jordi, estoy agradecido por todas las discusiones de química que pudimos tener. Realmente ayuda tener a alguien tan apasionado como tú en el laboratorio. Pol, eres mi motivación diaria para aprender español y estaré orgulloso de mí mismo el día que entienda todos los chistes que dices en el día. Me encantaría ver otro espectáculo tuyo. Gracias a los compañeros heterogéneos, Anna, mi amiga de tortilla y amante de la brillantina, y Angie por tu hospitalidad y buenas vibraciones. Daniel, my man, thank you for being you. I value all the life conversations we had sharing a nice cold beer at Twins. My beach volley

partner in those last month, I'm proud of you son. Sara, no puedo agradecerte lo suficiente por todo el buen tiempo que pasamos juntos. Gracias por compartir tu pasión por The Office y Bad Bunny conmigo. Gracias por enseñarme las herramientas para seguir las noticias en español y por ser la persona más paciente que conozco cuando se trata de entender lo que quiero decir. Definitivamente tienes un nivel C1 ahora. Gracias por tu constante apoyo y cuidado guapa, pero sobre todo gracias por el permanganato. Cheers to Sami, Ghassen and Antonio for the nice moments we had those last months.

Me gustaría agradecer a todos los técnicos que trabajan para la universidad, haciendo nuestras vidas más fáciles. Raquel, gracias por la ayuda que brindas a todos aquí con tu alegría interminable, siempre es un placer verte entrar al laboratorio. Gracias a Josep por tu disponibilidad. Gracias a Ramon por los experimentos de RMN que hicimos y por los consejos sobre la tortilla. Gracias a Sonia por ayudarme con el HPLC cuando tengo problemas.

Muchas gracias, Óscar, por haberme podido ayudar con los HPLC en esta última recta y por estar disponible para hablar de química orgánica. Gracias Sergio por todas tus explicaciones y tus buenos consejos. Gracias tambien a Carmen, Montse, Anna y Elena por las amables palabras.

I'm thankful to Prof. Philippe Serp in LCC for the collaboration that was possible for the single atom catalysts. Thank you Prof. Philippe Kalck for the discussions we had about hydroaminomethylation and for your kindness. Thanks to Dr. Jérôme Volkmann and Dr. Odile Dechy Cabaret for the brainstorming about organic chemistry and NMR issues. I'd like to thank my lab partners in Toulouse especially Mathieu Vidaloca for your generosity, kindness and the work we did together. Thank you Meriem for introducing me to the way things work in LCC and for teaching me a few stuff in the lab. Thank you Jeremy, for your honesty and friendship during this year. Quentin, thank you for your generosity and passion for cooking. Thanks to

Abbas, Edoardo, the newbies of team C. Again, thanks to the tech team Laurent and Idaline for fixing my issues with the GC or the reactors!

I have to exprime my gratitude to Italmatch Chemicals in Arese, Italy for hosting me for 3 months during my secondment period. Many thanks to Dr. Frédéric Bruyneel for help, guidance, reactivity, and kindness in every situation. Eric, thank you for the warm welcome in the team. I am deeply grateful for all the people I met during this internship where I could learn from each and every one of you. Thanks to Diego, Giorgio, Chiara, Zambo and Maria for your nice welcome. Big thanks for Matteo and Marta for the good mood and teaching me many things about Italian culture and chemistry. Mattia, thank you so much for the good time we spend in the lab and in your car in the way back to Milan. I wish you all the best, grazie mille!!!

Bien sûr je remercie ma famille pour le soutien moral et financier que vous me donnez depuis le début. J'ai de la chance d'avoir mes parents qui m'ont toujours poussé à donner le meilleur de moi-même depuis petit. Merci de m'avoir fait découvrir tant de choses et le gout pour le voyage. Merci à toi Jéjé d'être un super grand frère, de toujours me laisser gagner à FIFA et de solutionner tous les problèmes du monde avec le théorème de Pythagore. Merci Zazou d'être toujours ma fan numéro un, d'être venu à Tarragone pour me remonter le moral et de m'aider sur mes graphismes. Merci Anna et François pour tous ces beaux moments et de faire partie de cette belle famille. Le plus dur dans tout cela c'était toujours d'être loin de vous tous.

J'ai toujours su bien m'entourer et je remercie sincèrement mes amis de Normandie pour tous les rires et toutes les aventures partagées. J'ai hâte de pouvoir passer plus de temps à vos côtés car vous êtes les plus belles personnes que j'ai pu rencontrer. Mention spécial pour Coco, Lulu, Fio, Juju, Pierro, Ronan qui sont passé par Tarragone ou Toulouse. Merci à Julou, Garouf, Titoune, Claire, Chouchou, Mimine et en particulier Solal, d'être venu et surtout pour l'énorme soutien que vous m'avez donné cette année, vous êtes le sang ! Merci Camcam pour ton aide dans mon

dernier rush ! Ce n'est pas la peine de faire une liste exhaustive de tout ce beau groupe de coutain, notre amitié va jusqu'à m'inspirer la couverture de cette thèse. Pour ces belles rencontres réalisées à l'ecpm : Merci à Javi, Isa, Pablo (x2) et Miquel pour m'avoir envie de découvrir l'Espagne. Merci à Baptiste, Coco, Dodo, Titoms et Mathieu pour être aussi généreux et une source d'inspiration. Merci Eva pour ta bienveillance, de ton rayonnement et de ton amitié qui m'est chère.

Finalement, merci à toi Mouf pour toutes ces années partagées à tes côtés entre Coutances, Caen, Strasbourg et Toulouse. Je suis si heureux d'avoir passé 10 ans avec toi. Ton amour et ton soutien a été une source de motivation et de force. Je suis fier de tout ce qu'on a vécu ensemble.

In conclusion, this thesis stands as a testament to the collaborative efforts and encouragement of numerous individuals. Their contributions have left an indelible mark on both my academic and personal journey. I am deeply humbled and grateful for their unwavering support.

Thanks to each and every one of you.

The project leading to this application has received funding from the European Union's Horizon 2020 research and innovation programme under the Marie Skłodowska-Curie grant agreement No 860322

Summary

Chiral amines are fundamental structural elements present in a range of natural substances, pharmaceuticals, and biologically significant compounds. Approximately 40–45% of small-molecule drugs, as well as various industrially relevant fine chemicals and agrochemicals, incorporate chiral amine moieties. Additionally, these chiral amines find utility as resolution agent, chiral auxiliaries, and essential building blocks for the creation of more sophisticated molecules, including natural products. Consequently, there is a substantial demand within life sciences for a reliable and sustainable means of producing enantiomerically pure amines.

In this manuscript, the works performed on the homogeneous asymmetric intermolecular hydroaminomethylation of various alkenes such as 1,1-diarylethenes and cyclopropylmethacrylamides, and the intramolecular hydroaminomethylation of amine-containing styrene derivatives, and our preliminary results for the development of heterogenized chiral catalysts for the hydroaminomethylation reaction under flow condition are described. In the asymmetric hydroformylation and hydroaminomethylation of 1,1-diarylethenes, two classes of ligands stood out, namely the sugar-based phosphite phosphoramidite **L14** and sugar-based bisphosphite **L15** with good conversions, moderate chemoselectivity and ee's up to 41%. Via the asymmetric hydroaminomethylation reaction, chiral amines were obtained in 30-47% yield with ee's between 23 and 36%. Using the protected phenol **3.20**, the chemoselectivity and enantioselectivity were slightly enhanced with ee's up to 46%. The chiral chromanols **3.8a-g** were obtained in 45-90% yield via asymmetric hydroformylation. These results constitute the first direct synthesis of Tolterodine and derivatives via asymmetric hydroaminomethylation of 1,1-diarylethenes. The work outlined in Chapter IV focused on the synthesis of a series of 2-cyclopropylmethacrylamides and the evaluation of their reactivity in Rh-catalyzed hydroformylation and hydroaminomethylation. The synthesized cyclopropylacrylamides were tested in the Rh-catalyzed hydroformylation and

hydroaminomethylation reactions using various ligands. The reactivity of tertiary amides revealed substrate dependent. 2-cyclopropylacrylamides undergo ring opening reaction under hydroformylation and hydroaminomethylation conditions. Hydroformylation of secondary 2-cyclopropylacrylamides provided new dihydropyridinone and linear aldehyde products both coming from ring opening of the VCP and subsequent linear or branched hydroformylation. In the hydroaminomethylation of secondary 2-cyclopropylacrylamides, the expected hydroaminomethylation products were not detected but new amines formed via cascade reaction and hydroamination were isolated. Aiming at the development of heterogenized catalysts for the asymmetric hydroformylation and hydroaminomethylation of 1,1-disubstituted alkenes, the syntheses of two new pyrene-tagged sugar-based amino-alcohol backbones were successfully conducted. However, only the ligand **5.11** was successfully obtained in 33% yield. The new pyrene-tagged ligand was reacted with $[Rh(COD)_2]BF_4$ and provided the complex **5.10**, which was successfully immobilized on multiwalled carbon nanotubes, reduced graphene oxide and carbon beads. The activity of the Rh/**5.11** catalytic system was tested in homogeneous hydroformylation and hydroaminomethylation of the substrate **5.22** and the results indicated that the introduction of the pyrene moiety did not significantly alter the properties of the ligand. The immobilized catalysts were tested in batch hydroformylation and although the catalysts presented a low activity, the catalyst **5.10@MWCNT** provided a good enantioselectivity of 61%. The reactivity of *ortho* substituted styrene derivatives containing an amine moiety was also evaluated in the Rh-catalyzed intramolecular hydroaminomethylation. In the Rh-catalyzed intramolecular hydroaminomethylation of these substrates, the hydrogenation of the enamine intermediate is the limiting factor for the reaction to proceed. Increasing the size of the enamine ring formed from 5 to 7-membered ring resulted in a more efficient hydrogenation under HAM conditions.

Résumé

Les amines chirales sont des éléments structuraux fondamentaux présents dans diverses substances naturelles, médicaments et composés biologiquement actifs. Environ 40 à 45% des médicaments à base de petite molécule, ainsi que divers produits chimiques fins et agrochimiques d'importance industrielle, intègrent des motifs d'amines chirales. Par conséquent, il existe une demande importante d'un moyen fiable et durable de produire des amines énantiomériquement pures.

Dans ce manuscrit, les travaux réalisés sur l'hydroaminomethylation (HAM) homogène asymétrique intermoléculaire de divers alcènes tels que les 1,1-diaryléthènes et les cyclopropylméthacrylamides, ainsi que l'HAM intramoléculaire de dérivés de styrène contenant un groupe amine, sont décrits. De plus, nos résultats préliminaires concernant le développement de catalyseurs chiraux hétérogénéisés pour la réaction d'HAM en conditions de flux sont présentés. Dans l'hydroformylation (HF) et l'HAM asymétriques de 1,1-diaryléthènes, deux classes de ligands se sont démarquées, à savoir le phosphite phosphoramidite **L14** à base de sucre et le bisphosphite **L15** à base de sucre, présentant de bonnes conversions, une chimiosélectivité modérée et des excès énantiomériques allant jusqu'à 41%. Via la réaction d'HAM asymétrique, des amines chirales ont été obtenues avec un rendement de 30 à 47% et des excès énantiomériques entre 23 et 36%. En utilisant le phénol protégé **3.20**, la chimiosélectivité et l'énantiosélectivité ont été légèrement améliorées, avec des excès énantiomériques allant jusqu'à 46%. Les chromanols chiraux **3.8a-g** ont été obtenus avec un rendement de 45 à 90% via l'hydroformylation asymétrique. Ces résultats constituent la première synthèse directe de la Tolterodine et de ses dérivés par HAM asymétrique de 1,1-diaryléthènes.

Le travail présenté dans le chapitre IV s'est concentré sur la synthèse d'une série de 2-cyclopropylméthacrylamides et sur l'évaluation de leur réactivité en HF et en HAM catalysées par le Rh. Les cyclopropylacrylamides synthétisés ont été testés dans les réactions d'HF et d'HAM catalysées par le Rh en utilisant divers ligands. La réactivité

des amides tertiaires s'est révélée dépendante du substrat. Les 2-cyclopropylacrylamides subissent une réaction d'ouverture de cycle en conditions d'HF et d'HAM, et l'HF des 2-cyclopropylacrylamides secondaires a fourni de nouveaux produits de dihydropyridinone ainsi qu'un aldehyde linéaire, les deux provenant d'une séquence d'ouverture de VCP suivi d'hydroformylation linéaire ou ramifiée. Dans l'HAM des 2-cyclopropylacrylamides secondaires, aucun produit attendu d'hydroaminomethylation n'a pu être détecté mais des nouvelles amines provenant d'une réaction en cascade ainsi qu'hydroamination ont pu être isolées. Dans l'optique du développement de catalyseurs hétérogénéisés pour l'HF et l'HAM asymétriques d'alcènes 1,1-disubstitués, la synthèse de deux nouveaux squelettes amino-alcools basés sur un sucre, contenant un pyrène, a été menée avec succès. Cependant, seul le ligand **5.11** a été obtenu avec succès avec un rendement de 33%. Le nouveau ligand contenant le pyrène réagit avec $[Rh(COD)_2]BF_4$ et fournit le complexe **5.10**, qui a été immobilisé avec succès sur des nanotubes de carbone à parois multiples, de l'oxyde de graphène réduit et des billes de carbone. L'activité du système catalytique Rh/**5.11** a été testée en HF et en HAM homogènes du substrat **5.22** et les résultats indiquent que l'introduction de la partie pyrène n'a pas significativement modifié les propriétés du ligand. Les catalyseurs immobilisés ont été testés en HF en batch et bien que les catalyseurs présentent une faible activité, le catalyseur **5.10@MWCNT** a fourni une bonne énantiosélectivité de 61%. La réactivité de dérivés de styrène substitués en position *ortho* contenant un groupe amine a également été évaluée dans l'HAM intramoléculaire catalysée par le rhodium. Dans cette réaction, l'hydrogénation de l'intermédiaire énamine constitue le facteur limitant. Augmenter la taille du cycle de l'énamine formé, passant d'un cycle de 5 à 7 atomes, a conduit à une hydrogénation plus efficace dans des conditions d'HAM.

Abbreviations and acronyms

A	AHF	asymmetric hydroformylation
	Å	Angström
	acac	acetylacetone
	API	active pharmaceutical ingredient
	atm	atmosphere
	ax	axial
B	BDP	bis-3,4-diazaphospholane
	BINAP	2,2'-bis(diphenylphosphino)-1,1'-binaphthyl
	BINOL	1,1’-Bi-2-naphthol
	BOP	benzotriazol-1-yloxy-tris-(dimethylamino)phosphonium hexafluorophosphate
	BPE	bisphospholanoethane
	BPPFA	1-[1',2-bis(diphenylphosphine)-ferrocenyl]ethyldimethylamine
	BPPM	2-(diphenylphosphinomethyl)-4-(diphenylphosphino)-N-(t-butoxycarbonyl)pyrrolidine
	bs	broad signal
C	*ca.*	approximately
	CBs	carbon beads
	CCR	chemokine CC receptor
	CDI	1,1'-carbonyldiimidazole
	CNTs	carbon nanotubes
	COD	1,5-cyclooctadiene
	Conv.	conversion
	COSY	correlation spectroscopy
	CSTR	continuous stirred tank reactor
D	dba	dibenzylideneacetone
	DBU	1,8-diazabicyclo[5.4. 0]undec-7-ene
	DCC	N,N’-dicyclohexylcarbodiimide
	DCE	1,2-dichloroethane
	DCM	dichloromethane
	dd	doublet of doublet
	DDQ	2,3-dichloro-5,6-dicyano-1,4-benzoquinone

	DEA	diethylamine
	DFT	density functional theory
	DIBAL	diisobutylaluminium hydride
	DIOP	2,2-dimethyl-4,5-bis(diphenylphosphinomethyl)-1,3-dioxolane
	DIPA	diisopropylamine
	DIPEA	N,N-diisopropylethylamine
	DMAP	4-dimethylaminopyridine
	DME	1,2-dimethoxyethane
	DMF	N,N-dimethylformamide
	DPE	diphenyl ether
	DPPB	1,4-bis(diphenylphosphino)butane
	dppf	1,1'-bis(diphenylphosphino) ferrocene
	DPPP	1,3-bis(diphenylphosphino)propane
	DTBM	ditertbutylmethyl
E	EDC	1-ethyl-3-(3-dimethylaminopropyl)carbodiimide
	ee	enantiomeric excess
	eq	equatorial
	equiv.	equivalents
	ESI-TOF	electrospray ionization time-of-flight
	EtOAc	ethyl acetate
	EWG	electron-withdrawing group
G	GABA	γ-amino butyric acids
H	h	hours
	HAM	hydroaminomethylation
	HATU	hexafluorophosphate azabenzotriazole tetramethyl uronium
	HEH	Hantzsch ester
	HF	hydroformylation
	HIV	human immunodeficiency virus
	HMBC	heteronuclear multiple bond correlation
	HP	high-pressure
	HPLC	high performance liquid chromatography
	HSQC	heteronuclear single quantum coherence
	Hz	hertz(s)

I	ICP	induced coupled plasma
	IR	infrared
J	*J*	coupling constant
L	L	ligand
M	m	multiplet
	m/z	mass over charge
	MS	mass spectrometry
	MWCNTs	multi-walled carbon nanotubes
N	nbd	norbornadiene
	NHC	N-heterocyclic carbene
	NMI	N-methylimidazole
	NMP	N-methyl-2-pyrrolidone
	NMR	nuclear magnetic resonance
	NOESY	nuclear overhauser effect spectroscopy
	NP	nanoparticule
O	OAB	overactive bladder
P	PCC	pyridinium chlorochromate
	PE	petroleum ether
	PTSA	para-toluenesulfonic acid
	PyBOP	benzotriazol-1-yloxytripyrrolidinophosphonium hexafluorophosphate
R	r.t	room temperature
	RAME	randomly methylated
	rGO	reduced graphene oxide
	rpm	rotation per minute
S	SN	nucleophilic subsitution
	syngas	synthesis gas
T	T	temperature
	t	time
	t (in NMR)	triplet

	TBDPS	tert-butyldiphenylsilyl
	TBP	trigonal bipyramid
	tdt	triplet of doublet of triplet
	TFA	trifluoroacetic acid
	TFMLA	trifluoromethyllactic acid
	THF	tetrahydrofuran
	TLC	thin layer chromatography
	TMEDA	tetramethylethylenediamine
	TOF	turnover frequency
	TON	turnover number
	TPPTS	triphenylphosphine-3,3’,3’’-trisulfonic acid trisodium salt
V	VCP	vinylcyclopropane
X	XRD	x-ray diffraction

Table of contents

CHAPTER I

INTRODUCTION

1.1. General introduction

The use of carbon monoxide as C1 building block via metal-catalyzed carbonylation processes has revealed an efficient tool for the functionalization of organic molecules; moreover, the atom-economic nature of this type of reaction has increased the interest of both academia and industry.[1] The production of acetic acid through the carbonylation of methanol,[2] and the production of aldehydes by the hydroformylation of propene[3] are the two main homogeneous processes currently applied in industry. Nonetheless, metal-catalyzed carbonylations are not only limited to bulk chemistry and can also be applied for the synthesis of fine chemicals such as chiral molecules through enantioselective processes.[4]

Among the metals that catalyze carbonylation reactions, rhodium was largely studied due to its intrinsic properties that provide high activity and selectivity for this type of reaction.[5] Recently, an attractive strategy combining the efficiency of rhodium catalysts in carbonylation and C-H activation reactions has emerged for the construction of more complex cyclic skeletons.[6]

Rhodium catalyzed hydroformylation constitutes an attractive strategy for the synthesis of aldehydes from readily available starting materials such as alkenes in a high atom economy process.[7] The reaction consists in the addition of "synthesis gas" (syngas), a mixture of CO and H_2, to olefins in the presence of a catalyst. A formyl group and hydrogen are added through the π system of the alkene for the formation of aldehydes. Currently, several million tons of oxo-products are manufactured per year, mainly through the hydroformylation of propene **1.1**. The products *iso*-butyraldehyde **1.2** and *n*-butanal **1.3** are important intermediates to synthesize esters, acrylates, and 2-ethylhexanol (Scheme 1).[3]

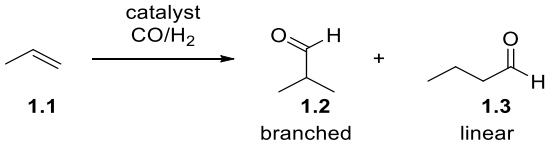

Scheme 1. Hydroformylation of propene

From an organic point of view, aldehydes are products of interest due to their potential in terms of subsequent functionalization, that can lead to the formation of new carbon-carbon and carbon-heteroatom bonds.[8] However, despite the clear potential of asymmetric hydroformylation for the synthesis of chiral aldehydes, the application of this process at a large scale has not yet been completed. Aldehydes are generally not isolated as final products since the products of interest are usually derivatives. In this context, tandem processes with hydroformylation as the initial step constitute an interesting strategy. Indeed, the possibility to carry out several catalytic transformations in "one-pot" is even more attractive from an environmental and efficiency point of view. In this context, tandem catalytic processes are described as sequential catalytic transformations of the substrate through two, or even more, mechanistic pathways (Scheme 2).[9]

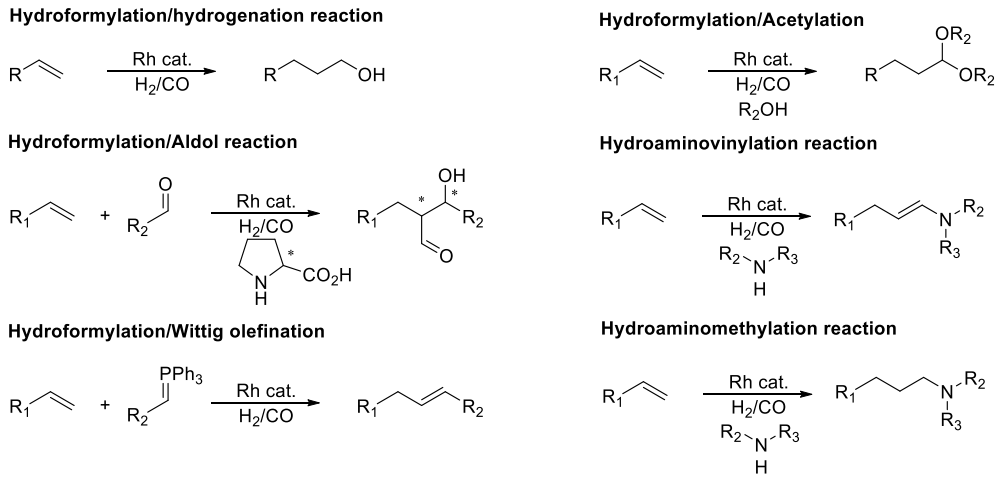

Scheme 2. Examples of hydroformylation tandem processes.

When hydroformylation is the first step of such processes, alcohols can be prepared by in situ reduction of the aldehyde using the hydrogen pressure present in the medium.[10] In the presence of a carbonyl compound such as an aldehyde and an organocatalyst, aldol reactions take place to expand the structure of the molecule.[11] It is also possible to create new C-C bonds if the aldehyde reacts with a phosphorus ylide via a Wittig reaction.[12] On the other hand, aldehydes can act as electrophiles

and react with a nucleophile present in the media. If the nucleophile is an alcohol, hemiacetals or acetals can be created.[13] In the presence of a primary or secondary amine, imines and enamines can be easily prepared.[14] When these imines or enamines are hydrogenated to produce the corresponding amine, the reaction is called hydroaminomethylation (HAM).

In this chapter, advances in the field of asymmetric hydroaminomethylation of alkenes is described. A part will also be devoted to the hydroformylation which is the first step of this tandem reaction. After a brief introduction of these reactions, the mechanisms of the processes will be detailed, and the most relevant catalytic results will be described according to the alkenes substrates.

1.2. Rh-catalyzed hydroaminomethylation of alkenes

1.2.1. Interest

The efficient and selective synthesis of amines using readily available and abundant precursors is a long-standing goal of chemical research since they are powerful building blocks for the synthesis of pharmaceuticals, peptides, alkaloids and agrochemical, dyes, and monomers for polymerization.[15]

Chiral amine moieties are present in ca. 40% of pharmaceutical products. The introduction of these chiral units is therefore of high importance and usually performed through multistep processes.[16,17] As enantiomerically pure amines are required in large quantities in the pharmaceutical and agrochemical industry, the development of efficient methodologies for their preparation is of great significance and highly desirable. In the context of green chemistry, research on organometallic catalysis is still progressing to access and produce optically pure chiral amines. The main enantioselective metal-catalyzed reactions for the synthesis of chiral amines are reductive amination, hydroamination, hydroaminoalkylation and hydroaminomethylation (Scheme 3).[18]

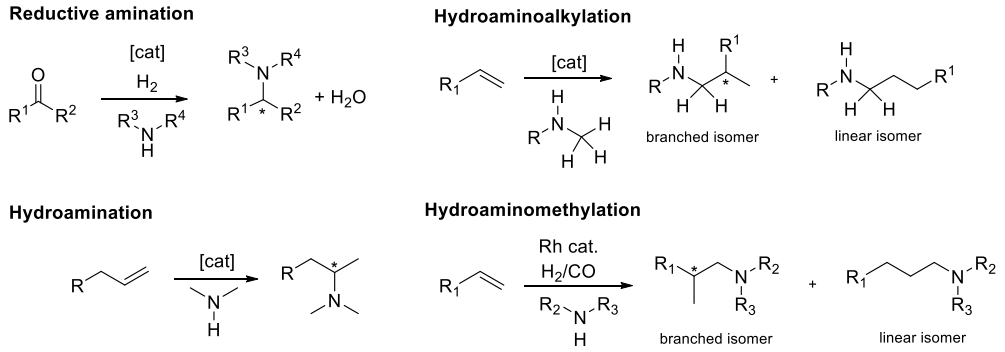

Scheme 3. Transition metal catalyzed processes to access chiral amines

In this context, the metal catalyzed hydroaminomethylation reaction constitutes an attractive alternative to the classical multistep organic synthetic routes. The reaction was discovered by Reppe and co-workers between 1928 and 1944 at BASF when they were studying the production of acrylamide by reaction of acetylene, carbon monoxide and ammonia using nickel and iron carbonyl catalysts. The authors studied first the reaction with ethylene to obtain propylamine, and then extended the reaction to various alkenes.

1.2.2. Mechanism

HAM is a tandem reaction involving in the first step the hydroformylation of an alkene. The achiral version of this reaction was significantly investigated and some reviews have recently appeared.[19, 20, 21] The rhodium-catalyzed HAM represents an attractive atom economy reaction providing amines from alkenes in a one-pot method. This tandem reaction is composed of three successive steps. The aldehydes produced during the hydroformylation step react with primary or secondary amines present in the medium to afford the corresponding imines or enamines. In most cases, isomerization between imine and enamine occurs and hydrogenation of these intermediates in the second catalytic cycle results in the formation of the desired amines. The mechanism thus includes the successive catalytic hydroformylation and hydrogenation cycles (Scheme 4).

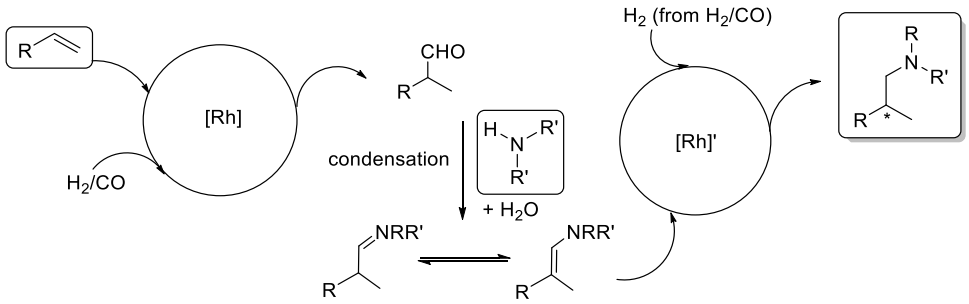

Scheme 4. Hydroaminomethylation reaction of olefins

The hydroformylation of alkenes, formerly discovered by Otto Roelen,[22] is currently one of the most principal industrial applications of homogeneous catalysis.[3,23]

Since Wilkinson reported that phosphine-containing rhodium complexes could provide enhanced catalytic performance compared with the first generation of cobalt catalysts,[24] ligand tuning has constituted the main axis of research to improve the outcome of hydroformylation.[25]

In the low-pressure hydroformylation of internal alkenes, the chemoselectivity (and simultaneously regioselectivity) is one of the main issues due to the substantial decrease of reactivity as the number of alkene substituents increases and usually rely on the use of strong π-acceptor ligands.[26] However, a high tendency towards alkene isomerization is usually observed and does not provide position-selective hydroformylation of internal alkenes.

The regioselectivity of the hydroformylation of alkenes depends on many aspects and insights into its origin often relied on quantum chemical calculations.[27] These include intrinsic substrate properties, directing effects caused by functional groups of the substrate, and catalyst effects. In order to better grasp substrate intrinsic regioselectivity trends, alkenes must be classified according to the number and nature of their substituents (Scheme 5).[7,28]

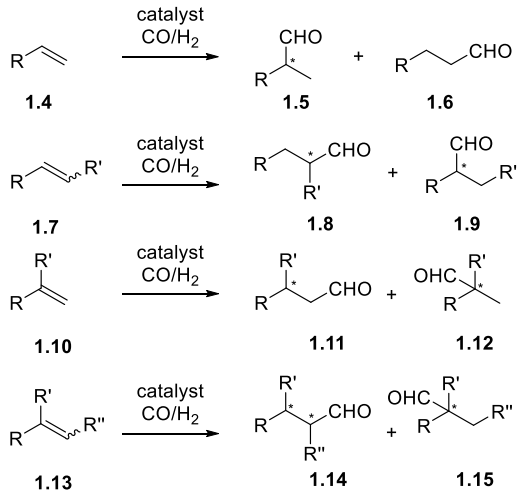

Scheme 5. Regioselective trends on hydroformylation of different alkenes.

Terminal and 1,2-disubstituted alkenes **1.7** are the substrates that present the most important regioselectivity issues. For alkyl-substituted terminal alkenes **1.4,** a slight preference is usually observed in favor of the linear product **1.6**. In contrast, when the reaction is performed using terminal alkenes **1.4** bearing an electron-withdrawing substituent, high selectivity to the branched product **1.5** can be achieved, independently of the catalyst used. For 1,2-disubstituted alkenes **1.7**, the branched aldehyde **1.9** is generally obtained when R is an electron withdrawing group while **1.8** can be obtained if R is a bulky substituent. When the substrates are 1,1-disubstituted alkenes **1.10** and trisubstituted **1.13,** only one regioisomer is usually obtained (**1.11** and **1.14**, respectively) in agreement with Keuleman´s rule, which states that the addition of the formyl group usually avoids the formation of a quaternary carbon center.[29]

Although chiral aldehydes can be obtained in a single step via asymmetric hydroformylation, this reaction has not yet been applied at industrial scale due to several technical issues such as the low reaction rates under the conditions required for high selectivity and the difficulty to control simultaneously the regio- and the enantioselectivity.[3]

1.2.2.1. Rh-catalyzed hydroformylation mechanism

The mechanism of the Rh-catalyzed hydroformylation proposed by Heck,[30] which corresponds to Wilkinson's dissociative mechanism is described for bidentate ligands (Scheme 6).[51] In this process, a great understanding of the mechanism was made possible by the structural characterization of the catalyst resting state using *in situ* spectroscopic techniques (HP-IR, HP-NMR).[8,31] In this mechanism, the coordination mode of the bidentate ligands (L-L) can be equatorial-equatorial (eq-eq) or equatorial-axial (eq-ax), depending on the ligand's structural properties such as their bite angle.

The common starting complex is the $[RhH(L\text{-}L)(CO)_2]$ species **1.16** from which dissociation of the equatorial CO provides the square planar intermediate **1.17**. Coordination of the alkene substrate gives complexes **1.18**, where the ligand can again be coordinated in two isomeric forms eq-ax and eq-eq, having a hydride in an apical position and alkene coordinated in the equatorial plane. It was proposed that the regioselectivity is determined by the coordination of the alkene to the square planar intermediate **1.17** to give the pentacoordinate intermediates **1.18**.[27e] This step is also enantioselectivity-determining since the enantioface discrimination occurs between **1.17** and **1.19**, and particularly from **1.17** to **1.18**. The rate of the reaction is usually governed by the reaction of **1.17** with either CO or the alkene to form **1.16** or **1.18**.[27i]

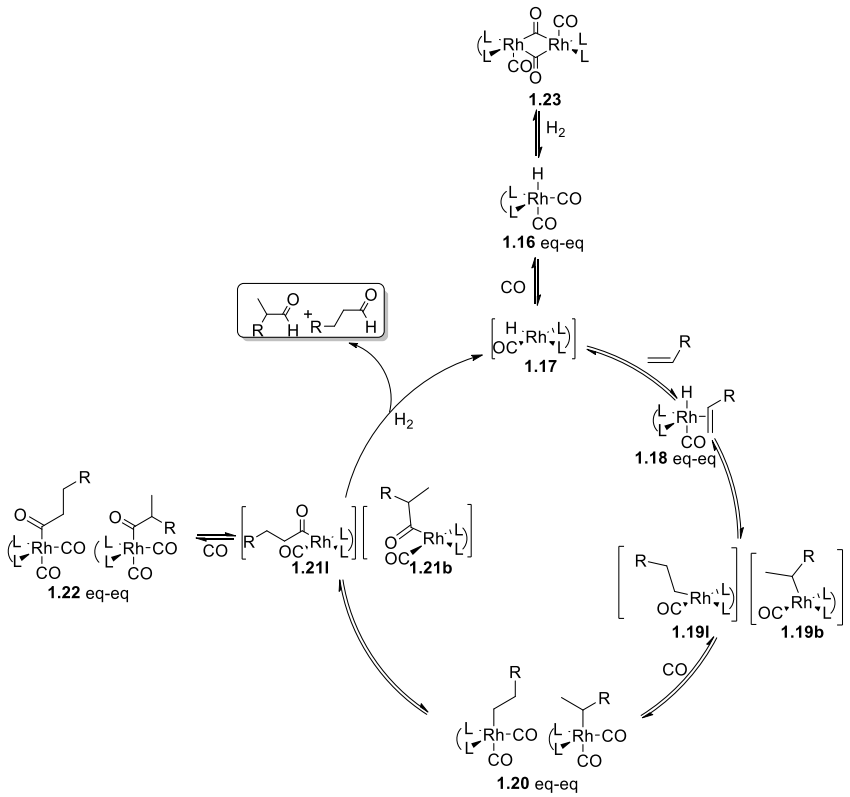

Scheme 6. Mechanism of the Rh-catalyzed hydroformylation in the presence of bidentate ligand (L-L) coordinated in eq-eq mode.

Experiments using deuterated substrates suggest that alkene coordination and insertion into the Rh-H bond can be reversible, especially at low pressure and all steps are usually described as reversible except the final hydrogenolysis. Complexes **1.18** undergo migratory insertion to give the square planar alkyl complexes **1.19**. These species can undergo β-hydride elimination, or can react with CO to form the trigonal bipyramid (TBP) complexes **1.20**. Under low pressure of CO, a higher degree of isomerization may then be expected. At low temperatures (< 70°C) and high pressures of CO (> 10 bar), the insertion reaction is usually irreversible and the regioselectivity and enantioselectivity of the overall process are therefore determined at this point. Complexes **1.20** undergo the second migratory insertion to form the acyl complex **1.21**, which can react with CO to form the 18-electron acyl intermediates **1.22** or with H_2 to give the aldehyde product and regenerate the

unsaturated intermediate **1.17**. The reaction with H_2 could involve oxidative addition and subsequent reductive elimination, but no Rh (III) intermediates were detected.[32] It is noteworthy that at low hydrogen pressures and high rhodium concentrations, the formation of dirhodium dormant species such as **1.23** becomes significant.[33] The full catalytic cycle for monophosphine Rh complexes was investigated using DFT calculations.[34]

1.2.2.2. Rh-catalyzed reductive amination mechanism

While amine condensation can proceed without the need of a catalyst, it was observed that rhodium often plays a non-innocent role in the chemoselectivity.[35]

It is necessary to carefully design the catalytic system to obtain not only high chemoselectivity but also regioselectivity to the branched or linear final amine. The hydrogenation reaction represents the rate-determining step in HAM. Recent investigations into the mechanism demonstrated that an equilibrium between the neutral $[Rh(H)(CO)_2L_2]$ **1.24** and the cationic $[Rh(CO)(X)L_2]^+$ **1.25** species exists to perform the two catalytic cycles.[36] It is probable that the neutral rhodium-hydride species catalyzes the hydroformylation reaction whereas the cationic species performs the hydrogenation reaction. In order to increase both catalytic activity and amine selectivity, an appropriate rhodium system able to generate *in situ* the two catalytic active species is necessary, instead of using simultaneously cationic and neutral rhodium precursors (Scheme 7).

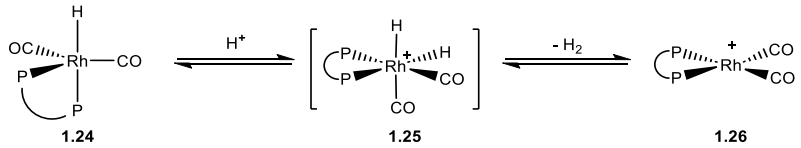

Scheme 7. Equilibrium between the two neutral and cationic rhodium species[36]

The second catalytic cycle concerning hydrogenation is described in Scheme 8. Classically, the cationic active species, represented as $[Rh]^+$, reacts with dihydrogen forming the Rh-η^2- dihydrogen complex **1.28**. Then the enamine coordinates to the

complex via the nitrogen atom giving **1.29**. Two consecutive hydrogen transfers generate the iminium **1.30** and the final amine, restoring the $[Rh]^+$ active species.

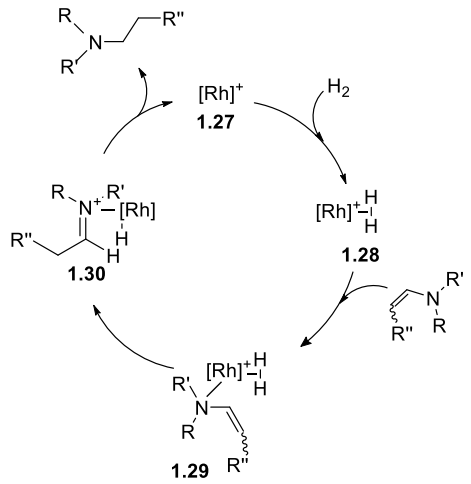

Scheme 8. Proposed hydrogenation catalytic cycle of an enamine[21]

The tandem reaction is generally carried out at temperatures between 90-130°C and 30-60 bar of $CO:H_2$ pressure to obtain amines in good yields. These operating conditions are somewhat harsher than those used for the hydroformylation reaction, consistent with a rate-determining step for the hydrogenation reaction of imines/enamines. The CO/H_2 composition generally varies from 1:1 to 1:5, depending on the experimental procedures.

1.2.3. Previous results in the HAM reaction of alkenes

The hydroaminomethylation of monosubstituted alkenes was reported by several groups over the last decade. Among them, the most studied substrates were the arylalkenes, especially those derived from styrene, since arylethylamines exhibit pharmacological activity.[37] Eilbracht and co-workers reported the rhodium catalyzed hydroaminomethylation of 1,1-diaryl-allyl-alcohols **1.31** and **1.32** and vinyl benzoazepine **1.33** using a non-modified $[Rh(\mu\text{-}Cl)(COD)]_2$ catalyst to afford antihistaminic drugs such as Difenidol, Fluspirilene precursor or biological active Trimipramine (Scheme 9).[38]

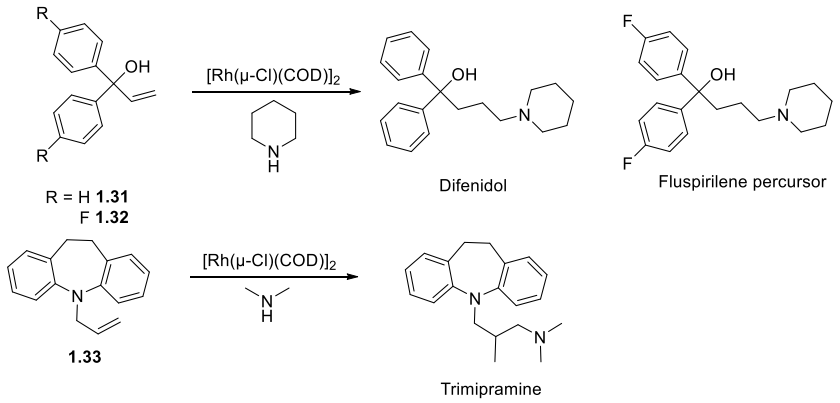

Scheme 9. Rh-catalyzed hydroaminomethylation of monosubstituted alkenes 1.31-1.33 using unmodified rhodium catalyst.

Despite these results with non-modified catalysts, the use of catalytic systems containing phosphorus ligands usually provide higher activity and selectivity for both hydroformylation and hydrogenation reactions.

In contrast to monodentate ligands, bidentate phosphorus ligands offer much stronger coordination and higher steric hindrance to the metal center. In consequence, diphosphine ligands tend to provide better chemo- and regioselectivities in the rhodium catalyzed hydroaminomethylation of monosubstituted alkenes. Beller and co-workers reported the use of Xantphos **L1** together with the cationic precursor $[Rh(COD)_2]BF_4$ for the hydroaminomethylation of several terminal alkyl alkenes, aryl alkenes, and vinyl arenes.[39] Excellent chemo- and regioselectivities to linear amines **1.34** and **1.36** were obtained (Scheme 10).

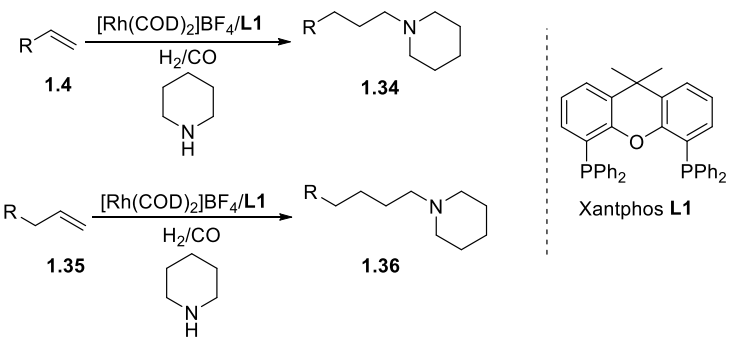

1.34	n:iso	amine (%)
R = Ph	82:18	95
R = C_4H_9	98:2	>99
R = $CH(OEt)_2$	99:1	>99
R = C_3H_6OH	99:1	98

1.36	n:iso	amine (%)
R = Ph	90:10	95
R = OPh	99:1	90

Scheme 10. Rh-catalyzed hydroaminomethylation of monosubstituted alkenes for the production of linear amines using the Xantphos ligand L1.

Vogt et. al. improved the results in terms of activity and regioselectivity to the linear amines using more π-acceptor diphosphorus ligands based on Xanthene.[40] Apart from linear amines, the production of branched arylethylamines **1.37** through the reaction of styrene with an amine is attractive due to the importance of these compounds in the pharmaceutical industry.[41] In this context, Beller et. al. achieved the production of branched amines from styrene and derivatives using 1,1'-bis(diphenylphosphino) ferrocene (dppf) **L2** as ligand with excellent regio- and chemoselectivities. The use of a cationic precursor in a mixture of methanol/toluene as solvent was necessary to afford the desired products (Scheme 11).[42] Moreover, the use of tetrafluoroboric acid (HBF_4) was necessary to afford amines in high yields.

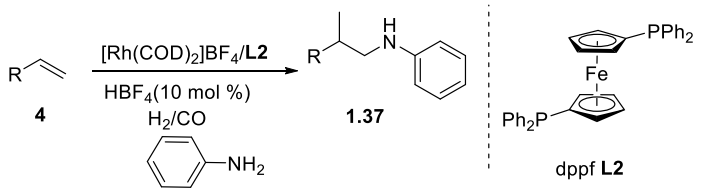

1.37	iso:n	amine (%)
R = Ph	88:12	96
R = 4-Cl-C_6H_4	85:15	98
R = 4-OMe-C_6H_4	88:12	97

Scheme 11. Rh-catalyzed hydroaminomethylation of styrene derivatives 1.4 for the production of branched amines 1.37 using dppf L2 as ligand.

Apart from these systems, other groups successfully employed diphosphine ligands for the selective hydroaminomethylation of monosubstituted alkenes obtaining either linear or branched amines.[43, 21]

As previously mentioned, diphosphite ligands can provide excellent results in the hydroformylation of several alkenes due to their π-acceptor character. Despite their sensitivity to hydrolysis, diphosphite ligands were also applied for the production of biological active compounds starting from monosubstituted alkenes.[44] Ibutilide, Aripiprazole or Tertefadine are some examples of molecules of interest produced via hydroaminomethylation of monosubstituted alkenes using the bidentate Biphephos derivative **L3** ligand (Scheme 12).

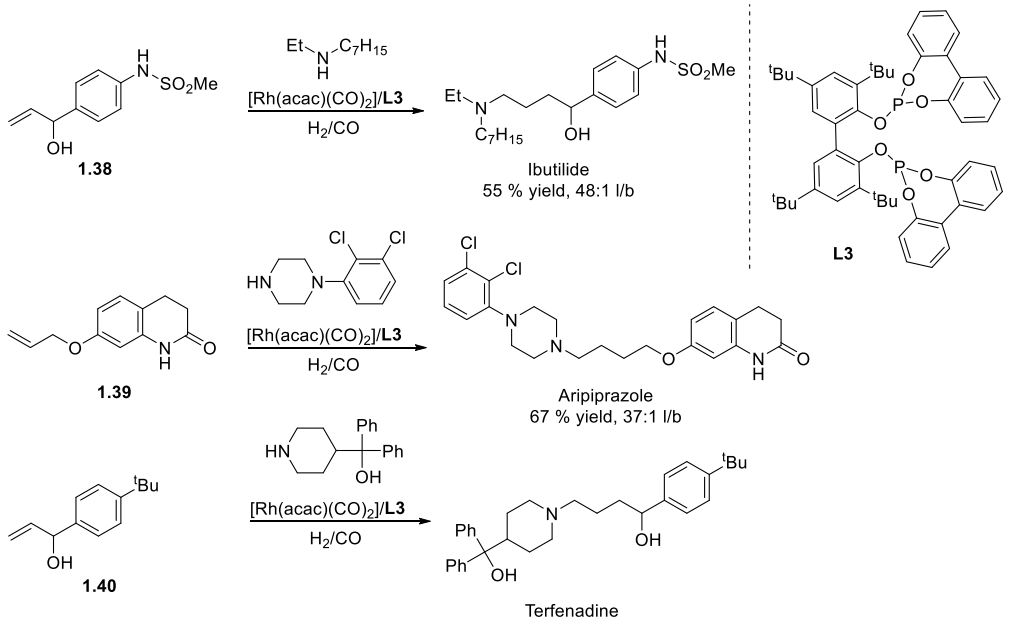

Scheme 12. Rh-catalyzed hydroaminomethylation of monosubstituted alkenes using ligand L3 for the production of biological active molecules.

In 2013, Zhang and co-workers reported that the tetraphosphorus ligand **L4** provided outstanding linear selectivity for the hydroaminomethylation of styrene and derivatives (up to >99:1 n/iso) (Scheme 13).[45] The high regioselectivity was explained by the steric hindrance provided by the ligand, together with the increased chelating effect due to the presence of four phosphorus atoms. Various amines from other terminal olefins such as 1-octene and 1-hexene were produced with high regioselectivities to the linear amine products using the ligand **L4** and other tetraphosphorus ligands.[46]

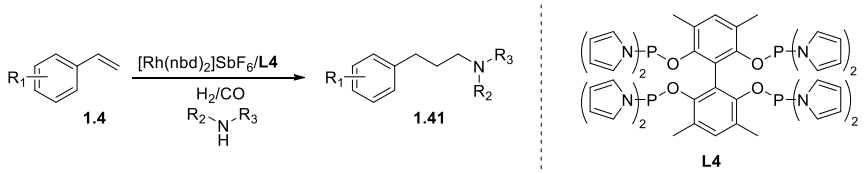

Scheme 13. Regioselective Rh-catalyzed hydroaminomethylation of styrene and derivatives using ligand L4

The hydroaminomethylation of 1,1-diarylethenes **1.43** gives access to 3,3-diarylpropylamines **1.44**, which are of pharmaceutical interest. In this context,

Eilbracht *et al*. reported the synthesis of these compounds using a catalyst bearing tributylphosphine **L5** with good selectivities towards the desired linear amines; however, high pressures (90/20 bar CO/H_2) were necessary (Scheme 14).[47] Later, Beller and co-workers reported the selective synthesis of 3,3-diarylpropylamines **1.44** via rhodium catalyzed hydroaminomethylation using the N-heterocyclic carbene **L6** ligand with low catalyst loading (0.1 mol%) (Scheme 14).[48] More recently, Zhang and co-workers reported the synthesis of the same compounds using the diphosphine Naphos **L7** with excellent selectivities, low pressure (20/10 bar CO/H_2), and catalyst loading (0.1 mol%).[49]

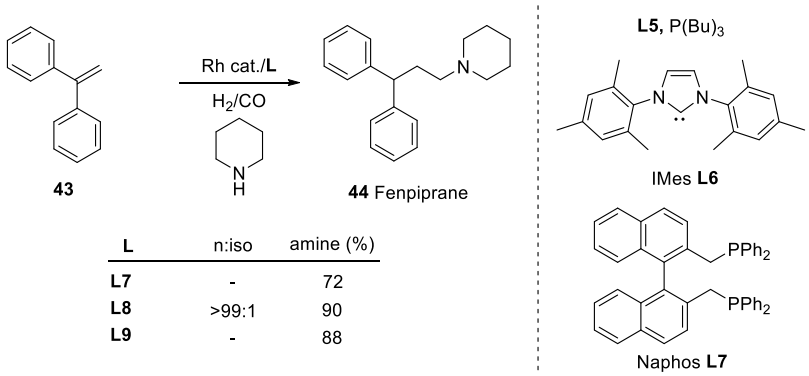

L	n:iso	amine (%)
L7	-	72
L8	>99:1	90
L9	-	88

Scheme 14.Synthesis of Fenpiprane 1.44 through hydroaminomethylation of ethene-1,1-diyldibenzene 1.43 using L5, L6 and L7 as ligands.

In conclusion, the rhodium catalyzed hydroaminomethylation reaction has demonstrated its potential for the direct synthesis of amines from alkenes. However, the asymmetric version of hydroaminomethylation is far less reported. Depending on the type of substrates, the chirality can be induced during the hydroformylation step (pathway A) or by the hydrogenation of imine/enamine (pathway B, Scheme 15).

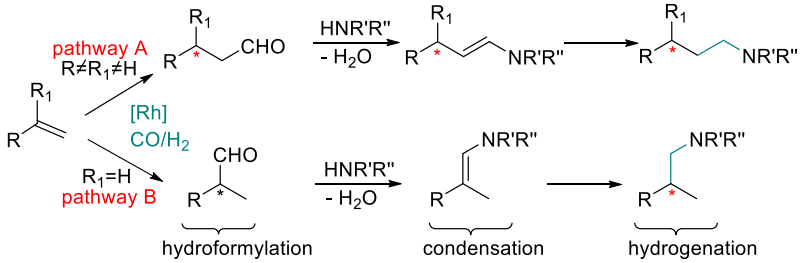

Scheme 15. Asymmetric induction in HAM

When 1,1-disubstituted alkenes are employed as substrates, asymmetric hydroformylation (AHF) generally provides the linear aldehyde creating a chiral center that is not racemized after condensation with the amine. In contrast, when monosubstituted alkenes are used, the branched aldehyde is usually favored creating a chiral aldehyde that loses its chiral information upon amine condensation. In this case, the asymmetric hydrogenation of these enamines is key to produce the desired chiral amines.

In this thesis, we focused on the asymmetric HAM of 1,1-disubstituted alkenes with a chiral center obtained via asymmetric hydroformylation, as well as on the intramolecular version of 2-propenyl aniline derivatives whose chiral center is obtained by hydrogenation. Thus, the following section presents a state of the art in asymmetric hydroaminomethylation, with a first section on the most relevant results obtained in hydroformylation of monosubstituted and 1,1-disubstituted alkenes.

1.3. Asymmetric hydroformylation and hydroaminomethylation of alkenes

1.3.1. Asymmetric hydroformylation

As previously mentioned, enantioselective hydroformylation presents a high potential to obtain a great variety of enantiomerically pure aldehydes. In this process, the first examples of high enantioselectivity (ee's up to 90%), were reported the same year by Stille and Consiglio using Pt diphosphite systems.[50] Nonetheless, such systems provided several disadvantages such as low reaction rates, tendency

to hydrogenate substrates and low regioselectivity to branched products. Later, these issues were mainly overcome using Rh-based catalysts.[51]

The first Rh-based systems reported in the asymmetric hydroformylation contained diphosphine ligands and provided *ee*'s up to 64% using styrene as substrate.[52] Later, the use of diphosphite and phosphine-phosphite ligands led to higher enantioselectivities.[23,25,28]

In the following sections the reactions are classified by the degree of substitution of the substrates and for each family of substrates, the most successful chiral ligands are described.

1.3.1.1. Asymmetric hydroformylation of monosubstituted alkenes

AHF of monosubstituted alkenes (Scheme 16) was lengthily investigated due to the interest in the enantioselective synthesis of 2-substituted branched aldehydes such as 2-aryl propionaldehydes, which are intermediates in the synthesis of 2-aryl propionic acids, the profen class of non-steroidal drugs.[23]

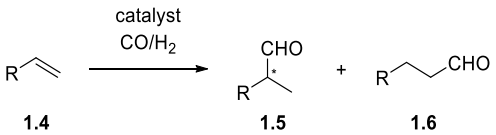

Scheme 16. Asymmetric hydroformylation of monosubstituted alkenes.

Several other monosubstituted alkenes such as allyl cyanide and vinyl acetate were also successfully converted.[23,28] 1,3-diphosphite and phosphine-phosphite ligands gave excellent results in these processes,[25] although bisphophacyclic ligands have recently emerged as an efficient alternative.[23,28]

1.3.1.1.1. 1,3-Diphosphite ligands

The diphosphite ligands proved efficient for these kinds of substrates.[21] The first successful ligand for the asymmetric hydroformylation of vinyl arenes was developed by Union Carbide and consisted in the (*2R*, *4R*)-pentane-2,4-diol diphosphite ligand **L8**. This system provided good chemo-, regio-, and enantioselectivities (up to 90% ee).[53] Apart from this structure, longer carbon chains between the oxygens atoms

were investigated but lower selectivities were obtained.[54] Furthermore, variations in the substituents on the biaryl moiety showed the importance of the groups in *ortho* and *para* positions. The best results were obtained with ligands **L8a** and **L8d** (Scheme 17). Another example of successful ligands in asymmetric hydroformylation of vinyl arenes is the family of diphosphite ligands derived from 1,2-*O*-isopropylidene-α-D-xylofuranose and 6-deoxy-1,2-*O*-isopropylidene-α-D-glucofuranose **L9** (Scheme 17).[55]

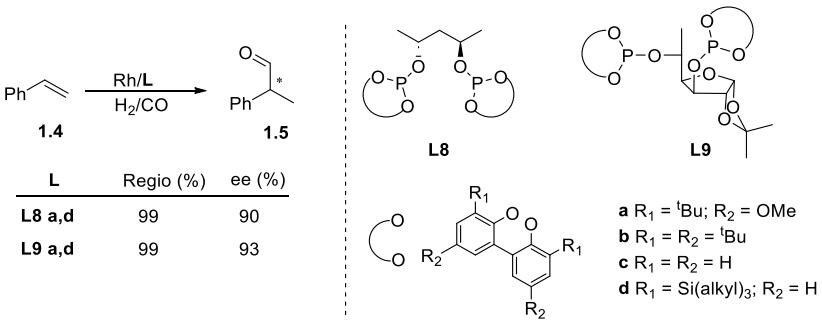

L	Regio (%)	ee (%)
L8 a,d	99	90
L9 a,d	99	93

Scheme 17. Rh-catalyzed asymmetric hydroformylation of styrene using ligands L8 and L9.

With **L9** type of ligands, the substituents on the biaryl moiety also proved to be crucial to provide high selectivities. Moreover, the absolute configuration at C5 is responsible in the high enantioselectivity and configuration of the product.

The Kelliphite ligand **L10** constitutes another example of a successful chiral diphosphite ligand for AHF developed by Dow Chemical Company.[56] In contrast with ligands **L8** and **L9**, the chirality in this ligand is located in the biaryl moiety whilst the backbone is achiral. This ligand provided good enantioselectivities (up to 88%) in the hydroformylation of allyl cyanide and vinyl acetate (Scheme 18).

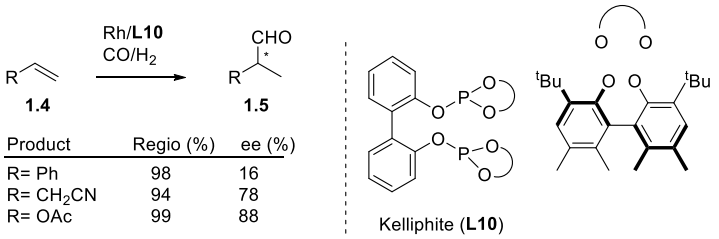

Scheme 18. Rh-catalyzed asymmetric hydroformylation of monosubstituted alkenes using the ligand Kelliphite (L10).

1.3.1.1.2. Phosphine-Phosphite ligands

The discovery of (*R*,*S*)-Binaphos (**L11**) and (*S*,*R*)-Binaphos (**L12**) ligands by Takaya and Nozaki in 1993, constituted a significant advance in the Rh-catalyzed asymmetric hydroformylation reaction (Scheme 19).[57]

Indeed, these ligands provided for the first time high enantioselectivity for several classes of monosubstituted alkenes such as vinyl arenes, vinyl acetate, and disubstituted 1,3-dienes (Scheme 19), and remains a reference to date.[58] Importantly, (*R*,*S*)-Binaphos (**L11**) or the (*S*,*R*)-Binaphos (**L12**) ligands yielded the two enantiomers of the product with high enantioselectivity.[59] However, the (*R*,*R*)- and (*S*,*S*)-Binaphos diastereoisomers of **L11** and **L12** generated much lower enantioselectivity in this process, thus demonstrating the importance of the combination of opposite configurations at the phosphine and phosphite moieties.

Using the **L11** ligand, De Vries and co-workers reported in 2003 the first Rh-catalyzed AHF of allylcyanide.[60]

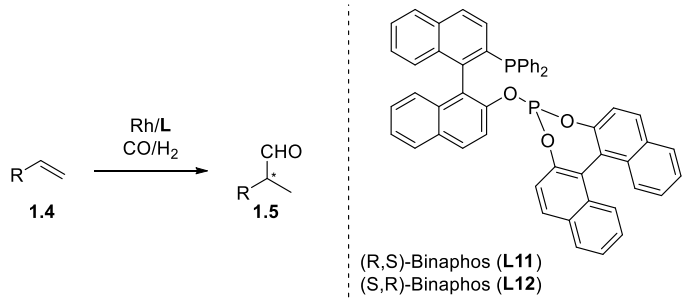

R	Ph	CH_2CN	OAc	C_6F_5	CF_3	Et	Phth	S(4-tolyl)
Regio (%)	90	72	86	96	95	21	89	96
ee (%)	94	66	92	98	93	83	85	74

Scheme 19. Rh-catalyzed asymmetric hydroformylation of monosubstituted alkenes using (R,S)- and (S,R)-Binaphos (L11 and L12).

In contrast with the eq-eq coordination of the previously mentioned diphosphite ligands at the Rh center, the Binaphos ligand coordinates to Rh in an eq-ax mode as a single isomer in the resting state $[RhH(CO)_2(L\text{-}L)]$.[60] DFT calculations indicated that the coordination of this ligand with the phosphite moiety in apical position is key for the stereoselectivity of this reaction and that the presence of a second chiral center plays a role in determining the *R* or *S* configuration of the aldehyde product.[61] They also showed that in the transition state determining the stereoselectivity, the main substrate-ligand interactions occur between the styrene and the phosphite moiety and that these interactions are repulsive in nature.

The introduction of 3-methoxy substituents on the arylphosphine units giving the **L13** ligand (Scheme 20)[58b,58c] and the replacement of the phosphite group by a phosphoramidite function giving the Yanphos **L14** ligand resulted in the second generation of Binaphos type ligands (Scheme 20).[62] The Rh/**L13** catalytic system increased the regio- and enantioselectivity in the AHF of styrene, vinylfuranes, and thiophenes (Scheme 20). Recently, the use of (*S,R*)-Bn-Yanphos (see **L14**, in which the ethyl group on the nitrogen atom is replaced by a benzyl one) was reported in the asymmetric hydroformylation reaction of vinyl-heteroarenes such as pyrroles and provided excellent regio- and enantioselectivities (up to 96%).[63]

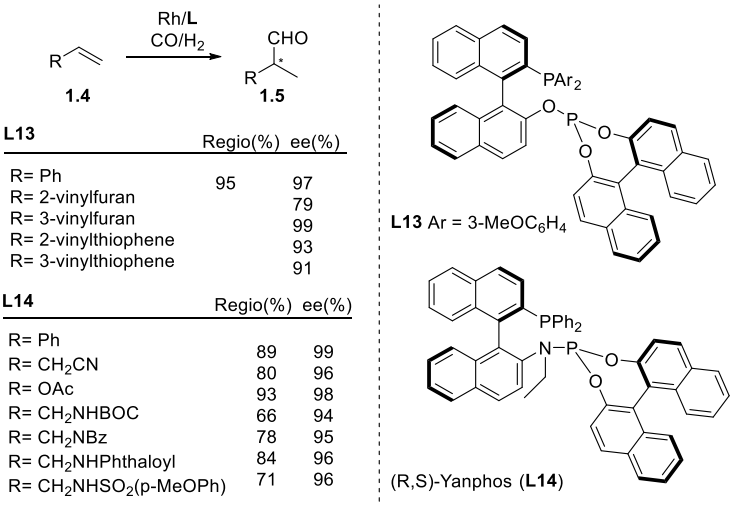

Scheme 20. Rh-catalyzed asymmetric hydroformylation of monosubstituted alkenes using the L13 and L14 ligands.

Higher enantioselectivity was achieved with Yanphos (**L14)** than that obtained with the Binaphos ligand without changing the regioselectivity in the reaction of styrene and vinyl acetate (ee up to 99 and 98%, respectively) (Scheme 20).[64]

More recently, **L14** was used in the Rh-catalyzed asymmetric hydroformylation of *N*-allylamides, *N*-allylphthalamides and *N*-allylsulfonamides and afforded good regioselectivities (up to 84%) with excellent ee's (up to 96%) and a turnover number (TON) up to 9700.[65]

Inspired by the excellent results reached with Binaphos **L13** and **L14** ligands, new phosphine-phosphite ligands presenting different backbones were synthesized over the last years but provided lower enantioselectivity (from 20 to 85%) than those previously achieved with the original Binaphos ligand.[66] However, some of these ligands helped to elucidate the correlation between the ee and the electronic withdrawing properties of the substituent on the alkene.[67]

The making of chiral aldehyde from simple terminal alkyl olefins with high regio- and enantioselectivity was a longstanding goal and a large set of ligands was tested in this reaction. Using these substrates, poor regioselectivity was usually obtained as the formation of linear aldehyde is preferred in most cases. In 2012, Clarke and co-

workers reported the first efficient production of branched aldehydes from alkyl alkenes with high regioselectivity and ee's using the Bobphos phosphine-phosphite ligand (**L15**) (Scheme 21).[68]

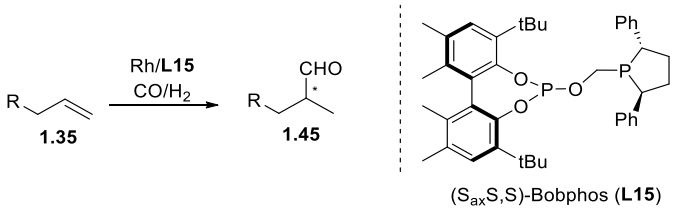

(S_{ax}S,S)-Bobphos (**L15**)

L15	regio (%)	ee (%)
R= Ph	80	90
R= C_6F_5	86	91
R= 4-t-BuC_6H_4	75	92
R= Bn	70	75
R= Pr	75	93
R= CN	89	71
R= CONPh(Me)	82	92

Scheme 21. Rh-catalyzed asymmetric hydroformylation of terminal alkyl alkenes using the Bobphos ligand L15.

The same group later developed the highly selective hydroformylation of propene towards *iso*-butanal using (R_{ax}, *R, R*)-Bobphos and octafluorotoluene. They applied their system in AHF of allylbenzene derivatives and produced the *iso*-aldehyde in 86% selectivity and 92% ee.[69]

1.3.1.1.3. Bisphosphacyclic ligands

Several chiral bisphospholane chiral ligands known as being efficient ligands for asymmetric hydrogenation were evaluated in AHF reaction (Scheme 22).[70]

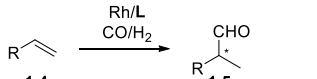

L	R= Ph		R= CH_2CN		R= OAc	
	Regio (%)	ee(%)				
L16	90	94	87	94	97	87
L17	93	90	88	93	97	83
L18	91	67			96	82
L19	98	94	88	90	99	82
L20					94	89
L21	97	82	83	87	98	96

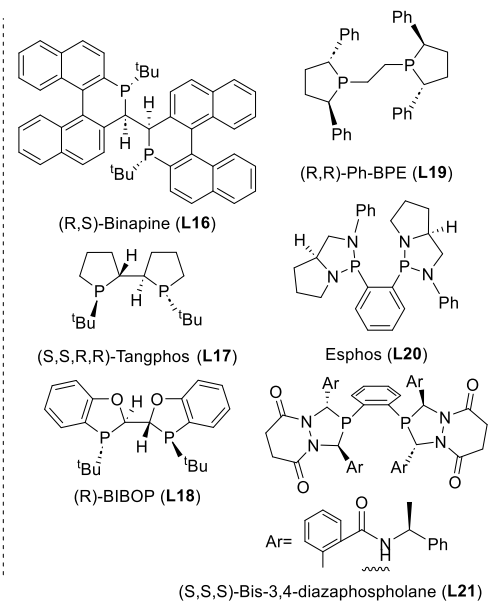

Scheme 22. Rh-catalyzed asymmetric hydroformylation of monosubstituted alkenes using the bisphospholane ligands L16-L21.

For instance, (*R*, *S*)-Binapine (**L16**) and (*S*,*S*,*R*,*R*)-Tangphos (**L17**) afforded excellent enantioselectivities in the AHF of styrene, allyl cyanide, and vinyl acetate (Scheme 22).[40] It is noteworthy that the enantioselectivities reached with these ligands are the highest ever reported for the allyl cyanide substrate. The ligand BIBOP **L18** also provided excellent results in the AHF of vinyl acetate and allylic substrates.[71] Moreover, ee´s up to 91% were obtained in the AHF of ethyl 2-vinylbenzoate providing a route to enantioenriched 4-methyl-3,4-dihydroisocoumarin after $NaBH_4$ reduction and *in situ* lactonization.[72]

Later, novel and improved bisphospholane-type ligands were discovered and the (*R*,*R*)-Ph-BPE ligand (**L19**) (Scheme 22) revealed an outstanding ligand affording excellent regio- and enantioselectivities in the AHF of styrene, allyl cyanide, and vinyl acetate.[73] The influence of spacers between the two phosphorus donor atoms was evaluated and the two carbon bridge of **L19** provided the highest selectivity for these three substrates.[74] This ligand was also successfully used in the Rh-catalyzed AHF of vinylarenes with ee's up to 95% using formaldehyde as syngas precursor.[75] It also

provided excellent results in the branched selective AHF of various 1-alkenes, as well as 1-dodecene, with regioselectivity up to 93% and ee up to 96%.[76]

A series of bis-2,5-diazaphospholane ligands was also evaluated in this process and the Esphos ligand (**L20**) provided the best results in the hydroformylation of vinyl acetate (*ee* up to 89%) (Scheme 22).[77] The (*S,S,S*)-bis-3,4-diazaphospholane ligand **L21** also offered excellent regio- and enantioselectivity (*ee* up to 96%) in this reaction (Scheme 22).[78] A detailed spectroscopic characterization of Rh intermediates bearing ligand **L21** was described for the hydroformylation of octene, vinyl acetate, allyl cyanide and 1-phenyl-1,3-butadiene.[79] Interestingly, when the tetrahydropyridazine-3,6-dione backbone of **L21** was reduced, the selectivity towards the branched aldehyde increased in the AHF of styrene, vinyl acetate and allyl cyanide.[80]

DFT calculations on a series of chiral Rh catalysts suggested an explanation for the high enantioinduction observed for Rh–CHIRAPHITE, –Binapine, –diazaphospholane, and Yanphos catalytic systems.[81] Concerning Binapine (**L16**) and Yanphos (**L14**) ligands, the main contribution to the selectivity was assigned to the naphthyl groups, while for CHIRAPHITE (**L8**) and diazaphospholane (**L21**) ligands, the *tert*-butyl and chiral amine groups were highlighted for the enantios induction. Significantly, the effective location of these groups to interact with the substrate is acquired through the coordination of phosphane moieties in the apical site of the complex.

1.3.1.2. Rh-catalyzed asymmetric hydroformylation of 1,1'-disubstituted alkenes

In 2011, Buchwald *et al*. reported the first AHF of various α-alkyl acrylates using a Rh-catalyst (Scheme 23).[82] Short reaction times and 10 bar of pressure were necessary for the transformation of the substrates, although the temperature required was 100 °C. The authors described that the P-stereogenic diphosphine (*R*,*R*)-BenzP* (**L22**) ligand provided 82% ee in the AHF of ethyl 2-benzylacrylate. Unprecedented enantioselectivities (81-94% ee) were obtained towards a selection of chiral linear aldehydes (Scheme 23). Moreover, the authors found the optimal CO/H_2 ratio of 1:5 to achieve good chemo- and regioselectivities and avoid side reactions. Alkenes bearing secondary alkyl substituents, such as isopropyl,

cyclohexyl, and cyclopentyl groups gave the highest yields and enantioselectivities (84-91% yield and 92-94% ee). The higher yields could be explained by the presence of those bulkier secondary alkyl groups that avoid the formation of the branched Rh-alkyl intermediate, leading to a better regioselectivity towards the chiral linear aldehydes.

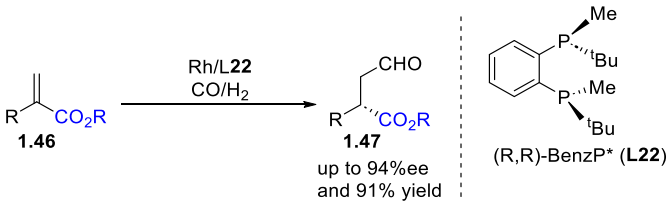

Scheme 23. Rh-catalyzed asymmetric hydroformylation of α-alkylacrylates with the (*R*,*R*)-BenzP* P-chirogenic phosphine ligand (L22).

The reaction of α-substituted acrylates was also achieved by Chin et al. in 2019 using the pyrrolylphosphinite ligand **L23**. A range of chiral aldehydes was obtained in good-to-high enantioselectivities (73%-86% ee) (Scheme 24) and good yields (up to 87%).[83]

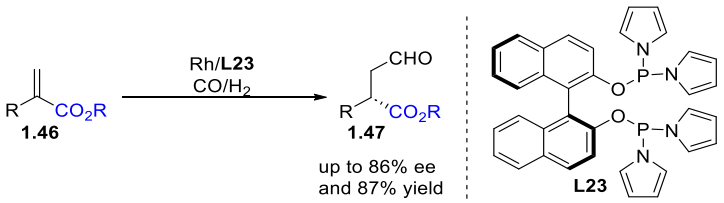

Scheme 24. Rh-catalyzed asymmetric hydroformylation of α-alkylacrylates with pyrrolylphosphinite ligand L23.

Zhang and co-workers made the most recent contribution to the AHF of α-substituted acrylates with a phosphine-phosphoroamidite ligand from the (*S*,*S*)-Yanphos family.[84] This ligand family was previously successfully applied in the AHF of 1,1'-disubstituted alkenes with weakly coordinating groups[85] and without coordinative groups[86] providing high activities and selectivities. They reported that the (*S*,*S*)-DTBM-Yanphos ligand (**L24**) provided the best catalytic performance for AHF of ethyl 2-benzylacrylate. With this ligand, a range of chiral linear aldehydes (Scheme 25) could be obtained with high enantioselectivities (88-96% ee) and high yields (up to 94%). A gram-scale AHF of α-methyl methacrylate could be performed

without compromising the yield and enantioselectivity while using a catalyst loading of 0.05 mol%.

The same catalytic system was reported for the AHF of allylic alcohols.[85] A broad range of these substrates were transformed with enantioselectivities ranging from 85 to 93% ee, independently of the nature of the aryl moiety. The afforded chiral linear aldehydes were then oxidized to the corresponding lactones. The AHF of allylic amines revealed more difficult since the corresponding lactams were obtained in lower yields and enantioselectivities (up to 69% yield and 80-86% ee, Scheme 25).

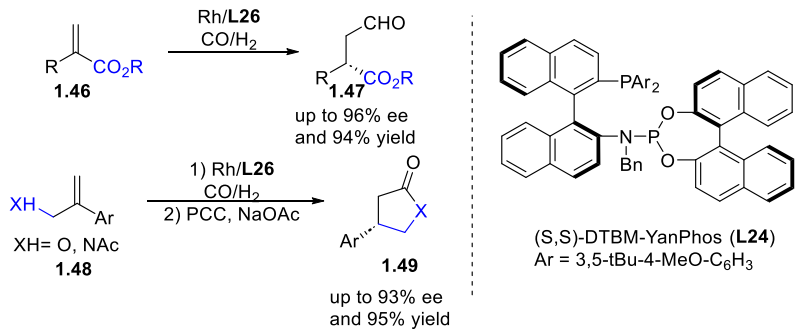

Scheme 25. Rh-catalyzed asymmetric hydroformylation of α-substituted acrylates and allylic alcohols and amines with (S,S)-DTBM-Yanphos (L24).

Only two publications reporting the AHF of α-substituted acrylamides appeared in 2020.[84,87] Godard et al. reported the first use of 1,3-phosphite-phosphoramidite ligands based on a sugar backbone derived from D-xylose in AHF of α-substituted acrylamides (**L25**, Scheme 26). The best catalytic performance was obtained with ligands bearing a bulky group on the nitrogen atom (R= Cy and R= (*S*)-CHMePh) and a (*Sax*,*Sax*)-biaryl moiety (Scheme 26). A broad range of acrylamides, with different substituents on the α-position and the amide group, were hydroformylated with high-to-excellent enantioselectivities (74-99% ee) and good-to-high yields (50-87%).[87] Furthermore, the reactions could be performed at only 60 °C. The catalytic system Rh/(*Sax*,*Sax*)-**L25** (R= Cy) was the most active for most of the substrates. When more sterically hindered alkenes ($R^2 = NEt_2$, $R^1 = {}^iPr$, cC_5H_9, Ph) were used, the ligand containing (*S*)-σ-methylbenzyl amine substituent provided the best results. Importantly, this catalytic system could efficiently transform substrates bearing a

phenyl substituent in α-position (R^1 = Ph, R^2 = NEt_2, azepane), which is present in several biologically active molecules whereas the catalysts previously reported[82, 84, 100] were only efficient for α-alkyl substituted substrates.

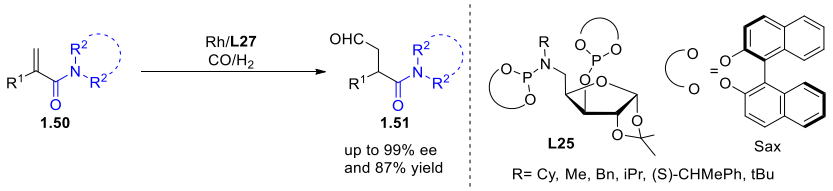

Scheme 26. Rh-catalyzed asymmetric hydroformylation of α-substituted acrylamides with sugar-based phosphite-phosphoramidite ligands L25.

The use of a Rh/(*S*,*S*)-Ph-BPE (**L19**) catalyst allowed the synthesis of a series of β[3]-aminoaldehydes via AHF of allyl phtalimides with enantioselectivities up to 95% ee (Scheme 27).[88] The system was sensitive to the length of the substrate's alkyl chain. Indeed, high enantioselectivities and chemoselectivities were only achieved with some substrates (Scheme 27). They showed the usefulness of this reaction to obtain chiral β[3]-amino acids and alcohols through oxidation or reduction of the N-phthalimide-protected aldehydes.

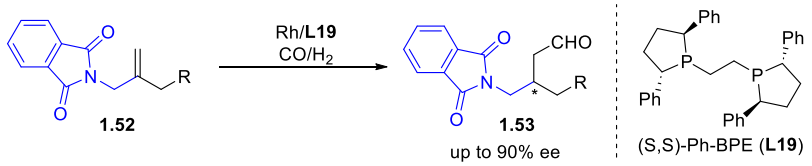

Scheme 27. Asymmetric hydroformylation of allyl phthalimides catalyzed by Rh/(S,S)-Ph-BPE (L19).

The first efficient catalyst providing the branched aldehyde as the major product was reported by Buchwald *et al.* on the AHF of 3,3,3-trifluoroprop-1-en-2-yl acetate.[89] With the (*R*,*R*)-QuinoxP* (**L26**) and (*R*,*R*,*S*,*S*)-Duanphos (**L27**) ligands, the chiral branched aldehyde was obtained with an enantioselectivity as high as 91% and 92% ee, respectively (Scheme 28). The origin of this unusual regioselectivity was suggested to come from the presence of the strongly electron-withdrawing trifluoromethyl group that favors the branched intermediate. The unexpected regioselectivity observed in the AHF of 3,3,3-trifluoroprop-1-en-2-yl acetate

permitted the one-pot preparation of the 2-trifluoromethyllactic acid (TFMLA), an important building block bearing a quaternary stereocenter in numerous active pharmaceutical compounds, with outstanding enantioselectivity (Scheme 28). Later, Zhang's group reported the AHF of the same substrate, using another P-stereogenic diphosphine ligand, the (*R*)-BIBOP **L18**,[90] however, a lower enantioselectivity (80% ee) was reached than those obtained with QuinoxP* or DuanPhos (Scheme 28).

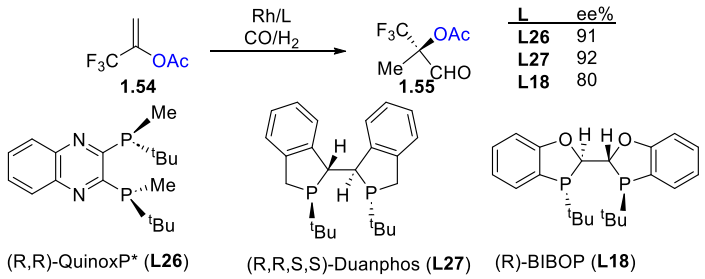

Scheme 28. Reported examples for the Rh-catalyzed asymmetric hydroformylation of 3,3,3-trifluoroprop-1-en-2-yl acetate.

In 2018, Landis et al. reported another branched selectivity on a broader scope of substrates using (*S*,*S*,*S*)-BisDiazaphos (**L21**) or (*S*,*S*)-Ph-BPE (**L19**) ligands under mild conditions (10 bar, 60 °C and 2-72 h).[91] In particular, high *i*-selectivities were reached with 1,1'-disubstituted alkenes containing electron-withdrawing groups, such as a fluorine, a trifluoromethyl or an acetate (Scheme 29). Interestingly, some acrylates without electron withdrawing groups also provided high *i*-selectivities (e.g. with Me or OMe).

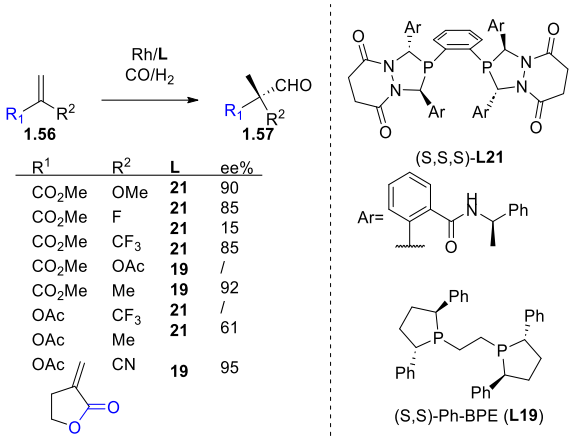

R^1	R^2	L	ee%
CO_2Me	OMe	**21**	90
CO_2Me	F	**21**	85
CO_2Me	CF_3	**21**	15
CO_2Me	OAc	**21**	85
CO_2Me	Me	**19**	/
OAc	CF_3	**19**	92
OAc	Me	**21**	/
OAc	CN	**21**	61
		19	95

Scheme 29. Selected results for the Rh-catalyzed asymmetric hydroformylation of acrylates and acetatates 1,1'-disubstituted alkenes with (S,S,S)-BisDiazaphos (L21) or (S,S)-Ph-BPE (L19).

In recent years, progress was made in the AHF of 1,1'-disubstituted alkenes containing functional groups that might coordinate to the metal center, with high levels of asymmetric induction. High enantioselectivity is even more challenging using unfunctionalized 1,1'-disubstituted alkenes and only very recently, the first examples of catalysts providing high selectivity for these substrates were reported.

Zhang et al. developed an improved AHF of 1,1'-dialkyl substrates via the introduction of a steric disulfonyl auxiliary, using the Rh/(*S*,*S*)-DTB-Yanphos (**L28**) catalytic system.[92] The incorporation of the disulfonyl moiety increased the yield of the reaction and considerably enhanced the enantioselectivity (Scheme 30(a) vs (b)). This methodology was applied over 20 substrates resulting in up to 97% yield and >99% ee.

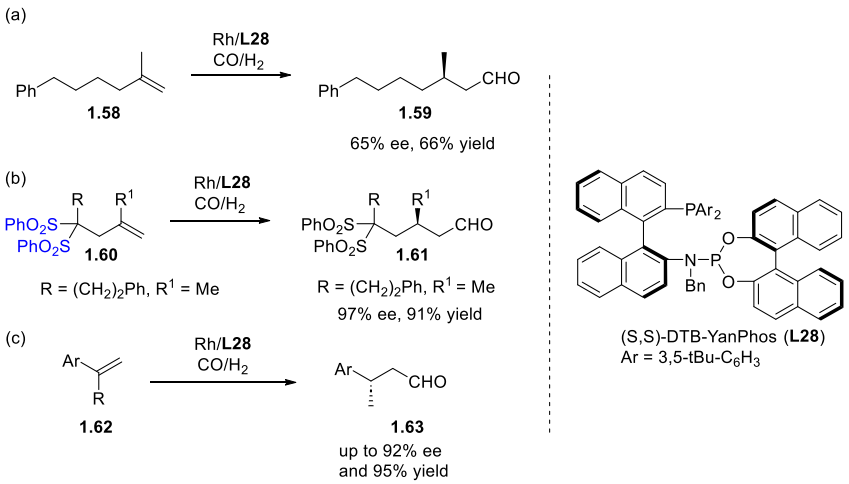

Scheme 30. Efficient Rh-catalyzed asymmetric hydroformylation of 1,1'-dialkylsubstituted alkenes via steric auxiliary help (a,b) and 1-aryl-1-alkyl disubstituted alkenes (c) with (*S*,*S*)-DTB-Yanphos (L28).

The same catalytic system was used for the AHF of α-methylstyrene producing the challenging aldehyde in 87% ee (Scheme 30).[86] The authors tested a series of Yanphos ligands and described that the key to reach high conversion and enantioselectivity was to use an (*S*,*S*)-configured-binol group on the phosphite moiety together with a hindered aryl group on the phosphine. Indeed, when using (*S*,*R*)-ligands, conversion and enantioselectivity drastically reduced.

Although the asymmetric HAM constitutes an interesting strategy to obtain chiral amines, scarce results were reported to date. They are described in the following section.

1.3.2. Asymmetric hydroaminomethylation

Although the asymmetric HAM constitutes an interesting strategy to obtain chiral amines, scarce results were reported to date. They are described in the following section.

1.3.2.1 Asymmetric HAM of monosubstituted alkenes

A thorough study was performed by Kalck and co-workers on the asymmetric hydroaminomethylation of styrene with piperidine, using a variety of chiral

diphosphine ligands which had been previously reported as very efficient in both asymmetric hydroformylation and hydrogenation reactions (Scheme 31).[93] The study also included ^{1}H and ^{31}P NMR investigations as well as DFT calculations.

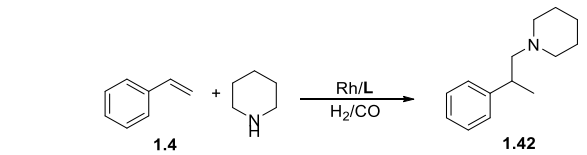

L	Conv. (%)	aldehyde (%)	enamine (%)	amine % (iso/n)	ee (%)
L29	65	4	85	5 (41:59)	0
L17	>99	8	40	48 (64:36)	0
L19	91	8	14	74 (75:25)	0
L30	>99	10	47	42 (48:52)	0

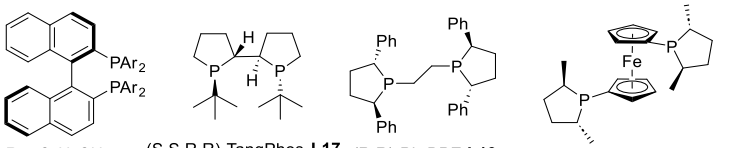

Scheme 31. Rh-catalyzed hydroaminomethylation of styrene using chiral diphosphine ligands.

It was observed that the hydroformylation and the condensation proceeded rapidly, whilst the hydrogenation step was rate determining. In this reaction, the enantioselectivity should be induced in the hydrogenation step, since the chiral information obtained in the hydroformylation step is lost after condensation of the amine with the chiral aldehyde to form the corresponding enamine.

High to full conversions were obtained, and good chemo- and regioselectivity towards the branched intermediates were also attained, even if only diphospholane ligand **L17** provided the amine with high selectivity (Scheme 31). However, in all cases, no enantiomeric excess was obtained.

As detected by NMR spectroscopy, upon condensation of the amine, both (*E*)- and (*Z*)-enamines are produced. This is a crucial fact as the asymmetric hydrogenation of these enamines will lead to the opposite enantiomers, namely the (*S*) or (*R*)-products, respectively. DFT calculations established that the hydrogenation of both enamines is very close in energy (Scheme 32), therefore supporting why no enantiomeric excess could be obtained.

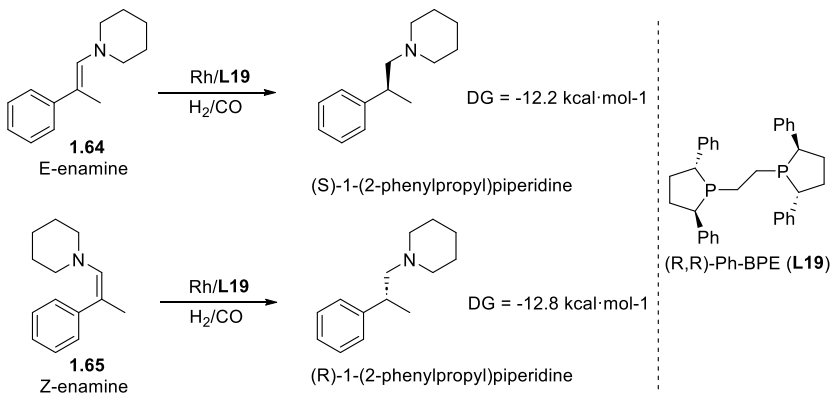

Scheme 32. Energy values for the hydrogenation of E- and Z-enamines

Several groups attempted to overcome this issue using alternative approaches. List and co-workers reported the catalytic asymmetric amination of aldehydes via dynamic kinetic resolution.[94] This strategy takes advantage of the imine-enamine equilibrium, through the use of a chiral phosphoric acid that promotes the formation of the iminium corresponding to an enantiomer reduced later with a Hantzsch ester (HEH) to give the desired chiral amine (Scheme 33).

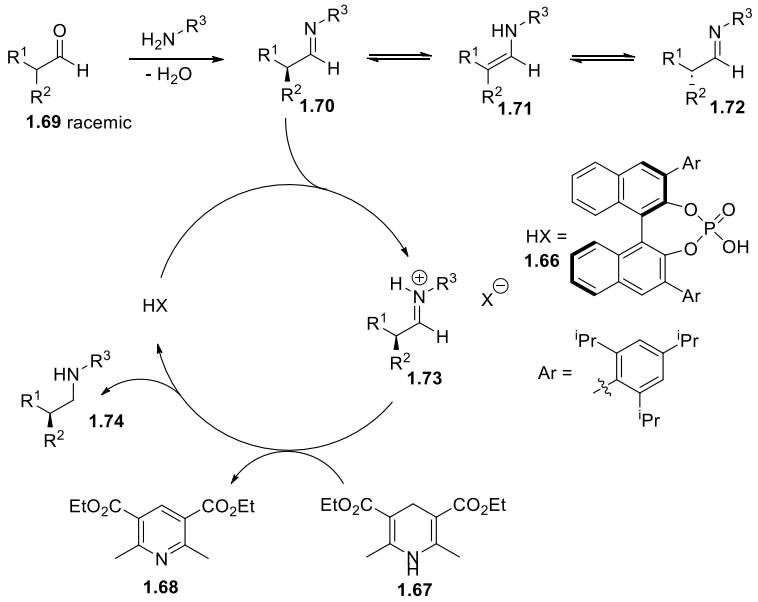

Scheme 33. Dynamic kinetic reductive amination of aldehydes developed by List et al.[94]

Xiao and co-workers adapted this methodology to the rhodium-catalyzed HAM to convert styrene and its derivatives into β-chiral amines with significant

enantioselectivity combining metal- and organocatalysts.[95] Indeed, the reaction was operated with the [Rh(acac)$(CO)_2$]/**L31** catalytic system under 11 bar CO/H_2 pressure, in the presence of the Hantzsch ester **1.67** as a hydride source, and the chiral TRIP phosphoric acid **1.66** for the asymmetric induction during the hydrogenation of the imine intermediate. The reaction proceeded slowly during 3 days with good to excellent isolated yields and enantioselectivities ranging from 79 to 91%.

Styrene derivatives were first converted into the corresponding branched aldehyde via rhodium-catalyzed hydroformylation using the ligand **L31**. Subsequently, the condensation took place in the presence of aniline and derivatives to give the corresponding imines, which were reduced via the same strategy depicted in Scheme 33 to produce the final amines in moderate to good yields and moderate to excellent enantioselectivities (Scheme 34). This system required stoichiometric amounts of Et-HEH, the use of a chiral phosphoric acid in catalytic amounts, long reaction times (up to 72h). Moreover, the system was limited to aniline derivatives.

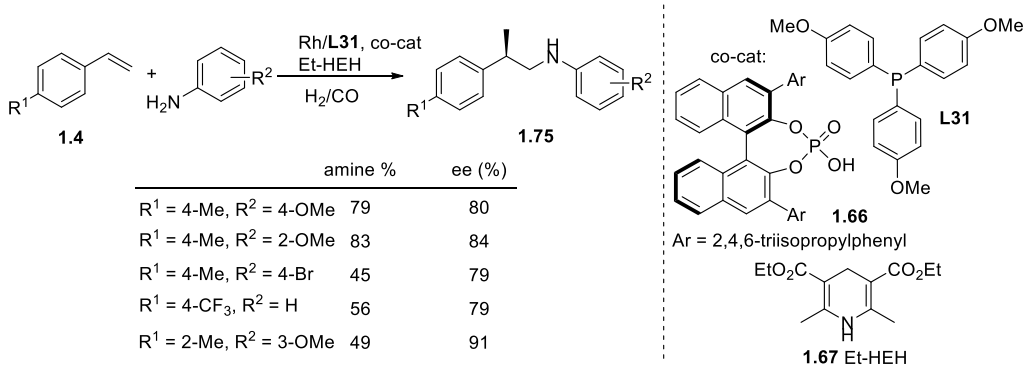

Scheme 34. Rh- and organocatalyzed asymmetric hydroaminomethylation of styrene and aniline derivatives.

Han et al. improved the system involving another bulky phosphoric acid, (*R,R*)-Ph-BPE (**L19**) ligand in the hydroformylation, and tBu-HEH **1.67b** as the reducing agent (Scheme 35).[96] These variations allowed reduction of the total pressure to 1 bar, and the lower temperatures, while providing chiral amines in higher yields (up to >99%) and enantioselectivities (up to >99.5:0.5 er). Moreover, the scope of styrene

derivatives was expanded to other aromatic cycles such as thiophene, naphthalene and non-aromatic alkenes such as acrylamides and acrylates. However, the reaction required long reaction times (up to 72 h) and additional stoichiometric reagents.

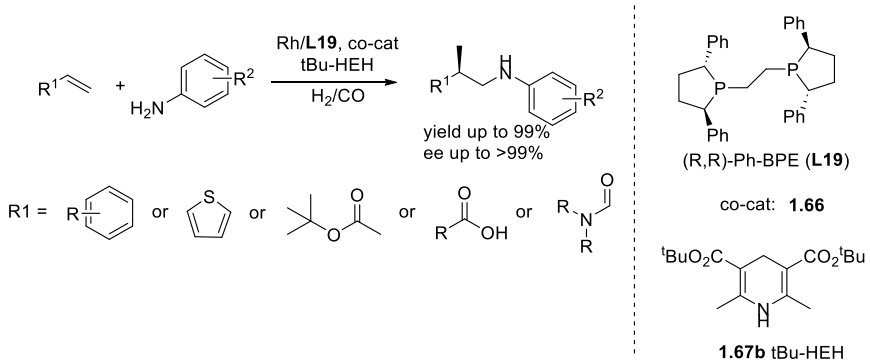

Scheme 35. Asymmetric HAM of various alkenes with anilines catalyzed by rhodium and organo-catalysts.

1.3.2.2. Asymmetric HAM of 1,2-disubstituted alkenes

Zhang et. al. adopted a different strategy to transform *trans*-1,2-disubstituted olefins. They reported an intramolecular HAM reaction following an approach called interrupted hydroaminomethylation (Scheme 36).[97] In order to circumvent the problem of the equilibrium between imines and enamines (Scheme 32), the formation of these species was interrupted by the use of external oxidants or reducing agents. The following strategy for conducting the reaction was applied: first, the Rh-catalyzed asymmetric hydroformylation of 3-substituted allylamines was carried out with a catalytic system involving the (*S,R*)-Yanphos ligand (**L14**). Then, intramolecular condensation yielded a stable hemiacetal that was subsequently either oxidized by pyridinium chlorochromate (PCC), to obtain chiral pyrrolidinones, or reduced using triethylsilane and boron trifluoride diethyl etherate to access chiral pyrrolidines.

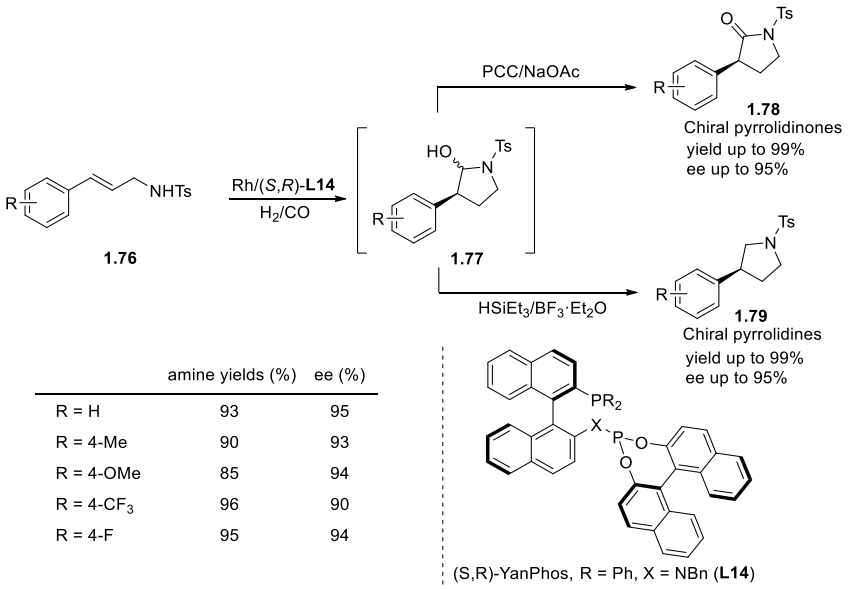

	amine yields (%)	ee (%)
R = H	93	95
R = 4-Me	90	93
R = 4-OMe	85	94
R = 4-CF_3	96	90
R = 4-F	95	94

Scheme 36. Interrupted asymmetric hydroaminomethylation of styrene derivatives using Rh/(S,R)-Yanphos catalytic system.

Both products were afforded in excellent yields and enantioselectivities up to 99% and 95%, respectively. The enantioselectivity was induced during the hydroformylation step in contrast to the classical approach where the enantioselectivity is induced in the hydrogenation step.

Interestingly, the system was also tolerant to naphthyl- and heteroaryl groups such as thiophene and furan. The corresponding products were obtained in high yields and excellent ee. However, the system suffered from drawbacks such as the requirement of additional reagents in stoichiometric amount, the restriction to tosyl group in the amine moiety and long reaction times (up to 70 h). Despite these disadvantages, the authors claimed that this reaction represents a new pathway for the synthesis of Vernakalant[98] and Enablex[99] drugs.

1.3.2.3. Asymmetric HAM of 1,1'-disubstituted alkenes

The first successful example of rhodium-catalyzed asymmetric hydroaminomethylation of α-alkyl acrylates using one single catalyst was recently reported by Godard and co-workers (Scheme 37).[100] The authors had previously

reported very interesting results on the regioselectivity of the reaction of α-substituted acrylates to access $\beta^{2,2}$-amino esters.[101] In this case, the products were not chiral, but provided $\beta^{2,2}$-amino acid derivatives containing a quaternary carbon center which are scaffolds present in various medicinal drugs.[102]

In another study, the authors focused on the $[Rh(COD)_2]BF_4$/(*R,R*)-QuinoxP* catalytic system to access chiral γ-aminobutyric esters in poor to high yields (up to 98%) and high enantioselectivities (up to 86%). A variety of acrylates were used and it was revealed that the steric hindrance in α-position was crucial to achieve high enantioselectivities. These final products were derivatives of γ-amino acids, which act as major inhibitory transmitters in the mammalian central nervous system.[103] Indeed, drugs containing γ-amino acids are currently commercialized as pharmaceutical agents.[104] In this case, (*R*,*R*)-QuinoxP* (**L26**) showed the best catalytic performance. For the first time, a single catalyst allowed the efficient and straightforward synthesis of chiral γ-aminobutyric esters from readily available acrylates. Different acrylates and amines were subjected to the HAM reaction releasing a range of synthetically valuable chiral γ-aminobutyric esters with ee's up to 86% (Scheme 37). Similarly to the Buchwald's system, the best results were achieved with substrates containing bulky secondary alkyl groups.

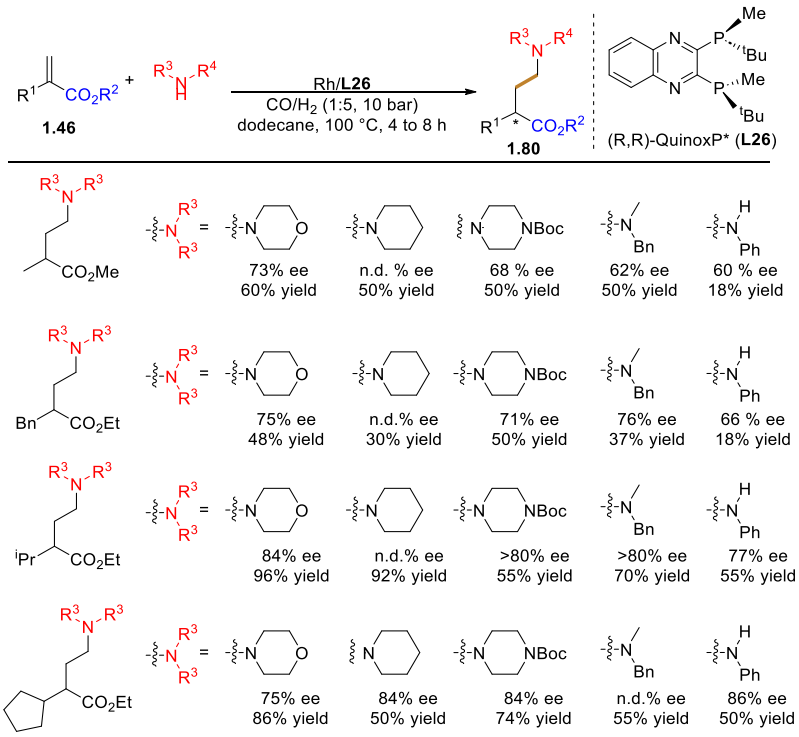

Scheme 37. Rh-catalyzed asymmetric intermolecular hydroaminomethylation of α-alkyl acrylates with (R,R)-QuinoxP* (L26).

In this amine synthesis strategy, as previously pointed out, the isomerization issue in the hydrogenation step was avoided since the chiral position was generated during the hydroformylation and not affected in the subsequent condensation and hydrogenation steps. The challenges in this approach relied on the use of the appropriate ligand to induce high enantioselectivity in the hydroformylation step. Mechanistic studies were conducted by HP-NMR experiments and revealed that the co-existence of a neutral rhodium hydride involved in the hydroformylation, and a cationic species involved in the hydrogenation is crucial (Scheme 38), in agreement with the results described previously.[36] It was also evidenced that a mixture of toluene/DCE was necessary to achieve the coexistence of both species.

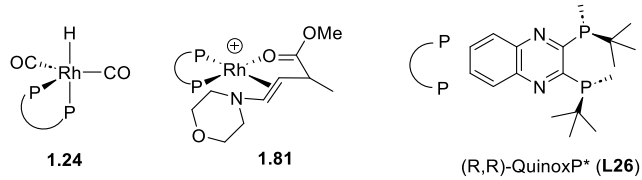

Scheme 38. Neutral and cationic rhodium species detected in the Rh-catalyzed asymmetric hydroaminomethylation of α-alkyl acrylates.

This new direct atom-efficient pathway was used by the same group for the synthesis of amide GABA derivatives from α-substituted acrylamides.[87] Indeed, these molecules are of great interest as this backbone is present in CCR2 antagonists for chronic inflammatory processes such as atherosclerosis, multiple sclerosis, and rheumatoid arthritis[105] and CCR5 antagonists for HIV drug,[106] or brain imaging.[107]

Following their results on the asymmetric hydroaminomethylation of α-acrylates, Godard and his group studied the asymmetric HAM of different α-substituted acrylamides using a series of amines with the [Rh(acac)(CO)$_2$]/(S_{ax},S_{ax})-**L25** (R= Cy) catalytic system. The latter turned out to be active to directly yield chiral γ-aminobutyric acid (GABA) derivatives, with good to high yields (59-70%) and high enantioselectivities (70-86%) (Scheme 39).

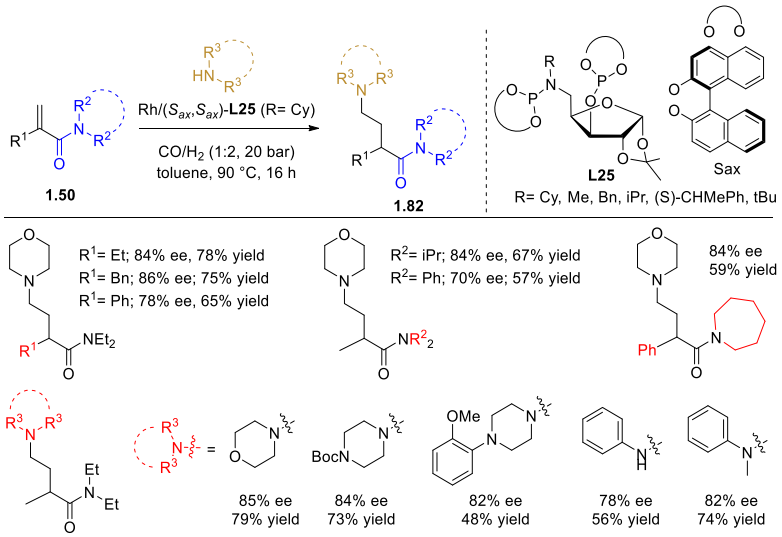

Scheme 39. Rh-catalyzed asymmetric hydroaminomethylation of α-substituted acrylamides with various amines

The synthetic potential of this method was demonstrated by the single-step synthesis of the brain imaging molecule RWAY (**83**, Scheme 40). The compound was obtained in 64% isolated yield and 82% ee by slightly varying the previously optimized conditions by using the mixture 2-Me-THF/toluene instead of DCE/toluene.

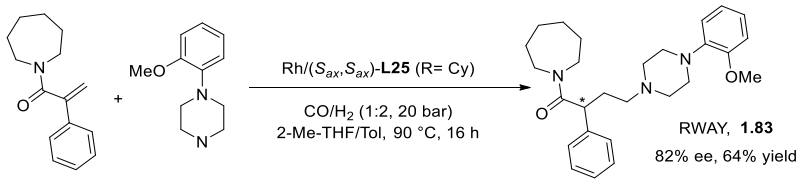

Scheme 40. Synthesis of RWAY via HAM reaction catalyzed by Rh/(S_{ax},S_{ax})-L25 (R= Cy).

1.4. Conclusions

As chiral amines represent important building blocks in the pharmaceutical and agrochemical industry, the HAM reaction appears as a powerful tool to obtain these products from readily available reagents. Rhodium is currently the metal of choice for catalyzing this reaction and it is necessary to adjust its coordination sphere in order to achieve high chemo-, regio- and enantioselectivities. The elucidation of the different steps of the catalytic cycle and the characterization of the resting state, together with the discovery of several types of ligands that are able to provide high enantioselectivities, have made the rhodium-catalyzed hydroformylation a synthetically useful tool. This process was widely studied mainly for monosubstituted alkenes. However, since the favored process is usually the introduction of this group in the less substituted carbon, this transformation is only useful for substrates containing electron-withdrawing group(s) (R= Ph, heteroatom) which direct the introduction of the formyl group on the most substituted carbon. Consequently, a regioselectivity problem must first be considered. The presence of a functional group at the allylic position, which contributes to stabilizing the double bond, always introduces an additional issue, since isomerization easily takes place. This isomerization can be controlled by the appropriate choice of ligand and reaction

conditions. For instance, increasing the CO pressure and/or decreasing the reaction temperature reduce the degree of isomerization.

The general trend is the introduction of the formyl group onto the less substituted carbon, thus creating the chiral center at the more substituted carbon atom Interestingly, it is also possible to introduce the formyl group at the more substituted carbon using Rh catalysts, creating a highly functionalized chiral quaternary center.

For years, ligands containing phosphite moieties such as diphosphites and phosphine-phosphites were considered as the most successful ligands to achieve high enantioselectivies. For instance, the phosphite-phosphine Binaphos or its derivatives like Yanphos were very successful ligands in terms of selectivity and scope. Recently, however, diphosphines in which the P atoms are incorporated in a ring have also shown to induce high levels of enantioselectivity in this process. Furthermore, diazaphospholane ligands are currently the most efficient ligands in the asymmetric hydroformylation of alkenes, with exceptional results in terms of regio- and enantioselectivity.

It can consequently be concluded that the key to achieve high enantioselectivities is not the type of phosphorus function involved in the coordination to the metal, but the particular spatial arrangement of the coordinated ligand. Furthermore, recently, supramolecular strategies were very successful in asymmetric hydroformylation, clearly indicating that the control of the second coordination sphere could be key to reach selectivity for challenging substrates.[108]

Since aldehydes are not usually isolated as final products because the real products of interest are generally derived products, tandem processes with hydroformylation as the initial step constitute an interesting strategy. The combination of CO/H_2 (syngas), alkene and amine, and a rhodium catalyst enables the rapid assembly of complex amine products with perfect atom economy and little environmental impact. The first successful direct Rh-catalyzed intermolecular asymmetric hydroaminomethylation of acrylates for the efficient synthesis of chiral γ-aminobutyric esters was reported. A wide variety of chiral γ-aminobutyric esters

were obtained in poor to excellent yields but high enantioselectivities. In contrast to previous reports, neither an external reducing agent nor a co-catalyst was required. The reaction was successfully extended to the transformation of α-substituted acrylamides using chiral phosphite-phosphoramidite ligands with high yields and high to excellent enantioselectivities. The system could tolerate different substituents at the acrylamide and various secondary amines and aniline could be applied.

The potential of asymmetric hydroaminomethylation proves its utility for the production of chiral amines, to attain pharmaceutical and agrochemical active products, such as vitamins, hormones, alkaloids, and neurotransmitters.

In this thesis, our strategies into the asymmetric hydroaminomethylation of alkenes to form chiral amines will be presented.

1.5. References

[1] Beller, M. *Catatlytic Carbonylation Reactions*, Beller, M., Springer-Verlag Berlin Heidelberg, Berlin, Germany, **2006**.

[2] [a)] Haynes, A. *Chapter 1 - Catalytic Methanol Carbonylation* in *Advances in Catalysis*, Gates, B. C.; Knözinger, H., Academic Press*, Vol. 53*, Amsterdam, The Netherlands, **2010**, pp. 1-45. [b)] Haynes, A.; Maitlis, P. M.; Morris, G. E.; Sunley, G. J.; Adams, H.; Badger, P. W.; Bowers, C. M.; Cook, D. B.; Elliott, P. I. P.; Ghaffar, T.; Green, H.; Griffin, T. R.; Payne, M.; Pearson, J. M.; Taylor, M. J.; Vickers, P. W.; Watt, R. J. Promotion of iridium-catalyzed methanol carbonylation: Mechanistic studies of the cativa process. *J. Am. Chem. Soc.* **2004**, *126*, 2847-2861.

[3] [a)] Cornils, B.; Herrmann, W. A. *Applied Homogeneous Catalysis with Organometallic Compounds, Vol. 1*, Cornils, B.; Herrmann, W. A., Wiley-VCH, Weinheim, Germany, **2002**. [b)] Weissermel, K.; Arpe, H.-J. *Industrial Organic Chemistry*, Weissermel, K.; Arpe, H.-J., Wiley-VCH, Weinheim, Germany, **2008**.

[4] [a)] Gehrtz, P. H.; Hirschbeck, V.; Ciszek, B.; Fleischer, I. Carbonylations of alkenes in the total synthesis of natural compounds. *Synthesis* **2016**, *48*, 1573-1596. [b)] Wu, X.-F.; Fang, X.; Wu, L.; Jackstell, R.; Neumann, H.; Beller, M. Transition-metal-catalyzed carbonylation reactions of olefins and alkynes: a personal account. *Acc. Chem. Res.* **2014**, *47*, 1041-1053.

[5] Claver C. Ed., "Rhodium Catalysis" *Top. Organomet. Chem*. Springer-Verlag, **2018**.

[6] Li, X.; Li, X.; Jiao, N. Rh-Catalyzed Construction of Quinolin-2(1H)-ones via C–H Bond Activation of Simple Anilines with CO and Alkynes. *J. Am. Chem. Soc.* **2015**, *137*, 9246-9249.

[7] Breit, B. Aldehydes: synthesis by hydroformylation of alkenes in Science of synthesis, Thieme, Vol. 25, Stuttgard, Germany, **2007**. Franke R., Selent D., Börner A., Applied Hydroformylation. *Chem. Rev*. **2012**, *112*, 5675-5732

[8] [a)] Trost, B. M. The atom economy—a search for synthetic efficiency. *Science* **1991**, *254*, 1471-1477. [b)] Breit, B. Synthetic aspects of stereoselective hydroformylation. *Acc. Chem. Res.* **2003**, *36*, 264-275.

[9] [a)] Fogg, D. E.; dos Santos, E. N. Tandem catalysis: a taxonomy and illustrative review. *Coord. Chem. Rev.* **2004**, *248*, 2365-2379. [b)] Wasilke, J.-C.; Obrey, S. J.; Baker, R. T.; Bazan, G. C. Concurrent tandem catalysis. *Chem. Rev.* **2005**, *105*, 1001-1020.

[10] Eilbracht, P.; Bärfacker, L.; Buss, C.; Hollmann, C.; Kitsos-Rzychon, B. E.; Kranemann, C. L.; Rische, T.; Roggenbuck, R.; Schmidt, A. Tandem Reaction Sequences under Hydroformylation Conditions: New Synthetic Applications of Transition Metal Catalysis. *Chem. Rev.* **1999**, *99*, 3329-3366.

[11] [a)] Chercheja, S.; Nadakudity, S. K.; Eilbracht, P. Combination of Enantioselective Metal Catalysis and Organocatalysis: Enantioselective Sequential Hydroformylation/Aldol Reactions. *Adv. Synth. Catal.*

2010, *352*, 637-643. [b)] Abillard, O.; Breit, B. Domino Hydroformylation/Enantioselective Cross-Aldol Addition. *Adv. Synth. Catal.* **2007**, *349*, 1891-1895.

[12] [a)] Breit, B.; Zahn, S. K. Domino hydroformylation-Wittig reactions. *Angew. Chem. Int. Ed.* **1999**, *38*, 969-971. [b)] Wong, G. W.; Landis, C. R. Iterative asymmetric hydroformylation/Wittig olefination sequence. *Angew. Chem. Int. Ed.* **2013**, *52*, 1564-1567.

[13] Diebolt, O.; Cruzeuil, C.; Müller, C.; Vogt, D. Formation of Acetals under Rhodium-Catalyzed Hydroformylation Conditions in Alcohols. *Adv. Synth. Catal.* **2012**, *354*, 670-677.

[14] [a)] Ahmed, M.; Bronger, R. P. J.; Jackstell, R.; Kamer, P. C. J.; van Leeuwen, P. W. N. M.; Beller, M. Highly selective hydroaminomethylation of internal alkenes to give linear amines. *Chem. Eur. J.* **2006**, *12*, 8979-8988. [b)] Moballigh, A.; Majeed, S. A.; Ralf, J.; Matthias, B. Highly Selective Synthesis of Enamines from Olefins. *Angew. Chem. Int. Ed.* **2003**, *42*, 5615-5619.

[15] Blunt, J. W.; Copp, B. R.; Keyzers, R. A.; Munro, M. H. G.; Prinsep, M. R. Marine natural products. *Natural Product Reports* **2012**, *29*, 144-222.

[16] Ghislieri, D.; Turner, N. J. Biocatalytic Approaches to the Synthesis of Enantiomerically Pure Chiral Amines. *Top. Catal.* **2014**, *57* (5), 284–300.

[17] Nugent, T. C., Chiral amines synthesis: methods, developments and applications. Wiley-VCH Weinheim, T.C. Nugent Ed. **2010,** Wiley-VCH Verlag GmbH & Co. KGaA, Weinheim.

[18] Cunillera A., Godard C., C. Claver C., Urrutigoïty M., Kalck Ph., Transition metal catalyzed chiral amines synthesis. *Methodologies in amine synthesis: challenges and applications*, Eds A. Ricci, L. Bernardi, Wiley-VCH ISBN: 978-3-527-34739-1, **2021**, p. 155-186

[19] Raoufmoghaddam, S., Recent advances in catalytic C–N bond formation: a comparison of cascade hydroaminomethylation and reductive amination reactions with the corresponding hydroaminomethylation and reductive amination reactions. *Org. Biomol. Chem.* **2014**, *12,* 7179-7193.

[20] Chen, C.; Dong, X. Q.; Zhang, X. recent progress in rhodium-catalyzed hydroaminomethylation. *Org*. *Chem*. *Front*. **2016**, *3*, 1359-1370.

[21] Kalck, P.; Urrutigoïty, M. Tandem Hydroaminomethylation Reaction to Synthesize Amines from Alkenes. *Chem. Rev.* **2018**, *118* (7), 3833–3861.

[22] a) Roelen, O.; Chem. Abstr. 1994, 38, 550; b) (Chemische Verwertungsgesellschaft, mBH Oberhausen), DE Patent 849-584, 1938/1952; c) US Patent 2, 317, 066, **1943**.

[23] a) Klosin, J.; Landis, C.R. Ligands for practical rhodium-catalyzed asymmetric hydroformylation. *Acc. Chem. Res*. **2007**, *40*, 1251-1259; b) Breit, B. Recent advances in alkene hydroformylation. *Top. Curr. Chem.* **2007**, *279*, 139-172; c) Ungvári, F. Application of transition metals in hydroformylation: Annual survey covering the year 2006. *Coord. Chem. Rev*. **2007**, *251*, 2087-2102; d) Ungvári, F. Application of

transition metals in hydroformylation: Annual survey covering the year 2005. *Coord. Chem. Rev*. **2007**, *251*, 2072-2086; e) Wiese, K.D.; Obst, D. Hydroformylation. *Top. Organomet. Chem*. **2006**, *18*, 1-33; f) Gual, A.; Godard, C.; Castillón, S.; Claver, C. Highlights of the Rh-catalyzed asymmetric hydroformylation of alkenes using phosphorus donor ligands. *Tetrahedron: Asymmetry* **2010**, *21*, 1135-1146; g) van Leeuwen, P. W. N. M.; Kamer, P. C. J.; Claver, C.; Pàmies, O.; Diéguez, M. Phosphite-containing ligands for asymmetric catalysis. *Chem. Rev.* **2011**, *111*, 2077-2118; h) Börner, A.; Franke R. *Hydroformylation: Fundamentals, Processes, and Applications in Organic Synthesis*, Wiley-VCH, **2016**; i) Taddei, M., Mann, A. (Eds.) *Hydroformylation for Organic Synthesis*, Springer, **2013**.

[24] a) Evans, D.A.; Osborn, J.A.; Wilkinson, G. Hydroformylation of alkenes by use of rhodium complex catalysts; *J. Chem. Soc. A* **1968**, 3133-3142; b) Evans, D.; Yagupsky, G.; Wilkinson, G. The reaction of hydridocarbonyltris(triphenylphosphine)rhodium with carbon monoxide, and of the reaction products, hydridodicarbonylbis(triphenylphosphine)rhodium and dimeric species, with hydrogen. *J. Chem. Soc. A*. **1968**, 2660-2665; c) Young, J.F.; Osborn, J.A.; Jardine, F.H.; Wilkinson, G. Hydride intermediates in homogeneous hydrogenation reactions of olefins and acetylenes using rhodium catalysts. *J. Chem. Soc. Chem. Comm.* **1965**, 131-132.

[25] van Leeuwen, P.W.N.M.; Claver, C. in Rhodium catalyzed hydroformylation, Kluwer, Dordrecht, 2000 and references therein.

[26] a) Jongsma, T.; Challa, G.; van Leeuwen, P.W.N.M. A mechanistic study of rhodium tri(o-t-butylphenyl)phosphite complexes as hydroformylation catalysts. *J. Organomet. Chem*. **1991**, *421*, 121-128; b) Selent, D.; Wiese, K.D.; Röttger, A. Börner, Novel Oxyfunctionalized Phosphonite Ligands for the Hydroformylation of Isomeric n-Olefins. *Angew. Chem. Int. Ed*. **2000**, *39*, 1639-1641; c) Breit, B.; Winde, R.; Mackewitz, T.; Paciello, R.; Harms, K. Phosphabenzenes as Monodentate π-Acceptor Ligands for Rhodium-Catalyzed Hydroformylation. *Chem. Eur. J*. **2001**, *7*, 3106-3121.

[27] a) Lazzaroni, R.; Settambolo, R.; Alagona, G.; Ghio, C. Investigation of alkyl metal intermediate formation in the rhodium-catalyzed hydroformylation: Experimental and theoretical approaches. *Coord. Chem. Rev*. **2010**, *254*, 696-706 and references therein; b) Gleich, D.; Schmid, R.; Herrmann, W. A. A Combined QM/MM Method for the Determination of Regioselectivities in Rhodium-Catalyzed Hydroformylation. *Organometallics* **1998**, *17*, 4828−4834; c) Gleich, D.; Schmid, R.; Herrmann, W. A. A Molecular Model To Explain and Predict the Stereoselectivity in Rhodium-Catalyzed Hydroformylation. *Organometallics* **1998**, *17*, 2141−2143; d) van der Veen, L. A.; Keeven, P. H.; Schoemaker, G. C.; Reek, J. N. H.; Kamer, P. C. J.; van Leeuwen, P. W. N. M.; Lutz, M.; Spek, A. L. Origin of the Bite Angle Effect on Rhodium Diphosphine Catalyzed Hydroformylation. *Organometallics* **2000**, *19*, 872−883; e) Rocha, W. A.; De Almeida, W. B. Insertion reaction of propene into Rh-H bond in $HRh(CO)(PH_3)_2(C_3H_6)$ compound:

A density functional study. *Int. J. Quantum Chem*. **2000**, *78*, 42−51; f) Carbó, J. J.; Maseras, F.; Bo, C.; van Leeuwen, P. W. N. M. Unravelling the Origin of Regioselectivity in Rhodium Diphosphine Catalyzed Hydroformylation. A DFT QM/MM Study. *J. Am. Chem. Soc*. **2001**, *123*, 7630−7637; g) Alagona, G.; Ghio, C.; Lazzaroni, R.; Settambolo, R. Olefin Insertion into the Rhodium−Hydrogen Bond as the Step Determining the Regioselectivity of Rhodium-Catalyzed Hydroformylation of Vinyl Substrates: Comparison between Theoretical and Experimental Results. *Organometallics* **2001**, *20*, 5394−5404; h) Kumar, M.; Subramaniam, B.; Chaudhari, R. V.; Jackson, T. A. Ligand Effects on the Regioselectivity of Rhodium-Catalyzed Hydroformylation: Density Functional Calculations Illuminate the Role of Long-Range Noncovalent Interactions. *Organometallics* **2014**, *33*, 4183−4191; i) Kumar, M.; Chaudhari, R. V.; Subramaniam, B.; Jackson, T. A. Importance of Long-Range Noncovalent Interactions in the Regioselectivity of Rhodium-Xantphos-Catalyzed Hydroformylation. *Organometallics* **2015**, *34*, 1062-1073.

[28] van Leeuwen, P.W.N.M. in Homogeneous Catalysis: Understanding the Art, Kluwer, Dordrecht, **2004** and references therein.

[29] Keulemans, A.I.M.; Kwantes, A.; van Bavel, T. *Rec. Trav. Chim. Pays Bas* **1948**, *67*, 298-308.

[30] Heck, R.F. Addition reactions of transition metal compounds. *Acc. Chem. Res*. **1969**, *2*, 10-16.

[31] Kamer, P.C. J.; van Rooy, A.; Schoemaker, G.C.; van Leeuwen, P.W.N.M. In situ mechanistic studies in rhodium catalyzed hydroformylation of alkenes. *Coord. Chem. Rev*. **2004**, *248*, 2409-2424.

[32] Deutsch, P.P.; Eisenberg, R. Synthesis and reactivity of propionyliridium complexes. Competitive reductive elimination of carbon-hydrogen and hydrogen-hydrogen bonds from a propionyldihydridoiridium complex. *Organometallics*. **1990**, *9*, 709-718.

[33] Castellanos-Páez, A.; Castillón, S.; Claver, C.; van Leeuwen, P.W.N.M.; de Lange, W.G.J. Diphosphine and Dithiolate Rhodium Complexes: Characterization of the Species under Hydroformylation Conditions. *Organometallics*, **1998**, *17*, 2543-2552.

[34] Jacobs, I.; de Bruin, B.; Reek, J. N. H. Comparison of the Full Catalytic Cycle of Hydroformylation Mediated by Mono- and Bis-Ligated Triphenylphosphine–Rhodium Complexes by Using DFT Calculations *ChemCatChem* **2015**, *7*, 1708-1718.

[35] Serrano-Maldonado, A.; Dang-Bao, T.; Favier, I.; Guerrero-Ríos, I.; Pla, D.; Gómez, M. Glycerol Boosted Rh-Catalyzed Hydroaminomethylation Reaction: A Mechanistic Insight. *Chem. - A Eur. J.* **2020**, *26* (55), 12553–12559.

[36] Crozet, D.; Gual, A.; McKay, D.; Dinoi, C.; Godard, C.; Urrutigoïty, M.; Daran, J.-C.; Maron, L.; Claver, C.; Kalck, P. Interplay between Cationic and Neutral Species in the Rhodium-Catalyzed Hydroaminomethylation Reaction. *Chem. Eur. J.* **2012**, *18,* 7128-7140.

[37] Chen, G.; Xia, H.; Cai, Y.; Ma, D.; Yuan, J.; Yuan, C. Synthesis and SAR Study of Diphenylbutylpiperidines as Cell Autophagy Inducers. *Bioorganic Med. Chem. Lett.* **2011**, *21* (1), 234–239.

[38] (a) Rische, T.; Müller, K. S.; Eilbracht, P. One-Pot Synthesis of Pharmacologically Active Diamines via Rhodium- Catalyzed Carbonylative Hydroaminomethylation of Heterocyclic Allylic Amines. *Tetrahedron* **1999**, *55* (32), 9801–9816. (b) Schmidt, A.; Marchetti, M.; Eilbracht, P. Regioselective Hydroaminomethylation of 1,1-Diaryl-Allyl-Alcohols: A New Access to 4,4-Diarylbutylamines. *Tetrahedron* **2004**, *60* (50), 11487–11492.

[39] Ahmed, M.; Seayad, A. M.; Jackstell, R.; Beller, M. Amines Made Easily: A Highly Selective Hydroaminomethylation of Olefins. *J. Am. Chem. Soc.* **2003**, *125* (34), 10311–10318.

[40] Hamers, B.; Kosciusko-Morizet, E.; Müller, C.; Vogt, D. Fast and Selective Hydroaminomethylation Using Xanthene-Based Amino-Functionalized Ligands. *ChemCatChem* **2009**, *1* (1), 103–106.

[41] Seayad, J.; Tillack, A.; Hartung, C. G.; Beller, M. Base-Catalyzed Hydroamination of Olefins: An Environmentally Friendly Route to Amines. *Adv. Synth. Catal.* **2002**, *344* (8), 795–813.

[42] Routaboul, L.; Buch, C.; Klein, H.; Jackstell, R.; Beller, M. An Improved Protocol for the Selective Hydroaminomethylation of Arylethylenes. *Tetrahedron Lett.* **2005**, *46* (43), 7401–7405.

[43] Chen, C.; Dong, X. Q.; Zhang, X. Recent Progress in Rhodium-Catalyzed Hydroaminomethylation. *Org. Chem. Front.* **2016**, *3* (10), 1359–1370.

[44] Briggs, J. R.; Klosin, J.; Whiteker, G. T. Synthesis of Biologically Active Amines via Rhodium-Bisphosphite-Catalyzed Hydroaminomethylation. *Org. Lett.* **2005**, *7* (22), 4795–4798.

[45] Li, S.; Huang, K.; Zhang, J.; Wu, W.; Zhang, X. Rhodium-Catalyzed Highly Regioselective Hydroaminomethylation of Styrenes with Tetraphosphorus Ligands. *Org. Lett.* **2013**, *15* (12), 3078–3081.

[46] Yan, Y.; Zhang, X.; Zhang, X. Retaining Catalyst Performance at High Temperature: The Use of a Tetraphosphine Ligand in the Highly Regioselective Hydroformylation of Terminal Olefins. *Adv. Synth. Catal.* **2007**, *349* (10), 1582–1586.

[47] Rische, T.; Eilbracht, P. One-pot synthesis of pharmacologically active secondary and tertiary 1-(3, 3-diarylpropyl) amines via rhodium-catalyzed hydroaminomethylation of 1, 1-diarylethenes. *Tetrahedron* **1999**, *55*, 1915-1920.

[48] Ahmed, M.; Buch, C.; Routaboul, L.; Jackstell, R.; Klein, H.; Spannenberg, A.; Beller, M. Hydroaminomethylation with Novel Rhodium-Carbene Complexes: An Efficient Catalytic Approach to Pharmaceuticals. *Chem. - A Eur. J.* **2007**, *13* (5), 1594–1601.

[49] Li, S.; Huang, K.; Zhang, J.; Wu, W.; Zhang, X. Cascade Synthesis of Fenpiprane and Related Pharmaceuticals via Rhodium-Catalyzed Hydroaminomethylation. *Org. Lett.* **2013**, *15* (5), 1036–1039.

[50] a) Consiglio, G.; Nefkens, S. C. A.; Borer, A. Platinum-catalyzed enantioselective hydroformylation with (R,R)-[bicyclo[2.2.2]octane-2,3-diylbis(methylene)]bis(5H-benzo[b]phosphindole) and related chiral ligands.*Organometallics* **1991**, *10*, 2046-2051. b) Stille, J. K.; Su, H.; Brechot, P.; Parrinello, G.; Hegedus, L. S. Platinum-catalyzed asymmetric hydroformylation of olefins with (-)-BPPM/$SnCl_2$-based catalyst systems. *Organometallics* **1991**, *10*, 1183-1189.

[51] a) Agbossou, F.; Carpentier, J.-F.; Mortreux, A. Asymmetric hydroformylation. *Chem. Rev.* **1995**, *95*, 2485-2506. b) Gladiali, S.; Bayón, J. C.; Claver, C. Recent advances in enantioselective hydroformylation. *Tetrahedron: Asymmetry* **1995**, *6*, 1453-1474.

[52] Masdeu-Bultó, A.M.; Orejon, A.; Castillón, S.; Claver, C. Asymmetric hydroformylation of styrene using a rhodium catalyst with BDPP as the chiral ligand. *Tetrahedron: Asymmetry* **1996**, *7*, 1829-1834.

[53] a) Babin, J.E.; Whiteker, G.T. Asymmetric Synthesis, World Patent, WO 9303839, 1993; b) Whiteker, G.T.; Briggs, J.R.; Babin, J.E.; Barne, G.A. in Asymmetric Catalysis Using Biphosphite Ligands in Chemical Industries, Marcel Dekker, New York, *vol. 89*, **2003**.

[54] Buisman, G.J.H.; van der Veen, L.A.; Kamer, P.C.J.; van Leeuwen, P.W.N.M. Fluxional Processes in Asymmetric Hydroformylation Catalysts [HRhL⌒L(CO)2] Containing C2-Symmetric Diphosphite Ligands. *Organometallics*. **1997**, *16*, 5681-5687.

[55] a) Buisman, G.J.H.; Martin, M.E.; Vos, E.J.; Klootwijk, A.; Kamer, P.C.J.; van Leeuwen, P.W.N.M. Rhodium catalyzed asymmetric hydroformylation with diphosphite ligands based on sugar backbones. *Tetrahedron: Asymmetry* **1995**, *6*, 719-738; b) Pàmies, O.; Net, G.; Ruiz, A.; Claver, C. Diphosphite ligands based on ribosa backbone as suitable ligands in the hydrogenation and hydroformylation of prochiral olefins. *Tetrahedron: Asymmetry* **2000**, *11*, 1097-1108; c) Diéguez, M.; Pàmies, O.; Ruiz, A.; Castillón, S.; Claver, C. Chiral diphosphites derived from D-glucose: New ligands for the asymmetric catalytic hydroformylation of vinyl arenes. *Chem. Eur. J.* **2001**, *7*, 3086-3094; d) Diéguez, M.; Pàmies, O.; Ruiz, A.; Claver, C. Asymmetric hydroformylation of styrene catalyzed by carbohydrate diphosphite-Rh(I) complexes. *New. J. Chem*. **2002**, *26*, 827-833.

[56] a) Cobley, C.J.; Klosin, J.; Qin, C.; Whiteker, G.T. Parallel Ligand Screening on Olefin Mixtures in Asymmetric Hydroformylation Reactions. Org. Lett. **2004**, 6, 3277-3280; b) Cobley, C.J.; Gardner, K.; Klosin, J.; Praquin, C.; Hill, C.; Whiteker, G.T.; Zanotti-Gerosa, A. Synthesis and Application of a New Bisphosphite Ligand Collection for Asymmetric Hydroformylation of Allyl Cyanide. J. Org. Chem. **2004**, 69, 4031-4040

[57] Sakai, N.; Mano, S.; Nozaki, K.; Takaya, H. Highly enantioselective hydroformylation of olefins catalyzed by new phosphine phosphite-rhodium(I) complexes. *J. Am. Chem. Soc.* **1993**, *115*, 7033-7034.

[58] a) Nozaki, K. Unsymmetric bidentate ligands in metal-catalyzed carbonylation of alkenes. *Chem. Record* **2005**, *5*, 376-384 and ref. therein; b) Tanaka, R.; Nakano, K.; Nozaki, K Synthesis of α-Heteroarylpropanoic Acid via Asymmetric Hydroformylation Catalyzed by Rh(I)-(R,S)-BINAPHOS and the Subsequent Oxidation. *J. Org. Chem*. **2007**, *72*, 8671-8676; c) Nakano, K.; Tanaka, R.; Nozaki, K. Asymmetric Hydroformylation of Vinylfurans Catalyzed by {(11bS)-4-{[(1R)-2'-Phosphino[1,1'-binaphthalen]-2-yl]oxy}dinaphtho[2,1-d:1',2'-f]- [1,3,2]dioxaphosphepin}rhodium(I) [RhI{(R,S)-Binaphos}] Derivatives. *Helv. Chim. Acta* **2006**, *89*, 1681-1686; d) Shibahara, F.; Nozaki, K.; Hiyama, T. Solvent-Free Asymmetric Olefin Hydroformylation Catalyzed by Highly Cross-Linked Polystyrene-Supported (R,S)-BINAPHOS−Rh(I) Complex. *J. Am. Chem. Soc.* **2003**, *125*, 8555-8560; e) Nozaki, K.; Matsuo, T.; Shibahara, F.; Hiyama, T. High-Pressure IR Studies on the Asymmetric Hydroformylation of Styrene Catalyzed by Rh(I)-(R,S)-BINAPHOS. *Organometallics* **2003**, *22*, 594-600; f) Shibahara, F.; Nozaki, K.; Matsuo, T.; Hiyama, T.; Asymmetric hydroformylation with highly crosslinked polystyrene-supported (R,S)-BINAPHOS–Rh(I) complexes: the effect of immobilization position. *Bioorg. Med. Chem. Lett.* **2002**, *12*, 1825–1827; g) Nozaki, K.; Matsuo, T.; Shibahara, F.; Hiyama, T. Substituent Effect in Asymmetric Hydroformylation of Olefins Catalyzed by Rhodium(I) Complexes of (R,S)-BINAPHOS Derivatives: A Protocol for Improvement of Regio- and Enantioselectivities. *Adv. Synth. Catal.* **2001**, *343*, 61-63; h) Horiuchi, T.; Ohta, T.; Shirakawa, E.; Nozaki, K.; Takaya, H. Asymmetric hydroformylation of conjugated dienes catalyzed by chiral phosphine-phosphite-Rh(I) complex. *Tetrahedron* **1997**, *53*, 7795-780; i) Nozaki, K.; Nanno, T., Takaya, H. Asymmetric hydroformylation catalyzed by an Rh(I)-(R, S)-BINAPHOS complex: substituent effects in olefins on the regioselectivity. *J. Organomet. Chem*. **1997**, *527*, 103-108; j) Nozaki, K.; Li, W.G.; Horiuchi, T.; Takaya, H. A New Stereocontrolled Approach to 1β-Methylcarbapenem: Asymmetric Hydroformylation of 4-Vinyl β-Lactams Catalyzed by Rh(I) Complexes of Chiral Phosphine−Phosphites and Phosphine−Phosphinites. *J. Org. Chem*. **1996**, *61*, 7658-7659; k) Horiuchi, T. Ohta, T.; Nozaki, K.; Takaya, H. Asymmetric hydroformylation of conjugated dienes catalyzed by [(R)-2-diphenylphosphino-1,1'-dinaphthalen-2'-yl][(S)-1,1'-dinaphthalene-2,2'-diyl]phosphite–rhodium(I). *Chem. Commun*. **1996**, 155-156; l) Nanno, T.; Sakai, N.; Nozaki, K.; Takaya, H. Asymmetric hydroformylations of sulfur-containing olefins catalyzed by BINAPHOS—Rh(I) complexes. *Tetrahedron: Asymmetry* **1995**, *6*, 2583-2591.

[59] a) Nozaki, K.; Sakai, N.; Nanno, T.; Higashijima, T.; Mano, S.; Horiuchi, T.; Takaya, H. Highly Enantioselective Hydroformylation of Olefins Catalyzed by Rhodium(I) Complexes of New Chiral Phosphine−Phosphite Ligands. *J. Am. Chem. Soc.* **1997**, *119*, 4413-4423; b) Nozaki, K.; Ito, Y.; Shibahara, F.; Shirakawa, E.; Otha, T.; Takaya, H.; Hiyama, T. Asymmetric Hydroformylation of Olefins in a Highly Cross-Linked Polymer Matrix. *J. Am. Chem. Soc.* **1998**, 120, 4051-4052.

[60] Lambers-Verstappen, M.M.H.; de Vries, J.G. Rhodium-Catalyzed Asymmetric Hydroformylation of Unsaturated Nitriles. *Adv. Synth. Catal*. **2003**, *345*, 478-482.

[61] Aguado-Ullate, S.; Saureu, S.; Guasch, L; Carbó, J. Theoretical studies of asymmetric hydroformylation using the Rh-(R,S)-BINAPHOS catalyst--origin of coordination preferences and stereoinduction. J. *Chem. Eur. J.* **2012**, *18*, 995-1005.

[62] Yan, Y.; Zhang, X. A Hybrid Phosphorus Ligand for Highly Enantioselective Asymmetric Hydroformylation. *J. Am. Chem. Soc.* **2006**, *128*, 7198-7202.

[63] Wei, B.; Chen, C.; You, C.; Lv, H.; Zhang, X. Efficient Synthesis of (S, R)-Bn-Yanphos and Rh/(S, R)-Bn-Yanphos Catalyzed Asymmetric Hydroformylation of Vinyl Heteroarenes. *Org. Chem. Front.* **2017**, *4* , 288–291.

[64] Zhang, X.; Cao, B.; Yan, Y.; Yu, S.; Ji, B.; Zhang, X. Synthesis and application of modular phosphine-phosphoramidite ligands in asymmetric hydroformylation: Structure-selectivity relationship. *Chem. Eur. J.* **2010**, *16*, 871-877.

[65] Zhang, X.; Cao, B.; Yu, S.; Zhang, X. Rhodium-Catalyzed Asymmetric Hydroformylation of n-Allylamides: Highly Enantioselective Approach to B2-Amino Aldehydes. *Angew. Chem. Int. Ed.* **2010**, *49*, 4047–4050.

[66] a) Deeremberg, S.; Kamer, P.C.J.; van Leeuwen, P.W.N.M. New Chiral Phosphine–Phosphite Ligands in the Enantioselective Rhodium-Catalyzed Hydroformylation of Styrene. *Organometallics* **2000**, *19*, 2065-2072; b) Pàmies, O.; Net, G.; Ruiz, A.; Claver, C. Asymmetric hydroformylation of styrene catalyzed by furanoside phosphine–phosphite–Rh(I) complexes. *Tetrahedron: Asymmetry* **2001**, *12*, 3441-3445; c) Arena, C.G.; Faraone, F.; Graiff, C.; Tiripicchio, A. Rhodium(I), Palladium(II), and Platinum(II) Complexes Containing New Mixed Phosphane−Phosphite Ligands − Effect of the Catalytic System Stability on the Enantioselective Hydroformylation of Styrene. *Eur. J. Inorg. Chem*. **2002**, 711-716; d) Rubio, M.; Suárez, A.; Álvarez, E.; Bianchini, C.; Oberhauser, W.; Peruzzini, M.; Pizzano, A. Asymmetric Hydroformylation of Olefins with Rh Catalysts Modified with Chiral Phosphine-Phosphite Ligands. *Organometallics* **2007**, *26*, 6428-6436; e) Robert, T.; Abiri, Z.; Wassenaar, J.; Sandee, A.J.; Meeuwissen, J.; Sandee, A. J.; Bruin, B. de; Siegler, M. A.; Spek A. L.; Reek, J. N. H. Phosphinoureas: Cooperative Ligands in Rhodium-Catalyzed Hydroformylation? On the Possibility of a Ligand-Assisted Reductive Elimination of the Aldehyde. *Organometallics*, **2010**, *29*, 2413-2421; f) Arribas, I.; Vargas, S.; Rubio, M.; Suárez, A.; Domene, C.; Alvarez, E.; Pizzano, A. Chiral Phosphine−Phosphite Ligands with a Substituted Ethane Backbone. Influence of Conformational Effects in Rhodium-Catalyzed Asymmetric Olefin Hydrogenation and Hydroformylation Reactions. *Organometallics* **2010**, *29*, 5791-5804.

[67] Doro, F.; Reek, J. N. H.; Leeuwen, P. W. N. M. Isostructural Phosphine−Phosphite Ligands in Rhodium-Catalyzed Asymmetric Hydroformylation. *Organometallics* **2010**, *29*, 4440-4447.

[68] Noonan, G.M.; Fuentes, J.A.; Cobley, C.J.; Clarke, M.L., An Asymmetric Hydroformylation Catalyst that Delivers Branched Aldehydes from Alkyl Alkenes. *Angew. Chem. Int. Ed*. **2012**, *51,* 2477-2480.

[69] Iu, L.; Fuentes, J. A.; Janka, M. E.; Fontenot, K. J.; Clarke, M. L. High Iso Aldehyde Selectivity in the Hydroformylation of Short-Chain Alkenes. *Angew. Chem. Int. Ed*. **2019**, *58,* 2120-2124.

[70] Axtell, A.T.; Klosin, J.; Abboud, K.A. Evaluation of Asymmetric Hydrogenation Ligands in Asymmetric Hydroformylation Reactions. Highly Enantioselective Ligands Based on Bis-phosphacycles. *Organometallics*, **2006**, *25*, 5003-5009.

[71] Tan, R.; Zheng, X.; Qu, B.; Sader, C. A.; Fandrick, K. R.; Senanayake, C. H.; Zhang, X. Tunable P-Chiral Bisdihydrobenzooxaphosphole Ligands for Enantioselective Hydroformylation. *Org. Lett.* **2016**, *18*, 3346–3349.

[72] Qu, B.; Tan, R.; Herling, M. R.; Haddad, N.; Grinberg, N.; Kozlowski, M. C.; Zhang, X.; Senanayake, C. H. Enantioselective Synthesis of 4-Methyl-3,4-Dihydroisocoumarin via Asymmetric Hydroformylation of Styrene Derivatives. *J. Org. Chem.* **2019**, *84* (8), 4915–4920.

[73] Axtell, A.T.; Colbey, C.J.; Klosin, J.; Whiteker, G.T.; Zanotti-Gerosa, A.; Abboud, K.A. Highly Regio- and Enantioselective Asymmetric Hydroformylation of Olefins Mediated by 2,5-Disubstituted Phospholane Ligands. *Angew. Chem. Int. Ed.* **2005**, *44*, 5834-5838.

[74] Axtell, A.T.; Klosin, J.; Whiteker, G.T.; Cobley, C.J.; Fox, M.E.; Jackson, M.; Abboud, K.A. Bridging Group Effects in Chelating Bis(2,5-diphenylphospholane) Ligands for Rhodium-Catalyzed Asymmetric Hydroformylation. *Organometallics*, **2009**, *28*, 2993-2999.

[75] Morimoto, T.; Fujii, T.; Miyoshi, K.; Makado, G.; Tanimoto, H.; Nishiyama, Y.; Kakiuchi, K. Accessible protocol for asymmetric hydroformylation of vinylarenes using formaldehyde. *Org. Biomol. Chem*., **2015**, *13*, 4632–4636.

[76] Yu, Z.; Eno, M.S.; Annis, A.H.; Morken, J.P. Enantioselective Hydroformylation of 1-Alkenes with Commercial Ph-BPE Ligand. *Org. Lett.* **2015**, *17*, 3264−3267.

[77] Clarkson, G.J.; Ansell, J.R.; Cole-Hamilton, D.J.; Pogorzelec, P.J.; Whittell, J.; Wills, M. Bis(diazaphospholidine) ligands for asymmetric hydroformylation: use of ESPHOS and derivatives based on ferrocene and diarylether backbones *Tetrahedron: Asymmetry*, **2004**, *15*, 1787-1792.

[78] Clark, T.P.; Landis, C.R.; Freed, S.L.; Klosin, J.; Abboud, K.A. Highly Active, Regioselective, and Enantioselective Hydroformylation with Rh Catalysts Ligated by Bis-3,4-diazaphospholanes. *J. Am. Chem. Soc*. **2005**, *127*, 5040-5042.

[79] Nelsen, E. R.; Brezny, A. C.; Landis C. R. Interception and Characterization of Catalyst Species in Rhodium Bis(diazaphospholane)-Catalyzed Hydroformylation of Octene, Vinyl Acetate, Allyl Cyanide, and 1-Phenyl-1,3-butadiene. *J. Am Chem. Soc*. **2015**, *137*, 14208-14219.

[80] Wildt, J.; Brezny, A. C.; Landis, C. R. Backbone-Modified Bisdiazaphospholanes for Regioselective Rhodium-Catalyzed Hydroformylation of Alkenes. *Organometallics* **2017**, *36*, 3142–3151.

[81] Aguado-Ullate, S.; Guasch, L.; Urbano-Cuadrado, M.; Bo, C.; Carbó, J. J. 3D-QSPR Models for Predicting the Enantioselectivity and the Activity for Asymmetric Hydroformylation of Styrene Catalyzed by Rh-Diphosphane. *Catal. Sci. Technol.* **2012**, *2*, 1694–1704.

[82] Wang, X.; Buchwald, S. L. Rh-catalyzed asymmetric hydroformylation of functionalized 1, 1-disubstituted olefins. *J. Am. Chem. Soc.* **2011**, *133*, 19080−19083.

[83] Xiaofei, J.; Xinyi, R.; Zheng, W.; Chungu, X.; Kuiling, D. Pyrrolyl-Based Phosphoramidite/Rh Catalyzed Asymmetric Hydroformylation of 1,1-Disubstituted Olefins. *J. Chinese Chem. Soc.* **2019**, *39*, 207–214.

[84] Li, S.; Li, Z.; You, C.; Li, X.; Yang, J.; Lv, H.; Zhang, X. Rhodium-Catalyzed Enantioselective Anti-Markovnikov Hydroformylation of α-Substituted Acryl Acid Derivatives. *Org. Lett.* **2020**, *22*, 1108−1112.

[85] You, C.; Li, S.; Li, X.; Lv, H.; Zhang, X. Enantioselective Rh-Catalyzed Anti-Markovnikov Hydroformylation of 1,1-Disubstituted Allylic Alcohols and Amines: An Efficient Route to Chiral Lactones and Lactams. *ACS Catal.* **2019**, *9*, 8529−8533.

[86] You, C.; Li, S.; Li, X.; Lan, J.; Yang, Y.; Chung, L.; Lv, H.; Zhang, X. Design and Application of Hybrid Phosphorus Ligands for Enantioselective Rh-Catalyzed Anti-Markovnikov Hydroformylation of Unfunctionalized 1,1-Disubstituted Alkenes. *J. Am. Chem. Soc.* **2018**, *140*, 4977–4981.

[87] Miró, R.; Cunillera, A.; Margalef, J.; Lutz, D.; Börner, A.; Pamiès, O.; Diéguez, M.; Godard, C. Rh-Catalyzed Asymmetric Hydroaminomethylation of α-Substituted Acrylamides: Application in the Synthesis of RWAY. *Org. Lett.* **2020**, *22*, 9036−9040.

[88] Zheng, X.; Cao, B.; Liu, T.-l.; Zhang, X. Rhodium-Catalyzed Asymmetric Hydroformylation of 1,1-Disubstituted Allylphthalimides: A Catalytic Route to β3-Amino Acids. *Adv. Synth. Catal.* **2013**, *355*, 679–684.

[89] Wang, X.; Buchwald, S. L. Synthesis of optically pure 2-trifluoromethyl lactic acid by asymmetric hydroformylation. *J. Org. Chem.* **2013**, *78*, 3429−3433.

[90] Tan, R.; Zheng, X.; Qu, B.; Sader, C. A.; Fandrick, K. R.; Senanayake, C. H.; Zhang, X. Tunable P-Chiral Bisdihydrobenzooxaphosphole Ligands for Enantioselective Hydroformylation. *Org. Lett.* **2016**, *18*, 3346−3349.

[91] Eshon, J.; Foarta, F.; Landis, C. R.; Schomaker, J. M. α-Tetrasubstituted aldehydes through electronic and strain-controlled branch-selective stereoselective hydroformylation. *J. Org. Chem.* **2018**, *83*, 10207−10220.

[92] Zhang, D.; You, C.; Li, X.; Wen, J.; Zhang, X. Asymmetric Linear-Selective Hydroformylation of 1,1-Dialkyl Olefins Assisted by a Steric-Auxiliary Strategy. *Org. Lett.* **2020**, *22*, 4523–4526.

[93] Crozet, D.; Kefalidis, C. E.; Urrutigoïty, M.; Maron, L.; Kalck, P. Hydroaminomethylation of Styrene Catalyzed by Rhodium Complexes Containing Chiral Diphosphine Ligands and Mechanistic Studies: Why Is There a Lack of Asymmetric Induction? *ACS Catal.* **2014**, *4* (2), 435–447.

[94] Hoffmann, S.; Nicoletti, M.; List, B. Catalytic Asymmetric Reductive Amination of Aldehydes via Dynamic Kinetic Resolution. *J. Am. Chem. Soc.* **2006**, *128* (40), 13074–13075.

[95] Villa-Marcos, B.; Xiao, J. Metal and Organo-Catalyzed Asymmetric Hydroaminomethylation of Styrenes. *Chinese J. Catal.* **2015**, *36* (1), 106–112.

[96] Meng, J.; Li, X. H.; Han, Z. Y. Enantioselective Hydroaminomethylation of Olefins Enabled by Rh/Brønsted Acid Relay Catalysis. *Org. Lett.* **2017**, *19* (5), 1076–1079.

[97] Chen, C.; Jin, S.; Zhang, Z.; Wei, B.; Wang, H.; Zhang, K.; Lv, H.; Dong, X. Q.; Zhang, X. Rhodium/Yanphos-Catalyzed Asymmetric Interrupted Intramolecular Hydroaminomethylation of Trans-1,2-Disubstituted Alkenes. *J. Am. Chem. Soc.* **2016**, *138* (29), 9017–9020.

[98] Limanto, J.; Ashley, E. R.; Yin, J.; Beutner, G. L.; Grau, B. T.; Kassim, A. M.; Kim, M. M.; Klapars, A.; Liu, Z.; Strotman, H. R.; Truppo, M. D. A Highly Efficient Asymmetric Synthesis of Vernakalant. *Org. Lett.* **2014**, *16* (10), 2716–2719.

[99] Cross, P. E.; MacKenzie, A. R., U.S. Patent 005096890A, **1992**.

[100] Cunillera, A.; De Los Bernardos, M. D.; Urrutigoïty, M.; Claver, C.; Ruiz, A.; Godard, C. Efficient Synthesis of Chiral γ-Aminobutyric Esters: Via Direct Rhodium-Catalyzed Enantioselective Hydroaminomethylation of Acrylates. *Catal. Sci. Technol.* **2020**, *10* (3), 630–634.

[101] Cunillera, A.; Ruiz, A.; Godard, C. Synthesis of B2,2-Amino Esters via Rh-Catalyzed Regioselective Hydroaminomethylation. *Adv. Synth. Catal.* **2019**, *361* (18), 4201–4207.

[102] (a) Corey, E. J.; Guzman-Perez, A. The Catalytic Enantioselective Construction of Molecules with Quaternary Carbon Stereocenters. *Angew. Chemie Int. Ed.* **1998**, *37* (4), 388–401. (b) Fuji, K. *Asymmetric Creation of Quaternary Carbon Centers*; *Chem. Rev.* **1993**, *93*, 2037-2066.

[103] Abdel-Halim, H.; Hanrahan, J. R.; Hibbs, D. E.; Johnston, G. A. R.; Chebib, M. A Molecular Basis for Agonist and Antagonist Actions at $GABA_C$ Receptors. *Chem. Biol. Drug Des.* **2008**, *71* (4), 306–327.

[104] Kumar, K.; Sharma, S.; Kumar, P.; Deshmukh, R. Therapeutic Potential of GABAB Receptor Ligands in Drug Addiction, Anxiety, Depression and Other CNS Disorders. *Pharmacology Biochemistry and Behavior*. **2013**, *110*, 174–184.

[105] a) Strunz, A. K.; Zweemer, A. J. M.; Weiss, C.; Schepmann, D.;Junker, A.; Heitman, L. H.; Koch, M.; Wünsch, B. Synthesis and biological evaluation of spirocyclic antagonists of CCR2 (chemokine CC receptor subtype 2). *Bioorg*. *Med*. *Chem*. **2015**, *23*, 4034−4049. b) Butora, G.; Morriello, G. J.; Kothandaraman, S.; Guiadeen, D.;Pasternak, A.; Parsons, W. H.; MacCoss, M.; Vicario, P. P.; Cascieri, M. A.; Yang, L. 4-Amino-2-alkyl-butyramides as small molecule CCR2 antagonists with favorable pharmacokinetic properties. *Bioorg*. *Med*. *Chem*. *Lett*. **2006**, *16*, 4715−4722.

[106] Zhang, H.; Feng, D.; Chen, L.; Long, Y. Discovery of novel(S)-α-phenyl-γ-amino butanamide containing CCR5 antagonists via functionality inversion approach. *Bioorg*. *Med*. *Chem*. *Lett*. **2010**, *20*, 2219−2223.

[107] McCarron, J.; Zoghbi, S.; Shetty, H.; Vermuelen, E.; Wikström, H.; Ichise, M.; Yasuno, F.; Halldin, C.; Innis, R.; Pike, V. Synthesis and initial evaluation of [11C](R)-RWAY in monkey- a new, simply labeled antagonist radioligand for imaging brain 5-HT1A receptors with PET. *Eur*. *J*. *Nucl*. *Med*. *Mol*. *Imaging* **2007**, *34*, 1670−1682.

[108] a) Jongkind, L. J.; Reek, J. N. H. Asymmetric Hydroformylation Using a Rhodium Catalyst Encapsulated in a Chiral Capsule. *Chem. Asian J.* **2020**, *15*, 867–875. b) García-Simón, C.; Gramage-Doria, R.; Raoufmoghaddam, S.; Parella, T.; Costas, M.; Ribas, X.; Reek, J. N. H. Enantioselective Hydroformylation by a Rh-Catalyst Entrapped in a Supramolecular Metallocage. *J. Am. Chem. Soc.* **2015**, *137*, 2680-2687.

CHAPTER II

OBJECTIVES

The main objective of this work deals with the direct synthesis of chiral amines via the development of efficient catalytic systems for the rhodium catalyzed asymmetric hydroaminomethylation of alkenes. For this purpose, the present work includes the study of the homogeneous asymmetric intermolecular hydroaminomethylation of various alkenes such as 1,1-diarylethenes and cyclopropylmethacrylamides, the intramolecular hydroaminomethylation of amine-containing styrene derivatives, and our preliminary results for the development of heterogenized chiral catalysts for the hydroaminomethylation reaction under flow conditions.

In view of the state-of-the-art described in Chapter 1, the following specific objectives were defined:

Objective 1: Study the asymmetric hydroaminomethylation of 1,1-disubstituted alkenes.

The work described in Chapter III aims at the asymmetric hydroformylation and hydroaminomethylation of 1,1-diarylethenes to produce molecules of high biological interest such as Tolterodine. In this strategy, the enantioinduction must take place during the hydroformylation step of the process.

Objective 2: Synthesis of 2-cyclopropylmethacrylamide derivatives and their reactivity in hydroformylation and hydroaminomethylation.

The work outlined in Chapter IV focuses on the synthesis of a series of 2-cyclopropylmethacrylamides and the evaluation of their reactivity in Rh-catalyzed hydroformylation and hydroaminomethylation.

Objective 3: Development of heterogenized catalysts for the asymmetric hydroformylation and hydroaminomethylation of 1,1-disubstituted alkenes.

The results presented in Chapter V describe the synthesis of a new pyrene tagged phosphite-phosphoramidite ligand derived from xylose and the application of the corresponding rhodium complexes in homogeneous asymmetric hydroformylation

and hydroaminomethylation of alkenes. In a second part, the immobilization of the rhodium complexes on carbon support is reported and their evaluation in batch catalysis.

Objective 4: Intramolecular asymmetric hydroaminomethylation of monosubstituted alkenes.

The work exposed in Chapter VI deals with the reactivity of *ortho* substituted styrene derivatives containing an amine moiety in the intramolecular hydroaminomethylation. In this strategy, the chirality is induced during the asymmetric hydrogenation of the enamine/imine intermediate.

Objective 5: Scale-up of a sugar-based phosphite phosphoramidite ligand.

Chapter VII presents the work performed during a 3-month secondment in Italmatch Chemicals, Arese, Italy. The goals of this chapter were the scale-up of the synthesis of a chiral ligand as well as the development of a new Betti-base based ligand.

CHAPTER III

RHODIUM CATALYZED ASYMMETRIC HYDROAMINOMETHYLATION OF 1,1-DIARYLETHENE TOWARDS TOLTERODINE AND ITS DERIVATIVES

3.1. Introduction

Following the strategy developed by our group for the production of chiral amines via the asymmetric hydroaminomethylation of 1,1-disubstituted alkenes forming chiral 1,1-disubstituted propylamines, the work presented in this chapter aimed at the synthesis of molecules of biological interest such as chiral 3,3'-diarylpropylamines (Figure 1).

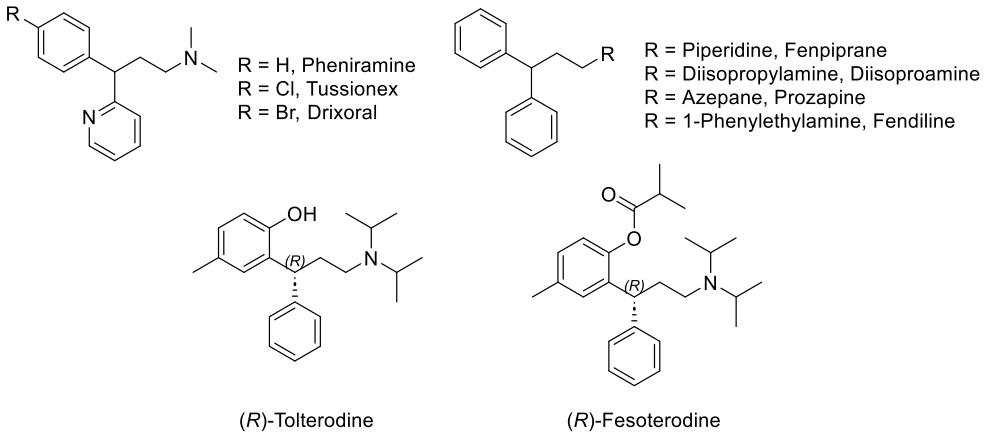

Figure 1. Representative examples of drugs based on the 3,3'-diarylpropylamine fragment

More precisely, the study presented here deals with the asymmetric hydroaminomethylation of 1,1-diarylethene for the production of Tolterodine derivatives (Scheme 1).

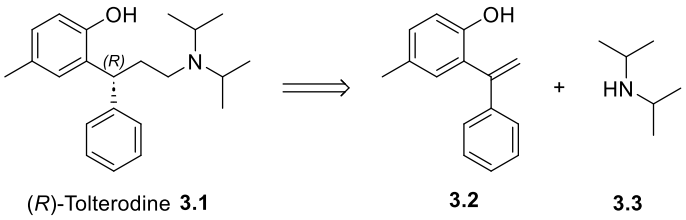

Scheme 1. Retrosynthetic analysis of Tolterodine 3.1 via hydroaminomethylation.

In the following section, the importance of this molecule and the synthetic pathways reported for the formation of Tolterodine and its derivatives will be described.

3.1.1. Relevance of Tolterodine derivatives

Tolterodine (Figure 1) stands as a notable pharmaceutical compound within the realm of medicinal chemistry, categorized as an antimuscarinic drug that has garnered considerable attention for its remarkable efficacy in treating overactive bladder (OAB) and its associated urinary symptoms.[1] Overactive bladder is a prevalent medical condition that presents a substantial challenge in the field of urological disorders. The pursuit of novel and effective agents to tackle this condition has led to the development of Tolterodine, which functions as a potent antagonist of muscarinic receptors in the bladder, thereby modulating the actions of acetylcholine, the neurotransmitter responsible for initiating detrusor muscle contractions. This unique mechanism of action offers promising therapeutic potential by improving the undesirable symptoms of OAB.

The annual bulk production of this active pharmaceutical ingredient (API) reaches approximately 0.5 tons in industrialized countries worldwide. In 2020, it ranked as the 271st most frequently prescribed medication in the United States, with over 1 million prescriptions dispensed.[2] This significant production is achieved through the original synthesis process, which involves a chemical resolution of racemic Tolterodine or a late-stage intermediate compound.

3.1.2. Synthetic approaches for Tolterodine and its derivatives

3.1.2.1. Racemic synthesis of Tolterodine

The initial approach for synthesizing Tolterodine was detailed in a patent by Kabi Pharmacia AB in 1998 (Scheme 2).[3] This method relied on the reaction between *p*-cresol **3.4** and cinnamic acid **3.5**, carried out in the presence of sulfuric acid at high temperature. The outcome of this reaction was the formation of 6-methyl-4-phenylchroman-2-one **3.6**. Subsequently, the process involved simultaneous opening of the lactone ring using methanol and phenolic hydroxyl etherification, performed in a solution of refluxing methanol and acetone containing K_2CO_3 and MeI. This led to the formation of 2-hydroxy-3-phenylpropanoate **3.7**. The next step

entailed the reduction of this compound to produce 2-(3-hydroxy-1-phenylpropyl)-4-methylphenol, which was then subjected to tosylation to yield the desired electrophile. This product was subsequently reacted with diisopropylamine, leading to the formation of protected Tolterodine. The methoxy fragment was cleaved using phosphorus tribromide in dichloromethane. This series of reactions ultimately yielded racemic Tolterodine **3.1rac**, which was then resolved using L-(+)-tartaric acid in ethanol yielding optically enriched Tolterodine **3.1** in the desired (*R*)-(+) enantiomer in 30% yield.

This route thus includes 8 consecutive synthetic steps and an overall yield < 13%. The synthesis also employed non-environmentally friendly chemicals including pyridine, phosphorus tribromide, and dichloromethane.

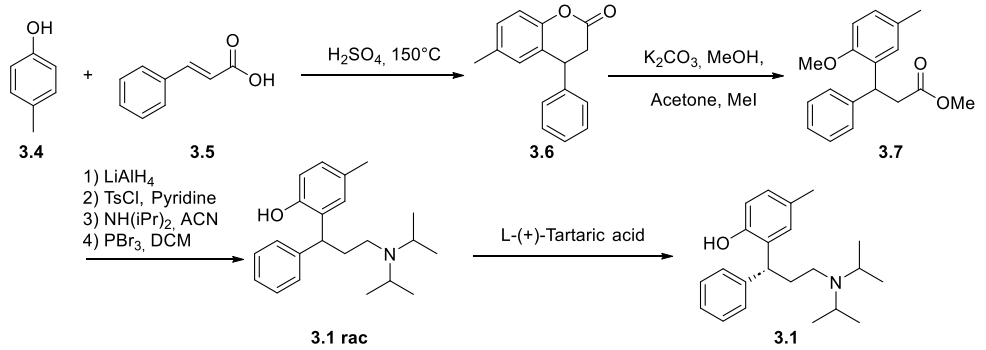

Scheme 2. Synthesis of Tolterodine 3.1 patented by Kabi Pharmacia AB

Another strategy also described in a patent[4] includes the reduction of dihydrocoumarin **3.6** using diisobutylaluminium hydride (DIBAL) to get the chromanol intermediate **3.8,** which was reacted with the amine in the presence of palladium and hydrogen to obtain the racemic Tolterodine **3.1rac** (Scheme 3).

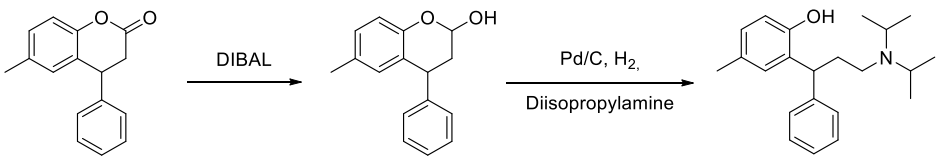

3.6 3.8 3.1 rac

Scheme 3. Synthesis of racemic Tolterodine from dihydrocoumarin intermediate 3.6

Despite these patents that initially provide a racemic mixture, more general strategies to access Tolterodine **3.1** are based on the synthesis of the chiral dihydrocoumarin intermediate **3.6** using asymmetric catalysis, followed by the sequential reduction to form **3.7** and reductive amination. In the next section, the asymmetric reactions yielding the dihydrocoumarin intermediate **3.6** are described.

*3.1.2.2. Asymmetric synthesis of the coumarin intermediate **3.6***

Hayashi and co-workers devised an exceptionally efficient enantioselective synthesis of (*R*)-Tolterodine via a Rh-catalyzed asymmetric 1,4-addition reaction (Scheme 4).[5] When coumarin **3.9** was subjected to reaction with phenylboronic acid in large excess at 60°C in a dioxane/water mixture, utilizing 3 mol% of Segphos **L1** and a Rh(I) precatalyst, the 1,4-adduct was attained in 88% yield with an impressive 99.6% enantiomeric excess (ee). Reduction of the lactone with DIBAL at -20°C provided the corresponding lactol in 95% yield, which was then subjected to a hydrogenative reductive amination to reach the desired compound.

Hayashi's approach thus only required three steps starting from commercially available compounds, which constituted a notable improvement. The overall yield was elevated to 76%.

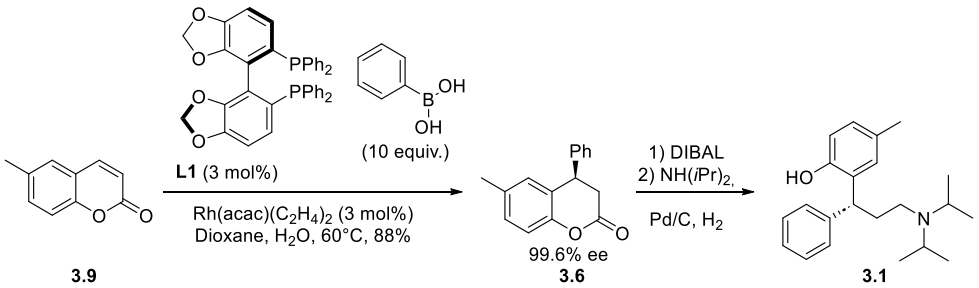

Scheme 4. Rh-catalyzed asymmetric 1,4-addition reaction leading dihydrocoumarin intermediate

Ever since, this methodology to afford Tolterodine has been the most studied[6]. A DFT based approach led to the design of a new catalytic system using a modified BIPHEP ligand. The computationally designed ligand enabled the significant decrease of catalyst and boronic acid loading.

Access to dihydrocoumarin **3.6** was recently reported via the asymmetric hydroesterification of diarymethyl carbinols (Scheme 5).[7] This method provided a 4-step asymmetric synthesis of (*R*)-Tolterodine from readily available reagents. The diol was converted to the 1,1-diaryl olefin *in situ* in acidic medium. Interestingly, without *p*-toluenesulfonic acid, no conversion of the alkene was observed.

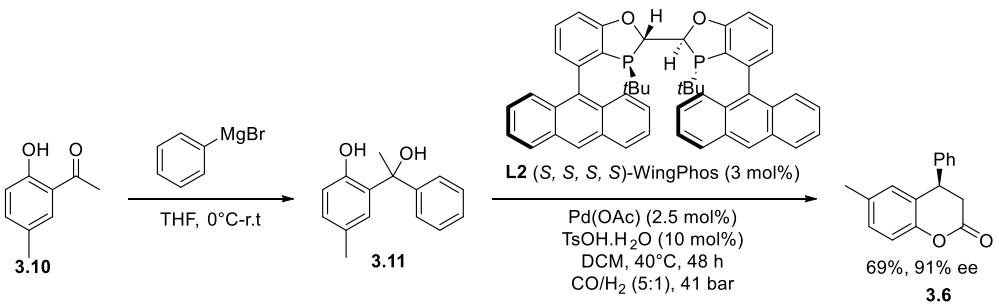

Scheme 5. Pd-catalyzed asymmetric hydroesterification reaction leading dihydrocoumarin intermediate

3.1.2.3. Synthesis of Tolterodine via asymmetric hydrogenation

Asymmetric hydrogenation of both chromanone[8] and styrene-type of olefins bearing a 2'-hydroxyl substituent was reported (Scheme 6).[9] The enantiomer of major interest was synthesized using the commercially available catalyst along with lithium

*tert*butoxyde to free the phenol from internal hydrogen bonding. Interestingly when the phenol was protected by a methyl group, the ee decreased below 20%, demonstrating the necessity of an hydroxy moiety in this system.

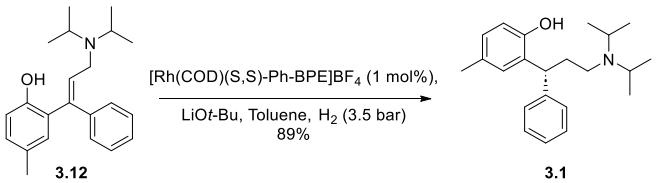

Scheme 6. Access to (*R*)-Tolterodine via Rh-catalyzed asymmetric hydrogenation

Hull and co-workers described the asymmetric synthesis of γ-branched amines via rhodium-catalyzed reductive amination and applied this methodology in the synthesis of Terikalant and Tolterodine.[10] This enantioselective approach is based on tandem isomerization-enamine exchange transfer hydrogenation process (Scheme 7).

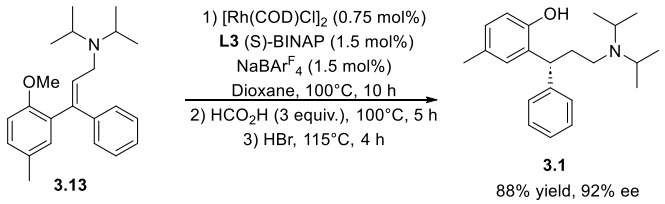

Scheme 7. Synthesis of Tolterodine via Rh-catalyzed tandem isomerization-enamine exchange transfer hydrogenation

3.1.2.4. Synthesis of Tolterodine via hydroformylation and hydroaminomethylation of 1,1-diarylethene substrates

Tolterodine was also obtained using hydroformylation as the key step of the process. This methodology was described by Piccolo and co-workers in 2002.[11] One important advantage of this route is to directly obtain the chromanol intermediate, avoiding the use of expensive and sensitive DIBAL reducing agent. In a first part of their study, the authors described the hydroformylation reaction using achiral ligands (Table 1). High conversion and selectivity towards **3.8** was obtained in most cases. Moreover, using an aqueous biphasic system with [Rh(COD)(μ-Cl)]$_2$/TPPTS as catalytic system (Entry 8), they achieved commendable reaction rates and nearly complete

chemoselectivity. Remarkably, even after subjecting the catalytic solution to five cycles, the loss in efficiency remained minimal (<5%).

Table 1. Rh-catalyzed hydroformylation of 1,1-diarylethene

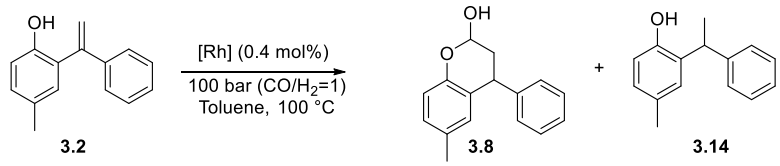

3.2 **3.8** **3.14**

Entry	Catalytic system	time (h)	conv. (%)	**3.8** (%)	**3.14** (%)
1	$[Rh(COD)(\mu\text{-}Cl)]_2$	72	96	94	2
2	$[HRh(CO)(PPh_3)_3]$	48	95	92	4
3	$[Rh(acac)(CO)_2]/PPh_3$	72	51	43	9
4	$[Rh(acac)(CO)_2]$/DPPB	72	83	75	9
5	$[Rh(acac)(CO)_2]$/Xantphos	72	90	83	7
6a	$[Rh(acac)(CO)_2]$/Xantphos	72	26	8	18
7	$[Rh(acac)(CO)_2]$/Xantphos	24	10	6	4
8b	$[Rh(COD)(\mu\text{-}Cl)]_2$/TPPTS	48	99	99	-

Ligand/Rh (molar ratio) = 1.1/1, [a] Ligand/Rh (molar ratio) = 2.2/1, [b] Ligand/Rh (molar ratio) = 3/1, solvent = toluene/H_2O

Having proved that the racemic synthesis of the intermediate was feasible, the authors reported the use of a few chiral ligands (Table 2). However, using the $[Rh(acac)(CO)_2]$/(S,R)-Binaphos catalytic system, only the hydrogenated product was observed. Thus, the authors protected the phenol group by an acetate in order to boost the chemoselectivity. Unfortunately, after 168 hours of reaction at 60°C and 80 bar, the conversion was only 51% with a poor chemo- and enantioselectivity towards the aldehyde. Ferrocene based diphosphines also resulted in a poor chemoselectivity and did not improve the enantioselectivity.

Table 2. Rh-catalyzed asymmetric hydroformylation of 1,1-diarylethene

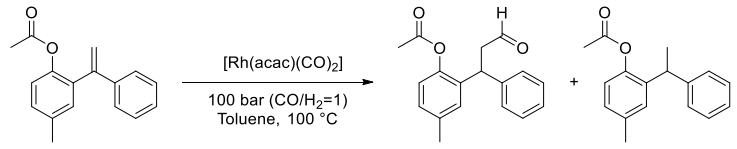

3.15 **3.16** **3.17**

Entry	Ligand	time (h)	conv. (%)	**3.16** (%)	ee (%)	**3.17** (%)
1a	**L4** (S,R)-Binaphos	168	51	25	8	27
2	**L5**	216	99	38	1	59
3	**L6**	216	66	22	-	44
4	**L7**	144	59	18	-	41

Ligand/Rh (molar ratio)=4/1, [a] 80 bar (CO/H_2=1), 60°C

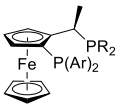

L5 = R = Cy, Ar = 3,5-CF_3-Ph
L6 = R = Ph, Ar = Ph
L7 = R = *t*Bu, Ar = Ph

To date, reports on the asymmetric hydroformylation (HF) of 1,1-disubstituted alkenes remain limited and to the best of our knowledge, the example by Piccolo described above is the only one for this transformation using 1,1-diaryl alkenes.[12,13] Moreover, there is no example of asymmetric hydroaminomethylation of this type of substrates. Only four examples of HAM of 1,1-diaryl alkenes were reported to date in its racemic version.[14a-d] The first example (Scheme 8, route a) was reported using the $[Rh(COD)(\mu\text{-}Cl)]_2/PBu_3$ (1% Rh, L/Rh = 16) catalytic system,[14a] achieving *ca*. 70% yield of amines in 3 days at 120 °C under 110 bar of syngas. The $[Rh(COD_2]BF_4$/Xantphos catalytic system was reported to produce Fenpiprane in 59% yield after 36 h at 135°C (Scheme 8, route b).[14b] The use of the rhodium-NHC complex at 125°C for 24 h afforded a variety of pharmaceuticals containing amines (see Figure 1) in ca. 85% yield (Scheme 8, route c). Lastly, the $[Rh(nbd)_2]BF_4$/Naphos catalytic system was reported for the synthesis of Fenpiprane and related pharmaceuticals in ca. 83% yield (Scheme 8, route d). All the systems reported needed temperature >120°C, high internal pressure, and long reaction time.

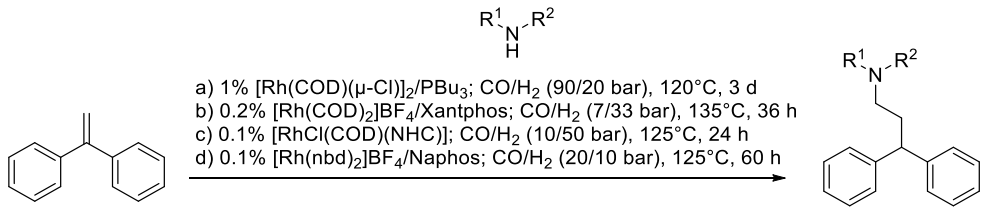

Scheme 8. Racemic hydroaminomethylation of 1,1-diarylethenes leading to 3,3'-diarylpropylamines.

This work described in the following section represents the first Rh-catalyzed asymmetric hydroformylation and hydroaminomethylation of 1,1-diarylethene, leading to Tolterodine and derivatives.

3.2. Results and discussion

3.2.1. Synthesis of substrates

In this section, the results obtained in the synthesis of 1,1-diarylethenes substrates are described.

3.2.1.1. Synthesis of 1,1-diarylethenes

1,1-diarylethenes were synthesized using a modified reported procedure.[15] Regioselective hydroarylation was performed using phenols **3.18** (1.5 equiv.) and phenylacetylenes **3.19** (1 equiv.) in the presence of an alumina-sulfuric acid heterogeneous catalyst at 160°C using microwave heating. It is noteworthy that with the conditions described in the literature (120°C, 4 h), low conversion of the acetylenes **3.19a-e** was observed. Four days in refluxing toluene were necessary to reach full conversion of the acetylenes under classic conditions. Therefore, the microwave assisted synthesis described constitutes a fast and effective manner of accessing these substrates using readily available products, in 30 to 60% yield after purification by column chromatography (Scheme 9).

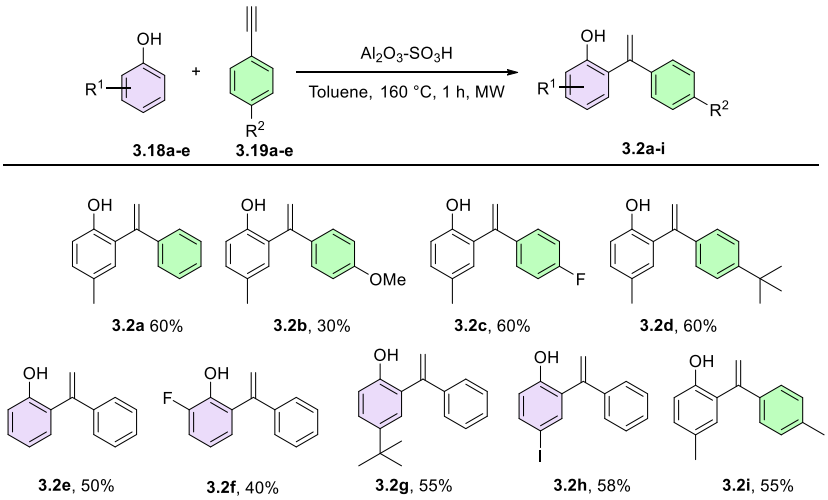

Scheme 9. Synthesis of 1,1-diarylethenes via microwave assisted catalysis.

In order to study the influence of the phenol on the catalytic outcome of the hydroformylation and hydroaminomethylation reactions, the protection of this group was carried out and will be described in the next section.

*3.2.1.2. Protection of phenol **3.2a***

First, the phenol **3.2a** was protected with an ester group by reaction with pivaloyl chloride in triethylamine and acetonitrile (Scheme 10). The ester **3.20** was obtained in 49% isolated yield after column chromatography.

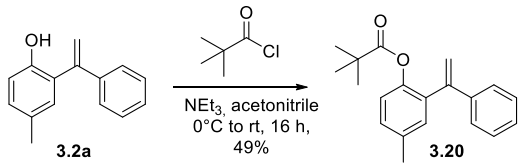

Scheme 10. Protection of phenol 3.2a with pivaloyl chloride generating the ester 3.20.

To introduce a bulkier protecting group that may favour the enantioinduction in the following asymmetric catalytic tests, the phenol **3.2a** was also treated with *tert*-Butyldiphenylsilyl chloride in presence of imidazole and DMF. The bulky silyl ether **3.21** was obtained in 54% isolated yield after column chromatography (Scheme 11).

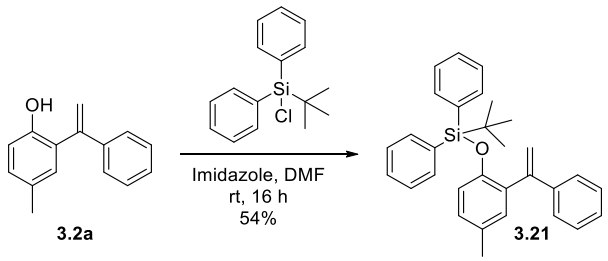

Scheme 11. Protection of phenol 3.2a with TBDPSCl producing the silyl ether 3.21.

3.2.2. Rh-catalyzed racemic hydroaminomethylation and hydroformylation of the 1,1-diarylethenes **3.2a-i**, **3.20** and **3.21**.

Prior to the testing in the asymmetric processes, the racemic reactions were first optimized in order to determine the methods for the HPLC analysis of the chiral products.

3.2.2.1. Rh-catalyzed racemic hydroaminomethylation of 3.2a-i

3.2.2.1.1. Optimization of conditions

A brief optimization of conditions was performed for the hydroaminomethylation of **3.2a** and the conditions are described in Table 3. The catalysis was performed with [Rh(acac)$(CO)_2$] as precursor while di-*tert*-butylphenylphosphine **L8** and DPEPhos **L9** were used as ligands. The reaction was performed with one equivalent of diisopropylamine **3.3** in MeTHF and under 30 bar of syngas pressure. Initially, the reaction was carried using **L9** at 90 °C for 66 h with a ratio CO:H_2 = 1. However, under these conditions, full conversion of **3.2a** was observed into the hydrogenated product **3.14a** (Entry 1). When the reaction was repeated using **L8** and increasing the partial pressure of CO, full conversion was obtained with a selectivity of 30% to the amine **3.1a** (Entry 2). Under these conditions but using the diphosphine ligand **L9** (Entry 3), only 18% conversion was measured with a poor chemoselectivity (13%) towards the amine **3.1a**. Therefore, **L8** was used for the subsequent tests. First, the reaction time was reduced to 24 h and the CO:H_2 ratio was increased to 3 (Entry 4). In this case, a drop in conversion and chemoselectivity was observed and the chromanol **3.8a** was detected indicating that the amine condensation was not efficient. Then, the CO:H_2 ratio was changed to 2 and the temperature increased to 125°C to improve the conversion. After 24h, 98% of **3.2a** was mainly converted into **3.14a** and only 27% of **3.1** were obtained (Entry 5). When the reaction time was decreased to 20 h, the same selectivity was observed (Entry 6). These conditions were thought to be good enough to isolate the racemic **3.1a**.

Table 3. Optimization of conditions for the racemic hydroaminomethylation of 3.2a towards 3.1a

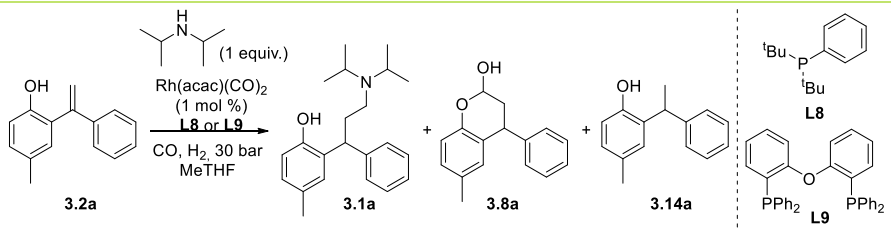

Entry[a]	Ligand	CO:H_2	Temp. (°C)	Time (h)	% Conv.	% 3.1a	%3.8a	% 3.14a
1	**L8**	1:1	90	66	100	0	0	100
2	**L8**	2:1	90	66	100	30	0	70
3[b]	**L9**	2:1	90	66	18	13	0	87
4	**L8**	3:1	90	24	23	10	10	80
5	**L8**	2:1	125	24	98	27	0	73
6	**L8**	2:1	125	20	98	27	0	73

[a] ***Reaction conditions**: **3.1a** (0.12 mmol), **3.3a** (0.12 mmol), Rh = [Rh(acac)(CO)$_2$] (1 mol%), **L** (5 mol %), 30 bar (CO:H_2), MeTHF (0.2 ml), 400 r.p.m.* [b] ***L** (2 mol %).*

Then, we applied the conditions obtained in entry 6 for the racemic hydroaminomethylation of the substrates **3.2a-g**.

3.2.2.1.2. Catalytic tests

The catalysis was performed with [Rh(acac)(CO)$_2$] as precursor with di-*tert*-butylphenylphosphine **L8** (5 mol%) as ligand. The reaction was performed with one equivalent of diisopropylamine **3.3** in MeTHF at 125°C for 20 h under 30 bar of syngas pressure with a ratio CO:H_2 = 2. The racemic amines **3.1a-g** were obtained in a range of 17-24% yield after column chromatography (Table 4). Notably, no chromanol was observed for the hydroaminomethylation of **3.2a-g** demonstrating the effectiveness of the amine condensation and enamine hydrogenation using **L8** under these conditions. The racemic amines were fully characterized by NMR and separated by chiral HPLC to obtain the retention times of the enantiomers.

Table 4. Racemic Rh-catalyzed hydroaminomethylation of 3.2a-g to the racemic amines 3.1a-g using L8.

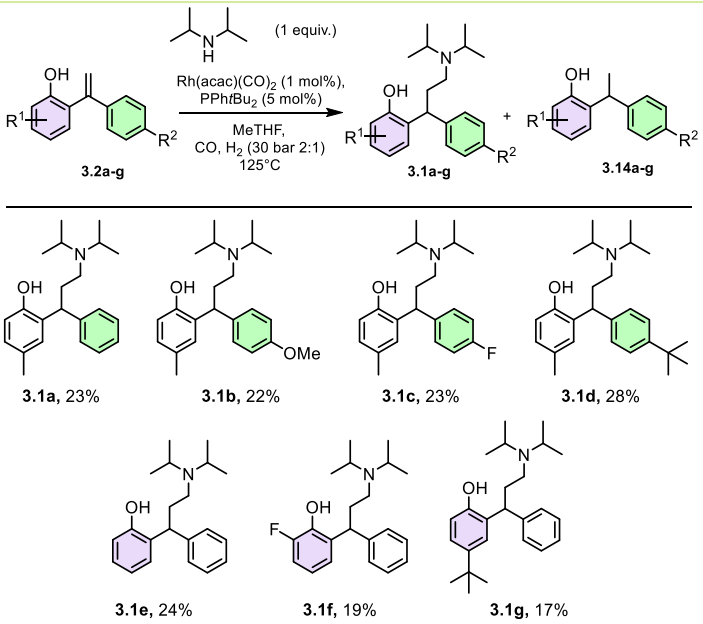

Entry	Substrate	Conv (%)	% **3.1**	% **3.14**
1	**3.2a**	98	27	73
2	**3.2b**	97	27	73
3	**3.2c**	96	26	74
4	**3.2d**	97	33	67
6	**3.2f**	98	29	71
7	**3.2g**	96	23	77
8	**3.2h**	95	21	79

***Reaction conditions**: **3.2** (0.3 mmol), **3.3** (0.3 mmol), Rh = [Rh(acac)(CO)$_2$] (1 mol%), **L** (1.2 mol %), P = 30 bar (CO:H$_2$, 2:1), MeTHF (0.6 ml), T = 125 °C, t = 20 h, 400 r.p.m.*

*3.2.2.2. Rh-catalyzed racemic hydroaminomethylation of **3.20** and **3.21***

The racemic hydroaminomethylation of **3.20** was performed with the same [Rh(acac)(CO)$_2$]/**L8** catalytic system. The reaction was performed with one equivalent of diisopropylamine **3.3** in MeTHF at 125°C for 36 h under 30 bar of syngas pressure with a ratio CO:H$_2$ = 2 (Scheme 12). The substrate was converted in 98%

with a 58% chemoselectivity towards **3.22** and 42% towards **3.24**. No aldehyde **3.23** was observed using these conditions. The amine was obtained in 51% yield and the enantiomers were separated using chiral HPLC.

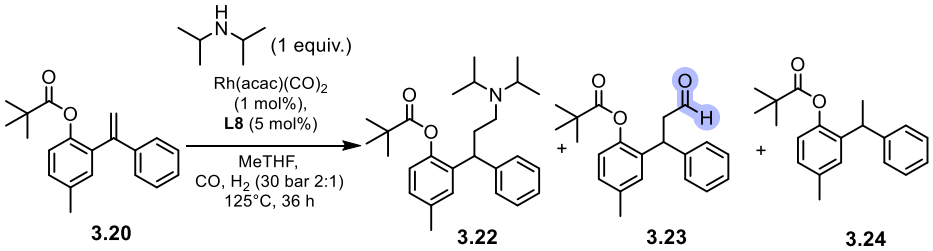

Scheme 12. Racemic Rh-catalyzed hydroaminomethylation of 3.20 to the racemic amine 3.22 using L8.

The racemic hydroaminomethylation of **3.21** was also studied using the same conditions (Scheme 13) and gave 99% conversion towards 43% of amine **3.25** and 57% of the hydrogenated product **3.26**.

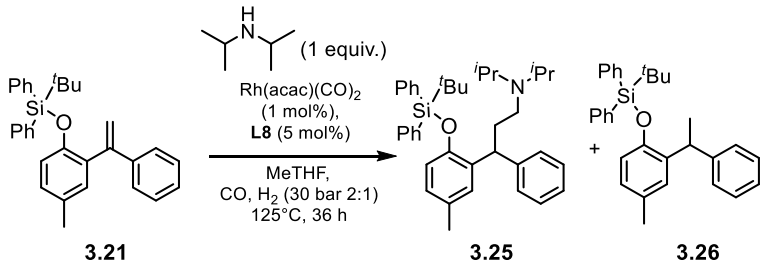

Scheme 13. Racemic Rh-catalyzed hydroaminomethylation of 3.21 to the racemic amine 3.25 using L8.

The product was fully characterized but we couldn't separate the enantiomers using chiral HPLC. Having optimized the racemic hydroaminomethylation and observed that the CO partial pressure was crucial for the chemoselectivity, the Rh-catalyzed racemic hydroformylation of **3.2a-i** was performed under the same conditions.

*3.2.2.3. Rh-catalyzed racemic hydroformylation of **3.2a-i***

The racemic hydroformylation of these substrates was performed using [Rh(acac)$(CO)_2$] as precatalyst and ditertbutylphenyl phosphine as ligand in MeTHF at 125°C with 30 bars of pressure of syngas (CO:H_2=2). Using these conditions, the

chemoselectivity towards chromanols **3.8a-g** was between 44% (**Table 5**, entry 6) and 74% (Table 5, entry 1). The chromanols **3.8a-g** and the hydrogenated products **3.14a-g** were the only products detected. The higher chemoselectivities obtained in hydroformylation revealed the negative effect of the presence of the amine, favoring the hydrogenation in the hydroaminomethylation reaction. Surprisingly, no conversion was observed for **3.2h** and only 7% conversion was detected for **3.2i**. The presence of two diastereomers of products **3.8a-g** were observed by ^{1}H NMR (Figure 2). The d.e. obtained was between 47 (**Table 5**, entry 7) and 58% (**Table 5**, entry 1 and 3). These d.e. are in accordance with those reported for the synthesis of chromanols.[21] The racemic crude products were purified by column chromatography on silica gel yielding the products **3.8a-g** in 26-52% yield.

Table 5. Racemic Rh-catalyzed hydroformylation of 3.2a-g to the racemic chromanols 3.1a-g using L8.

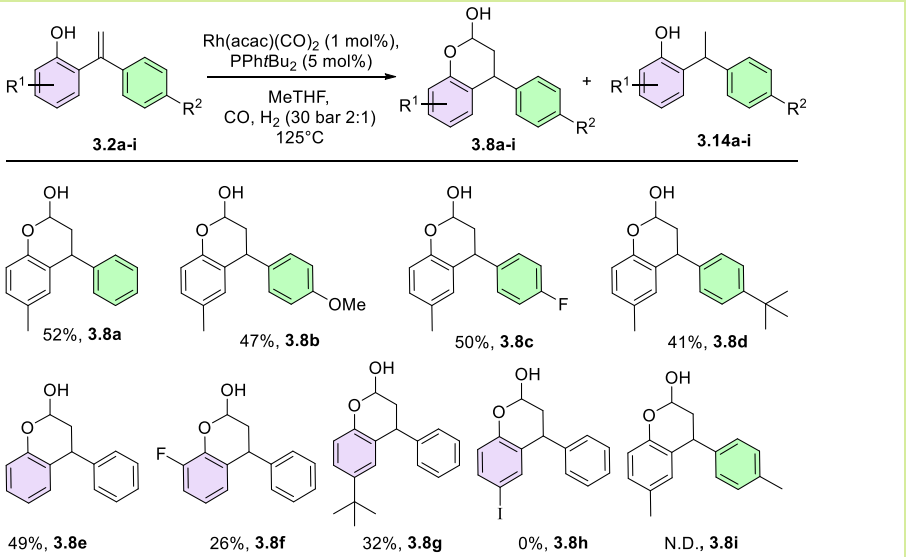

Entry	Substrate	Conv (%)	% **3.8**	% **3.14**	d.e (%)
1	**3.2a**	96	74	26	58
2	**3.2b**	90	73	27	51
3	**3.2c**	91	72	28	58
4	**3.2d**	92	63	37	56
5	**3.2e**	92	66	34	46
6	**3.2f**	92	44	56	54
7	**3.2g**	93	47	53	47
8	**3.2h**	0	-	-	N.D.
9	**3.2i**	7	100	-	N.D.

***Reaction conditions**: **3.2a** (0.3 mmol), Rh = [Rh(acac)(CO)$_2$] (1 mol%), **L** (1.2 mol %), P = 30 bar (CO:H$_2$, 2:1), MeTHF (0.6 ml), T = 125 °C, t = 20 h, 400 r.p.m.*

In all the catalysis, only the cyclic form of the products was observed, indicating that the intramolecular cyclization of the aldehyde with the free phenol was very fast.

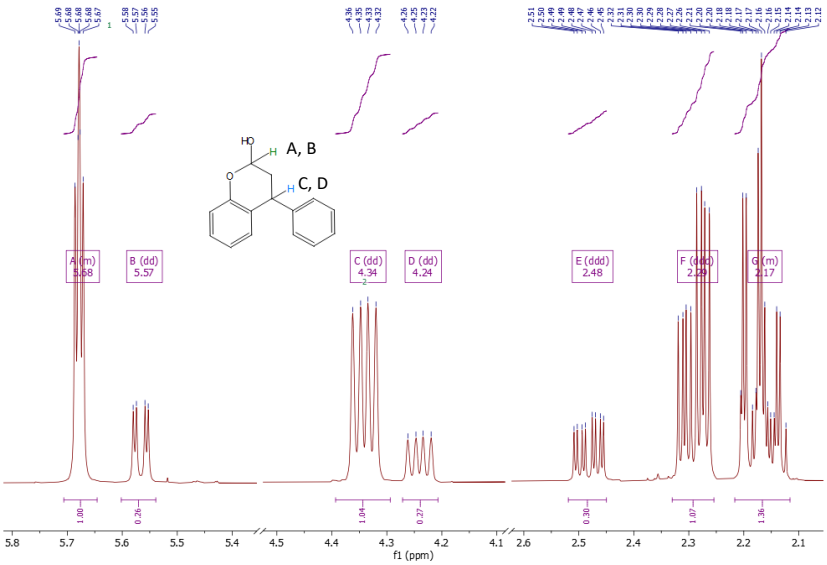

Figure 2. Selected region of the ^{1}H NMR spectrum of chromanol 3.8e.

Since the separation of the diasteroisomers by column chromatography revealed challenging and the determination of the HPLC methods for the chromanols separation was not always straightforward, the intermediate mixture of diastereoisomers was oxidized using PCC to get the chromanones compounds thus containing only one pair of enantiomers (Scheme 14). The racemic chromanones **3.6a-g** were obtained in quantitative yield from **3.8a-g**.

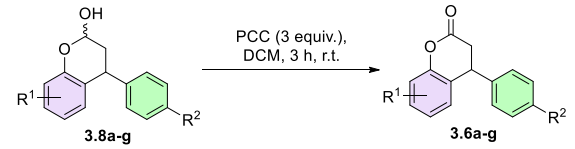

R^1 = 4-Me, H, 2-F, 4-^{t}Bu
R^2 = H, 4-OMe, 4-F, 4-^{t}Bu

R^1 = 4-Me, H, 2-F, 4-^{t}Bu
R^2 = H, 4-OMe, 4-F, 4-^{t}Bu

Scheme 14. Oxidation of racemic chromanols

Finally, the racemic amines were thus successfully obtained by Rh-catalyzed hydroaminomethylation of **3.2a-g** while the chromanols and chromanones were produced via the Rh-catalyzed hydroformylation of **3.2a- g** using **L8** as ligand.

At this stage, with the conditions for enantiomers separation by HPLC developed via the analysis of the racemic, we next focus on the asymmetric version of these processes.

3.2.3. Rh-catalyzed asymmetric hydroaminomethylation and hydroformylation of the 1,1-diarylethenes **3.2a-i** and **3.20**

*3.2.3.1. Rh-catalyzed asymmetric hydroaminomethylation of **3.2a-g***

Since the optimization with the racemic ligands indicated that the substrates were prone to hydrogenation, a new optimization was performed using more π-acceptor ligands.

3.2.3.1.1. Optimization of conditions

The phosphite phosphoramidite ligand **L14a** was used for the optimization of reaction conditions. Initially, the temperature was set to 125°C, the partial pressure to CO = 30 bar with a $CO:H_2$ ratio of 2 with 3 mol% Rh and a Rh:L ratio of 2 (Table 6). Under these conditions, a conversion of 80% was obtained with 54% of selectivity to amine **3.1a**. 20% of chromanol **3.8** and 26% of hydrogenation product **3.14a** were also observed (Entry 1). When 2 equiv. of $NH(^iPr)_2$ were used, similar results were obtained (Entry 2). However, when the catalyst loading was lowered in the presence of 1 equiv. of amine, a greater selectivity to the desired amine product was reached although the conversion decreased to 72% (Entry 3). Moreover, the molarity of the reaction mixture revealed to greatly affect the chemoselectivity since at higher concentration, lower selectivity to the chromanol **3.8** was obtained (Entries 7-11). Reducing the Rh/L ratio to 1.2 was also beneficial to the chemoselectivity of the reaction in favor of the amine **3.1**. After variation of the total syngas pressure and $CO:H_2$ ratio, the most favorable conditions were set to 30 bar of $CO:H_2$ (2/1) with a molarity of 0.7 using 1 mol% of Rh, Rh/L = 1.2 and 1 equivalent of amine per substrate (Entry 6). Under these conditions, 75% conversion was reached with 70% selectivity to **3.1**, 6% of **3.8a** and 24% of **3.14a**.

Table 6. Optimization conditions of Rh-catalyzed HAM of 3.2a using L14a

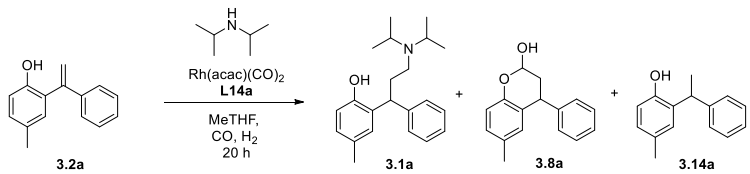

Entry	P (CO:H_2) (bar)	Rh mol%: L mol%	Molarity	Conv (%)	% 3.1a	% 3.8a	% 3.14a
1	30 (2:1)	3:6	0.4	80	54	20	26
2[a]	30 (2:1)	3:6	0.4	86	52	18	30
3	30 (2:1)	1:2	0.4	72	74	3	23
4[a]	30 (2:1)	1:2	0.4	94	51	24	25
5[a]	30 (2:1)	1:1.2	0.4	61	66	6	28
6	30 (2:1)	1:1.2	0.7	75	70	6	24
7	30 (4:1)	1:1.2	0.7	66	69	6	25
8	20 (4:1)	1:1.2	0.7	26	54	-	46
9	40 (4:1)	1:1.2	0.7	34	54	15	31
10	30 (1:1)	1:1.2	0.7	61	59	-	41
11	20 (1:1)	1:1.2	0.7	54	45	15	41

***Reaction conditions**: **1a** (0.12 mmol), Rh = [Rh(acac)(CO)$_2$], **L14a**, P = 20-40 bar (CO:H_2), toluene, T = 125 °C, t = 20 h, 400 r.p.m. [a] 2 equiv. amine were used.*

Next, the ligands **L10-L15** were tested using the substrate **3.2a**, [Rh(acac)(CO)$_2$], MeTHF as solvent, under 30 bar H_2/CO (1:2), at 125 °C during 20 h (Table 7). The use of **L10** resulted in poor selectivity towards **3.1a** (Entry 1) whilst in the asymmetric HAM of α-alkyl acrylates,[16] **L10** provided great yields (up to 91%) and enantioselectivity (up to 94% *ee*). When the phosphine-phosphite (S_{ax},*S*,*S*)-BOBPhos **L11** was used, excellent conversion was obtained but with poor selectivity and no enantioselectivity (Entry 2). When **L12** was tested, only 34% conversion was obtained with 24% selectivity to **3.1a** (Entry 3). Both conversion and selectivity were improved when the diphosphites **L13** and **L15** or phosphite phosphoramidite **L14** ligands were used. While **L13** provided the best selectivity of the series, no enantioinduction was

observed (Entry 4). The phosphite phosphoramidite **L14c** provided 88% conversion, 54% selectivity and 31% *ee* (Entry 5). Moreover, the diphosphite ligand **L15a** outperformed the recently described **L14c** with 96% conversion, 49% selectivity and 41% *ee* (Entry 6). It was then decided to further explore the performance of other members of the families of the sugar-based ligands **L14** and **L15**.

Table 7. Screening of ligands for the asymmetric HAM of 3.2a

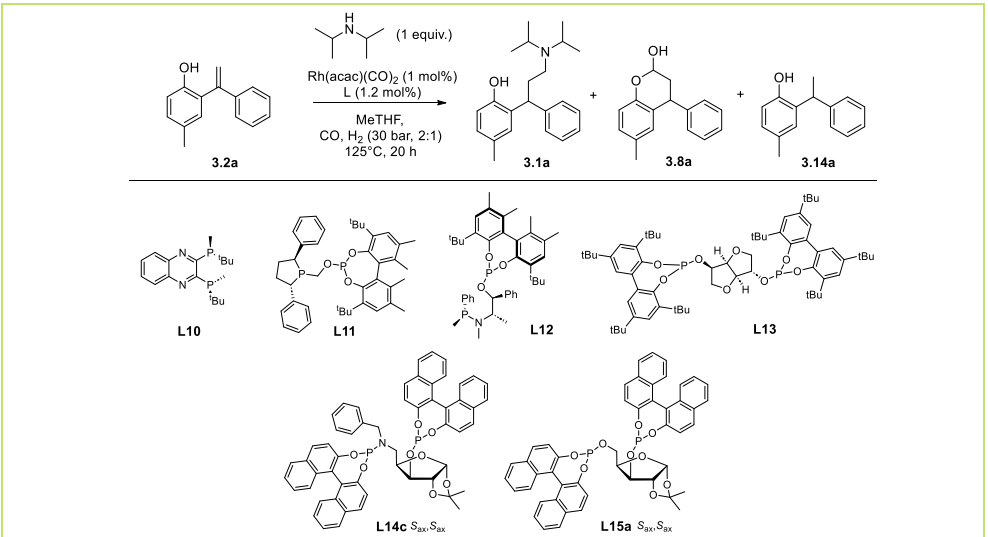

Entry[a]	Ligand	% Conv.	% 3.1a (%ee)	% 3.8a	%3.14a
1	**L10**	63	21 (-)	2	77
2	**L11**	99	36 (0)	8	56
3	**L12**	34	24 (-)	6	70
4	**L13**	99	63 (0)	0	31
5	**L14c**	88	54 (31)	27	19
6	**L15a**	96	49 (41)	41	10

[a] ***Reaction conditions**: **1a** (0.12 mmol), Rh = [Rh(acac)(CO)$_2$] (1 mol%), **L** (1.2 mol %), P = 30 bar (H$_2$/CO, 1:2), MeTHF (0.2 ml), T = 125 °C, t = 20 h, 400 r.p.m. % ee of **2a** determined by chiral HPLC.*

The family of sugar based phosphite phosphoramidite was first tested (Table 8) and the results revealed that the substituent at the nitrogen atom was not affecting the conversion nor the chemoselectivity of the reaction. However, variation in the enantiomeric excess from 9% when R=Me (entry 1) to 36% when R=(*S*)-α-methylbenzyl (entry 5) were measured. It is noteworthy that when the BINOL chirality is (*R*) at the phosphoramidite moiety, the conversion and the enantiomeric excess decreased but the chemoselectivity towards **3.1a** reached up to 80% (entries 6 and 8). Interestingly, when the diol moiety was replaced by a chiral biphenol (entries 9 and 10) at the phosphite position, the selectivity dropped to 32% with S_{ax} or to 21% with R_{ax}. However, when the diol was replaced by the bulky biphenol in both the phosphite and phosphoramidite moieties, the conversion was still good but the selectivity towards the amine was only 20%. The presence of the BINOL groups is therefore important for the chemoselectivity of the reaction in which the enantiomer used influences the enantioselectivity. However, despite the number of ligands tested in this family, the highest enantioselectivity obtained was 36%.

It is noteworthy that the ligand structure had a strong effect on the condensation reaction between the aldehyde and the amine, which could indicate the participation of the Rh center in this step.

Table 8. Screening of sugar-based phosphite phosphoramidite family

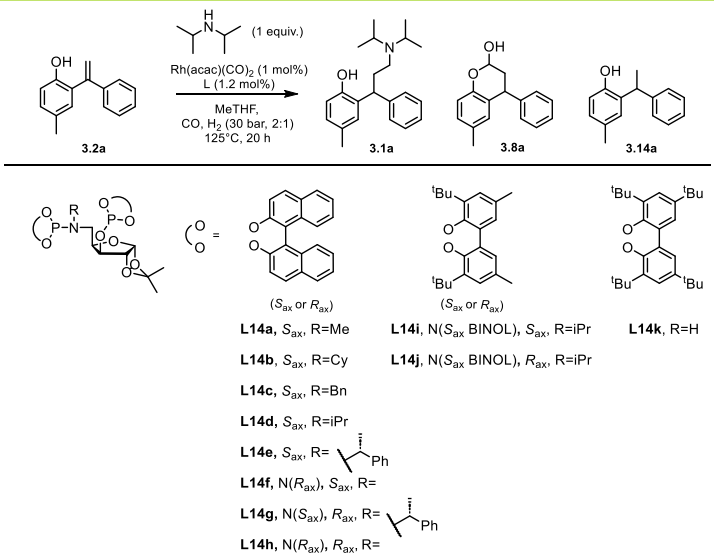

Entry[a]	Ligand	% Conv.	% 3.1a (%ee)	% 3.8a	% 3.14a
1	**L14a**	75	70 (9)	6	24
2	**L14b**	96	49 (26)	40	12
3	**L14c**	88	54 (31)	27	19
4	**L14d**	94	56 (34)	31	13
5	**L14e**	90	48 (36)	41	10
6	**L14f**	80	77 (15)	4	19
7	**L14g**	87	53 (10)	32	15
8	**L14h**	78	80 (6)	4	16
9	**L14i**	93	32 (N.D.)	45	23
10	**L14j**	93	21 (N.D.)	52	27
11	**L14k**	95	20 (N.D.)	43	37

[a] ***Reaction conditions**: **1a** (0.12 mmol), Rh = [Rh(acac)(CO)$_2$] (1 mol%), **L** (1.2 mol %), P = 30 bar (H$_2$/CO, 1:2), MeTHF (0.2 ml), T = 125 °C, t = 20 h, 400 r.p.m. % ee of **3.1a** determined by chiral HPLC.*

Next, the influence of the structure of the diphosphite family **L15** on the performance of the reaction was looked at (Table 9). When the xylose-derived ligands (**L15a-d** and **L15g**) were used (R=H), all conversions were above 94%. However, when the ligands **L15e** and **L15f** containing a glucose-derived backbone (R=CH$_3$) were involved, lower values were measured. Selectivity towards **3.1a** ranged

from 49% (entry 1) to 67% (entry 3). No enantioinduction was observed when the phosphite moieties contained a bulky biphenol (entry 7) was used instead of a chiral binaphthol, showing the importance of the axial chirality in this ligand rather than the chirality from the backbone.

In this series, the ligand structure again appeared to have a strong influence, and consequently the Rh center, on the efficiency of the condensation step since the selectivity of the chromanol ranged from 3 to 41% depending on the ligand used.

Table 9. Screening of sugar-based diphosphite ligands L15

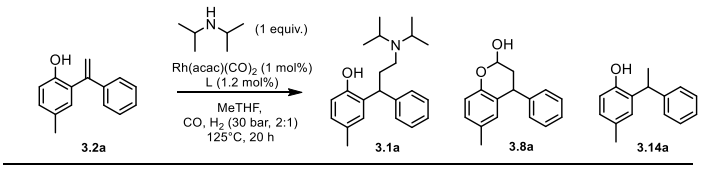

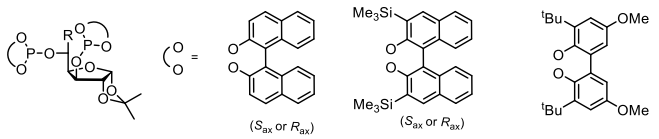

L15a, S_{ax}, R=H
L15b, R_{ax}, R=H
L15c, S_{ax}, R=H
L15d, R_{ax}, R=H
L15e, S_{ax}, R=CH_3
L15f, R_{ax}, R=CH_3
L15g, R=H

Entry[a]	Ligand	% Conv.	% 3.1a (% *ee*)	% 3.8a	% 3.14a
1	**L15a**	96	49 (41)	41	10
2	**L15b**	98	56 (12)	35	9
3	**L15c**	94	67 (7)	7	26
4	**L15d**	96	61 (25)	13	26
5	**L15e**	68	59 (17)	6	35
6	**L15f**	88	64 (27)	3	32
7	**L15g**	99	63 (0)	8	29

[a] ***Reaction conditions**: **1a** (0.12 mmol), Rh = [Rh(acac)(CO)$_2$] (1 mol%), **L** (1.2 mol %), P = 30 bar (H_2/CO, 1:2), MeTHF (0.2 ml), T = 125 °C, t = 20 h, 400 r.p.m. % ee of **3.1a** determined by chiral HPLC.*

3.2.3.2. Scope of substrates in the Rh-catalyzed asymmetric hydroaminomethylation of 1,1-diarylethenes.

At this stage, the scope of 1,1-diarylethene substrates that can be used in the Rh-catalyzed asymmetric hydroaminomethylation reactions was evaluated using ligand **L14e** (Table 10). In all cases, high conversions were obtained with ca. 50% chemoselectivity and ee's ranging from 14 to 36%. No clear conclusions could be drawn from the influence of the substrate substituents.

Table 10. Asymmetric Rh-catalyzed hydroaminomethylation of 3.2a-g to the chiral amines 3.1a-g using L14e.

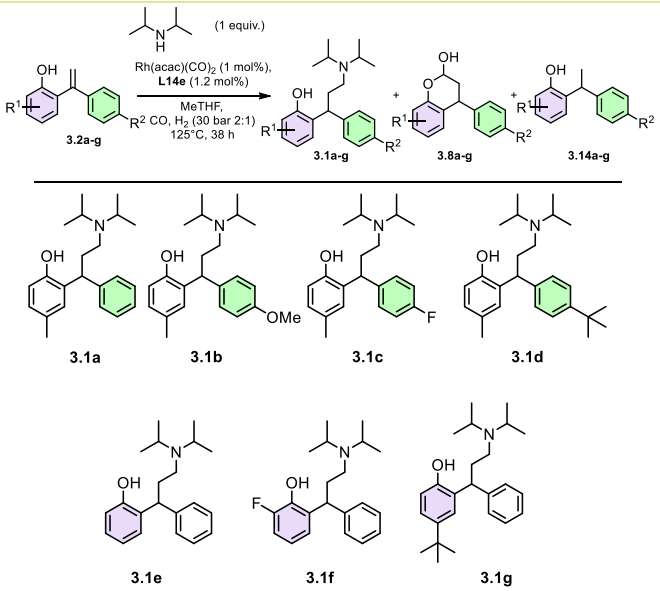

Entry	Substrate	Conv (%)	% **3.1** [yield]*	% ee (**3.1**)	% **3.8**	%**3.14**
1	**3.2a**	90	48 [42]	36	42	10
2	**3.2b**	85	46 [32]	32	41	13
3	**3.2c**	93	46 [39]	33	45	9
4	**3.2d**	84	44 [30]	17	38	18
5	**3.2e**	90	44 [36]	14	46	10
6	**3.2f**	97	51 [47]	27	40	9
7	**3.2g**	86	43 [34]	25	43	15

[a] ***Reaction conditions**: **1a** (0.12 mmol), Rh = [Rh(acac)(CO)$_2$] (1 mol%), **L14e** (1.2 mol %), P = 30 bar (H_2/CO, 1:2), MeTHF (0.2 mL), T = 125 °C, t = 38 h, 400 r.p.m. % ee of **3.1a** determined by chiral HPLC.* isolated yield.*

*3.2.3.3. Rh-catalyzed asymmetric hydroaminomethylation of protected phenol **3.20***

When the phenol-protected substrate **3.20** was tested in the Rh-catalyzed asymmetric hydroaminomethylation reaction (Table 11) using the ligands **L11**, **L13**, **L14** and **L15** (Scheme 15), only **L14c** (entry 4) outperformed the *ee* values obtained with the unprotected phenol substrates.

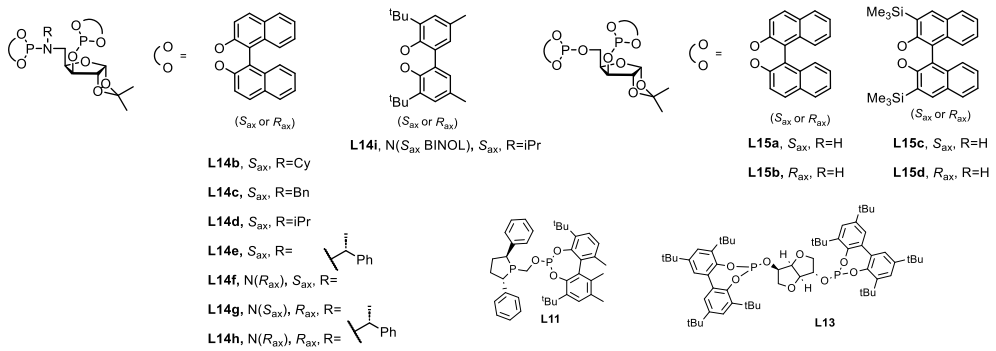

Scheme 15. Structure of ligands L11, L13-L15 used for the study of asymmetric HAM of 3.20

In other cases, **L15a** and also **L15c**, the *ortho*-$SiMe_3$ substituted BINOL gave disappointing activity with only 13% *ee* (entry 11) and 8%, respectively (entry 11 and 13). When the phenol **3.21** was substituted with a bulkier protecting group TBDPS, enantiomers separation was not possible using HPLC.

Table 11. Screening of ligands with substrate 3.20

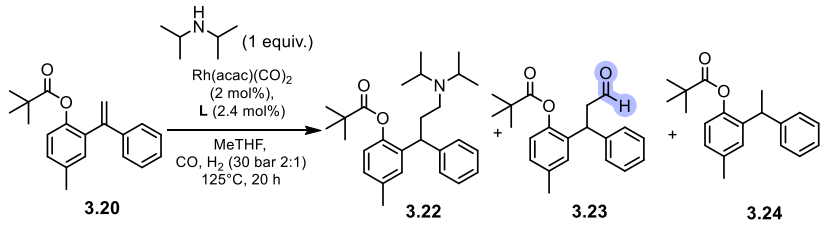

Entry	Ligand	Conv (%)	% **3.22** (%ee)	% **3.23**	% **3.24**
1	**L11**	53	82 (8)	2	16
2	**L13**	82	90 (3)	3	7
3	**L14b**	46	81 (28)	6	13
4	**L14c**	57	83 (46)	6	11
5	**L14d**	86	81 (25)	14	5
6[b]	**L14e**	62	84 (50)	10	6
7	**L14f**	34	96 (5)	0	4
8	**L14h**	17	65 (8)	22	13
9	**L14i**	48	79 (25)	7	15
10	**L14j**	58	84 (6)	6	10
11	**L14k**	53	75 (5)	7	18
12	**L15a**	100	90 (13)	5	5
13	**L15b**	76	95 (20)	3	2
14	**L15c**	19	81 (8)	8	12
15	**L15d**	60	79 (3)	2	19

[a] ***Reaction conditions**: 3.22 (0.12 mmol), Rh = [Rh(acac)(CO)$_2$] (2 mol%), L (2.4 mol %), P = 30 bar (H_2/CO, 1:2), MeTHF (0.2 ml), T = 125 °C, t = 20 h, 400 r.p.m. % ee of 3.22 determined by chiral HPLC.* [b] *t = 38 h.*

These results thus indicated that an increase in steric hindrance around the phenol group is not an efficient strategy to increase the enantioinduction with these catalytic systems.

*3.2.3.4. Rh-catalyzed asymmetric hydroformylation of **3.2a-g***

Next, we were interested in studying the asymmetric hydroformylation of substrates **3.2a-g** leading to the chromanols **3.8a-g** using the ligand **L14e**.

After the catalytic tests, the products **3.8** were isolated and oxidized into the chromanones **3.6** for determination of the enantiomeric excesses. The results are described in Table 12.

High conversions were obtained for all substrates (87-99%) with excellent chemoselectivity to the chromanol products (*ca.* 90%). In this reaction, the highest ee's (44 and 37%, entries 4 and 7 respectively) were obtained when a *tert*-butyl group was present in *para* position of one of the aryl substituents of the substrates. It is noteworthy that slightly higher chemo- and enantioselectivities were obtained in this hydroformylation reaction when compared to the results obtained in hydroaminomethylation. This again indicated that the presence of amine in the medium negatively affected the catalytic process.

Table 12. Asymmetric Rh-catalyzed hydroformylation of 3.2a-g to the chiral chromanols 3.8a-g using L14e.

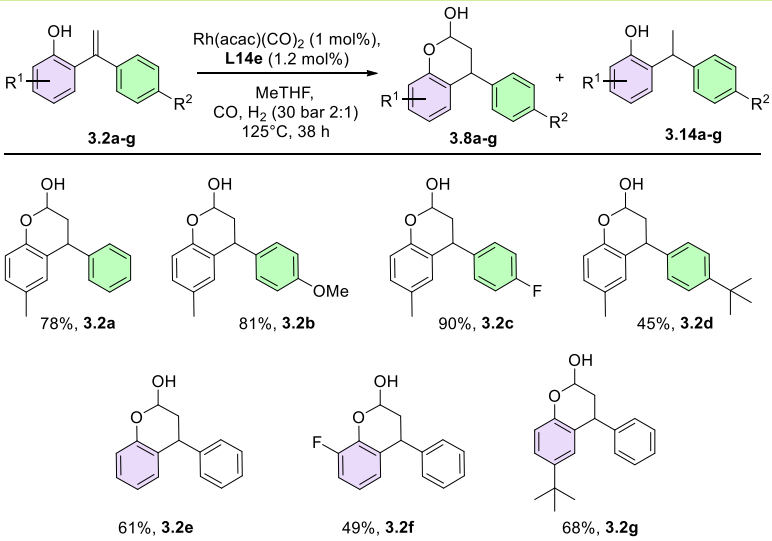

Entry	Substrate	Conv. (%)	% **3.8** [yield]*	ee **3.6** (%)	% **3.14**
1	**3.2a**	97	90 [78]	21	10
2	**3.2b**	87	88 [81]	22	12
3	**3.2c**	96	95 [90]	35	5
4	**3.2d**	96	88 [45]	44	12
5	**3.2e**	99	91 [61]	14	9
6	**3.2f**	99	94 [49]	28	6
7	**3.2g**	98	94 [68]	37	6

[a] ***Reaction conditions**: **1a** (0.12 mmol), Rh = [Rh(acac)(CO)$_2$] (1 mol%), **L14e** (1.2 mol %), P = 30 bar (H_2/CO, 1:2), MeTHF (0.2 ml), T = 125 °C, t = 38 h, 400 r.p.m. % ee of **3.1a** determined by chiral HPLC. *isolated yield.*

3.3. Conclusions

- The synthesis of 1,1-diarylethenes **3.2a-i** was performed using modified reported procedure. The optimized synthesis involved the use of microwave, providing the substrates in a straightforward manner and a short time.
- The racemic hydroaminomethylation was briefly optimized using the phosphine ligand **L8**. High temperature and high CO partial pressure were necessary to drive the reaction towards the formation of the amines products **3.1**.
- Racemic hydroaminomethylation of substrates **3.2a-g**, **3.20** and **3.21** was performed providing the racemic amines in moderate yield to good yield. The enantiomers were separated, except **3.25**, by chiral HPLC for subsequent analysis of the asymmetric reactions.
- Racemic hydroformylation of substrates **3.2a-g** was performed providing the racemic chromanols **3.8a-g** in moderate yield. The racemic products were oxidized to the chromanones **3.6a-g** which were separated by chiral HPLC.
- The asymmetric hydroaminomethylation of **3.2a** was optimized by screening the effect of the temperature, pressure, partial pressure, molarity and stoichiometry of the reaction using the chiral ligand **L14a**.
- A chiral ligand screening for the asymmetric hydroaminomethylation of **3.2a** was performed. The activity of the catalytic system was assessed in terms of conversion, chemoselectivity and enantioselectivity. Two classes of ligands stood out of the series tested, namely the sugar-based phosphite phosphoramidite **L14** and sugar-based bisphosphite **L15**.
- The ligand **L14e** was selected to evaluate the scope of substrates **3.2** in the asymmetric hydroaminomethylation reaction. Chiral amines were obtained in 30-47% yield and between 23 and 36% ee.
- In the asymmetric hydroaminomethylation of the protected phenol **3.20**, a second ligand screening was carried out. The chemoselectivity and

enantioselectivity were slightly enhanced compared to the hydroaminomethylation of the analog **3.2a**.

- The ligand **L14e** was selected for the asymmetric hydroformylation of **3.2**. The chiral chromanols **3.8a-g** were obtained in 45-90% yield. The oxidation of these compounds produced chromanones **3.6a-g** which were analyzed by chiral HPLC. The enantiomeric excesses obtained spanned from 14 and 44% demonstrating the importance of the substituents in the phenyl ring to reach high enantioselectivity.
- This methodology, beside the moderate enantioselectivity obtained, stands as the first direct asymmetric hydroaminomethylation of 1,1-diarylethenes towards Tolterodine and derivatives.

3.4. Experimental part

General considerations

All the reactions were carried out using Schlenk-line inert atmosphere techniques or glovebox techniques. Anhydrous solvents were collected from the system Braun MB SPS-800. Commercially available reagents and solvents were purchased at the highest commercial quality from Sigma-Aldrich, Fluka, Alfa Aesar, Fluorochem, Strem and were used as received, without further purification. Al_2O_3-SO_3H was synthesized via a reported procedure.[15]

^1H and $^{13}C\{^1H\}$ NMR spectra were recorded using a Varian Mercury VX 400 (400 and 100.6 MHz respectively). Chemical shift values (δ) are reported in ppm relative to TMS (^1H and $^{13}C\{^1H\}$) and coupling constants are reported in Hertz. The following abbreviations are used to indicate the multiplicity: s, singlet; d, doublet; t, triplet; q, quartet; quint, quintuplet; sext, sextuplet; sept, septet; oct, octet; m, multiplet; bs, broad signal. High-resolution mass spectra (HRMS) were recorded on a Bruker Daltonics Microtof Focus and/or Maxis Impact using ESI-TOF (electrospray ionization-time of flight). Samples were introduced to the mass spectrometer ion source by direct injection using a syringe pump and were externally calibrated using sodium formate. Enantiomeric excess was measured using HPLC Agilent instrument with Daicel Chiralpak IA, IC, ID, IF, AD-H and OD-H columns. Reactions were monitored by TLC carried out on 0.25 mm E. Merck silica gel 60 F_{254} aluminum plates. Developed TLC plates were visualized under a short-wave UV lamp (254 nm) and by heating plates that were dipped in potassium permanganate. Flash column chromatography was carried out using forced flow of the indicated solvent, on Merck silica gel 60 (230-400 mesh). The Rh-catalyzed hydroformylation reaction and Rh-catalyzed hydroaminomethylation reaction were set up in a CAT7 autoclave from HEL Inc. and stirred with a Teflon-coated magnetic stir bar.

General Procedure A. Synthesis of 1,1-disubstituted alkenes using MW

3.18a-e **3.19a-e** **3.2a-i**

The reaction was carried out in a 10 mL tube with a CEM Discover microwave system. Phenol (3 mmol), acetylene (2 mmol), Al_2O_3-SO_3H (200 mg) and toluene 1.2 mL were added inside the tube equipped with a magnetic stir bar. The mixture was stirred at 160°C for 1 h. Reaction mixture was filtered and purified with distillation under vacuum or flash chromatography using petroleum ether and ethyl acetate to afford the diphenylethene as a yellow oil in a range of 30-60% yield.

4-methyl-2-(1-phenylvinyl)phenol[15] (3.2a)

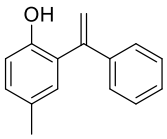

Synthesized according to general procedure A. The product was obtained as yellow oil in 60% yield. ^{1}H NMR (400 MHz, $CDCl_3$) δ 7.44 – 7.33 (m, 5H), 7.09 (dd, *J* = 8.2, 2.3 Hz, 1H), 6.98 (d, *J* = 2.4 Hz, 1H), 6.89 (dd, *J* = 8.3, 1.8 Hz, 1H), 5.88 (d, *J* = 1.4 Hz, 1H), 5.44 (d, *J* = 1.3 Hz, 1H), 5.05 (s, 1H), 2.31 (s, 3H). These signals are in agreement with those reported in the literature.

2-(1-(4-methoxyphenyl)vinyl)-4-methylphenol[17] (3.2b)

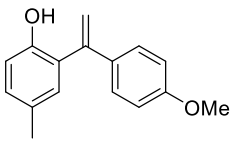

Synthesized according to general procedure A. The product was obtained as yellow oil in 30% yield. 1H NMR (400 MHz, $CDCl_3$) δ 7.38 – 7.29 (m, 2H), 7.07 (ddd, J = 8.3, 2.3, 0.8 Hz, 1H), 7.00 – 6.94 (m, 1H), 6.92 – 6.83 (m, 3H), 5.76 (d, J = 1.3 Hz, 1H), 5.30 (d, J = 1.3 Hz, 1H), 5.09 (s, 1H), 3.82 (s, 3H), 2.29 (d, J = 0.8 Hz, 3H). These signals are in agreement with those reported in the literature.

2-(1-(4-fluorophenyl)vinyl)-4-methylphenol (3.2c)

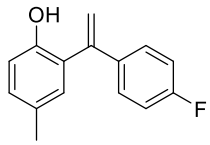

Synthesized according to general procedure A. The product was obtained as yellow oil in 60% yield. ^{1}H NMR (400 MHz, $CDCl_3$) δ 7.39 – 7.27 (m, 2H), 7.08 – 6.99 (m, 3H), 6.90 (d, J = 2.2 Hz, 1H), 6.85 (d, J = 8.2 Hz, 1H), 5.80 (d, J = 1.1 Hz, 1H), 5.37 (d, J = 1.2 Hz, 1H), 4.99 (s, 1H), 2.27 (d, J = 0.8 Hz, 3H).

^{13}C NMR (101 MHz, $CDCl_3$) δ 163.06 (d, J_{CF} = 248.3 Hz), 150.91, 144.55, 135.87 (d, J_{CF} = 3.2 Hz), 130.78, 130.25, 129.82, 128.94 (d, J_{CF} = 8.1 Hz), 127.22, 116.33 (d, J_{CF} = 1.6 Hz), 115.78 (d, J_{CF} = 3.3 Hz), 115.55, 20.56.

^{19}F NMR (377 MHz, $CDCl_3$) δ -113.31 (s).

HRMS (ESI) for **$C_{15}H_{13}FO$**. Calculated **M:** 228.0950, **$[M\text{-}H^+]^-$:** 227.0878, found: 227.0876.

2-(1-(4-(tert-butyl)phenyl)vinyl)-4-methylphenol[7] (3.2d)

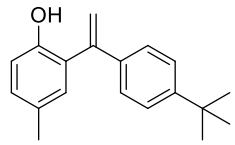

Synthesized according to general procedure A. The product was obtained as yellow oil in 60% yield. ^{1}H NMR (400 MHz, $CDCl_3$) δ 7.41 – 7.28 (m, 4H), 7.11 – 7.01 (m, 1H), 6.96 (dt, *J* = 2.2, 0.6 Hz, 1H), 6.85 (d, *J* = 8.2 Hz, 1H), 6.73 (d, *J* = 8.5 Hz, 1H), 5.84 (d, *J* = 1.3 Hz, 1H), 5.36 (d, *J* = 1.3 Hz, 1H), 5.01 (s, 1H), 2.28 (s, 3H), 1.32 (s, 9H). These signals are in agreement with those reported in the literature.

2-(1-phenylvinyl)phenol[15] (3.2e)

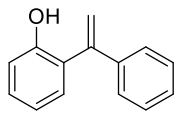

Synthesized according to general procedure A. The product was obtained as yellow oil in 50% yield. Synthesized via general procedure A. ^{1}H NMR (400 MHz, $CDCl_3$) δ 7.75 – 7.70 (m, 2H), 7.47 – 7.42 (m, 1H), 7.29 (ddt, *J* = 5.3, 2.6, 1.5 Hz, 2H), 7.26 – 7.19 (m, 5H), 6.27 (d, *J* = 1.3 Hz, 1H), 5.54 (s, 1H), 5.45 (d, *J* = 1.4 Hz, 1H). These signals are in agreement with those reported in the literature.

2-fluoro-6-(1-phenylvinyl)phenol (3.2f)

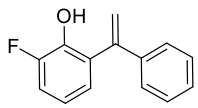

Synthesized according to general procedure A. The product was obtained as yellow oil in 40% yield. ^{1}H NMR (400 MHz, $CDCl_3$) δ 7.46 – 7.27 (m, 5H), 7.08 (ddd, *J* = 10.5, 8.1, 1.7 Hz, 1H), 6.96 (dt, *J* = 7.8, 1.5 Hz, 1H), 6.86 (td, *J* = 8.0, 5.1 Hz, 1H), 5.84 (d, *J* = 1.1 Hz, 1H), 5.44 (d, *J* = 1.1 Hz, 1H), 5.14 (s, 1H).

^{13}C NMR (101 MHz, $CDCl_3$) δ 151.37 (d, J_{CF} = 240.4 Hz), 144.85 (d, J_{CF} = 2.9 Hz), 141.58 (d, J_{CF} = 13.1 Hz), 139.78, 130.43 (d, J_{CF} = 1.8 Hz), 128.67, 128.44, 126.99, 126.09 (d, J_{CF} = 3.3 Hz), 120.16 (d, J_{CF} = 7.4 Hz), 117.09, 115.43 (d, J_{CF} = 18.2 Hz).

^{19}F NMR (377 MHz, $CDCl_3$) δ -138.84 (s).

HRMS (ESI) for **$C_{14}H_{11}FO$**. Calculated **M:** 214.0793, **[M-H$^+$]$^-$:** 213.0721, found: 213.0726.

4-(tert-butyl)-2-(1-phenylvinyl)phenol[18] (3.2g)

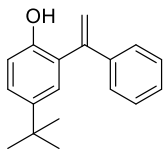

Synthesized according to general procedure A. The product was obtained as yellow oil in 55% yield. 1H NMR (400 MHz, $CDCl_3$) δ 7.41 – 7.23 (m, 5H), 7.14 (d, J = 2.5 Hz, 1H), 6.88 (d, J = 8.5 Hz, 1H), 6.81 – 6.72 (m, 1H), 5.87 (d, J = 1.3 Hz, 1H), 5.42 (d, J = 1.3 Hz, 1H), 4.98 (s, 1H), 1.29 (s, 9H). These signals are in agreement with those reported in the literature.

4-iodo-2-(1-phenylvinyl)phenol[15] (3.2h)

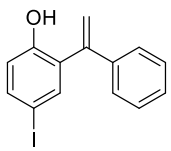

Synthesized according to general procedure A. The product was obtained as yellow oil in 58% yield. ^{1}H NMR (400 MHz, $CDCl_3$) δ 7.53 (dd, *J* = 8.5, 2.3 Hz, 1H), 7.46 (d, *J* = 2.3 Hz, 1H), 7.35 (s, 5H), 6.73 (d, *J* = 8.6 Hz, 1H), 5.87 (d, *J* = 1.0 Hz, 1H), 5.42 (d, *J* = 1.0 Hz, 1H), 5.09 (s, 1H). These signals are in agreement with those reported in the literature.

4-methyl-2-(1-(p-tolyl)vinyl)phenol[7] (3.2i)

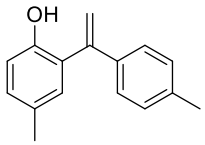

Synthesized according to general procedure A. The product was obtained as yellow oil in 55% yield. ^{1}H NMR (400 MHz, $CDCl_3$) δ 7.30 – 7.20 (m, 2H), 7.20 – 7.11 (m, 3H), 7.05 (dd, J = 8.2, 2.2 Hz, 1H), 6.95 (dt, J = 2.1, 1.0 Hz, 1H), 6.85 (dt, J = 8.1, 1.3 Hz, 1H), 5.80 (q, J = 1.2 Hz, 1H), 5.35 (t, J = 1.2 Hz, 1H), 5.02 – 4.97 (m, 1H), 2.36 (d, J = 1.2 Hz, 4H), 2.30 – 2.25 (m, 3H). These signals are in agreement with those reported in the literature.

General procedure B. Protection of the substrates

Pivaloyl chloride (265 mg, 269 µL, 1.1 Eq, 2.20 mmol) was added dropwise slowly to a solution of 4-methyl-2-(1-phenylvinyl)phenol (421 mg, 388 µL, 1 Eq, 2.00 mmol) and triethylamine (607 mg, 836 µL, 3 Eq, 6.00 mmol) in acetonitrile (13 mL) over 30 minutes at 0 °C. The mixture was then stirred at r.t. for 15 h. Reaction mixture was diluted with Et_2O and it was washed with aqueous 1N HCl (20 mL x 2), saturated aqueous $NaHCO_3$ (20 mL x 2) and brine (20 mL x 2). The organic phase was dried with $MgSO_4$ and concentrated under vacuum. The crude product was purified via column chromatography with silica gel to afford the protected phenol as an uncolored oil with 70% yield. (PE/EtOAC 99:1)

4-methyl-2-(1-phenylvinyl)phenyl pivalate (3.20)

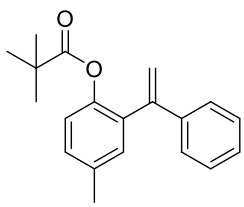

Synthesized according to general procedure B. The product was obtained as uncolored oil in 49% yield. ^{1}H NMR (400 MHz, $CDCl_3$) δ 7.35 – 7.20 (m, 6H), 7.19 – 7.12 (m, 1H), 7.12 – 7.08 (m, 1H), 6.92 (d, J = 8.2 Hz, 1H), 5.72 (d, J = 1.3 Hz, 1H), 5.27 (d, J = 1.3 Hz, 1H), 2.35 (d, J = 0.8 Hz, 3H), 1.01 (s, 9H).

^{13}C NMR (101 MHz, $CDCl_3$) δ 176.77, 174.08, 146.42, 145.78, 140.21, 135.42, 134.43, 131.97, 129.38, 128.27, 127.77, 126.79, 122.42, 116.07, 40.29, 38.88, 26.92, 26.61, 20.92.

HRMS (ESI) for **$C_{20}H_{22}O_2$**. Calculated **M:** 294.1619, **$[M+Na^+]^+$**: 317.1517, found: 317.1511.

tert-butyl(4-methyl-2-(1-phenylvinyl)phenoxy)diphenylsilane (3.21)[19]

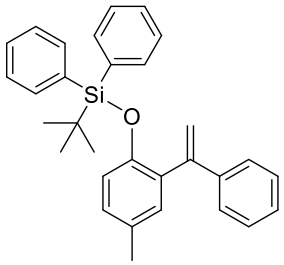

tert-Butyldiphenylsilyl chloride (181 mg, 169 µL, 0.66 mmol) was added dropwise to a stirred solution of **3.2a** (126 mg, 0.60 mmol) and imidazole (81.6 mg, 1.2 mmol) in DMF (0.4 mL) at room temperature. The reaction mixture was stirred for 16 h. Then, water (2 mL) was added and the resulting mixture was extracted with diethyl ether (5 mL) three times. Combined organic layers were dried over anhydrous $MgSO_4$ and concentrated under high vacuum. The crude product was purified by column chromatography on silica gel (hexane:ethyl acetate, 90:10) to yield **3.21** as a white solid (146 mg, 54% yield).

^{1}H NMR (400 MHz, $CDCl_3$) δ 7.64 – 7.56 (m, 4H), 7.45 – 7.36 (m, 4H), 7.35 – 7.28 (m, 6H), 7.25 – 7.21 (m, 1H), 7.06 (d, *J* = 2.5 Hz, 1H), 6.67 (ddd, *J* = 8.3, 2.4, 0.8 Hz, 1H), 6.27 (d, *J* = 8.3 Hz, 1H), 5.82 (d, *J* = 1.5 Hz, 1H), 5.35 (d, *J* = 1.5 Hz, 1H), 2.22 (s, 3H), 0.70 (s, 9H).

^{13}C NMR (101 MHz, $CDCl_3$) δ 150.66, 147.84, 140.89, 135.55, 133.05, 132.57, 132.28, 129.98, 129.82, 128.91, 128.29, 127.79, 127.60, 126.68, 118.97, 114.99, 26.08, 20.59, 19.18.

HRMS (ESI) for **$C_{31}H_{32}OSi$**. Calculated **M:** 448.2222, **$[M+H^+]^+$:** 449.2300, found: 449.2288.

General procedure C: Rh-catalyzed asymmetric hydroaminomethylation of 1,1-diphenylethenes.

A 5 mL glassware reactor tube was charged with 1,1-diphenylethene (0.15 mmol), amine (0.15 mmol), dicarbonyl(acetylacetonato)rhodium(I) (1 mol%) in MeTHF (0.1 mL) and chiral ligand (1.2 mol%) in MeTHF (0.1 mL). The reaction tube was placed in the reactor which was purged with 5 bars of CO (x3) and pressurized at 30 bars ($CO:H_2$ = 2:1). The reactor was stirred at 400 rpm and heated at 125°C for 20 h. The reaction was stopped by cooling the reactor with an ice bath followed by carefully venting of the system in a well-ventilated fumehood. The mixture was purified by chromatographic column using a Pasteur pipette (eluent PE to remove the starting materials and AcOEt, NEt_3 to isolate the product). The enantiomeric excess of the resulting amine was analyzed by chiral HPLC.

2-(3-(diisopropylamino)-1-phenylpropyl)-4-methylphenol[21] (3.1a)

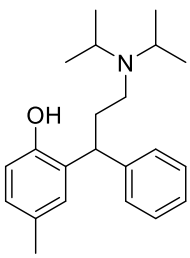

Synthesized according to general procedure C. The product was obtained as yellow oil in 42% yield. ^{1}H NMR (400 MHz, $CDCl_3$) δ 11.20 – 8.00 (br s, 1H), 7.37 – 7.17 (m, 5H), 6.89 – 6.77 (m, 2H), 6.55 (d, *J* = 2.1 Hz, 1H), 4.53 – 4.44 (m, 1H), 3.23 (hept, *J* = 6.7 Hz, 2H), 2.77 – 2.67 (m, 1H), 2.46 – 2.26 (m, 2H), 2.12 (s, 3H), 1.11 (dd, *J* = 21.5, 6.7 Hz, 12H). These signals are in agreement with those reported in the literature.

Enantiomers were separated by HPLC using Daicel Chiralpak ADH column with a gradient 95:5 nHexane/iPrOH + 0.1% DEA, flow rate 1 mL/mn, λ = 270 nm: tr_1= 8.74 min, tr_2 = 9.56 min or ID 98/02 tr_1= 8.16 min, tr_2 = 9.22 min. The major product (tr_2) was found to be (R)-**3.1a** according to the order of elution described in the literature.[20]

2-(3-(diisopropylamino)-1-(4-methoxyphenyl)propyl)-4-methylphenol (3.1b)

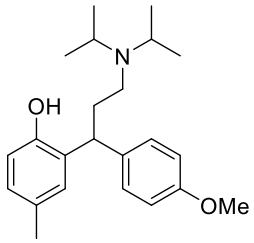

Synthesized according to general procedure C. The product was obtained as yellow oil in 32% yield. ^{1}H NMR (400 MHz, $CDCl_3$) δ 11.72 – 8.13 (br s, 1H), 7.28 – 7.22 (m, 2H), 6.87 (dd, J = 9.3, 2.6 Hz, 2H), 6.84 – 6.78 (m, 2H), 6.54 (d, J = 2.1 Hz, 1H), 4.43 (dd, J = 11.2, 3.8 Hz, 1H), 3.81 (s, 3H), 3.23 (hept, J = 6.6 Hz, 2H), 2.78 – 2.66 (m, 1H), 2.42 – 2.25 (m, 2H), 2.13 (s, 3H), 1.10 (dd, J = 21.6, 6.7 Hz, 12H).

^{13}C NMR (101 MHz, $CDCl_3$) δ 158.03, 153.27, 136.99, 132.84, 129.50, 129.45, 128.71, 127.77, 118.23, 113.80, 55.39, 48.02, 42.26, 38.68, 33.79, 25.49, 20.89, 20.08, 19.73.

HRMS (ESI) for **$C_{23}H_{33}NO_2$**. Calculated **M:** 355.2511, **$[M\text{-}H^+]^-$:** 354.2433, found: 354.2439.

Enantiomers were separated by HPLC using Daicel Chiralpak ADH column with a gradient 95:5 nHexane/iPrOH + 0.1% DEA, flow rate 1 mL/mn, λ = 270 nm: tr_1= 8.74 min, tr_2 = 9.56 min

2-(3-(diisopropylamino)-1-(4-fluorophenyl)propyl)-4-methylphenol (3.1c)

Synthesized according to general procedure C. The product was obtained as yellow oil in 39% yield. ^{1}H NMR (400 MHz, $CDCl_3$) δ 7.30 – 7.23 (m, 2H), 7.03 – 6.97 (m, 2H),

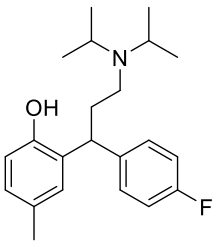

6.96 – 6.89 (m, 1H), 6.84 (dd, J = 2.2, 0.7 Hz, 1H), 6.50 (d, J = 2.2 Hz, 1H), 4.47 (dd, J = 11.5, 3.8 Hz, 1H), 3.22 (hept, J = 6.7 Hz, 2H), 2.76 – 2.68 (m, 1H), 2.36 – 2.31 (m, 2H), 2.13 (d, J = 0.8 Hz, 3H), 1.10 (dd, J = 22.0, 6.7 Hz, 12H).

^{13}C NMR (101 MHz, $CDCl_3$) δ 161.43 (d, J_{CF} = 244.1 Hz), 153.25, 140.61 (d, J_{CF} = 3.2 Hz), 132.37, 129.92 (d, J_{CF} = 7.7 Hz), 129.58, 128.65, 127.96, 118.36, 115.10 (d, J_{CF} = 21.0 Hz), 48.06, 42.20, 38.76, 33.64, 25.47, 20.86, 20.07, 19.68.

^{19}F NMR (377 MHz, $CDCl_3$) δ -117.06 (s).

HRMS (ESI) for **$C_{22}H_{30}FNO$**. Calculated **M:** 343.2311, **$[M\text{-}H^+]^-$:** 342.2233, found: 342.2229.

Enantiomers were separated by HPLC using Daicel Chiralpak ADH column with a gradient 98:2 nHexane/iPrOH + 0.1% DEA, flow rate 1 mL/mn, λ = 270 nm: tr_1= 15.75 min, tr_2 = 16.81 min OR Chiralpak IA column with a gradient 95:5 nHexane/iPrOH + 0.1% DEA, flow rate 1 mL/mn, λ = 270 nm: tr_1= 6.53 min, tr_2 = 6.88 min

2-(1-(4-(tert-butyl)phenyl)-3-(diisopropylamino)propyl)-4-methylphenol (3.1d)

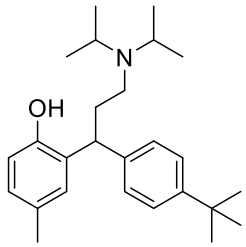

Synthesized according to general procedure C. The product was obtained as yellow oil in 30% yield. ^{1}H NMR (400 MHz, $CDCl_3$) δ 7.38 – 7.29 (m, 2H), 7.25 (d, *J* = 8.4 Hz, 2H), 6.88 – 6.76 (m, 2H), 6.59 (d, *J* = 2.1 Hz, 1H), 4.45 (dd, *J* = 11.3, 3.9 Hz, 1H), 3.24 (hept, *J* = 6.7 Hz, 2H), 2.76 – 2.68 (m, 1H), 2.43 – 2.30 (m, 1H), 2.14 (s, 3H), 1.32 (s, 9H), 1.13 (d, *J* = 6.7 Hz, 7H), 1.07 (d, *J* = 6.7 Hz, 6H).

^{13}C NMR (101 MHz, $CDCl_3$) δ 153.35, 149.00, 141.79, 132.70, 129.49, 128.78, 128.19, 127.83, 125.31, 118.36, 47.91, 42.07, 38.92, 34.51, 33.41, 31.54, 20.93, 20.17, 19.55. **HRMS** (ESI) for **$C_{26}H_{39}NO$**. Calculated **M:** 381.3031, **$[M\text{-}H^+]^-$:** 380.2953, found: 380.2965.

Enantiomers were separated by HPLC using Daicel Chiralpak IC column with a gradient 95:5 nHexane/iPrOH + 0.1% DEA, flow rate 1 mL/mn, λ = 270 nm: tr_1= 3.81 min, tr_2 = 3.99 min

2-(3-(diisopropylamino)-1-phenylpropyl)phenol (3.1e)

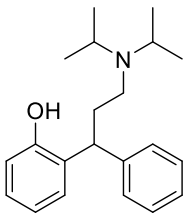

Synthesized according to general procedure C. The product was obtained as yellow oil in 36% yield. ^{1}H NMR (400 MHz, $CDCl_3$) δ 7.36 – 7.16 (m, 6H), 7.05 (ddd, *J* = 8.0, 6.0, 2.8 Hz, 1H), 6.95 – 6.87 (m, 1H), 6.79 – 6.67 (m, 2H), 4.55 – 4.47 (m, 1H), 3.25 (hept, *J* = 6.7 Hz, 2H), 2.79 – 2.68 (m, 1H), 2.48 – 2.30 (m, 2H), 2.18 – 2.02 (m, 2H), 1.12 (dd, *J* = 19.7, 6.7 Hz, 12H).

^{13}C NMR (101 MHz, $CDCl_3$) δ 155.76, 144.71, 132.81, 128.67, 128.46, 128.43, 127.31, 126.37, 120.43, 118.51, 48.43, 42.44, 39.70, 33.25, 27.23, 19.94, 19.64.

HRMS (ESI) for **$C_{21}H_{29}NO$**. Calculated **M:** 311.2249, **$[M\text{-}H^+]^-$:** 310.2170, found: 310.2171.

Enantiomers were separated by HPLC using Daicel Chiralpak ADH column with a gradient 95:5 nHexane/iPrOH + 0.1% DEA, flow rate 1 mL/mn, λ = 270 nm: tr_1= 6.68 min, tr_2 = 7.03 min

2-(3-(diisopropylamino)-1-phenylpropyl)-6-fluorophenol (3.1f)

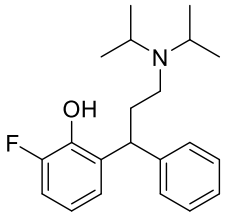

Synthesized according to general procedure C. The product was obtained as yellow oil in 47% yield. ^{1}H NMR (400 MHz, $CDCl_3$) δ 7.49 – 7.10 (m, 5H), 6.87 – 6.74 (m, 1H), 6.58 (td, *J* = 7.9, 5.0 Hz, 1H), 6.47 (dt, *J* = 7.9, 1.4 Hz, 1H), 4.49 (dd, *J* = 11.5, 3.9 Hz, 1H), 3.24 (hept, *J* = 6.8 Hz, 2H), 2.77 – 2.60 (m, 2H), 2.43 – 2.28 (m, 2H), 2.18 – 2.01 (m, 1H), 1.15 – 1.02 (m, 12H).

^{13}C NMR (101 MHz, $CDCl_3$) δ 153.55 (d, J_{CF} = 241.6 Hz), 144.56 (d, J_{CF} = 12.0 Hz), 144.44, 135.75 (d, J_{CF} = 2.0 Hz), 128.52, 128.46, 126.47, 123.43 (d, J_{CF} = 3.3 Hz), 119.28 (d, J_{CF} = 7.5 Hz), 113.61 (d, J_{CF} = 19.2 Hz), 48.19, 41.85, 39.57 (d, J_{CF} = 2.7 Hz), 32.95, 19.95, 19.27.

^{19}F NMR (377 MHz, $CDCl_3$) δ -136.47.

HRMS (ESI) for **$C_{21}H_{28}FNO$**. Calculated **M:** 329.2154, **$[M\text{-}H^+]^-$:** 328.2076, found: 328.2075.

Enantiomers were separated by HPLC using Daicel Chiralpak ADH column with a gradient 90:10 nHexane/iPrOH + 0.1% DEA, flow rate 1 mL/mn, λ = 270 nm: tr_1= 4.21 min, tr_2 = 5.10 min

4-(tert-butyl)-2-(3-(diisopropylamino)-1-phenylpropyl)phenol (3.1g)

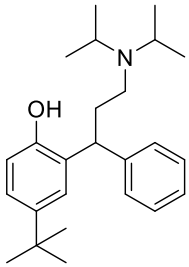

Synthesized according to general procedure C. The product was obtained as yellow oil in 34% yield. ^{1}H NMR (400 MHz, $CDCl_3$) δ 7.36 – 7.29 (m, 4H), 7.24 – 7.19 (m, 1H), 7.05 (dd, J = 8.4, 2.5 Hz, 1H), 6.83 – 6.77 (m, 2H), 4.46 (dd, J = 10.6, 4.1 Hz, 1H), 3.23 (hept, J = 6.7 Hz, 2H), 2.78 – 2.66 (m, 1H), 2.45 – 2.31 (m, 2H), 1.15 – 1.05 (m, 21H).

^{13}C NMR (100 MHz, $CDCl_3$) δ 153.11, 144.86, 142.81, 131.76, 128.68, 128.33, 126.26, 125.28, 123.93, 117.38, 48.22, 42.64, 40.13, 34.17, 33.95, 31.63, 29.85, 20.00.

HRMS (ESI) for **$C_{25}H_{37}NO$**. Calculated **M:** 367.2875, **$[M\text{-}H^+]^-$**: 366.2796, found: 366.2799.

Enantiomers were separated by HPLC using Daicel Chiralpak ADH column with a gradient 98:2 nHexane/iPrOH + 0.1% DEA, flow rate 1 mL/mn, λ = 270 nm: tr_1= 12.84 min, tr_2 = 18.55 min

2-(3-(diisopropylamino)-1-phenylpropyl)-4-methylphenyl pivalate (3.22)

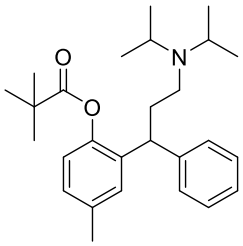

Synthesized according to general procedure C. The product was obtained as transparent oil in 65% yield. ^{1}H NMR (400 MHz, $CDCl_3$) δ 7.31 – 7.21 (m, 4H), 7.20 – 7.12 (m, 1H), 7.09 (d, J = 2.1 Hz, 1H), 6.99 (dd, J = 8.4, 2.0 Hz, 1H), 6.84 (d, J = 8.2 Hz, 1H), 4.08 (t, J = 7.6 Hz, 1H), 2.99 (p, J = 6.4 Hz, 2H), 2.35 (td, J = 8.5, 3.7 Hz, 2H), 2.29 (s, 3H), 2.14 (d, J = 15.5 Hz, 2H), 1.37 (s, 9H), 0.94 (dd, J = 6.8, 2.4 Hz, 12H).

^{13}C NMR (101 MHz, $CDCl_3$) δ 177.13, 146.68, 144.39, 136.50, 135.53, 129.01, 128.43, 128.04, 127.73, 126.17, 122.10, 48.94, 44.11, 41.49, 39.30, 27.48, 21.24, 20.84, 20.63.

Enantiomers were separated by HPLC using Daicel Chiralpak ADH column with a gradient 98:2 nHexane/iPrOH + 0.1% DEA, flow rate 1 mL/mn, λ = 270 nm: tr_1= 4.20 min, tr_2 = 4.82 min

HRMS (ESI) for **$C_{27}H_{39}NO_2$**. Calculated **M:** 409.2980, **$[M+H^+]^+$:** 410.3059, found: 410.3057.

3-(2-((tert-butyldiphenylsilyl)oxy)-5-methylphenyl)-N,N-diisopropyl-3-phenylpropan-1-amine (3.25)

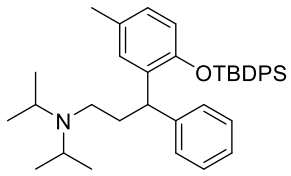

Synthesized according to general procedure C. The product was obtained as transparent oil in 38% yield. ^{1}H NMR (400 MHz, $CDCl_3$) δ 7.79 – 7.70 (m, 2H), 7.68 – 7.59 (m, 2H), 7.52 – 7.25 (m, 10H), 7.22 – 7.13 (m, 1H), 7.03 (d, *J* = 2.2 Hz, 1H), 6.50 (ddd, *J* = 8.3, 2.3, 0.8 Hz, 1H), 6.29 (d, *J* = 8.2 Hz, 1H), 4.80 (t, *J* = 7.7 Hz, 1H), 3.02 (hept, *J* = 6.5 Hz, 2H), 2.54 (ddd, *J* = 13.9, 9.1, 6.9 Hz, 1H), 2.48 – 2.34 (m, 1H), 2.29 – 2.17 (m, 2H), 2.15 (s, 3H), 1.33 – 1.23 (m, 2H), 1.09 (s, 9H), 0.97 (t, *J* = 6.5 Hz, 12H).

^{13}C NMR (101 MHz, $CDCl_3$) δ 150.52, 145.90, 135.56, 135.54, 134.36, 133.02, 132.84, 130.15, 129.94, 129.90, 128.94, 128.36, 128.17, 127.91, 126.88, 125.86, 118.76, 49.10, 44.47, 40.70, 38.14, 27.25, 26.73, 21.01, 20.88, 20.59, 19.57.

HRMS (ESI) for **$C_{38}H_{49}NOSi$**. Calculated **M:** 563.3583, **$[M+H^+]^+$:** 564.3661, found: 564.3664.

General procedure D: Rh-catalyzed asymmetric hydroformylation of 1,1-diphenylethenes.

A 5 mL glassware reactor tube was charged with 1,1-diphenylethene (116 µmol) dicarbonyl(acetylacetonato)rhodium(I) (1 mol%) in MeTHF (0.1 mL) and chiral ligand (1.2 mol%) in MeTHF (0.1 mL). The reaction tube was placed in the reactor which was purged with 5 bars of CO (x3) and pressurized at 30 bars ($CO:H_2$ = 2:1). The reactor was stirred at 400 rpm and heated at 125°C for 20 h. The reaction was stopped by cooling the reactor with an ice bath followed by carefully venting of the system in a well-ventilated fumehood. The mixture was purified by chromatographic

column using a Pasteur pipette with eluent AcOEt/PE (95/5). The enantiomeric excess of the resulting amine was analyzed by chiral HPLC.

6-methyl-4-phenylchroman-2-ol[21] (3.8a)

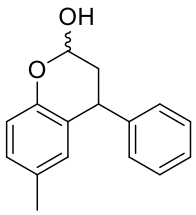

Synthesized according to general procedure D. The product was obtained as transparent oil in 78% yield. ^{1}H NMR (400 MHz, $CDCl_3$) δ 7.90 (s, 0H), 7.16 (s, 0H), 7.07 (ddd, *J* = 8.4, 5.2, 2.5 Hz, 3H), 6.92 (t, *J* = 8.7 Hz, 3H), 6.85 (dd, *J* = 8.2, 2.2 Hz, 1H), 6.69 (t, *J* = 8.3 Hz, 1H), 6.45 (q, *J* = 1.3 Hz, 1H), 6.42 – 6.38 (m, 0H), 5.57 – 5.51 (m, 1H), 5.41 (dd, *J* = 8.7, 2.2 Hz, 0H), 4.21 (dd, *J* = 11.2, 5.7 Hz, 1H), 4.13 – 4.00 (m, 0H), 2.86 (s, 1H), 2.79 (s, 1H), 2.32 (ddd, *J* = 13.3, 6.0, 2.1 Hz, 0H), 2.15 (ddd, *J* = 13.5, 5.7, 3.5 Hz, 1H), 2.06 (s, 4H), 2.04 – 1.95 (m, 2H), 1.52 – 1.39 (m, 1H), 1.25 – 1.01 (m, 4H), 0.78 (tdd, *J* = 9.0, 6.9, 2.0 Hz, 6H). These signals are in agreement with those reported in the literature.

Enantiomers (major) were separated by HPLC using Daicel Chiralpak IA column with a gradient 80:20 nHexane/iPrOH, flow rate 1 mL/mn, λ = 243 nm: tr_1= 6.08 min, tr_2 = 7.68 min.

4-(4-methoxyphenyl)-6-methylchroman-2-ol (3.8b)

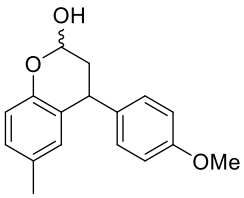

Synthesized according to general procedure D. The product was obtained as transparent oil in 81% yield. ^{1}H NMR (400 MHz, $CDCl_3$) δ 7.17 – 7.07 (m, 3H), 6.94 (ddt, *J* = 8.2, 2.2, 0.7 Hz, 1H), 6.91 – 6.83 (m, 3H), 6.78 (dd, *J* = 11.0, 8.2 Hz, 1H), 6.61 – 6.52 (m, 1H), 5.63 (d, *J* = 3.0 Hz, 1H), 5.51 (t, *J* = 7.0 Hz, 0H), 4.25 (dd, *J* = 11.0, 5.7 Hz, 1H), 3.82 (d, *J* = 0.7 Hz, 4H), 2.98 (d, *J* = 3.3 Hz, 1H), 2.42 (ddd, *J* = 13.2, 5.9, 2.4 Hz, 0H), 2.23 (ddd, *J* = 13.4, 5.8, 3.5 Hz, 1H), 2.15 (s, 4H), 2.12 – 2.05 (m, 1H).

^{13}C NMR (101 MHz, $CDCl_3$) δ 158.44, 149.86, 136.62, 130.21, 129.93, 129.86, 128.58, 125.43, 116.73, 114.12, 91.46, 55.39, 36.65, 36.23, 20.68.

HRMS (ESI) for **$C_{17}H_{18}O_3$**. Calculated **M:** 270.1255, **$[M+Na^+]^+$:** 293.1148, found: 293.1158.

Enantiomers (major) were separated by HPLC using Daicel Chiralpak ADH column with a gradient 80:20 nHexane/iPrOH, flow rate 1 mL/mn, λ = 243 nm: tr_1= 7.34 min, tr_2 = 10.54 min.

4-(4-fluorophenyl)-6-methylchroman-2-ol (3.8c)

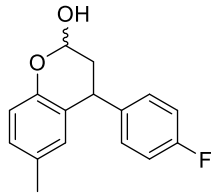

Synthesized according to general procedure D. The product was obtained as transparent oil in 90% yield. ^{1}H NMR (400 MHz, $CDCl_3$) δ 7.40 – 7.16 (m, 6H), 6.99 – 6.92 (m, 1H), 6.85 – 6.76 (m, 1H), 6.63 – 6.53 (m, 1H), 5.65 (p, *J* = 2.3 Hz, 1H), 5.53 (d, *J* = 7.6 Hz, 0H), 4.32 (dd, *J* = 11.0, 5.8 Hz, 1H), 4.20 (dd, *J* = 11.1, 5.9 Hz, 0H), 3.44 (d, *J* = 15.6 Hz, 1H), 2.46 (ddd, *J* = 13.2, 5.9, 2.4 Hz, 0H), 2.28 (dddd, *J* = 13.4, 5.9, 3.6, 0.9 Hz, 1H), 2.16 (d, *J* = 2.8 Hz, 5H), 1.30 (s, 0H), 0.99 – 0.83 (m, 1H).

^{13}C NMR (101 MHz, $CDCl_3$) δ 161.80 (d, J_{C-F} = 244.5 Hz), 149.83, 140.30 (d, J_{C-F} = 3.3 Hz), 130.35 (d, J_{C-F} = 7.7 Hz), 129.81, 128.77, 124.97, 116.86, 115.55 (d, *J* = 21.1 Hz), 91.29, 36.67, 36.35, 20.66.

^{19}F NMR (377 MHz, $CDCl_3$) δ -116.07 (0.23F), -116.36 (1F).

HRMS (APCI) for **$C_{16}H_{15}FO_2$**. Calculated **M:** 258.1056, **$[M\text{-}OH^-]^+$:** 241.1023, found: 241.1024.

Enantiomers (major) were separated by HPLC using Daicel Chiralpak IA column with a gradient 90:10 nHexane/iPrOH, flow rate 1 mL/mn, λ = 243 nm: tr_1= 8.89 min, tr_2 = 11.90 min.

4-(4-(tert-butyl)phenyl)-6-methylchroman-2-ol (3.8d)

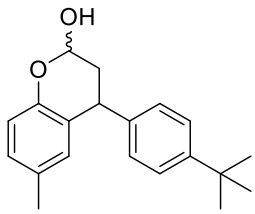

Synthesized according to general procedure D. The product was obtained as transparent oil in 45% yield. ^{1}H NMR (400 MHz, $CDCl_3$) δ 7.35 (d, *J* = 8.1 Hz, 3H), 7.13 (d, *J* = 8.2 Hz, 3H), 6.95 (dd, *J* = 8.2, 2.2 Hz, 1H), 6.80 (t, *J* = 9.3 Hz, 1H), 6.63 (s, 1H), 5.62 (dd, *J* = 3.9, 2.4 Hz, 1H), 4.28 (dd, *J* = 10.6, 5.9 Hz, 1H), 3.14 (s, 1H), 2.25 (ddd, *J* = 13.5, 6.0, 4.0 Hz, 1H), 2.17 (s, 5H), 1.37 – 1.32 (m, 11H).

^{13}C NMR (101 MHz, $CDCl_3$) δ 149.98, 149.55, 141.46, 130.23, 130.05, 128.62, 128.49, 125.77, 125.60, 116.77, 91.50, 42.44, 36.76, 36.66, 31.54, 20.70.

HRMS (ESI) for **$C_{20}H_{24}O_2$**. Calculated **M:** 296.1776, **$[M+Na^+]^+$:** 319.1669, found: 319.1670.

Enantiomers (major) were separated by HPLC using Daicel Chiralpak ADH column with a gradient 80:20 nHexane/iPrOH, flow rate 1 mL/mn, λ = 243 nm: tr_1= 4.78 min, tr_2 = 6.35 min.

4-phenylchroman-2-ol[21] (3.8e)

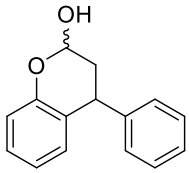

Synthesized according to general procedure D. The product was obtained as transparent oil in 61% yield. ^{1}H NMR (400 MHz, $CDCl_3$) δ 7.39 – 7.09 (m, 8H), 6.94 – 6.72 (m, 4H), 5.72 – 5.65 (m, 1H), 4.34 (dd, *J* = 11.2, 5.8 Hz, 1H), 3.06 (s, 1H), 2.29 (ddd, *J* = 13.5, 5.8, 3.4 Hz, 1H), 2.22 – 2.13 (m, 1H). These signals are in agreement with those reported in the literature.

Enantiomers (major) were separated by HPLC using Daicel Chiralpak ADH column with a gradient 80:20 nHexane/iPrOH, flow rate 1 mL/mn, λ = 243 nm: tr_1= 5.48 min, tr_2 = 7.25 min

8-fluoro-4-phenylchroman-2-ol (3.8f)

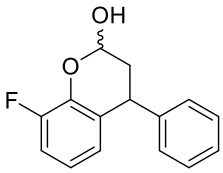

Synthesized according to general procedure D. The product was obtained as transparent oil in 49% yield. ^{1}H NMR (400 MHz, $CDCl_3$) δ 7.37 – 7.27 (m, 4H), 7.23 – 7.20 (m, 2H), 6.99 – 6.91 (m, 2H), 6.73 (td, *J* = 8.0, 5.1 Hz, 1H), 6.53 (dd, *J* = 7.9, 1.4 Hz, 1H), 5.79 (t, *J* = 2.8 Hz, 1H), 5.64 (dd, *J* = 8.5, 2.4 Hz, 0.3H), 4.35 (dd, *J* = 11.7, 5.7 Hz, 1H), 4.25 (dd, *J* = 10.9, 6.2 Hz, 0.3H), 3.32 (s, 1H), 2.50 (ddd, *J* = 13.5, 5.9, 2.4 Hz, 0H), 2.36 – 2.28 (m, 1H), 2.23 – 2.14 (m, 1H), 1.26 (d, *J* = 1.5 Hz, 5H).

^{19}F NMR (377 MHz, $CDCl_3$) δ -137.51.

^{13}C NMR (101 MHz, $CDCl_3$) δ 152.78, 151.71 (d, J_{CF} = 244.2 Hz), 143.66, 131.42, 128.76 (d, J_{CF} = 2.7 Hz), 128.42, 127.48, 126.96, 124.53 (d, J_{CF} = 3.5 Hz), 124.14 (d, J_{CF} = 19.7

Hz), 120.16 (d, J_{CF} = 7.4 Hz), 117.79, 114.13 (d, J_{CF} = 18.1 Hz), 91.50, 36.47 (d, J_{CF} = 2.6 Hz), 35.74.

HRMS (ESI) for **$C_{15}H_{13}FO_2$**. Calculated **M:** 244.0899, **$[M+Na^+]^+$:** 267.0792, found: 267.0800.

Enantiomers (major) were separated by HPLC using Daicel Chiralpak IF column with a gradient 80:20 nHexane/iPrOH, flow rate 1 mL/mn, λ = 243 nm: tr_1= 4.51 min, tr_2 = 4.82 min

6-(tert-butyl)-4-phenylchroman-2-ol (3.8g)

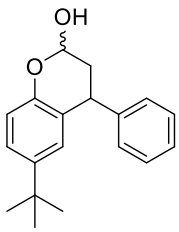

Synthesized according to general procedure D. The product was obtained as transparent oil in 68% yield. ^{1}H NMR (400 MHz, $CDCl_3$) δ 7.37 – 7.27 (m, 4H), 7.24 – 7.15 (m, 4H), 6.89 – 6.75 (m, 3H), 5.63 (s, 1H), 5.54 (s, 0.3H), 4.33 (dd, *J* = 10.7, 5.8 Hz, 1H), 4.24 (dd, *J* = 10.6, 5.9 Hz, 0.3H), 2.99 (s, 1H), 2.47 (ddd, *J* = 13.3, 5.9, 2.4 Hz, 0H), 2.27 (ddd, *J* = 13.5, 5.8, 3.8 Hz, 1H), 2.19 – 2.10 (m, 1H), 1.15 (s, 11H).

^{13}C NMR (101 MHz, $CDCl_3$) δ 149.82, 144.61, 143.77, 128.90, 128.68, 126.77, 126.68, 124.97, 124.36, 116.33, 91.49, 37.36, 36.69, 34.19, 31.54.

HRMS (ESI) for **$C_{19}H_{22}O_2$**. Calculated **M:** 282.1619, **$[M+Na^+]^+$:** 305.1512, found: 305.1516.

General procedure E: Oxidation of chromanols 3.8a-g to chromanones 3.6a-g. [21]

To a solution of chromanols **3.8** (1 equiv) in DCM (0.1 M) was added PCC (3 equiv). The reaction mixture was stirred at room temperature for 3 h. The reaction mixture was diluted with DCM and washed with water. The aqueous layer was extracted with DCM and the organic phase was washed with brine, dried over $MgSO_4$, filtered, and dried under vacuum to afford the product as an orange oil.

6-methyl-4-phenylchroman-2-one[21] (3.6a)

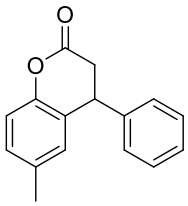

Synthesized according to general procedure E. The product was obtained as an orange oil in quantitative yield. ^{1}H NMR (400 MHz, $CDCl_3$) δ 7.40 – 7.26 (m, 3H), 7.26 – 7.06 (m, 3H), 7.03 (d, *J* = 8.2 Hz, 1H), 6.79 (d, *J* = 2.1 Hz, 1H), 4.30 (t, *J* = 6.7 Hz, 1H), 3.11 – 2.95 (m, 2H), 2.26 (s, 3H). These signals are in agreement with those reported in the literature.

Enantiomers (major) were separated by HPLC using Daicel Chiralpak ODH column with a gradient 95:5 nHexane/iPrOH, flow rate 0.8 mL/mn, λ = 243 nm: tr_1= 16.36 min, tr_2 = 18.70 min

4-(4-methoxyphenyl)-6-methylchroman-2-one[22] (3.6b)

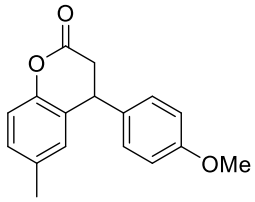

Synthesized according to general procedure E. The product was obtained as an orange oil in quantitative yield. ^{1}H NMR (400 MHz, $CDCl_3$) δ 7.04 (dd, *J* = 23.4, 7.5 Hz, 4H), 6.88 (d, *J* = 7.9 Hz, 2H), 6.78 (s, 1H), 4.26 (d, *J* = 6.7 Hz, 1H), 3.80 (s, 3H), 2.99 (qd, *J* = 15.5, 6.3 Hz, 2H), 2.26 (s, 3H). These signals are in agreement with those reported in the literature.

^{13}C NMR (101 MHz, $CDCl_3$) δ 168.00, 158.97, 149.62, 134.30, 132.47, 129.22, 128.61, 125.79, 116.84, 114.49, 55.32, 39.99, 37.36, 20.78.

Enantiomers were separated by HPLC using Daicel Chiralpak IA column with a gradient 95:5 nHexane/iPrOH, flow rate 0.8 mL/mn, λ = 243 nm: tr_1= 18.89 min, tr_2 = 23.88 min

4-(4-fluorophenyl)-6-methylchroman-2-one[6] (3.6c)

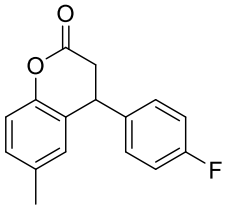

Synthesized according to general procedure E. The product was obtained as an orange oil in quantitative yield. ^{1}H NMR (400 MHz, $CDCl_3$) δ 7.16 – 7.08 (m, 3H), 7.04 (t, *J* = 8.1 Hz, 3H), 6.79 – 6.74 (m, 1H), 4.29 (t, *J* = 6.5 Hz, 1H), 3.05 (dd, *J* = 15.9, 5.8 Hz, 1H), 2.96 (dd, *J* = 15.8, 7.3 Hz, 1H), 2.27 (s, 3H). These signals are in agreement with those reported in the literature.

^{13}C NMR (101 MHz, $CDCl_3$) δ 167.58, 162.11 (d, J_{CF} = 246.3 Hz), 149.61, 136.27, 134.47, 129.50, 129.13 (d, J_{CF} = 8.0 Hz), 128.55, 125.13, 117.00, 116.04 (d, J_{CF} = 21.3 Hz), 40.08, 37.30, 20.77.

^{19}F NMR (377 MHz, $CDCl_3$) δ -114.73.

Enantiomers were separated by HPLC using Daicel Chiralpak IA column with a gradient 95:5 nHexane/iPrOH, flow rate 0.8 mL/mn, λ = 243 nm: tr_1= 14.45 min, tr_2 = 18.83 min

4-(4-(tert-butyl)phenyl)-6-methylchroman-2-one[7] (3.6d)

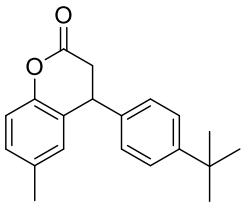

Synthesized according to general procedure E. The product was obtained as an orange oil in quantitative yield. ^{1}H NMR (400 MHz, $CDCl_3$) δ 7.39 – 7.31 (m, 2H), 7.16 – 6.98 (m, 4H), 6.85 – 6.80 (m, 1H), 4.27 (t, *J* = 6.5 Hz, 1H), 3.10 – 2.94 (m, 2H), 2.27 (s, 3H), 1.31 (s, 9H). These signals are in agreement with those reported in the literature.

^{13}C NMR (101 MHz, $CDCl_3$) δ 168.03, 150.47, 149.67, 137.47, 134.28, 129.22, 128.74, 127.09, 126.01, 125.49, 116.86, 77.22, 40.32, 37.20, 34.51, 31.31, 20.78.

Enantiomers were separated by HPLC using Daicel Chiralpak ODH column with a gradient 95:5 nHexane/iPrOH, flow rate 1 mL/mn, λ = 243 nm: tr_1= 8.53 min, tr_2 = 10.80 min

4-phenylchroman-2-one[21] (3.6e)

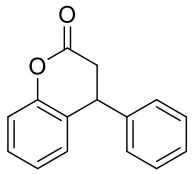

Synthesized according to general procedure E. The product was obtained as an orange oil in quantitative yield. ^{1}H NMR (400 MHz, $CDCl_3$) δ 7.39 – 7.27 (m, 4H), 7.20 – 7.01 (m, 4H), 7.01 – 6.95 (m, 1H), 4.39 – 4.31 (m, 1H), 3.14 – 2.96 (m, 2H). These signals are in agreement with those reported in the literature.

Enantiomers were separated by HPLC using Daicel Chiralpak ODH column with a gradient 98:2 nHexane/iPrOH, flow rate 0.8 mL/mn, λ = 243 nm: tr_1= 30.55 min, tr_2 = 32.86 min

8-fluoro-4-phenylchroman-2-one (3.6f)

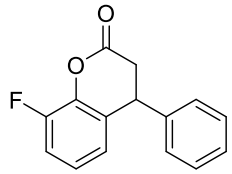

Synthesized according to general procedure E. The product was obtained as an orange oil in quantitative yield. ^{1}H NMR (400 MHz, $CDCl_3$) δ 7.39 – 7.28 (m, 3H), 7.18 – 7.14 (m, 2H), 7.10 (ddd, *J* = 9.9, 8.2, 1.5 Hz, 1H), 7.02 (td, *J* = 8.0, 4.9 Hz, 1H), 6.78 – 6.71 (m, 1H), 4.38 (t, *J* = 6.9 Hz, 1H), 3.16 – 3.00 (m, 2H).

^{13}C NMR (100 MHz, $CDCl_3$) δ 166.22, 150.46 (d, J_{CF} = 250.0 Hz) 139.81, 129.39, 128.89 (d, J_{CF} = 2.5 Hz), 128.04, 127.64, 127.10, 124.66 (d, J_{CF} = 6.7 Hz), 123.34 (d, J_{CF} = 3.7 Hz), 115.96 (d, J_{CF} = 17.7 Hz), 40.97, 36.86.

^{19}F NMR (377 MHz, $CDCl_3$) δ -132.77.

HRMS (ESI) for **$C_{15}H_{11}FO_2$**. Calculated **M:** 242.0743, **$[M+Na^+]^+$:** 265.0640, found: 265.0635.

Enantiomers (major) were separated by HPLC using Daicel Chiralpak IA column with a gradient 95:5 nHexane/iPrOH, flow rate 1 mL/mn, λ = 243 nm: tr_1= 13.17 min, tr_2 = 14.13 min

6-(tert-butyl)-4-phenylchroman-2-one (3.6g)

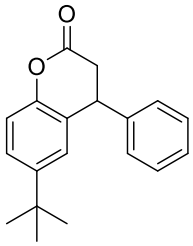

Synthesized according to general procedure E. The product was obtained as an orange oil in quantitative yield. ^{1}H NMR (400 MHz, $CDCl_3$) δ 7.38 – 7.28 (m, 4H), 7.18 – 7.13 (m, 2H), 7.07 (d, *J* = 8.5 Hz, 1H), 7.01 (dd, *J* = 2.4, 0.8 Hz, 1H), 4.33 (t, *J* = 6.5 Hz, 1H), 3.70 – 3.63 (m, 1H), 3.11 – 2.98 (m, 2H), 1.24 (s, 9H).

^{13}C NMR (101 MHz, $CDCl_3$) δ 168.06, 140.80, 129.23, 127.71, 127.63, 125.89, 125.39, 124.91, 116.73, 41.17, 37.50, 31.49, 29.85, 22.84, 14.27.

HRMS (ESI) for **$C_{19}H_{20}O_2$**. Calculated **M:** 280.1463, **$[M+H^+]^-$:** 281.1541, found: 281.1535.

Enantiomers were separated by HPLC using Daicel Chiralpak IA column with a gradient 95:5 nHexane/iPrOH, flow rate 1 mL/mn, λ = 243 nm: tr_1= 7.95 min, tr_2 = 9.00 min

3.5. References

[1] Nilvebrant, L.; Hallen, B.; Larsson, G. Tolterodine - a new bladder-selective muscarinic receptor antagonist: preclinical pharmacological and clinical data. *Life Sci.* **1997**, *60*, 1129–1136.

[2] Tolterodine - Drug Usage Statistics. *ClinCalc*. Retrieved 7 October 2022.

[3] Joensson, N. A.; Sparf, B. A.; Mikiver, L.; Moses, P.; Nilvebrant, L.; Glas, G. 3, 3- Diphenylpropylamines as drugs, especially anticholinergic agents, and their preparation and formulations containing them, EP 325571 (1998).

[4] Gage, J. R.; Cabaj, J. E. (Pharmacia & Upjohn Co.). U.S. Patent 5,922,914, 1999.

[5] Chen, G.; Tokunaga, N.; Hayashi, T. Rhodium-Catalyzed Asymmetric 1,4-Addition of Arylboronic Acids to Coumarins: Asymmetric Synthesis of (R)-Tolterodine. *Org. Lett.* **2005**, *7* (11), 2285–2288.

[6] Lai, J.; Yang, C.; Csuk, R.; Song, B.; Li, S. Palladium Catalyzed Enantioselective Hayashi–Miyaura Reaction for Pharmaceutically Important 4-Aryl-3,4-Dihydrocoumarins. *Org. Lett*. **2022**, *24* (6), 1329–1334.

[7] Tian, D.; Xu, R.; Zhu, J.; Huang, J.; Dong, W.; Claverie, J.; Tang, W. Asymmetric Hydroesterification of Diarylmethyl Carbinols. *Angew. Chemie Int. Ed.* **2021**, *60* (12), 6305–6309.

[8] Ulgheri, F.; Marchetti, M.; Piccolo, O. Enantioselective Synthesis of (S)- and (R)-Tolterodine by Asymmetric Hydrogenation of a Coumarin Derivative Obtained by a Heck Reaction. *J. Org. Chem.* **2007**, *72* (16), 6056–6059.

[9] Wang, X.; Guram, A.; Caille, S.; Hu, J.; Preston, J. P.; Ronk, M.; Walker, S. Highly Enantioselective Hydrogenation of Styrenes Directed by 2′-Hydroxyl Groups. *Org. Lett.* **2011**, *13* (7), 1881–1883.

[10] Wu, Z.; Laffoon, S. D.; Hull, K. L. Asymmetric Synthesis of γ-Branched Amines via Rhodium-Catalyzed Reductive Amination. *Nat. Commun.* **2018**, *9* (1), 1–7.

[11] Botteghi, C.; Corrias, T.; Marchetti, M.; Paganelli, S.; Piccolo, O. A New Efficient Route to Tolterodine. *Org. Process Res. Dev.* **2002**, *6* (4), 379–383.

[12] Margalef, J.; Langlois, J.; Garcia, G.; Godard, C.; Diéguez, M. Evolution in the Metal-Catalyzed Asymmetric Hydroformylation of 1,1′-Disubstituted Alkenes. In *Advances in Catalysis*; **2021**; Vol. 69, pp 181–215.

[13] Chakrabortty, S.; Almasalma, A. A.; de Vries, J. G. Recent Developments in Asymmetric Hydroformylation. *Catal. Sci. Technol.* **2021**, *11* (16), 5388–5411.

[14] (a) Rische, T.; Eilbracht, P. One-Pot Synthesis of Pharmacologically Active Secondary and Tertiary 1-(3,3-Diarylpropyl)Amines via Rhodium-Catalysed Hydroaminomethylation of 1,1- Diarylethenes. *Tetrahedron* **1999**, *55* (7), 1915–1920. (b) Ahmed, M.; Seayad, A. M.; Jackstell, R.; Beller, M. Amines Made Easily: A Highly Selective Hydroaminomethylation of Olefins. *J. Am. Chem. Soc.* **2003**, *125* (34),

10311–10318. (c) Ahmed, M.; Buch, C.; Routaboul, L.; Jackstell, R.; Klein, H.; Spannenberg, A.; Beller, M. Hydroaminomethylation with Novel Rhodium-Carbene Complexes: An Efficient Catalytic Approach to Pharmaceuticals. *Chem. - A Eur. J.* **2007**, *13* (5), 1594–1601. (d) Li, S.; Huang, K.; Zhang, J.; Wu, W.; Zhang, X. Cascade Synthesis of Fenpiprane and Related Pharmaceuticals via Rhodium-Catalyzed Hydroaminomethylation. *Org. Lett.* **2013**, *15* (5), 1036–1039.

[15] Pramanik, A.; Ghatak, A.; Khan, S.; Bhar, S. Hydroarylation of Alkynes and Alkenes through Alumina-Sulfuric Acid Catalyzed Regioselective C–C Bond Formation. *Tetrahedron Lett.* **2019**, *60* (16), 1091–1095.

[16] Cunillera, A.; De Los Bernardos, M. D.; Urrutigoïty, M.; Claver, C.; Ruiz, A.; Godard, C. Efficient Synthesis of Chiral γ-Aminobutyric Esters: Via Direct Rhodium-Catalysed Enantioselective Hydroaminomethylation of Acrylates. *Catal. Sci. Technol.* **2020**, *10* (3), 630–634.

[17] Wang, Z.; Ai, F.; Wang, Z.; Zhao, W.; Zhu, G.; Lin, Z.; Sun, J. Organocatalytic Asymmetric Synthesis of 1,1-Diarylethanes by Transfer Hydrogenation. *J. Am. Chem. Soc.* **2015**, *137* (1), 383–389.

[18] Hu, F.; Xia, Y.; Ye, F.; Liu, Z.; Ma, C.; Zhang, Y.; Wang, J. Rhodium(III)-Catalyzed Ortho Alkenylation of n-Phenoxyacetamides with n-Tosylhydrazones or Diazoesters through C-H Activation. *Angew. Chemie - Int. Ed.* **2014**, *53* (5), 1364–1367..

[19] Mir, R.; Dudding, T. Phase-Transfer Catalyzed O-Silyl Ether Deprotection Mediated by a Cyclopropenium Cation. *J. Org. Chem.* **2017**, *82* (1), 709–714.

[20] Hedberg, C.; Andersson, P. G. Catalytic Asymmetric Total Synthesis of the Muscarinic Receptor Antagonist (R)-Tolterodine. *Adv. Synth. Catal.* **2005**, *347* (5), 662–666.

[21] Wang, L.; Zhou, P.; Lin, Q.; Dong, S.; Liu, X.; Feng, X. Chiral Fe(II) Complex Catalyzed Enantioselective [1,3] O-to-C Rearrangement of Alkyl Vinyl Ethers and Synthesis of Chromanols and Beyond. *Chem. Sci.* **2020**, *11* (37), 10101–10106.

[22] Chen, G.; Tokunaga, N.; Hayashi, T. Rhodium-Catalyzed Asymmetric 1,4-Addition of Arylboronic Acids to Coumarins: Asymmetric Synthesis of (R)-Tolterodine. *Org. Lett.* **2005**, *7* (11), 2285–2288.

CHAPTER IV

RH-CATALYZED HYDROAMINOMETHYLATION OF 1,1-CYCLOPROPYLMETHACRYLAMIDES

4.1. Introduction

Among amine containing molecules, amino acids are the most crucial molecules in human life, since they present relevant biological activity and act as precursors in the synthesis of hormones and low-molecular weight nitrogenous substances having biological importance.[1]

γ-amino acids act as major inhibitory transmitters in the mammalian central nervous system.[2] Furthermore, gamma-aminobutyric acid (GABA) derivatives with substituents in the carbon chain were applied in the treatment of diseases and disorders including anxiety, depression, epilepsy, autism spectrum disorder, stroke, drug and neurodegenerative disorders: Huntington's disease, Parkinson's disease and Alzheimer's disease.[3] Some examples of drugs containing *γ*-amino acid motif commercialized by pharmaceutical agents are Baclofen,[4] Pregabalin,[5] Vigabatrin,[6] and Phenibut.[7] Moreover, compounds featuring the GABA motif with amide groups were recently assessed as CCR2 antagonists for addressing chronic inflammatory conditions like atherosclerosis, multiple sclerosis, and rheumatoid arthritis. Nevertheless, the production of these compounds demands substantial synthetic efforts. For instance, the synthesis of the CCR2 antagonist molecule **4.1** is usually achieved in 5 steps (Scheme 1) in an overall yield <1%.

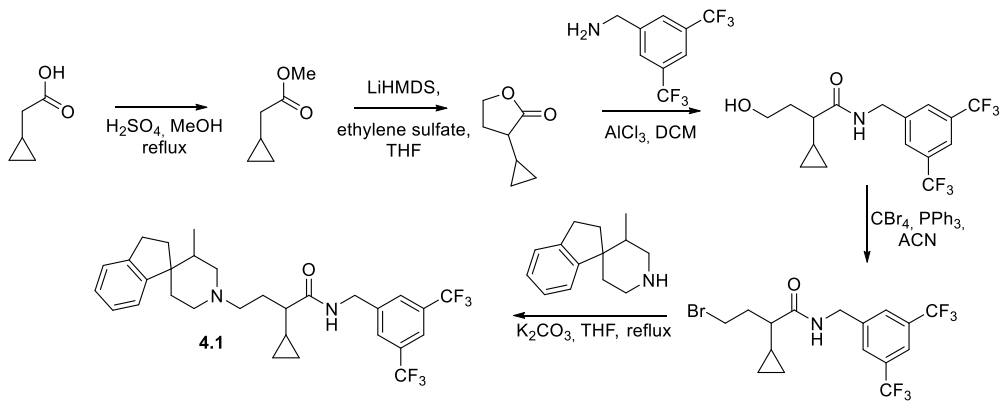

Scheme 1. Synthesis of CCR2 antagonist 4.1.

The possibility to access chiral GABA and derivatives through a more direct approach to reduce the number of synthetic steps would thus be of interest. In this context, the rhodium catalyzed asymmetric hydroaminomethylation would be an attractive and simple approach to access the α-substituted-γ-aminobutyric acid scaffold. On one hand, the number of synthetic steps would be reduced, and on the other hand, the production of enantio-enriched GABA motifs would not require the use of chiral auxiliaries to induce enantioselectivity, and would avoid an enantioresolution process to separate the enantiomers. As such, the asymmetric HAM of the cyclopropyl acrylamide **4.2** with the spirocyclic amine **4.3** could yield **4.1** based on the retrosynthetic route described in Scheme 2.

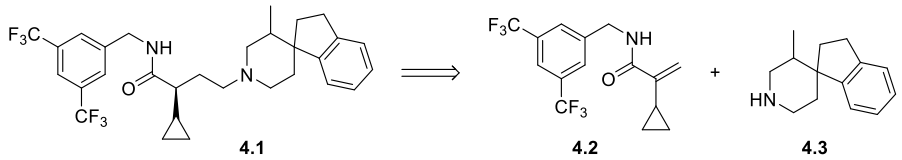

Scheme 2. Retrosynthetic analysis for the production of CCR2 antagonist 4.1 via HAM.

A drawback of this strategy involved the presence of a vinylcyclopropyl moiety in the starting material, which could undergo undesired side reactions. The reactivity of molecules bearing such a group is summarized in the next section.

4.1.1. Reactivity of vinylcyclopropanes

Vinylcyclopropanes (VCPs) have found extensive application in transition-metal-catalyzed cycloaddition reactions due to the presence of an olefin group that guides the transition-metal towards the selective cleavage of C–C bonds.[8] Additionally, the considerable strain energy of VCPs (approximately 28 kcal/mol) facilitates the energetically favorable opening of the cyclopropane ring, generating active π-allyl-metal complexes. Consequently, the transition-metal-catalyzed activation of VCPs, when combined with a wide array of unsaturated acceptors, has led to the emergence of novel cycloaddition patterns in organic synthesis. The bonding arrangement in VCPs allows for an s-trans–gauche conformational equilibrium, optimizing the orbital overlap between the p-orbitals of the cyclopropane ring and

the π-or π*-orbitals of the vinyl unit (Scheme 3). Generally, VCPs are categorized based on the substitution pattern of the activated cyclopropane: activated VCPs feature potent electron-withdrawing groups (EWGs), while non-activated VCPs lack these EWGs (refer to Scheme 3c). Depending on whether the vinyl substituent participates in the cycloaddition, VCPs can act as either three- or five-carbon building blocks. In their role as three-carbon building blocks, VCPs primarily engage in [3 + 2] and [3 + 2 + 1] cycloadditions, yielding five- and six-membered rings. As five-carbon building blocks, VCPs partake in a diverse range of cycloadditions, including [5 + 1], [5 + 2], [5 + 2 + 1], and [5 + 1 + 2 + 1], leading to the formation of mono- or fused six-, seven-, and even eight-membered ring systems. Through the utilization of VCPs as either three- or five-carbon building blocks, both intramolecular and intermolecular cycloaddition reactions were employed to efficiently produce a wide variety of skeletal structures.

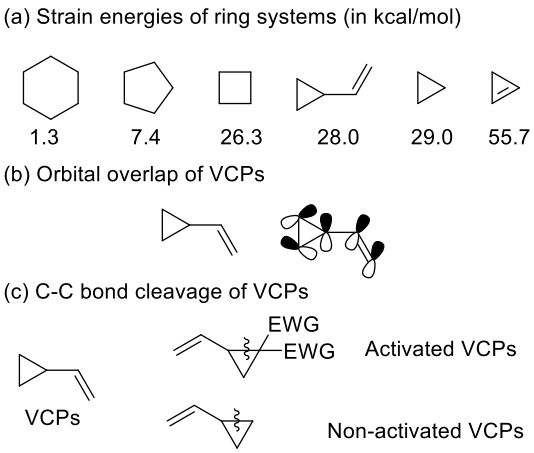

Scheme 3. VCPs particularities.[8]

VCPs were reported in reactions with Ru, Ni, Pd, Ir, Co, Fe and Rh based metal catalysts.[8] Among them, Rh was one of the most studied as it was active in both C-C bond cleavage of activated and non-activated VCPs in either inter- or intramolecular processes. In the next section, only Rh-based C-C bond cleavage is described.

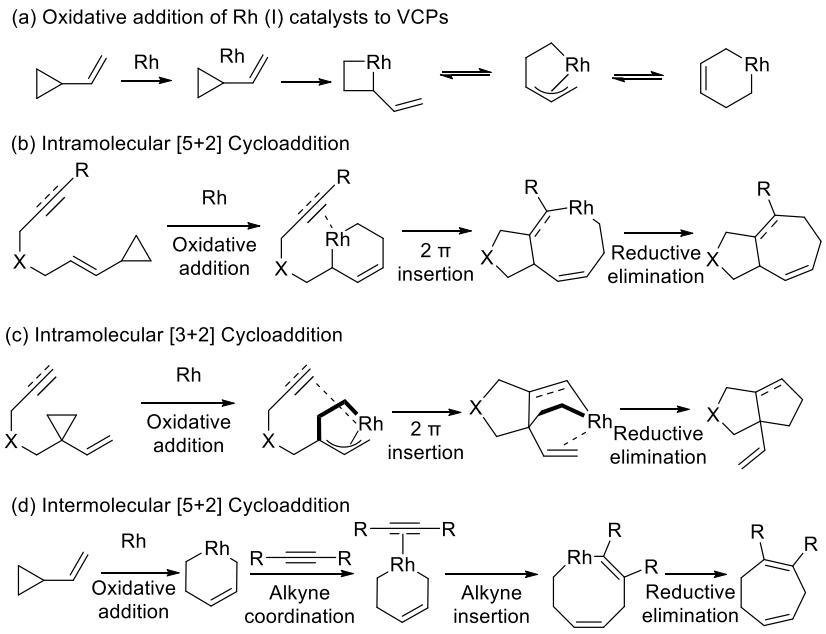

Scheme 4. Reactivity of VCPs with Rh.[8]

As a relevant example of reactivity in the context of this work, a cationic Rh(I) catalyst was reported for the carbonylative [5+1] cycloaddition of VCPs and CO.[9] VCPs were tested with [Rh(dppp)]OTf (10 mol%) under carbon monoxide atmosphere (0.2 atm) with 4Å molecular sieves in dichloroethane at 85 °C. β,γ-cyclohexenones and α,β-cyclohexenones were obtained selectively depending on the reactions conditions. When no external base was used, β,γ-cyclohexenones were obtained in a range of 41-80% yield. When DBU was further added, β,γ-cyclohexenones were isomerized to the α,β-cyclohexenones quantitatively.

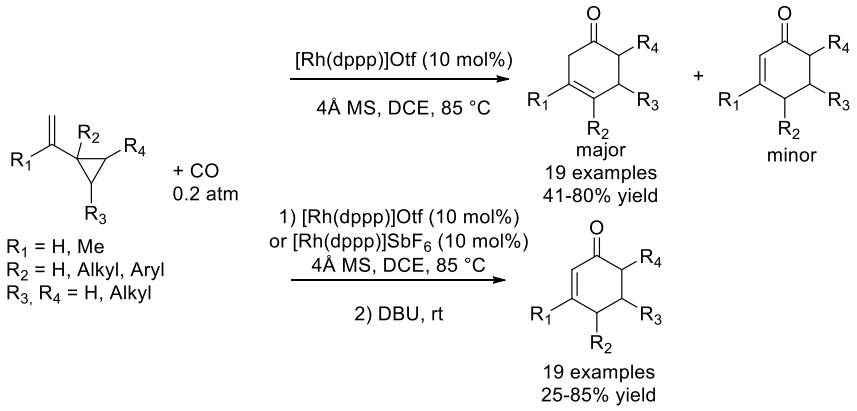

Scheme 5. Rh(I)-catalyzed [5 + 1] cycloaddition of vinylcyclopropanes and CO

VCPs present a particular reactivity with transition metals such as rhodium leading to complexes molecules. Yu and co-workers presented the rhodium-catalyzed [(5+2)+1] reaction of ene-VCPs with CO leading to a 5,8-fused carbocycle (Scheme 6) as a key intermediate for the synthesis of (+)-Asteriscanolide.[10]

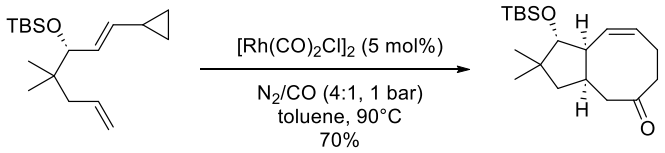

Scheme 6. Rhodium-catalyzed [(5+2)+1] reaction of ene-VCPs with CO

Their reactivity in cycloaddition reaction was well described but to date, no hydroformylation or hydroaminomethylation was reported with these substrates. As such, we decided to test alkenes bearing cyclopropyl and amide moieties as substrates in these reactions.

In the following sections, the synthesis of 1,1-disbstituted alkenes bearing a cyclopropyl and an amide moieties is described as well as their use as substrate in Rh-catalyzed hydroformylation and some hydroaminomethylation reactions.

4.2. Results and discussion

4.2.1. Synthesis of substrates

*4.2.1.1. Retrosynthetic analysis for the target alkene **4.2***

From the literature, we envisioned three possible pathways for the synthesis of the target alkene **4.2**. The first pathway involved the S_N2 substitution at the C-Br bond of the cyclopropyl bromide **4.5** by the nucleophile generated at the activated methylene position of the diethylmalonate **4.4**. The resulting α-substituted diethylmalonate **4.6** could be transformed into a diacid by ester hydrolysis. The formed diacid would then be treated with diethylamine and paraformaldehyde to form α-substituted acrylic acid **4.7**. The acid can then be transformed into the amide **4.2** by any of the classical amidation reactions (Scheme 7, route 1).

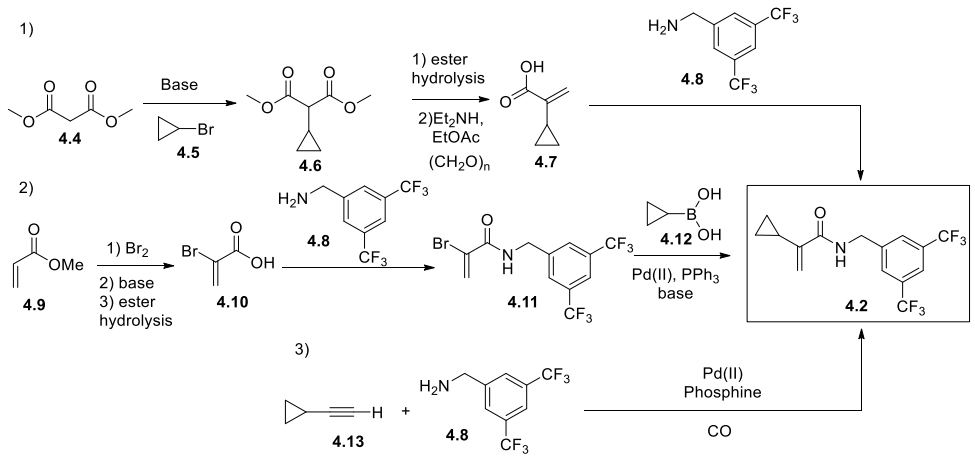

Scheme 7. Possible pathways envisaged towards the synthesis of the alkene 4.2.

The second pathway involves the Suzuki-Miyaura reaction as a key step to synthesize the 1,1-disubstituted alkene **4.2** (Scheme 7, route 2). The synthesis starts with a sequential dibromination of methylacrylate **4.9**, elimination in the presence of a base and hydrolysis of the ester yielding the α-bromoacrylic acid **4.10**. The acid could be transformed into the amide **4.2** by a classical amidation reaction with the amine **4.8**. In the final step, the target alkene **4.2** could be synthesized by treating the α-

bromoacrylamide **4.11** with cyclopropyl boronic acid **4.12** under classical Suzuki-Miyaura cross coupling conditions.

The third pathway involves a one-step synthesis of the target alkene **4.2** via a palladium-catalyzed hydroaminocarbonylation reaction of the corresponding cyclopropyl acetylene **4.13**, in the presence of amine **4.8** and carbon monoxide (Scheme 7, route 3). In this case, the reaction must be highly regioselective to form the 1,1-disubstituted alkene.

These 3 synthetic routes were tested and are described in the following sections.

*4.2.1.2. Synthetic route based on S_N2 substitution at the diethylmalonate **4.4***

First, the reaction of diethylmalonate **4.4** with on equivalent of cyclopropyl bromide **4.5** in the presence of a base (1 equiv.) was attempted. Three bases were tested: NaH, MeONa and LiHMDS. Performing the reaction at room temperature overnight and at 50 °C for 3 days in THF resulted in no product formation, indicating the unsuitability of this process (Scheme 8).

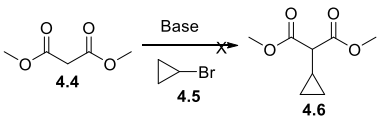

Scheme 8. S_N2 substitution reaction of cyclopropyl bromide 4.5.

Subsequently, a Grignard reaction using cyclopropyl bromide **4.5** and diethyloxalate **4.15** was tested. The Grignard reagent **4.14** was first formed *in situ* with cyclopropyl bromide **4.5** and treated with diethyloxalate **4.15** in THF at -78 °C for 4h. The reaction resulted in 30 % conversion of the starting material into the required product **4.16** (Scheme 9).

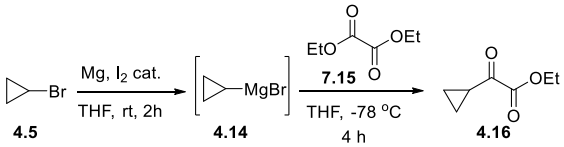

Scheme 9. Grignard reaction of cyclopropyl bromide 4.5 with diethyl oxalate 4.15

4.2.1.3. Synthetic pathway based on Suzuki-Miyaura coupling

For the second pathway, an addition reaction was performed with methylacrylate **4.9** and Br_2 in DCM as the solvent at 0 °C. The reaction proceeded cleanly to give 92% yield of the dibrominated product **4.17**. The latter **4.17** was then treated with triethylamine in diethyl ether to provide the α-bromoacrylate **4.18** in 82% yield (Scheme 10).

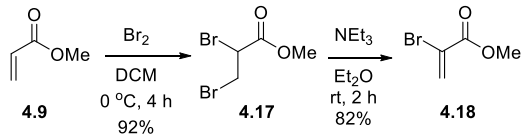

4.9 **4.17** **4.18**

Scheme 10. Synthesis of the Suzuki-Miyaura coupling partner 4.18.

This product **4.18** was then tested in the Suzuki-Miyaura coupling to introduce the cyclopropyl moiety at the α-position of the acrylate (**Table 1**).

Three palladium precursors and three bases were selected for the initial screening: the palladium precursors were $Pd(OAc)_2$, $Pd(dba)_2$ and $Pd(TFA)_2$ and the bases were K_3PO_4, K_2CO_3 and Cs_2CO_3. Each palladium precursor was tested with all three bases under standard Suzuki-Miyaura reaction conditions. The reaction was performed using a Pd (II) precursor, PPh_3 and base in toluene at 100 °C for 14 h and the results are summarized in Table 1.

Table 1. Screening of catalysts for the Suzuki-Miyaura reaction of α-bromoacrylate 4.18 with cyclopropylboronic acid 4.12.

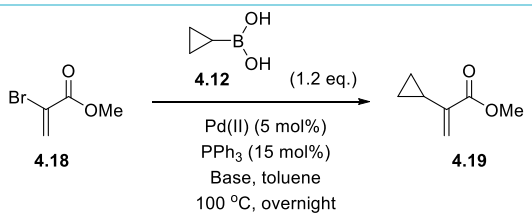

Entry	Pd. Catalyst	Base	% Conversion[a]	% Selectivity[a]
1	$Pd(OAc)_2$	K_3PO_4	100	30
2	$Pd(OAc)_2$	K_2CO_3	90	52
3	$Pd(OAc)_2$	Cs_2CO_3	100	57
4	$Pd(dba)_2$	K_3PO_4	80	10
5	$Pd(dba)_2$	K_2CO_3	80	<5
6	$Pd(dba)_2$	Cs_2CO_3	100	71
7	$Pd(TFA)_2$	Cs_2CO_3	100	22
8	$Pd(TFA)_2$	K_2CO_3	100	48
9	$Pd(TFA)_2$	K_3PO_4	100	90

***Reaction conditions**: **4.18** (0.5 mmol), **4.12** (1.2 equiv.), [Pd] (5 mol%), PPh_3 (15 mol %), base (3.5 equiv.), solvent (5 ml), T = 100°C, t = 16 h. [a]Conversion and selectivity were determined using ^1H NMR.*

Under these conditions, the conversion of the substrate was high (80-100%) in all cases. Using $Pd(OAc)_2$, the selectivity towards the product was low to moderate (Entries 1-3, 30% to 57%) and very low using $Pd(dba)_2$ and K_3PO_4 and K_2CO_3 as the bases (Entries 4 and 5). In contrast, when Cs_2CO_3 was used as the base, the selectivity increased to 71% (Entry 6). In the case of $Pd(TFA)_2$, when Cs_2CO_3 and K_2CO_3 were used as bases, the selectivity was 22% and 48%, respectively. Total conversion and excellent selectivity (Entry 9, 90%) towards the product was observed when the reaction was performed using $Pd(TFA)_2$ and K_3PO_4.

Based on this screening, $Pd(TFA)_2$ and K_3PO_4 were selected as catalytic system for this process. Attempts to isolate the product **4.19** using standard workup procedures followed by evaporation of the organic layer under reduced pressure failed due to the volatility of the product. Nonetheless, in view of the results obtained in the Suzuki-Miyaura reaction, this coupling was attempted using the 2-bromoacrylamide **4.11** to overcome the volatility issue.

The α-bromoacrylate **4.18** was then treated with LiOH in THF:H_2O as the solvent to perform the ester hydrolysis to give α-bromoacrylic acid **4.10** in 65% yield (Scheme 11).

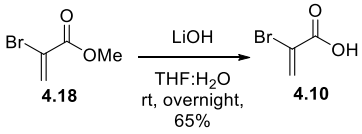

Scheme 11. Hydrolysis of 4.18

To form the amide, classical amidation strategies were tested. The α-bromoacrylic acid **4.10** was first treated with oxalyl chloride and a catalytic amount of DMF in DCM as the solvent to generate the acyl chloride **4.19** *in situ*, which was then treated with the amine **4.8** in the presence of triethylamine and a catalytic amount of DMAP. However, analysis of the reaction crude by GC-MS and ^1H NMR revealed that the major reaction product was compound **4.20** (Scheme 12).

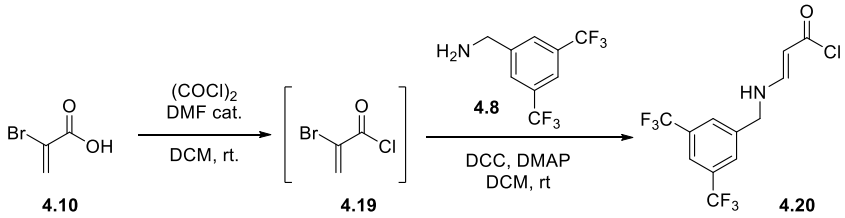

Scheme 12. Amidation of α-bromoacrylic acid 4.10 using oxalyl chloride.

At this point, the α-bromoacrylic acid **4.10** was then treated with the amine **4.8**, DCC and catalytic amount of DMAP to provide the desired amide **4.11** in 55% yield (Scheme 13).

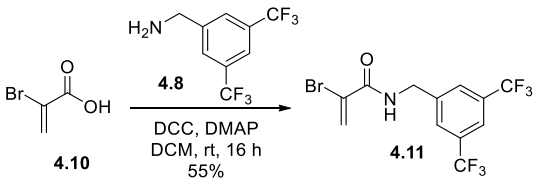

Scheme 13. Formation of α-bromo acrylamide 4.11

The α-bromoacrylamide **4.11** was then tested in the Suzuki-Miyaura coupling and a new screening of palladium precursors and bases was performed. Three palladium precursors and two bases were selected for screening: $Pd(OAc)_2$, $PdCl_2(PPh_3)_2$ and $Pd(TFA)_2$. The bases used were K_3PO_4 and KOH. The reactions were performed using the Pd (II) precursor, PPh_3 and base in toluene or toluene:H_2O at 100 ˚C overnight (Table 2).

Table 2 Screening of catalysts for the Suzuki-Miyaura reaction of α-bromoacrylamide 4.11.

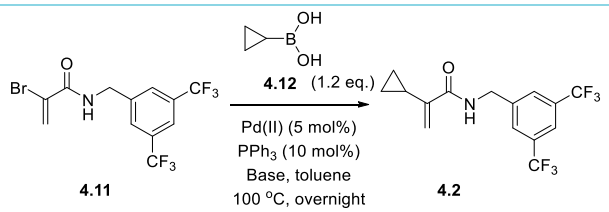

Entry	Pd. Catalyst	PPh_3	Base	Solvent	% Selectivity[b]
1	$Pd(TFA)_2$	10 mol%	K_3PO_4	Tol:H_2O(20:1)	55
2	$Pd(TFA)_2$	10 mol%	KOH	Tol:H_2O(20:1)	28
3	$Pd(PPh_3)_2Cl_2$	---------	K_3PO_4	Tol:H_2O(20:1)	27
4	$Pd(PPh_3)_2Cl_2$	---------	KOH	Tol:H_2O(20:1)	12
5	$Pd(OAc)_2$	10 mol%	K_3PO_4	Tol:H_2O(20:1)	62
6	$Pd(OAc)_2$	10 mol%	KOH	Tol:H_2O(20:1)	24
7[a]	$Pd(OAc)_2$	10 mol%	K_3PO_4	Toluene	85%

***Reaction conditions**: **4.11** (0.5 mmol), **4.12** (1.2 equiv.), [Pd] (5 mol%), PPh_3 (10 mol %), base (3.5 equiv.), solvent (5 ml), T = 100°C, t = 16 h. [a]3 eq. of boronic acid was used. [b]Conversion and selectivity were determined using ^1H NMR.*

Under these conditions, the conversion of the substrate was total in every tests. Using $Pd(TFA)_2$ the selectivity towards the product was low to moderate (28% to 55%, Entries 1-2) while using $Pd(PPh_3)_2Cl_2$, the selectivity was quite low (Entries 3-4). In the case of $Pd(OAc)_2$, when KOH is used as the base, the selectivity was 24%, (Entry 7) whereas when K_3PO_4 was used as the base the selectivity increased to 62% (Entry 6). Moreover, when KOH is used as the base, the free amine was observed, indicating that the hydrolysis of the amide bond had taken place. The highest conversion and selectivity of 85% towards the product was observed when $Pd(Oac)_2$ and K_3PO_4 were used as the metal precursor and base, respectively and toluene as the solvent.

Using these conditions, the product **4.2** was successfully isolated in 52% yield. The accessibility of this method was tested by synthesizing the corresponding α-bromoacrylamide **4.21** bearing a tertiary butyl amide moiety from **4.10**. The compound **4.22** was isolated in 72% yield using this methodology (Scheme 14).

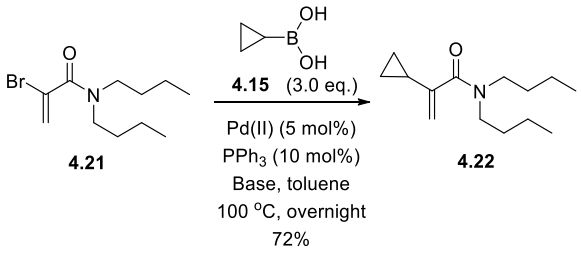

Scheme 14. Suzuki reaction of 4.21 with cyclopropylboronic acid 4.15

Even though the pathway involving the Suzuki-Miyaura reaction proved to be robust, this multistep reaction pathway was thought to be too tedious.

Next, the hydroaminocarbonylation pathway to synthesize the α-substituted acrylamide was investigated.

4.2.1.4. Synthetic route based on the Pd-catalyzed hydroaminocarbonylation of alkynes

Cyclopropyl acetylene **4.13** and different amines were tested as substrates in the Pd-catalyzed hydroaminocarbonylation reaction based on previous reports involving different alkynes.[11] The substrates were reacted with carbon monoxide gas in the

presence of $Pd(OAc)_2$ as the metal precursor and 1,3-bis(diphenylphosphino)propane (dppp) **L1** as ligand. For the synthesis of α-cyclopropyl acrylamide **4.27**, ammonium carbonate was used as the amine source and the reaction was run for 6h (Scheme 15).[12]

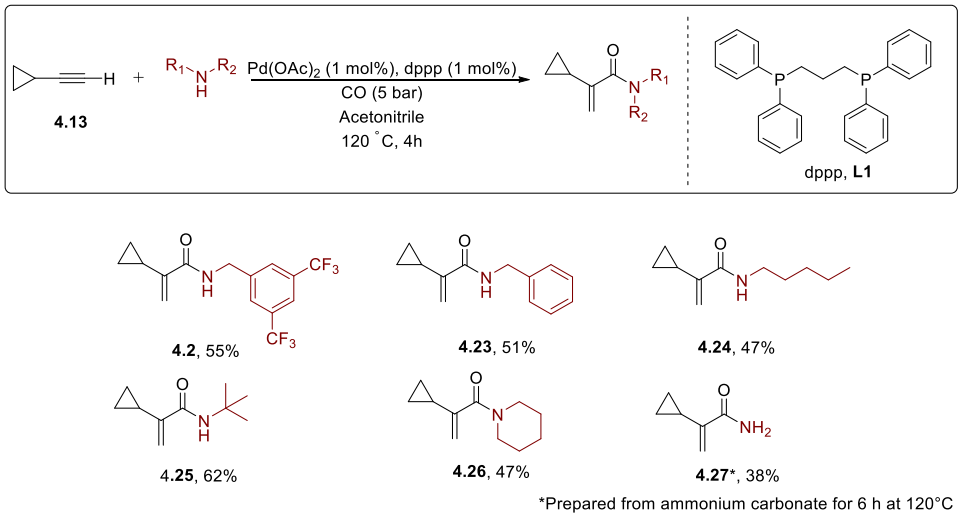

Scheme 15. Synthesis of 1,1 disubstituted alkenes via hydroaminocarbonylation

Various 1,1-disubstituted alkenes containing either primary, secondary or tertiary amide moieties were synthesized using this protocol. The primary amide **4.27** was synthesized in 38% yield and the four secondary amides **4.2**, **4.23**, **4.24** and **4.25** were synthesized in moderate to good yields (47 to 62%). The tertiary amide **4.26** was obtained in 47% yield. These yields were good considering that the alkenes were synthesized using a one-step process.

Liu and co-workers proposed a plausible catalytic cycle explaining the regioselectivity for the formation of the amide (Scheme 16). The carbamoylpalladium intermediate (**4.28**), formed by reaction of the palladium(II)-precursor with the amine and CO, was reported to be crucial for the reaction to yield the corresponding amide. As proposed in Scheme 16, the carbamoylpalladium intermediate (**4.28**) was readily formed upon the complexation of $Pd(OAc)_2$ with an organic amine under CO atmosphere. The subsequent insertion of a π-coordinated alkyne into the Pd–acyl bond (**4.29**) led to the formation of the intermediate complex (**4.31**) due to steric effects. The latter

(**4.31**) irreversibly underwent aminolysis to afford the branched α,β-unsaturated amide accompanied by the regeneration of the Pd amide complex **4.27**, which upon reaction with CO forms the carbamoylpalladium intermediate (**4.28**).

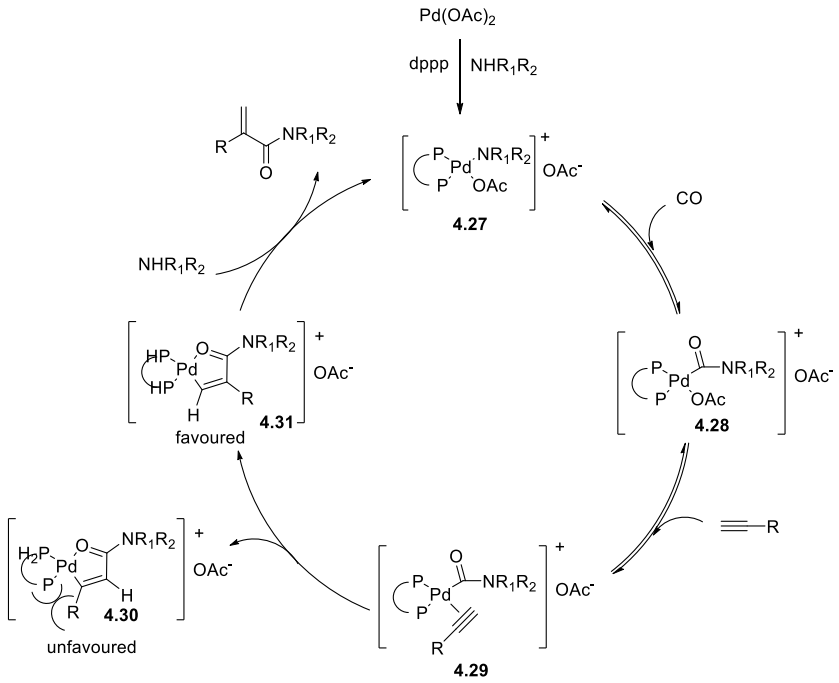

Scheme 16. Proposed catalytic cycle for the Pd-catalyzed hydroaminocarbonylation of alkynes

In view of these results, the hydroaminocarbonylation was selected as the method of choice for the synthesis of these substrates in one step. Moderate to good yields were obtained for these alkenes (30-60%) without further optimization of the conditions.

4.2.2. Rh-catalyzed hydroformylation of the synthesized substrates.

The synthesized amides were tested in the Rh-catalyzed hydroformylation and hydroaminomethylation reactions according to the degree of substitution of the amide functions.

4.2.2.1. Substrates bearing tertiary amides

For the rhodium-catalyzed asymmetric hydroformylation of α-cyclopropyl acrylamides, N,N-dibutyl-2-cyclopropylacrylamide **4.22** was initially used as substrate, [Rh(acac)$(CO)_2$] as Rh precursor, toluene as solvent, under 20 bar CO/H_2 (1:1), at 90°C during 16 h and using the ligands **L2**, **L3**, and **L4** (Scheme 17).

When the reaction was carried out using the achiral ligand **L2,** very low conversion of the substrate was observed. When the ligand **L3** was used in the reaction, the conversion of the substrate into aldehyde products was 28%. Four aldehyde products were detected by ^{1}H NMR, indicating that various reactions had taken place. The identity of the main aldehyde product could not be determined as the alkylic region of the spectrum was very crowded. The highest conversion (*ca*. 40%) of the substrate was observed when the chiral ligand **L4** was tested in the reaction although in this case, 6 aldehyde signals were observed in the NMR spectra, indicating a very low selectivity. The large number of products obtained suggested that the opening of the cyclopropyl moiety had taken place under these conditions. The complexity of the alkylic region of the ^{1}H spectrum did not permit to draw conclusions on the identity of these products.

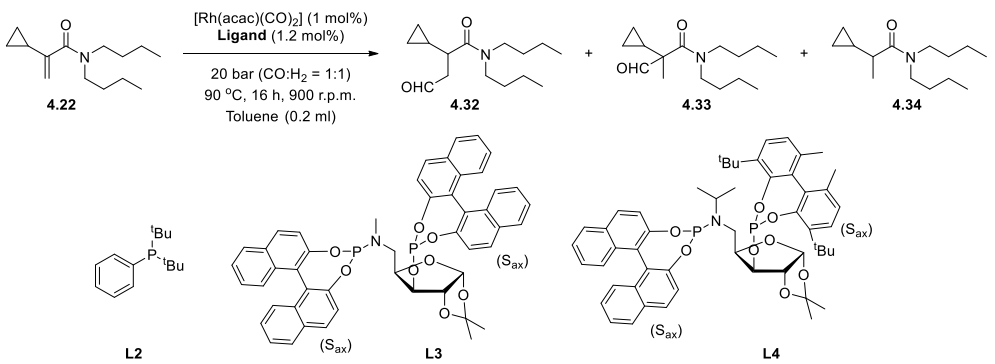

Scheme 17. Ligand screening for the hydroformylation of substrate 4.22

The other tertiary amide **4.26** was also tested in hydroformylation (Scheme 18). When ligand **L3** was tested in the reaction, the conversion (80%) was higher than that obtained for the substrate **4.22,** indicating that this substrate was more reactive

under these hydroformylation conditions. The selectivity towards the formation of one of the aldehydes was 76% (Scheme 18). The triplet multiplicity of the aldehyde signal in the ^{1}H spectrum indicated that this product had been formed by linear hydroformylation of the double bond of the substrate. It was therefore tentatively concluded that the linear hydroformylation product **4.35** was formed under these conditions.

In view of this promising result in hydroformylation, the reaction was repeated under hydroaminomethylation conditions with the addition of piperidine as the amine reactant. The reaction was performed in 16 h at 90 °C with 20 bar of a mixture of CO/H_2 (1:2). However, no conversion of substrate was observed, suggesting that the presence of piperidine in the reaction medium inhibited the reaction.

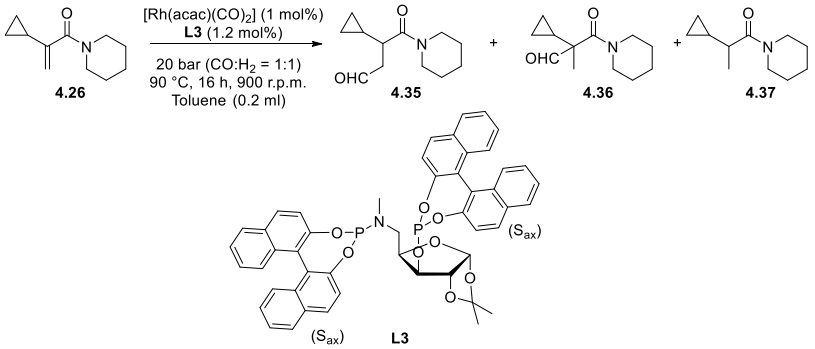

Scheme 18. Hydroformylation of 4.26 using L3

4.2.2.2. Substrates bearing secondary amides

We then focused our attention on the hydroformylation and hydroaminomethylation studies of secondary α-cyclopropylacrylamides. The first substrate that was tested was the N-(3,5-bis(trifluoromethyl)benzyl)-2-cyclopropylacrylamide **4.2**. First, the hydroformylation reaction was tested using the ligand **L3** with the conditions used for the tertiary amides. Under these conditions, 100% conversion of the substrate was observed. A ligand screening for the substrate **4.2** was performed using ligands **L3** and **L5-L8**.

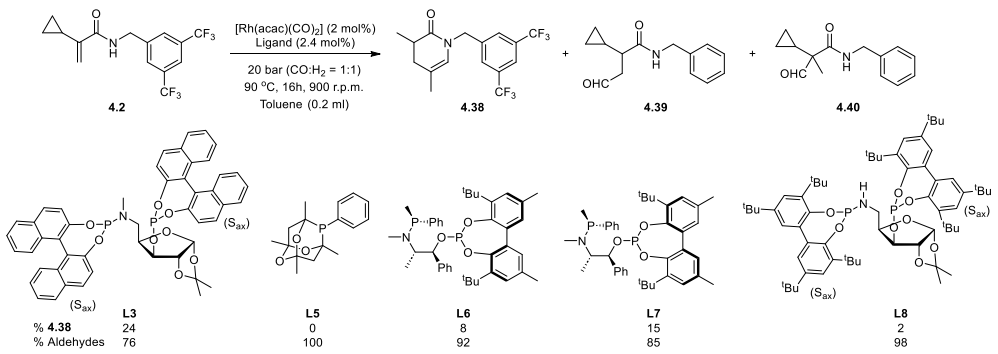

Scheme 19. Ligand screening for the HF of 4.2

The conversion of the substrate was >95% using all ligands. At least 3 aldehydes peaks were observed in ^{1}H NMR indicating a possible opening of the cyclopropyl. Using **L3**, a new signal in the alkene region of the ^{1}H NMR spectrum was observed. This peak was also detected with the tests using **L6**, **L7** and **L8** but not with the monodentate phosphine **L5**. Unfortunately, it was not possible to isolate the product of this test using **L3** due to the low selectivity. The catalysis using **L3** was applied for the test with N-benzyl-2-cyclopropylacrylamide **4.23** and presented 79% selectivity towards the new alkene product vs 21% aldehydes. The product was isolated in 40% yield after column chromatography.

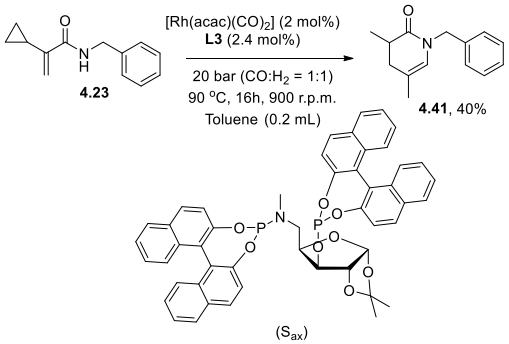

Scheme 20. Hydroformylation of 4.23 using L3

Surprisingly, the major product formed in this reaction did not exhibit any aldehyde signal in the corresponding ^{1}H NMR spectrum, nor resonances that could be assigned to a cyclopropyl fragment. One of the characteristic peaks in ^{1}H NMR spectra was a singlet resonance at 4.58 ppm attributed to the benzylic protons **d**. The multiplicity

of this signal indicated that the absence of adjacent N-H moiety and thus, that a tertiary amide moiety was contained in the molecule. Another characteristic peak was the singlet signal **e** at 5.68 ppm of the NMR spectra, indicating that a trisubstituted alkene was present. The diastereotopic protons of CH_2 at **g** resonated at 2.22 ppm and 1.99 ppm, which indicated the proximity of a chiral center. NMR characterization using bidimensional experiments such as COSY, ^{1}H-^{13}C HSQC, and ^{1}H-^{13}C HMBC was performed to determine the identity of this compound as the new dihydropyridinone product **4.38** (Figure 1). The identity of this compound was confirmed by GC-MS analysis with the detection of a peak at m/z= 215.

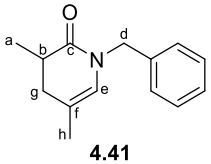

4.41

Figure 1. Structure of the major product 4.41 during the HF of 4.23

As **L3** is a chiral ligand, the enantioselectivity was assessed by HPLC. However, the enantioselectivity for the product **4.41** was determined to be only 8%. The other two secondary amides **4.24** and **4.25** were tested in hydroformylation conditions using the ligand **L3** (Scheme 21), and both substrates were mainly converted into the dihydropyridinone products **4.42** and **4.43**. Analysis of the reaction crude by ^{1}H NMR for the pentyl substituted substrate indicated the formation of 51% of **4.42** and 49% aldehydes while with for the tert-butyl counterpart, 37% of **4.43** against 63% of aldehydes were obtained. The dihydropyridinone product **4.42** was isolated in 39% yield. However, the catalysis with **4.25** led to the formation of various impurities that prevented the isolation of **4.43**.

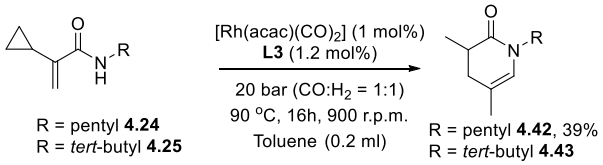

R = pentyl **4.24**
R = *tert*-butyl **4.25**

R = pentyl **4.42**, 39%
R = *tert*-butyl **4.43**

Scheme 21. Hydroformylation of 4.42 and 4.43 using ligand L3.

The formation of **4.41** was further evaluated without syngas and using achiral ligands. The $Rh(acac)(CO)_2$ precursor was tested in a control experiment at 90°C for 16 h and no conversion of **4.23** was observed (entry 1). In a second control experiment, the ligand **L3** was added with the rhodium precursor and the substrate **4.23** and stirred at 90°C for 16 h (entry 2). Again, no conversion of **4.23** was observed demonstrating that the reaction takes place only in the presence of syngas and indicating that the active species could be a rhodium hydride formed by reaction with syngas. The $Rh(acac)(CO)_2$ precursor was tested without additional ligand and provided a mixture of 50% **4.41** and 50% aldehydes products. Biphephos ligand **L9** was tested and provided good conversion of the substrate with a high chemoselectivity towards aldehydes (91% vs. 9% selectivity to **4.41**). The diphosphine ligand dppf **L10** provided the best selectivity towards aldehydes (99%) as almost no conversion towards **4.41** was observed. Notably, dppf provided a linear aldehyde in 69% as observed by the triplet pattern of the aldehyde signal in ^1H NMR. Interestingly, on standing during several days, X-Ray analysis of a single crystal formed in an NMR tube of entry 5 and 6 showed the formation of N1, N2-dibenzyloxalamide **4.44**. This unexpected product indicated the C-C bond breaking in α position of the carbonyl moiety.

Table 3. Ligand screening for the formation of 4.41

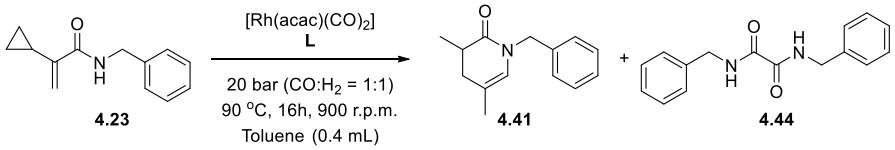

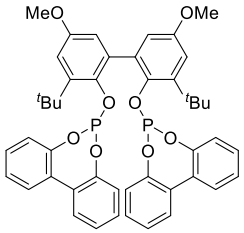

Biphephos, **L9**

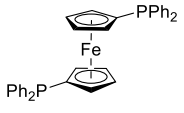

DPPF, **L10**

Entry	Ligand	Conversion %	% **4.41**	% Aldehydes
1[a]	None	0	0	0
2[a]	**L3**	0	0	0
3	None	-	50	50
4	**L3**	99	79	21
5	**L9**	98	9	91
6	**L10**	99	1	99

***Reaction conditions**: **4.23** (0.2 mmol), [Rh(acac)(CO)$_2$] (1 mol%), **Ligand** (2 mol %), P = 20 bar (CO/H$_2$, 1:1), toluene (0.4 mL), T = 90°C, t = 16 h, 900 r.p.m.[a] Without CO/H$_2$ pressure.*

To get more insights into the hydroformylation products obtained during catalysis, the reaction was performed at 1 mmol scale and the crude was treated with $NaBH_4$ in MeOH and purified by column chromatography (Scheme 22). The main product could be characterized by ^{1}H and ^{13}C NMR and identified as the alcohol **4.46.** The identity of this product thus revealed that the hydroformylation product was the aldehyde **4.45** where the cyclopropyl unit of the substrate had undergone C-C cleavage.

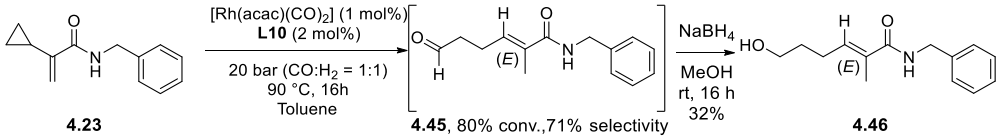

Scheme 22. Hydroformylation of 4.23 followed by reduction of the crude mixture.

The formation of products **4.41** and **4.45** could be explained through the mechanism displayed in Scheme 23. The formation of the cyclic dihydropyridinone **4.41** and the aldehyde **4.45** product indicated that C-C bond activation of cyclopropanes had taken place, as previously observed in the presence of Rh(I) catalysts. The possible mechanism described in Scheme 23 relies on the oxidative addition of Rh(I) into VCPs described in Scheme 4.[13] As the catalysis is performed under syngas pressure, a rhodium hydride species is present in the system. Oxidative addition of the rhodium into the cyclopropyl moiety of **4.23** forms a 4 member-ring rhodacycle intermediate **4.49** in equilibrium with the allyl species **4.50**. Coordination of the rhodium to the allyl forms the six-membered ring intermediate **4.51** which would undergo reductive elimination leading to Rh(I) **4.52**. The latter would perform β-elimination to regenerate the rhodium hydride catalyst and the diene **4.48**. From this intermediate, a rhodium catalyst, depending on the ligand present, can perform either linear or branched hydroformylation. Linear hydroformylation would be responsible of the formation of the aldehyde **4.45** while branched hydroformylation would provide the aldehyde **4.47**. Interestingly, **4.47** was not isolated but the dihydropyridinone **4.41** was formed. Thus, intramolecular condensation of the amide moiety onto the branched aldehyde would lead to the stabilized 6-membered ring **4.53** via the loss of a water molecule. Subsequent hydrogenation of the endocyclic double bond would lead to the isolated product **4.41.**

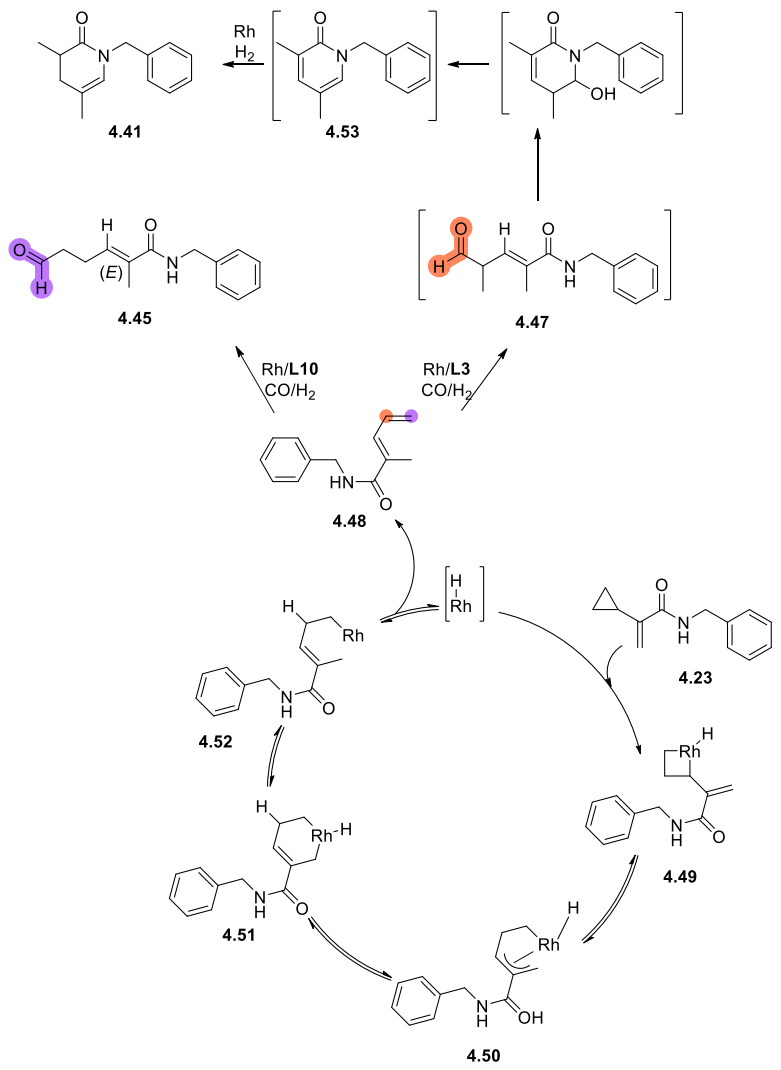

Scheme 23. Possible mechanism for the formation of dihydropyridinone 4.41 and aldehyde 4.45

To conclude, the catalytic tests of vinyl cyclopropyl secondary acrylamides under hydroformylation conditions presented a complex reactivity due to the presence of the vinylcyclopropane moiety resulting in the formation of various aldehydes. In the following section, the reactivity of these substrates was evaluated under hydroaminomethylation conditions.

4.2.3. Rh-catalyzed hydroaminomethylation of secondary acrylamides.

The reactivity of N-benzyl-2-cyclopropylacrylamide **4.23** was tested in hydroaminomethylation using $Rh(acac)(CO)_2$ as rhodium precursor, **L10** as ligand, and with 1 equivalent of piperidine. The reaction was carried out at 1 mmol scale under 20 bar of syngas for 16 h at 90 °C.

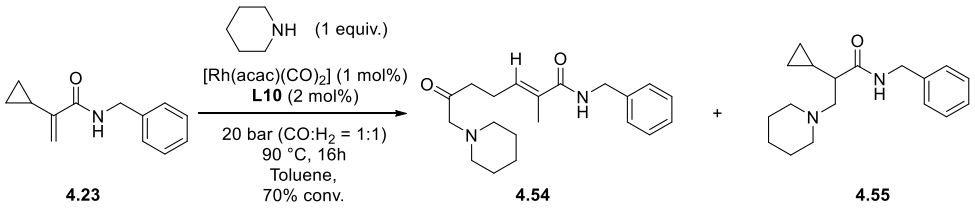

Scheme 24. Reactivity of 4.23 under hydroaminomethylation conditions with piperidine.

The substrate was converted in 70% in mainly in two products, **4.54** (44%) and **4.55** (48%). Surprisingly, the expected condensation of the amine on the resulting aldehyde **4.45** obtained previously in the hydroformylation of **4.23** with Rh/**L10** catalytic system was not detected. However, opening of the VCP occurred yielding the new product **4.54**. The second surprise was the formation of the cyclopropyl containing hydroamination product **4.55**. This unexpected result would suggest that a fast hydroamination would occur before the opening of the VCP. A test reaction without syngas will be performed in the near future to evaluate the formation of this the product **4.55** and the mechanism of formation of **4.54** is currently under investigation.

In view of these results, the influence of the benzyl amide moiety was looked at via the study of the reactivity of the secondary acrylamide **4.44**, which contained a methyl group instead of a cyclopropyl moiety. This compound was evaluated in the asymmetric hydroaminomethylation with the system $Rh(acac)(CO)_2$/phosphite phosphoramidite ligand **L13** using the reported procedure for hydroaminomethylation of tertiary acrylamides (Scheme 25).[14] The conversion of the substrate was >99% with 88% selectivity to the linear product **4.45**. The amine **4.45** was obtained in 34% yield and 36% enantiomeric excess, thus demonstrating

that the cyclopropyl moiety was responsible for the failed attempts using substrate **4.23**. In comparison to the asymmetric hydroformylation of tertiary acrylamide with the same ligand, the aldehyde reported was obtained in 81% ee. This result demonstrates the importance of the substitution in the amide moiety to reach high enantioselectivities.

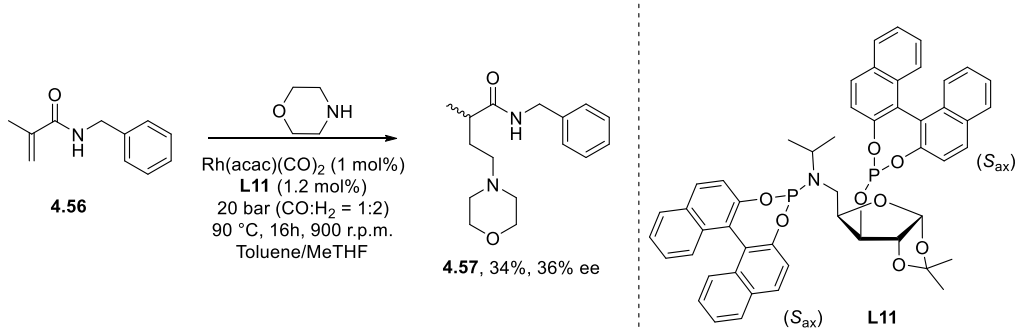

Scheme 25. Asymmetric hydroaminomethylation of 4.44 using Rh/L13.

It was therefore concluded that the hydroaminomethylation of secondary acrylamide bearing a cyclopropyl substituent undergoes ring opening that inhibits the effective linear hydroaminomethylation of the substrate. In contrast, hydroaminomethylation of the methyl substituted secondary acrylamide (**4.56**) was efficient and provided expected the chiral amine **4.57** in moderate enantioselectivity.

4.3. Conclusions

- The synthesis of the α-cyclopropyl acrylamides containing primary, secondary and tertiary amides were explored via three synthetic routes.
- The most appropriate pathway was based on the Pd-catalyzed hydroaminocarbonylation of cyclopropylacetylene **4.13.** Using a series of amines and $Pd(OAc)_2$ / dppp as catalytic system, the synthesis of the new 2-cyclopropylacrylamides **4.2**, **4.23-4.27** was successful with yields ranging from 40 to 60%.

- The synthesized cyclopropylacrylamides were tested in the Rh-catalyzed hydroformylation and hydroaminomethylation reactions using various ligands.
- The reactivity of tertiary amides revealed substrate dependent since using ligand **L3,** high conversion was measured in the case of substrate **4.26**, whereas the conversion of substrate **4.22** was much lower.
- 2-cyclopropylacrylamides undergo ring opening reaction under hydroformylation and hydroaminomethylation conditions.
- Hydroformylation of secondary 2-cyclopropylacrylamides provided new dihydropyridinone products which were isolated and fully characterized. Moreover, reduction of the catalytic crude revealed that the hydroformylation product **4.45** was also formed as the main linear aldehyde.
- In the hydroaminomethylation of secondary 2-cyclopropylacrylamides, no hydroaminomethylation products could be detected. Instead, ring opening of the cyclopropyl unit of the substrate was evidenced in **4.55** as long as the formation of hydroamination product **4.56** bearing the cyclopropyl moiety.

4.4. Experimental part

General considerations

All the reactions were carried out using Schlenk-line inert atmosphere techniques or glovebox techniques. Anhydrous solvents were collected from the system Braun MB SPS-800. Commercially available reagents and solvents were purchased at the highest commercial quality from Sigma-Aldrich, Fluka, Alfa Aesar, Fluorochem, Strem and were used as received, without further purification.

^{1}H and $^{13}C\{^{1}H\}$ NMR spectra were recorded using a Varian Mercury VX 400 (400 and 100.6 MHz respectively). Chemical shift values (δ) are reported in ppm relative to TMS (^{1}H and $^{13}C\{^{1}H\}$) and coupling constants are reported in Hertz. The following abbreviations are used to indicate the multiplicity: s, singlet; d, doublet; t, triplet; q, quartet; quint, quintuplet; sext, sextuplet; sept, septet; oct, octet; m, multiplet; bs, broad signal. High-resolution mass spectra (HRMS) were recorded on an Agilent Time-of-Flight 6210 using ESI-TOF (electrospray ionization-time of flight). Samples were introduced to the mass spectrometer ion source by direct injection using a syringe pump and were externally calibrated using sodium formate. The instrument was operating in the positive ion mode. Reactions were monitored by TLC carried out on 0.25 mm E. Merck silica gel 60 F_{254} aluminum plates. Developed TLC plates were visualized under a short-wave UV lamp (254 nm) and by heating plates that were dipped in potassium permanganate. Flash column chromatography was carried out using forced flow of the indicated solvent, on Merck silica gel 60 (230-400 mesh). The Rh-catalyzed hydroaminocarbonylation reaction was set up in a CAT24 autoclave from HEL Inc. and stirred with a Teflon-coated magnetic stir bar. The Rh-catalyzed hydroformylation reaction and Rh-catalyzed hydroaminomethylation reaction were set up in a CAT7 autoclave from HEL Inc. and stirred with a Teflon-coated magnetic stir bar.

methyl 2,3-dibromopropanoate (4.17)[15]

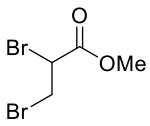

To a solution of methyl acrylate (3.0 g, 34.84 mmol) in DCM (30 mL), bromine (1.78 mL, 34.84 mmol) was slowly added using a dropping funnel at 0 °C. The resulting solution was allowed to stir at 0 °C for 1 h. The reaction was quenched by adding a saturated sodium thiosulfate solution. The resulting suspension was allowed to stir for 1 h at room temperature. The mixture was diluted with DCM (10 mL) and extracted with DCM (3 × 10 mL). The organic layers were washed with brine, dried over $MgSO_4$, and concentrated under reduced pressure to afford (7.88 g, 92%).

^{1}H NMR (400 MHz, $CDCl_3$) δ 4.38 (dd, *J* = 11.3, 4.4 Hz, 1H), 3.86 (dd, *J* = 11.3, 9.9 Hz, 1H), 3.78 (s, 3H), 3.61 (dd, *J* = 10.0, 4.4 Hz, 1H). These signals are in agreement with those reported in the literature.

IV

methyl 2-bromoacrylate (4.18)[15]

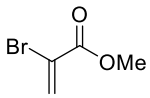

2, 3-dibromopropionate was dissolved in 65 mL of diethyl ether directly without further purification. To the resulting mixture was added 5.36 mL (38.46 mmol) of triethylamine, and the reaction was stirred at ambient temperature until reaction completion. The precipitate was filtered with a pad of Celite; the filtrate was diluted, dried over $MgSO_4$ and concentrated under reduced pressure to afford (4.33 g, 82%).

^{1}H NMR (400 MHz, $CDCl_3$) δ 6.90 (s, 1H), 6.20 (s, 1H), 3.77 (s, 3H). These signals are in agreement with those reported in the literature.

2-bromoacrylic acid (4.10)

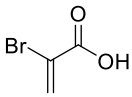

To a solution of methyl 2-bromoacrylate (4.33 g, 26.28 mmol) in THF/H_2O (v/v = 1:1) was added LiOH (1.88 g, 78.84 mmol) at room temperature. After being stirred at ambient temperature for 14 h, the reaction mixture was diluted with DCM and water. The water layer was washed with DCM. Subsequently, the water layer was acidified with 1 M HCl until pH < 3 and the

resulting suspension was extracted with DCM. The organic phase was dried over $MgSO_4$ and concentrated under reduced pressure to afford (2.57 g, 65%).

^{1}H NMR (400 MHz, $CDCl_3$) δ 7.04 (d, *J* = 1.8 Hz, 1H), 6.34 (d, *J* = 1.8 Hz, 1H), 5.70 (bs, 1H).

methyl 2-cyclopropylacrylate (4.19)

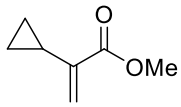

methyl 2-bromoacrylate (200 mg, 1.2 mmol), cyclopropyl boronic acid (123 mg, 1.44 mmol), $Pd(OAc)_2$ (13.5 mg, 0.06 mmol), triphenylphosphine (31.5 mg, 0.12 mmol) and K_3PO_4 (764 mg, 3.6 mmol) were charged to a Schlenk equipped with a stir bar. The Schlenk was then flushed with argon and toluene was added and the reaction was let to stir at 100 °C for 14h. The product was not isolated due to its volatility.

^{1}H NMR (400 MHz, $CDCl_3$) δ 6.03 (d, *J* = 1.0 Hz, 1H), 5.31 (t, *J* = 1.1 Hz, 1H), 3.78 (s, 3H), 1.79 – 1.71 (m, 1H), 0.82 – 0.77 (m, 2H), 0.52 – 0.48 (m, 2H).

General procedure A: Synthesis of α-bromo acrylamides

2-bromoacrylic acid (1 eq.), the corresponding amine (1 eq.), N,N'-Dicyclohexylcarbodiimide (DCC) (1 eq.) and 4-Dimethylaminopyridine (DMAP) (0.3 eq.) were added to a round-bottomed flask equipped with a stir bar and dissolved in of DCM at ambient temperature under N_2. After completion, the mixture was diluted in DCM and filtered. The filtrate was washed with water and saturated $NaHCO_3$ solution. The organic phase was dried and evaporated under reduced pressure. The residue was purified by flash chromatography on silica gel using petroleum ether (PE) / dichloromethane (DCM) to give the desired product.

N-(3,5-bis(trifluoromethyl)benzyl)-2-bromoacrylamide (4.11)

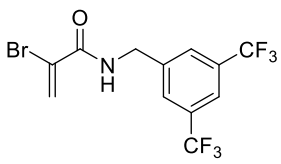

General procedure A was followed by employing 2-bromoacrylic acid **4.10** (1 g, 6.58 mmol), 3,5-bis(trifluoromethyl) benzylamine (1.6 g, 6.58 mmol), DCC (1.35 g, 6.58 mmol) and DMAP (241 mg, 1.97

mmol). Purification by flash chromatography on eluting with DCM in PE (50% v/v) afforded (1 g, 40.5%).

^{1}H NMR (400 MHz, $CDCl_3$) δ 7.82 (s, 1H), 7.76 (s, 2H), 7.12 (s, 1H), 7.09 (d, *J* = 1.6 Hz, 1H), 6.12 (d, *J* = 1.7 Hz, 1H), 4.64 (d, *J* = 6.1 Hz, 2H). ^{13}C NMR (100.6 MHz, $CDCl_3$) δ 161.57, 140.29, 132.26 (q, *J* = 33.5 Hz), 128.98, 128.00, 124.64, 121.97, 119.22, 43.81. ^{19}F NMR (377 MHz, $CDCl_3$) δ -62.89.

2-bromo-N,N-dibutylacrylamide (4.21)

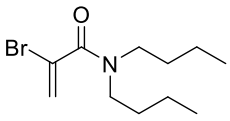

General procedure A was followed by employing 2-bromoacrylic acid (1.20 g, 7.90 mmol), dibutylamine (1.02 g, 7.90 mmol), DCC (1.63 g, 7.90 mmol) and DMAP (290 mg, 2.37 mmol). Purification by flash chromatography eluting with DCM in PE (50% v/v) afforded (621 mg, 30%).

^{1}H NMR (400 MHz, $CDCl_3$) δ 5.92 (dd, *J* = 2.6, 0.8 Hz, 1H), 5.77 (dd, *J* = 2.5, 0.8 Hz, 1H), 3.32 (dt, *J* = 15.5, 7.8 Hz, 4H), 1.55 (dq, *J* = 12.0, 8.7, 7.9 Hz, 4H), 1.36 – 1.26 (m, 4H), 0.93 (t, *J* = 7.3 Hz, 6H). ^{13}C NMR (100.6 MHz, $CDCl_3$) δ 166.02, 122.12, 120.03, 48.54, 44.44, 30.72, 29.19, 20.12, 13.88. **HRMS** (ESI) for **$C_{11}H_{20}BrNO$.** Calculated **M:** 261.0728**, $[M+H^+]^+$:** 262.0806, found: 262.0807.

General procedure B: Synthesis of α-cyclopropyl acrylamides

α-cyclopropyl acrylamide (1 eq.), cyclopropyl boronic acid (3 eq.), $Pd(OAc)_2$ (0.05 eq.), triphenylphosphine (0.10 eq.) and K_3PO_4 (3.5 eq.) were charged to a Schlenk equipped with a stir bar. The Schlenk was then flushed with argon and toluene was added and the reaction was stirred at 100 °C for 14h. The crude was purified by flash chromatography on silica gel using appropriate eluent to give the desired product.

General procedure C: Synthesis of α-cyclopropyl acrylamides

A 2 mL glassware reactor tube equipped with a stirring bar was charged with a mixture of alkyne (1 eq.), amine (1.25 eq.), $Pd(OAc)_2$ (1.0 mol%), Dppp (1.0 mol%) and CH_3CN (1 mL). The reactor tube was placed in the reactor and the reactor was

flushed three times with CO and then pressurized to 5 bar of CO. The reaction was stirred at 800 r.p.m. and heated to 120 °C for 4 hrs. The reaction was stopped by cooling the reactor in an ice bath for 20 min followed by venting of the system. The mixture was purified by chromatographic column to afford the product.

N,N-dibutyl-2-cyclopropylacrylamide (4.22)

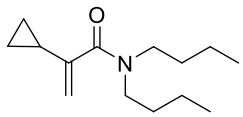

General procedure B was followed by employing 2-bromo-N,N-dibutylacrylamide (150 mg, 0.572 mmol), cyclopropyl boronic acid (148 mg, 1.716 mmol), Pd(OAc)2 (6.7.2 mg, 0.029 mmol), PPh_3 (15 mg, 0.057 mmol) and K_3PO_4 (7.25 mg, 2.00 mmol). Purification by flash chromatography using 1% v/v of NEt_3 in P.E afforded the product (126 mg, 71%).

^{1}H NMR (400 MHz, $CDCl_3$) δ 4.95 (s, 1H), 4.84 (d, *J* = 0.8 Hz, 1H), 3.23 (dt, *J* = 29.1, 7.9 Hz, 4H), 1.46 (m, *J* = 8.0 Hz, 5H), 1.30 – 1.16 (m, 4H), 0.86 (q, *J* = 7.2 Hz, 6H), 0.75 – 0.66 (m, 2H), 0.57 – 0.51 (m, 2H). ^{13}C NMR (100.6 MHz, $CDCl_3$) δ 170.95, 147.31, 110.30, 48.21, 43.80, 30.92, 29.53, 20.27, 14.61, 6.92.

N-(3,5-bis(trifluoromethyl)benzyl)-2-cyclopropylacrylamide (4.2)

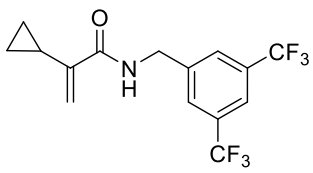

General procedure C was followed by employing cyclopropyl acetylene (198 mg, 3.00 mmol), 3,5-bis(trifluoromethyl) benzylamine (900 mg, 3.9 mmol), $Pd(OAc)_2$ (6.6mg, 1 mol%), Dppp (12.3 mg, 1mol%). Purification by flash chromatography using 60% v/v of DCM in P.E afforded the product **7.2** (126 mg, 71%).

^{1}H NMR (400 MHz, $CDCl_3$) δ 7.72 (s, 1H), 7.69 (s, 2H), 6.68 (s, 1H), 5.96 (d, *J* = 1.0 Hz, 1H), 5.26 (t, *J* = 1.4 Hz, 1H), 4.60 (d, *J* = 6.2 Hz, 2H), 1.53 – 1.44 (m, 1H), 0.84 – 0.74 (m, 2H), 0.55 – 0.50 (m, 2H). ^{13}C NMR (100.6 MHz, $CDCl_3$) δ 167.65, 143.38, 141.22, 131.99 (Q, *J* = 33.4 Hz), 127.67, 124.56, 121.86, 120.55, 7.2.77, 12.28, 6.37.

HRMS (ESI) for **$C_{15}H_{13}F_6NO$.** Calculated **M:** 337,0901, **$[M+H^+]^+$:** 338.0979, found: 338.0974.

2-cyclopropyl-1-(piperidin-1-yl)prop-2-en-1-one (4.26)

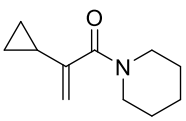

General procedure C was followed by employing cyclopropyl acetylene (198 mg, 3.00 mmol), Piperidine (330 mg, 3.9 mmol), $Pd(OAc)_2$ (6.6mg, 1 mol%), Dppp (12.3 mg, 1 mol%). Purification by flash chromatography using 60% v/v of DCM in P.E afforded the product (252 mg, 47%).

^{1}H NMR (401 MHz, $CDCl_3$) δ 4.96 (d, *J* = 1.6 Hz, 1H), 4.86 – 4.85 (m, 1H), 3.44 (dt, *J* = 7.8 Hz, 4H) 1.62 – 1.55 (m, 2H), 1.53 – 1.44 (m, 5H), 0.73 – 0.67 (m, 2H), 0.53 (m, *J* = 6.6, 4.5, 1.6 Hz, 2H). ^{13}C NMR (100.6 MHz, $CDCl_3$) δ 169.75, 146.97, 110.47, 48.02, 7.2.20, 24.61, 14.49, 6.72.

HRMS (ESI) for **$C_{11}H_{18}NO$.** Calculated **M:** 179.1310, **$[M+H^+]^+$:** 180.1388, found: 180.1388.

N-benzyl-2-cyclopropylacrylamide (4.23)

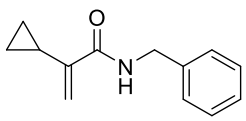

General procedure C was followed by employing cyclopropyl acetylene (198 mg, 3.00 mmol), benzylamine (390 mg, 3.9 mmol), $Pd(OAc)_2$ (6.6mg, 1 mol%), Dppp (12.3 mg, 1mol%). Purification by flash chromatography using DCM. afforded the product (308 mg, 51%).

^{1}H NMR (400 MHz, $CDCl_3$) δ 7.38 – 7.28 (m, 5H), 6.52 (s, 1H), 6.00 (t, *J* = 1.1 Hz, 1H), 5.26 (t, *J* = 1.4 Hz, 1H), 4.56 (d, *J* = 5.8 Hz, 2H), 1.53 (m, 1H), 0.85 – 0.78 (m, 2H), 0.59 – 0.53 (m, 2H). ^{13}C NMR (100.6 MHz, $CDCl_3$) δ 167.47, 144.12, 138.45, 128.91, 127.84, 127.67, 119.68, 43.86, 12.43, 6.49.

HRMS (ESI) for **$C_{13}H_{15}NO$**. Calculated **M:** 201.1153, **$[M+H^+]^+$:** 202.1231, found: 202.1229.

N-(tert-butyl)-2-cyclopropylacrylamide (4.25)

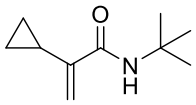

General procedure C was followed by employing cyclopropyl acetylene (198 mg, 3.00 mmol), *tert*-butyl amine (273 mg, 3.9 mmol), $Pd(OAc)_2$ (6.6mg, 1 mol%), Dppp (12.3 mg, 1mol%). Purification by flash chromatography using DCM. afforded the product (311 mg, 62%).

^{1}H NMR (400 MHz, $CDCl_3$) δ 6.07 (s, 1H), 5.84 (t, *J* = 1.1 Hz, 1H), 5.14 (t, *J* = 1.4 Hz, 1H), 1.53 – 1.43 (m, 1H), 1.39 (s, 9H), 0.86 – 0.71 (m, 2H), 0.63 – 0.47 (m, 2H). ^{13}C NMR (100.6 MHz, $CDCl_3$) δ 166.97, 145.55, 118.18, 51.23, 28.91, 12.63, 6.48.

HRMS (ESI) for **$C_{10}H_{17}NO$**. Calculated **M:** 167.1310, **$[M+H^+]^+$:** 168.1388, found: 168.1388.

2-cyclopropyl-N-pentylacrylamide (4.24)

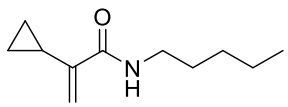

General procedure C was followed by employing cyclopropyl acetylene (198 mg, 3.00 mmol), pentylamine (330 mg, 3.9 mmol), $Pd(OAc)_2$ (6.6mg, 1 mol%), Dppp (12.3 mg, 1mol%). Purification by flash chromatography using DCM afforded the product (255 mg, 47%).

^{1}H NMR (401 MHz, $CDCl_3$) δ 6.24 (s, 1H), 5.93 (q, *J* = 1.2 Hz, 1H), 5.21 (q, *J* = 1.4 Hz, 1H), 3.33 (tdd, *J* = 7.1, 5.8, 1.0 Hz, 2H), 1.56 (q, *J* = 7.2 Hz, 2H), 1.50 (ddt, *J* = 8.4, 4.2, 1.9 Hz, 1H), 1.34 (dt, *J* = 8.0, 4.4 Hz, 4H), 0.94 – 0.86 (m, 3H), 0.84 – 0.79 (m, 2H), 0.55 (tdd, *J* = 5.1, 4.0, 0.9 Hz, 2H). ^{13}C NMR (100.6 MHz, $CDCl_3$) δ 167.49, 144.35, 119.12, 39.78, 29.40, 29.26, 22.50, 14.14, 12.44, 6.40.

HRMS (ESI) for **$C_{11}H_{19}NO$**. Calculated **M:** 181.1466, **$[M+H^+]^+$:** 182.1544, found: 182.157.2.

2-cyclopropylacrylamide (4.27)

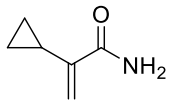

General procedure C was followed by employing cyclopropyl acetylene (198 mg, 3.00 mmol), pentylamine (570 mg, 6 mmol), $Pd(OAc)_2$ (6.6mg, 1 mol%), Dppp (12.3 mg, 1 mol%). Purification by flash chromatography using 60% v/v of EtOAc in P.E. afforded the product (127 mg, 38%). ^{1}H NMR (401 MHz, $CDCl_3$) δ 6.23 (s, 1H), 6.00 (t, *J* = 1.0 Hz, 1H), 5.92 (s, 1H), 5.30 (t, *J* = 1.3 Hz, 1H), 1.62 – 1.49 (m, 1H), 0.95 – 0.75 (m, 2H), 0.64 – 0.50 (m, 2H). ^{13}C NMR (101 MHz, $CDCl_3$) δ 169.85, 143.37, 120.80, 12.60, 6.51.

HRMS (ESI) for **C_6H_9NO**. Calculated **M:** 111.0684, **$[M+H^+]^+$:** 112.0762, found: 112.0760.

General procedure D: Hydroformylation of 1,1-disubstituted alkenes

A 2 mL glassware reactor tube was charged with α-cyclopropyl acrylamide **7.23** (0.100 mmol), $[Rh(acac)(CO)_2]$ (1.3 mg, 1 mol%) and chiral ligand **L3** (1.2 mol%) in toluene (0.4 mL). The reaction tube was placed in the reactor which was pressurized at the 20 bar (1:1 $CO:H_2$), heated to 60 or 90°C and left stirring at 900 rpm. The reaction was stopped after 16 h by cooling the reactor in an ice bath for 20 min followed by venting of the system.

General Procedure E: Hydroaminomethylation of 1,1-disubstituted alkenes

A 2 mL glassware reactor tube was charged with α-cyclopropyl acrylamide **7.23** (0.100 mmol), amine (0.100 mmol), $[Rh(acac)(CO)_2]$ (2 mol%) and **L** (2.4 mol%) in toluene (0.2 mL). The reaction tube was placed in the reactor, which was pressurized at the desired pressure, heated to 90°C and left stirring at 900 rpm. The reaction was stopped after the desired time by cooling the reactor in an ice bath for 20 min followed by venting of the system.

1-benzyl-3,5-dimethyl-3,4-dihydropyridin-2(1H)-one (4.41)

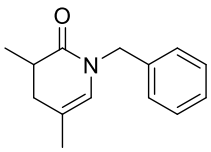

General procedure D was followed by employing N-benzyl-2-cyclopropylacrylamide (0.200 mmol), $Rh(acac)(CO)_2$ (2 mol%) and chiral ligand (**L3**) (2.4 mol%). Purification by flash chromatography on silica gel by eluting with 1% v/v NEt_3 in P.E. afforded the product (17 mg, 40%).

^{1}H NMR (400 MHz, $CDCl_3$) δ 7.25 (dd, *J* = 8.0, 6.4 Hz, 2H), 7.21 – 7.14 (m, 3H), 5.68 (t, *J* = 1.8 Hz, 1H), 4.58 (s, 1H), 2.53 (dp, *J* = 10.8, 7.0 Hz, 1H), 2.22 (dd, *J* = 16.6, 7.0 Hz, 1H), 1.99 (dd, *J* = 16.7, 10.7 Hz, 1H), 1.61 (s, 3H), 1.18 (d, *J* = 6.8 Hz, 3H). ^{13}C NMR (100.6 MHz, $CDCl_3$) δ 171.97, 137.71, 128.73, 127.71, 127.46, 123.65, 115.49, 49.10, 35.30, 34.22, 19.85, 16.16.

The enantiomeric excess was determined to be 8% by HPLC analysis using Daicel Chiralpak IC column with a gradient 80:20 nHexane/iPrOH, flow rate 1 mL/mn, λ = 220 nm: $t_{r\ major}$= 11.51 min, $t_{r\ minor}$ = 12.29 min.

3,5-dimethyl-1-pentyl-3,4-dihydropyridin-2(1H)-one (4.42)

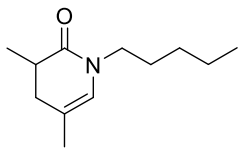

General procedure D was followed by employing N-benzyl-2-cyclopropylacrylamide (0.200 mmol), $Rh(acac)(CO)_2$ (2 mol%) and chiral ligand (**L3**) (2.4 mol%). Purification by flash chromatography on silica gel by eluting with 5% EtOAc in P.E. afforded the product in 39% yield.

^{1}H NMR (400 MHz, $CDCl_3$) δ 5.74 (p, *J* = 1.7 Hz, 1H), 3.48 – 3.30 (m, 2H), 2.49 (dp, *J* = 10.7, 7.0 Hz, 1H), 2.24 (dd, *J* = 16.6, 7.0 Hz, 1H), 2.00 (ddt, *J* = 16.7, 10.7, 1.5 Hz, 1H), 1.71 (s, 3H), 1.51 (p, *J* = 7.4 Hz, 2H), 1.35 – 1.27 (m, 4H), 1.18 (d, *J* = 7.0 Hz, 3H), 0.88 (t, *J* = 7.0 Hz, 3H). ^{13}C NMR (100.6 MHz, $CDCl_3$) δ 171.55, 124.01, 114.69, 46.18, 35.15, 34.03, 28.88, 28.26, 22.44, 19.74, 16.00, 14.03.

(E)-N-benzyl-2-methyl-6-oxohex-2-enamide (4.45)

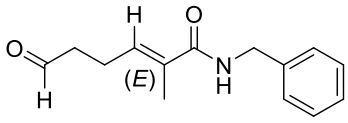

General procedure D was followed by employing N-benzyl-2-cyclopropylacrylamide (1 mmol), $Rh(acac)(CO)_2$ (1 mol%) and dppf (**L10**) (2 mol%). The peaks of the product could be extracted from the spectras as followed.

^{1}H NMR (401 MHz, $CDCl_3$) δ 9.79 (q, J = 1.1 Hz, 1H), 7.39 – 7.28 (m, 5H), 6.33 (tq, J = 7.4, 1.6 Hz, 1H), 6.03 – 5.92 (br s, 1H), 4.50 (d, J = 5.7 Hz, 2H), 2.61 (dt, J = 7.4, 1.0 Hz, 2H), 2.25 (qd, J = 7.4, 1.0 Hz, 2H), 1.89 (d, J = 1.3 Hz, 3H).^{13}C NMR (101 MHz, $CDCl_3$) δ 201.13, 168.94, 133.89, 132.14, 128.85, 127.97, 127.65, 119.52, 43.99, 42.85, 20.98, 12.93.

(E)-N-benzyl-6-hydroxy-2-methylhex-2-enamide (4.46)

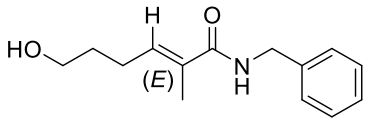

The crude mixture of **4.45** was dissolved in MeOH (1.5 mL) and $NaBH_4$ (56.7 mg, 1.5 equiv.) was added and the reaction mixture was stirred at room temperature for 16 h. Water and Et_2O were added and the phases were separated. The aqueous phase was extracted with Et_2O. The combined organic phases were washed with brine, dried with $MgSO_4$, filtered and concentrated under vacuum. The crude product was purified by column chromatography on silica gel by eluting 5% MeOH in DCM affording the alcohol as an uncolored oil in 32% yield.

^{1}H NMR (401 MHz, $CDCl_3$) δ 7.39 – 7.24 (m, 5H), 6.40 (tq, J = 7.4, 1.5 Hz, 1H), 6.04 (s, 1H), 4.50 (d, J = 5.6 Hz, 2H), 3.66 (t, J = 6.4 Hz, 2H), 2.25 (q, J = 7.4 Hz, 2H), 1.87 (q, J = 1.1 Hz, 3H), 1.69 (p, J = 7.4 Hz, 2H). ^{13}C NMR (101 MHz, $CDCl_3$) δ 169.29, 138.56, 135.85, 131.28, 128.87, 128.00, 127.65, 62.32, 44.00, 31.78, 24.82, 12.88.

HRMS (ESI) for **$C_{14}H_{19}NO_2$**. Calculated **M:** 233.1415, **$[M+H^+]^+$:** 234.1494, found: 234.1491.

(E)-N-benzyl-2-methyl-6-oxo-7-(piperidin-1-yl)hept-2-enamide (4.54)

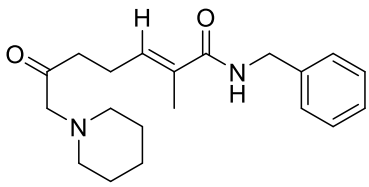

General procedure E was followed by employing **4.23** (1 mmol), $Rh(acac)(CO)_2$ (1 mol%) and **L10** (2 mol%). Purification by flash chromatography on silica gel by eluting with 5% MeOH in DCM afforded the product as an uncolored oil in 25% yield.

^{1}H NMR (401 MHz, $CDCl_3$) δ 7.39 – 7.25 (m, 5H), 6.31 (tq, J = 7.3, 1.5 Hz, 1H), 5.98 (s, 1H), 4.49 (d, J = 5.7 Hz, 2H), 3.10 (s, 2H), 2.60 (t, J = 7.3 Hz, 2H), 2.46 – 2.35 (m, 6H), 1.88 (t, J = 1.2 Hz, 3H), 1.60 (p, J = 5.6 Hz, 4H), 1.48 – 1.37 (m, 2H). ^{13}C NMR (101 MHz, $CDCl_3$) δ 208.67, 169.12, 138.53, 134.59, 131.85, 128.88, 128.04, 127.66, 68.91, 55.13, 44.01, 39.13, 25.96, 23.98, 22.53, 12.94.

HRMS (ESI) for **$C_{20}H_{28}N_2O_2$**. Calculated **M:** 328.2150, **$[M+H^+]^+$:** 329.2224, found: 329.2232.

N-benzyl-2-cyclopropyl-3-(piperidin-1-yl)propenamide (4.55)

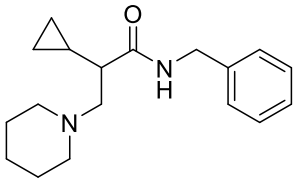

General procedure E was followed by employing **4.23** (1 mmol), $Rh(acac)(CO)_2$ (1 mol%) and **L10** (2 mol%). Purification by flash chromatography on silica gel by eluting with 10% MeOH in DCM afforded the product as an uncolored oil in 20% yield.

^{1}H NMR (401 MHz, $CDCl_3$) δ 8.40 (s, 1H), 7.37 – 7.18 (m, 5H), 4.49 (dd, J = 14.7, 5.7 Hz, 1H), 4.38 (dd, J = 14.7, 5.2 Hz, 1H), 2.72 (dd, J = 12.9, 10.7 Hz, 1H), 2.45 – 2.43 (m, 3H), 2.34 – 2.26 (m, 2H), 1.63 (td, J = 10.3, 3.3 Hz, 1H), 1.45 – 1.32 (m, 6H), 0.90 (dtt, J = 9.9, 8.1, 5.0 Hz, 1H), 0.69 (dddd, J = 9.1, 8.2, 5.8, 4.7 Hz, 1H), 0.48 (dddd, J = 9.0, 8.0, 5.7, 4.5 Hz, 1H), 0.36 (ddt, J = 9.3, 5.7, 4.8 Hz, 1H), 0.11 – 0.03 (m, 1H).

^{13}C NMR (101 MHz, $CDCl_3$) δ 174.55, 139.07, 128.66, 127.91, 127.28, 61.18, 54.52, 47.68, 43.46, 25.83, 24.06, 12.17, 5.40, 3.50.

HRMS (ESI) for **$C_{18}H_{26}N_2O$**. Calculated **M:** 286.2045, **$[M+H^+]^+$:** 287.2118, found: 287.2126.

N-benzyl-2-methyl-4-morpholinobutanamide (4.56)

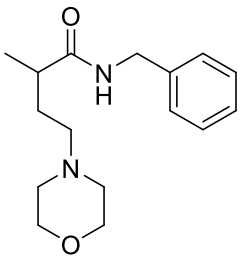

General procedure E was followed by employing **4.44** (0.200 mmol), $Rh(acac)(CO)_2$ (2 mol%) and chiral ligand (**L13**) (2.4 mol%). Purification by flash chromatography on silica gel by eluting with 10% MeOH in DCM afforded the product in 34% yield.

^{1}H NMR (401 MHz, $CDCl_3$) δ 7.38 – 7.19 (m, 5H), 6.58 (s, 1H), 4.51 (dd, *J* = 14.4, 6.0 Hz, 1H), 4.34 (dd, *J* = 14.4, 5.1 Hz, 1H), 3.57 (t, *J* = 4.7 Hz, 4H), 2.44 – 2.31 (m, 4H), 2.29 – 2.11 (m, 3H), 1.76 (dddd, *J* = 14.2, 9.7, 6.9, 4.6 Hz, 1H), 1.64 (dddd, *J* = 14.1, 8.9, 7.0, 5.1 Hz, 1H), 1.18 (d, *J* = 6.9 Hz, 3H).

^{13}C NMR (101 MHz, $CDCl_3$) δ 175.71, 138.70, 128.73, 128.03, 127.56, 66.87, 56.07, 53.33, 43.57, 38.57, 30.67, 17.85.

HRMS (ESI) for **$C_{16}H_{25}N_2O_2$**. Calculated **M:** 276.1837, **$[M+H^+]^+$:** 277.1916, found: 277.1916.

The enantiomeric excess was determined to be 36% by HPLC analysis using Daicel Chiralpak ADH column with a gradient 90:10 nHexane/iPrOH, flow rate 1 mL/mn, λ = 220 nm: $t_{r\ major}$= 10.70 min, $t_{r\ minor}$ = 11.70 min.

4.5. Annexes

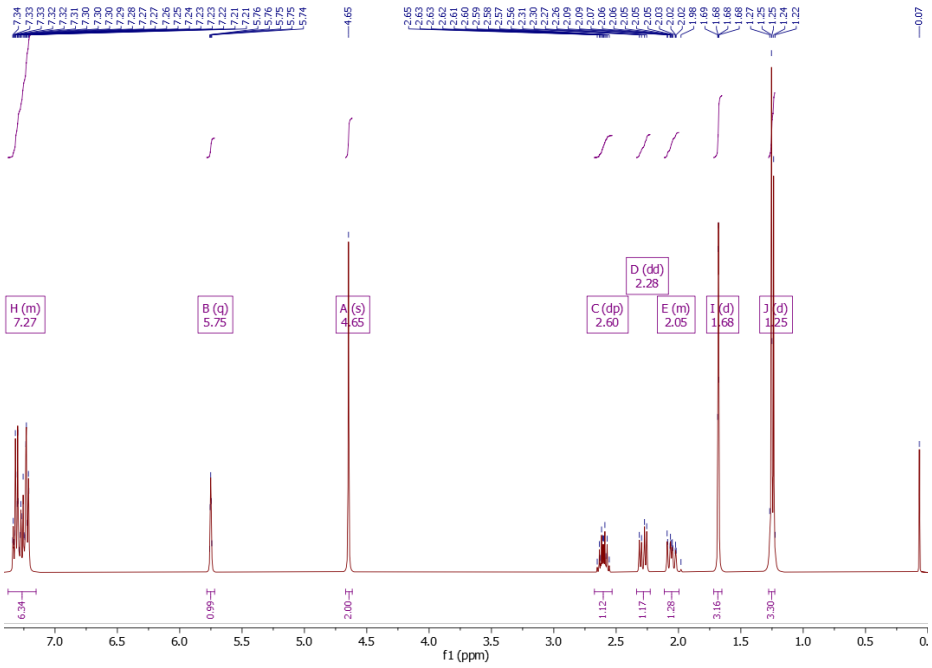

Figure 2. ^{1}H NMR of 4.41

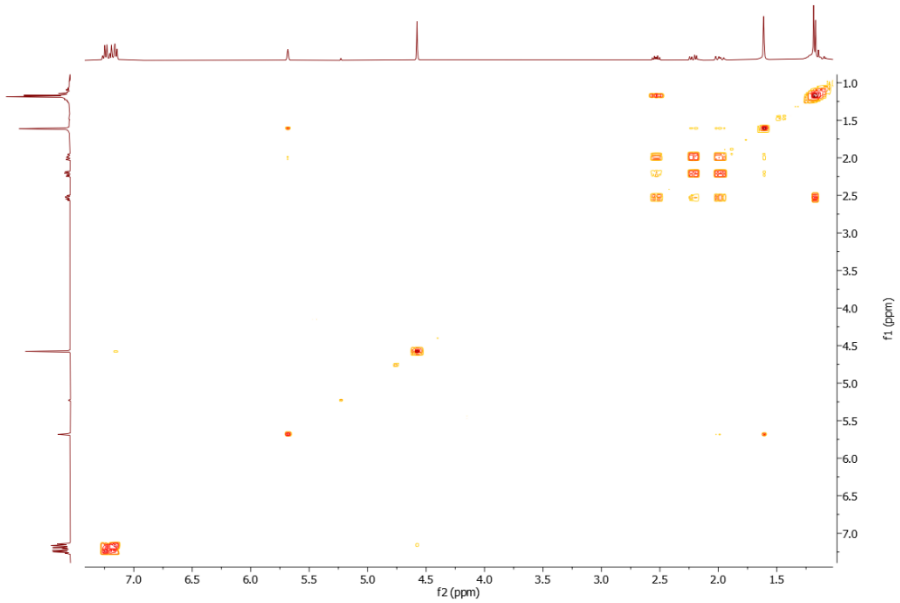

Figure 3.COSY (^{1}H-^{1}H) NMR of 4.41

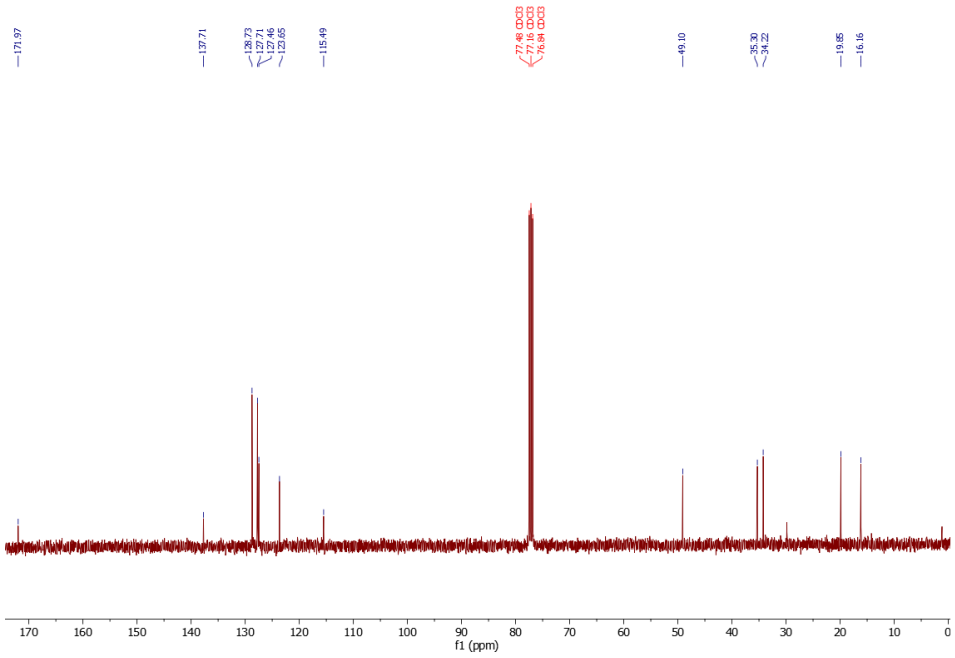

Figure 4. ^{13}C NMR of 4.41

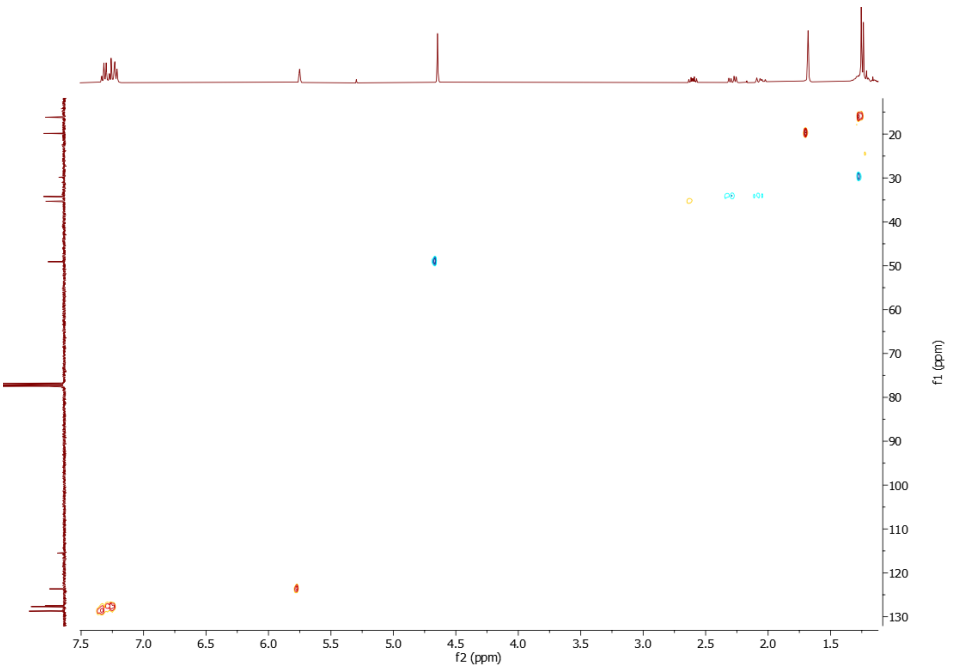

Figure 5. HSQC (^{1}H-^{13}C) NMR of 4.41

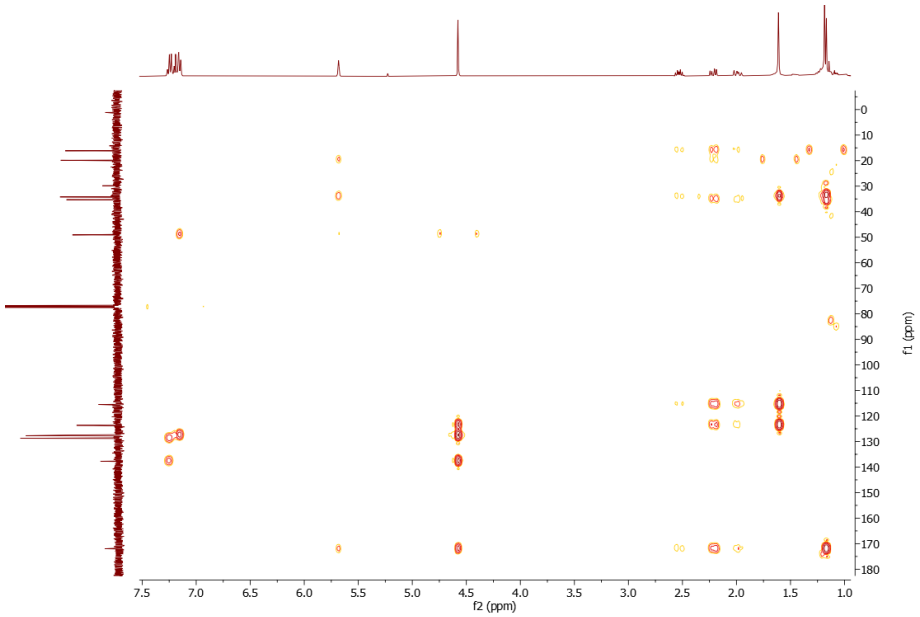

Figure 6. HMBC (^{1}H-^{13}C) NMR of 4.41

4.6. References

[1] Wu, G. Amino acids: metabolism, functions, and nutrition. *Amino Acids*. **2009**, *37*, 1-17. b) Wagner, I.; Musso, H. *New Naturally Occurring Amino Acids*. Angew. Chem. Int. Ed. **1983**, *22*, 816-828.

[2] Brown, K. M.; Roy, K. K.; Hockerman, G. H.; Doerksen, R. J.; Colby, D. A. Activation of the γ-Aminobutyric Acid Type B (GABAB) Receptor by Agonists and Positive Allosteric Modulators. *J. Med. Chem.* **2015**, *58*, 6336-6347.

[3] Abdel-Halim, H.; Hanrahan, J. R.; Hibbs, D. E.; Johnston, G. A. R.; Chebib, M. A Molecular Basis for Agonist and Antagonist Actions at $GABA_C$. Receptors. *Chem. Biol. Drug Des.* **2008**, *71*, 306-327.

[4] a) Mann, A.; Boulanger, T.; Brandau, B.; Durant, F.; Evrard, G.; Heaulme, M.; Desaulles, E.; Wermuth, C. G. Synthesis and biochemical evaluation of baclofen analogs locked in the baclofen solid-state conformation. *J. Med. Chem.* **1991**, *34*, 1307-1313. b) Fromm, G. H.; Terrence, C. F.; Chattha, A. S.; Glass, J. D. Baclofen in Trigeminal Neuralgia Its Effect on the Spinal Trigeminal Nucleus: A Pilot Study. *Archives of Neurology.* **1980**, *37*, 768-771.

[5] a) Hoekstra, M. S.; Sobieray, D. M.; Schwindt, M. A.; Mulhern, T. A.; Grote, T. M.; Huckabee, B. K.; Hendrickson, V. S.; Franklin, L. C.; Granger, E. J.; Karrick, G. L. Chemical Development of CI-1008, an Enantiomerically Pure Anticonvulsant. *Org. Process Res. Dev.* **1997**, *1*, 26-38. b) Chandrasekhar, S.; Mohapatra, S. Asymmetric synthesis of anti-convulsive drug (S)-Vigabatrin®. *Tetrahedron Lett.* **1998**, *39*, 6415-6418.

[6] Lippert, B.; Metcalf, B. W.; Jung, M. J.; Casara, P. 4-amino-hex-5-enoic acid, a selective catalytic inhibitor of 4-aminobutyric-acid aminotransferase in mammalian brain. *Eur. J. Biochem.* **1977**, *74*, 441-445.

[7] Lapin, I. Phenibut (beta-phenyl-GABA): a tranquilizer and nootropic drug. *CNS Drug Rev*. **2001**, *7*, 471-481.

[8] Wang, J.; Blaszczyk, S. A.; Li, X.; Tang, W. Transition Metal-Catalyzed Selective Carbon-Carbon Bond Cleavage of Vinylcyclopropanes in Cycloaddition Reactions. *Chem. Rev.* **2021**, *121* (1), 110–139.

[9] Jiang, G. J.; Fu, X. F.; Li, Q.; Yu, Z. X. Rh(I)-Catalyzed [5 + 1] Cycloaddition of Vinylcyclopropanes and CO for the Synthesis of α,β- and β,γ-Cyclohexenones. *Org. Lett.* **2012**, *14* (3), 692–695.

[10] Liang, Y.; Jiang, X.; Yu, Z. X. Enantioselective Total Synthesis of (+)-Asteriscanolide via Rh(I)-Catalyzed [(5+2)+1] Reaction. *Chem. Commun.* **2011**, *47* (23), 6659–6661.

[11] Wang, D. L.; Guo, W. Di; Liu, L.; Zhou, Q.; Liang, W. Y.; Lu, Y.; Liu, Y. Pd-Catalyzed Hydroaminocarbonylation of Alkynes with Aliphatic Amines and Its Mechanism Study. *Catal. Sci. Technol.* **2019**, *9* (6), 1334–1337.

[12] Wang, D.; Guo, W.; Zhou, Q.; Liu, L.; Lu, Y.; Liu, Y. Hydroaminocarbonylation of Alkynes to Produce Primary α,β-Unsaturated Amides Using NH_4HCO_3 Dually as Ammonia Surrogate and Brønsted Acid Additive. *ChemCatChem* **2018**, *10*, 4264–4268.

[13] Dalling, A. G.; Yamauchi, T.; McCreanor, N. G.; Cox, L.; Bower, J. F. Carbonylative C–C Bond Activation of Electron-Poor Cyclopropanes: Rhodium-Catalyzed (3+1+2) Cycloadditions of Cyclopropylamides. *Angew. Chemie - Int. Ed.* **2019**, *58* (1), 221–225.

[14] Miró, R.; Cunillera, A.; Margalef, J.; Lutz, D.; Börner, A.; Pamies, O.; Diéguez, M.; Godard, C. Rh-Catalyzed Asymmetric Hydroaminomethylation of α-Substituted Acrylamides: Application in the Synthesis of RWAY. *Org. Lett.* **2020**, *22* (22), 9036–9040.

[15] Moon, B.; Han, S.; Kim, D. Efficient Synthesis of Highly Functionalized Cyclic Aminimides. *Org. Lett.* **2005**, *7* (15), 3359–3361.

CHAPTER V

RHODIUM CATALYZED ASYMMETRIC HYDROAMINOMETHYLATION TOWARDS CONTINUOUS FLOW

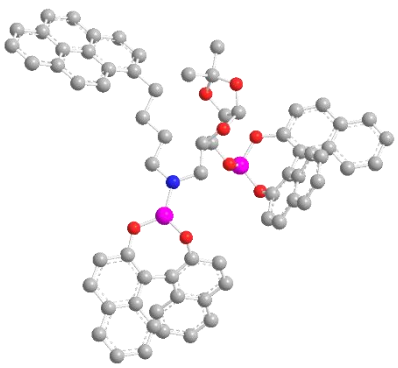

5.1. Introduction

Currently, over 90% of all industrial chemicals are produced through catalytic processes.[1] Whether via homogeneous, heterogeneous, or even enzymatic catalysis, these processes are fundamentally molecular in nature, involving the conversion of molecules into new compounds. Despite the benefits offered by homogeneous and heterogeneous catalysis, there are significant challenges that need to be addressed in both cases.[2]

The main type of heterogeneous catalysts are oxides and metal supported particles, which are in a distinct phase from the reagents and the products.[3] This allows for straightforward recovery of the catalyst, thereby simplifying their integration into industrial processes. However, harsh reaction conditions such as elevated temperatures and pressures are typically necessary to enhance the diffusion rate of reactants towards the catalytic core, as well as for processes like reactant adsorption and product desorption. Furthermore, identifying and modifying the active site of heterogeneous catalysts is often challenging, leading to lower efficiency. Despite these drawbacks, most bulk industrial processes rely on heterogeneous catalysis.

In homogeneous catalysis, both the catalyst and reagents share the same phase, typically in a liquid state. These catalysts exhibit high levels of activity and selectivity, including chemo-, regio-, and enantioselectivity, primarily due to the capacity to fine-tune their performance through variations in ligand structure. Additionally, modern spectroscopic techniques like multinuclear NMR offer insights into atomic-level mechanisms, contributing to the development of more effective catalysts. Nevertheless, a significant drawback of homogeneous catalysts lies in their challenging separation from reaction products, which restricts opportunities for recovery and reutilization.[4]

Hence, an important challenge in modern chemistry is the discovery of catalytic systems that combine the merits of both homogeneous (selectivity) and heterogeneous (recycling) catalysis. Numerous techniques were devised to retrieve

and reuse homogeneous catalysts, as well as to efficiently separate the catalyst from the products. Among these methods, one of the prevailing approach involves anchoring homogeneous catalysts onto solid supports, resulting in the so-called "heterogenized catalysts". These heterogenized systems can be produced through various approaches (Figure 1).[5]

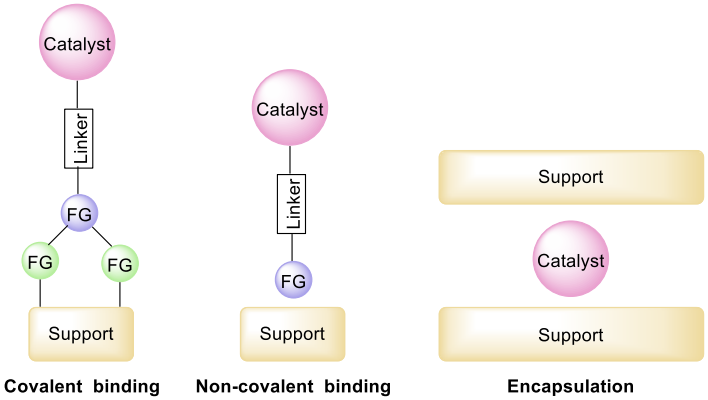

Figure 1. Main approaches for the immobilization of homogeneous catalysts onto solid supports.

In this work, we focused on the non-covalent immobilization of homogeneous catalysts for their application in hydroformylation and hydroaminomethylation reactions.

5.1.1. Homogeneous catalyst immobilization via π-π interactions

Graphitic materials have attracted significant interest as potential supports for anchoring homogeneous catalysts through π-π interactions. These interactions provide a stable foundation for the anchoring metal complexes and refer to non-covalent connections that arise between the electron densities of stacked aromatic systems. While benzene traditionally serves as the archetype for aromatic interactions, recent investigations have unveiled that larger aromatic systems, such as pyrene and coronene, provide even more resilient π-π stacking bonds with CNTs. In fact, a comprehensive exploration of π-interactions involving organic molecules encompassing benzene, 2,3-dichloro-5,6-dicyano-1,4-benzoquinone (DDQ), azulene, and pyrene - in conjunction with CNTs, demonstrated a remarkable difference in

stacking interaction strengths. Specifically, the pyrene component (at around 9.69 kcal/mol) exhibits a stacking strength nearly twice that of benzene (approximately 4.61 kcal/mol).[6] This highlights the importance of incorporating a pyrene or coronene moiety within the catalyst/ligand structure for achieving a stable heterogenized catalyst through such interactions. This methodology was applied in a few asymmetric reactions such as asymmetric hydrogenation of methyl acetamidocinnamate (Scheme 1).

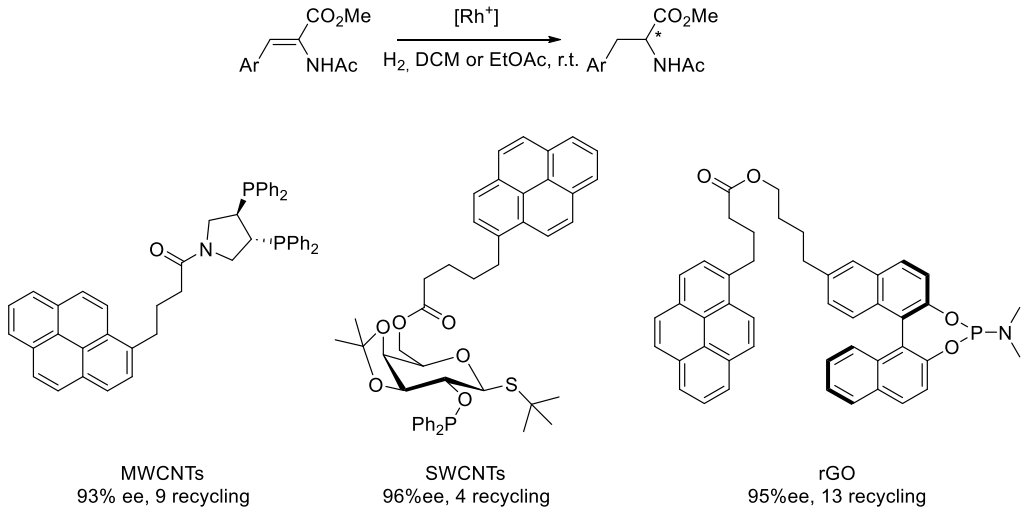

Scheme 1. Asymmetric hydrogenation of methylacetamidocinnamate with pyrene-tagged ligands.

Qi-Lin and co-workers developed the synthesis of a new pyrene tagged diphosphine by a simple amide coupling from (*3R,4R*)3,4-bis(diphenylphosphino)- pyrrolidine (Pyrphos).[7] They tested the adsorption properties of the catalysts on CNTs in THF (83%), MeOH (94%), DCM (50%) and EtOAc (97%). In view of these results, they performed the catalysis in DCM and recovered the catalyst by switching the solvent to EtOAc. Khiar and co-workers developed the same methodology with the carbohydrate-based mixed P/S ligand.[8] Indeed, they observed that the homogeneous catalyst afforded good enantioselectivity in DCM whereas in EtOAc, only 3% ee was obtained. Interestingly, when the pyrene chain was shortened to 2 carbons, no enantioinduction was reported. Shi and co-workers recently described

the *in situ* immobilization of a multicomponent chiral catalyst bearing the pyrene tagged monophos ligand on graphene.[9] The active catalyst was formed with two equivalents of the ligand with each pyrene moiety interacting with the graphene support. A control experiment without the pyrene moiety showed that the catalyst could not anchor on the carbon material, showing the importance of the pyrene unit. They described the asymmetric hydrogenation in EtOAc, making the catalyst easily recovered by a direct filtration of the reaction media. This strategy provided a constant enantioselectivity upon recycling tests although the reaction time needed to be extended to complete the conversion after the 7th recycling experiment.

Schulz and Didier reported the immobilization of anthracene and pyrene tagged bis(oxazoline) ligands on charcoal, fullerene and SWCNTs.[10] The copper complexes were evaluated in asymmetric Henry and ene reactions (Scheme 2). High stability of the catalysts was observed as the yield and enantioselectivity only showed a small drop. The more stable catalyst was the pyrene tagged bis(oxazoline) supported on SWCNT giving 84% yield and 62% ee after the 7th run.

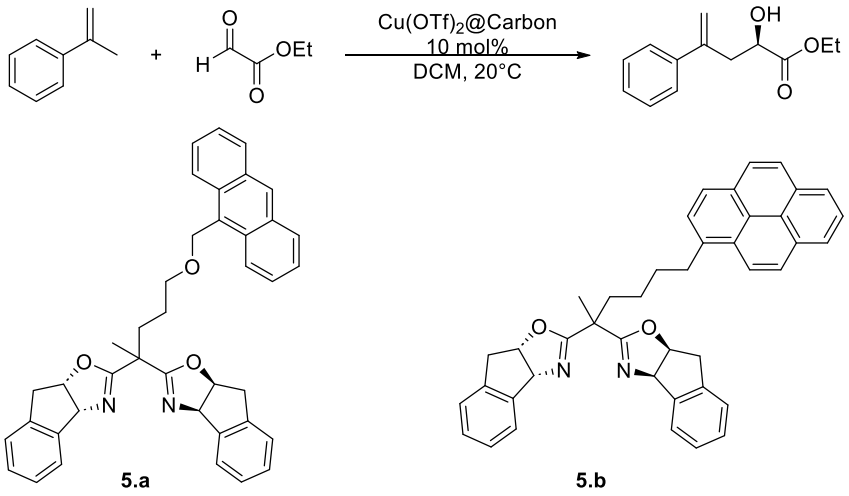

	Run 1		Run 7	
Catalyst	Yield (%)	ee (%)	Yield (%)	ee (%)
[**5.a**-Cu(OTf)$_2$@charcoal]	85	70	76	52
[**5.b**-Cu(OTf)$_2$@charcoal]	89	69	78	57
[**5.b**-Cu(OTf)$_2$@fullerene]	87	56	79	52
[**5.b**-Cu(OTf)$_2$@SWCNT]	89	64	84	62

Scheme 2. Anthracene and pyrene-tagged bis(oxazoline) ligands for asymmetric Henry reaction.

More recently, Schulz and co-workers developed the immobilization of chiral isothiourea as organocatalyst on rGO for asymmetric cycloaddition.[11] The same group also studied the asymmetric ring-opening of cyclohexane oxide and hetero

Diels-Alder cycloaddition using a pyrene-tagged chromium salen complex on rGO (Scheme 3).[12]

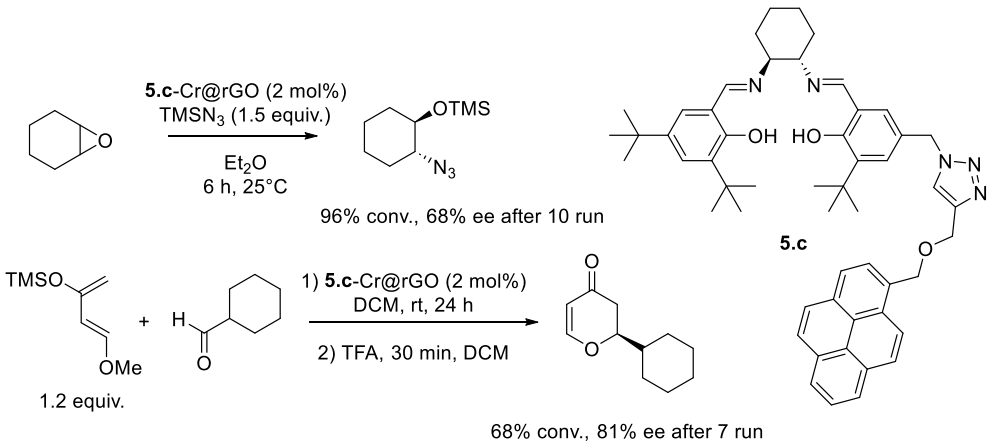

Scheme 3. Pyrene-tagged salen complex for asymmetric cycloaddition.

This strategy was more widely used in non-asymmetric reactions such as olefins methathesis with Ru-carbene complexes,[13] Au-catalyzed enyne cyclization,[14] Pd-CoNP catalyzed Suzuki-Miyaura coupling,[15] Ru-catalyzed water oxidation,[16] Cu-catalyzed C-H activation on rGO[17] or cycloaddition of CO_2 to epoxides[18] and click reaction.[19]

Peris and co-workers used pyrene tagged NHC ligands for Ru-catalyzed nitro reduction, ketone hydrogenation, dehydrofluorination or Rh-catalyzed hydrosilylation of alkynes and 1,4-addition to α,β-unsaturated ketones.[20] Even when employing less polar solvents like toluene and subjecting the system to elevated temperatures (up to 100°C), the catalysts could be reused for up to 10 cycles without loss of activity nor selectivity. The investigation also unveiled that incorporating two pyrene moieties within the complexes, as opposed to one, led to a reduction of the catalyst leaching.

Another example of the use of π–π interactions for the anchoring of chiral ligands was reported by our group for the asymmetric hydroformylation of norbornene under continuous flow (Scheme 4).[21] The ligand was a chiral bisphosphite based on a sugar backbone including a pyrene moiety and the catalysts were immobilized by

π-π interactions on three carbon support (MWCNTs, rGO and CBs). The chain length between the pyrene tag and the ligand backbone influenced the activity and a longer chain (n=4 vs n=1) had a beneficial impact on the catalysis. The catalysts suffered from a drastic rhodium leaching under batch conditions. In contrast, when the catalysts were tested in continuous flow using a U-shaped reactor, they exhibited higher stability, especially when carbon beads were used as support. This catalyst delivered a constant conversion of 28% and enantioselectivity of 71% under the optimized conditions. Interestingly, the ee obtained in continuous flow was higher than that reached under batch conditions. Using this catalyst, the AHF of norbornene could be performed for 6h in continuous flow with only an initial leaching of rhodium.

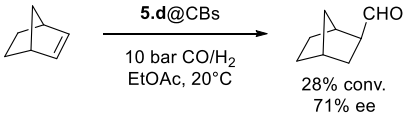

		t=80 min		t=240 min	
Support	Rh (wt%)	Conv. (%)	ee (%)	Conv. (%)	ee (%)
MWCNT	0.41	14	70	4	72
rGO	0.48	12	63	7	65
CBs	0.56	12.5	69	10	71

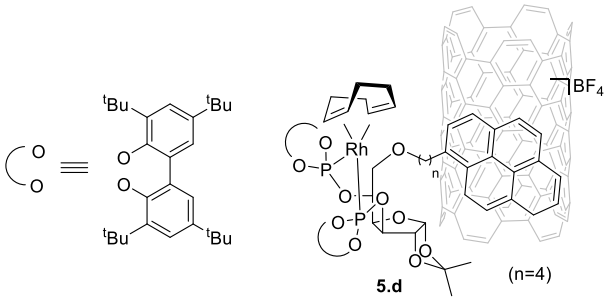

Scheme 4. Continuous flow AHF of norbornene using 5.d immobilized on carbon materials

5.1.2. Asymmetric hydroformylation in continuous flow

Apart from the latter study described in the last section, only a few examples of asymmetric hydroformylation were reported to date using heterogenized catalysts and their application under flow conditions. The initial study was conducted by Nozaki and coworkers, who outlined the process of attaching the BINAPHOS ligand

onto a cross-linked polymer matrix. [22] To achieve this, modifications were made to the BINAPHOS ligand by introducing a vinyl group into its backbone. The modified ligand underwent radical polymerization alongside a commercially available mixture of divinylbenzene, encompassing 1,2-, 1,3-, and 1,4-divinylbenzene. This led to the formation of the PS-BINAPHOS ligand in a 3:97 mixture ratio (BINAPHOS:divinylbenzenes). The authors noted that the catalyst was evenly distributed within the polymeric structure, preventing the formation of inactive dimeric species during catalysis.

Interestingly, when the immobilized catalyst was employed for the asymmetric hydroformylation of diverse alkenes like styrene, vinyl acetate, (Z)-2-butene, and 3,3,3-trifluoropropene, the outcomes in terms of activity and selectivity were very similar those observed in the homogeneous version (Scheme 5). Nonetheless, recycling experiments performed in batch mode for the asymmetric hydroformylation of styrene revealed a decline in activity during the second run. Subsequently, an increased reaction time was necessary in the third run to maintain the desired activity level. This drop in activity was attributed to the polymer to break down during the reaction caused by the mechanical stirring.

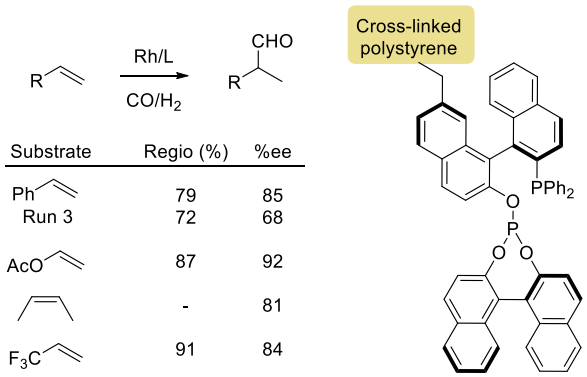

Scheme 5. Continuous flow AHF using immobilized BINAPHOS ligand

Later, the same research group explored the asymmetric hydroformylation of alkenes in a flow setup, utilizing the same ligand and supercritical CO_2 as a solvent. For the catalytic process, various injections of styrene solution mixed with syngas

were passed through the catalyst bed. This innovative approach enabled up to 7 cycles in the flow system without significant losses in either activity (retaining up to 90% activity) or selectivity. However, it was essential to maintain high pressures (around 120 atm) to uphold the activity at the desired level of 90%. If the pressure was reduced to 88 atm, the activity dropped to less than 20%.[23]

Additionally, this system was employed to hydroformylate various alkenes through different injection cycles. In all cases, good to exceptional selectivities were achieved. The same catalyst demonstrated its effectiveness across up to 6 different alkenes, with intermittent use of styrene to monitor activity levels.

More recently, Landis and collaborators undertook the immobilization of the bisdiazophospholane (BDP) ligand onto various amine resins (Scheme 6).[24] This study revealed that the separation between the support and the metal center held significance; longer separations correlated with enhanced selectivity. However, despite these findings, the regioselectivity and enantioselectivity achieved were lower in all cases when compared to the results obtained with the corresponding homogeneous catalyst.

The ligand's performance was assessed in batch mode, conducting up to 9 cycles in the Rh-catalyzed asymmetric hydroformylation of styrene, vinyl acetate and tertbutylsilylallylether. Variations in pressure during cycles 5, 7, and 9 exhibited a negative influence on enantioselectivity but a positive effect on the b:l ratio when higher pressures were applied in the case of styrene. Catalyst leaching was evaluated after each cycle, revealing the most substantial loss of catalyst during the initial cycles. Furthermore, the solvent's impact was scrutinized in cycle 7, with toluene being replaced by THF. This substitution led to a higher loss of metal catalyst. Lastly, a racemic variant of the immobilized system was employed in a plug flow reactor for the hydroformylation of vinyl acetate.

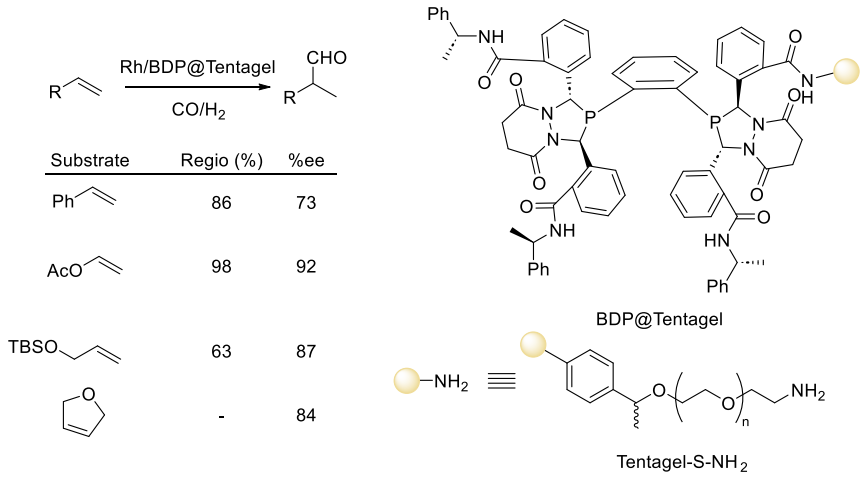

Scheme 6. Continuous flow AHF using BDP@Tentagel

The system remained active for 6 consecutive runs, roughly spanning 39 hours, demonstrating favorable regioselectivities for the branched product and complete conversion. The primary catalyst loss occurred in the initial cycle (reaching up to 6.1 wt%), followed by a sustained loss of 0.5 wt% per subsequent cycle.

5.1.3. Hydroaminomethylation in continuous flow

Only a few examples of continuous flow hydroaminomethylation were reported to date. Monflier, Vogt and Seidensticker used water as solvent, along with a water-soluble catalyst made from sulfoxantphos and $[Rh(acac)(CO)_2]$.[25] The key finding was the use of randomly methylated-β-cyclodextrins (RAME-β-cyclodextrins) to form an inclusion complex and make possible the catalysis even with such a polarity difference (Figure 2). This approach's potential was confirmed through recycling experiments involving the transferability of 1-octene hydroaminomethylation with diethylamines. Subsequently, a series of batch experiments were executed to establish optimal experimental conditions that could be smoothly adapted for continuous operation.

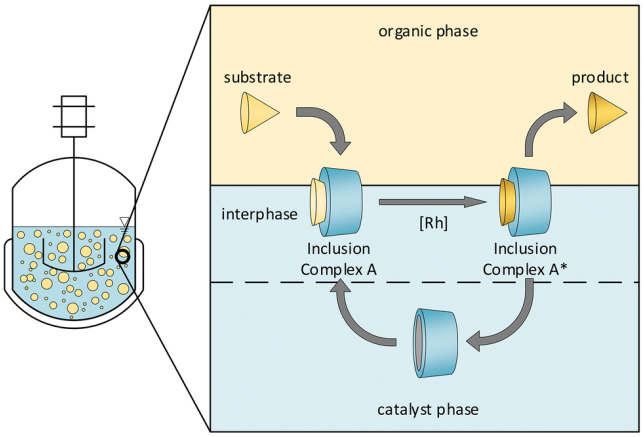

Figure 2. Biphasic HAM mediated by cyclodextrin.[25]

The overall conversion rate was predominantly influenced by the concentration of cyclodextrins. Nonetheless, a non-uniform reliance of the individual reaction rates within the HAM tandem catalytic reaction network on both cyclodextrin and catalyst concentrations could lead to an unfavorable alteration in product distribution. The identified favorable reaction conditions were then successfully employed in a continuously operated miniplant for the first time. Once the operating parameters were defined, further optimization was carried out while the process was running. Notably, elevated reaction temperatures not only augmented conversion rates but also improved the selectivity towards the main product.

When the reaction was performed in a Continuous Stirred-Tank Reactor (CSTR), distinct enhancements were observed in comparison to batch experiments, particularly in terms of selectivity. Over a duration of 80 hours, impressive yields reaching up to 70% were achieved, accompanied by a main product selectivity exceeding 80% and a linear-to-branched selectivity of over 96%. Notably, this achievement was obtained without the need for additional catalyst or ligand.[26]

Throughout this extended experiment, the leaching of the catalyst remained at extremely low levels, mostly below 0.003% per hour, which corresponded to a rhodium loss of less than 0.15 mg per kilogram of product. These results

demonstrated the potential applicability of this reaction system in large-scale industrial processes.

The other strategy developed was the use of thermomorphic multiphase system (TMS).[27] The authors reported that methanol and n-dodecane are two suitable solvents for a TMS that facilitates phase separation upon cooling. The system catalyzed by a complex made from sulfoxantphos and Rh(acac)(COD) was able to perform HAM of 1-decene with diethylamine. Very low leaching of Rh was observed. The drawback of this system is its tolerance to water accumulated during the reaction, that was changing the properties of the TMS over the course of the reaction. To avoid water accumulation, the system was improved by nanofiltration of the organic phase, also reducing the catalyst leaching.[28]

Recently, Ibrahim and Abolhasani presented HAM in segmented flow using a Rh/N-Xantphos catalyst along with 2-fluoro-4-methylbenzoic acid as a co-catalyst (Scheme 7).[29] They reported a cooperative effect, increasing by a 70-fold the reactivity in comparison with that of the Rh/Xantphos system under batch conditions. This new catalytic system favored the H-H cleavage, driving forward the enamine reduction that was the rate limiting step. The ionic catalyst developed could be recycled up to 4 times by changing the solvent to pentane without loss of activity.

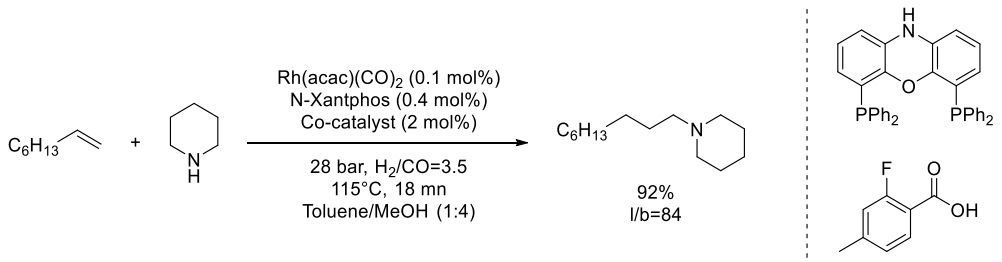

Scheme 7. Continuous segmented flow HAM using N-Xantphos and acid co-catalyst.

Therefore, good results were reported in the Rh-catalyzed hydroaminomethylation reaction under flow conditions. However, the asymmetric version of this process was not reported to date.

Hence, here, our objective was the preparation of heterogenized chiral Rh catalysts for their application in the asymmetric hydroaminomethylation of acrylamides under

batch and flow conditions. The design of the catalysts was based on a previous report from our group that described the efficient hydroaminomethylation of these substrates into chiral amines under homogeneous conditions.[30] These catalysts would be supported onto carbon support via π- π interaction by introduction of a pyrene moiety in the backbone of the phosphite-phosphoramidite ligands (Figure 3). In the following sections, the results obtained to reach this objective will be described.

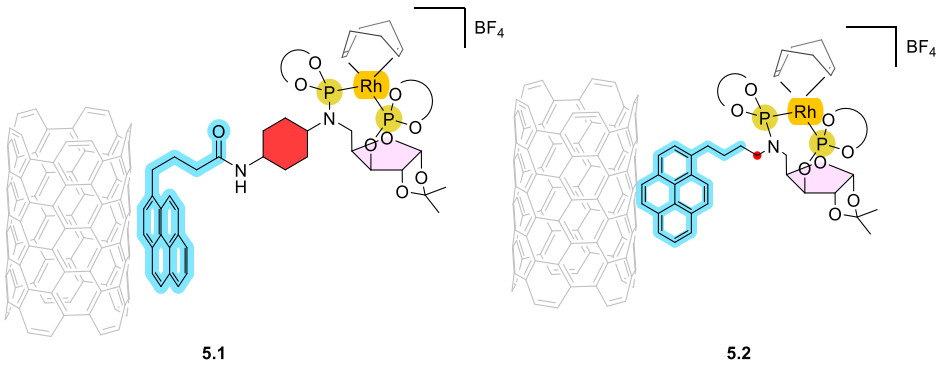

5.1 5.2

Figure 3. Aimed catalysts for the asymmetric HAM of acrylamides in continuous flow.

5.2. Results and discussion

5.2.1. Retrosynthesis of the catalysts for their immobilization

*5.2.1.1. Retrosynthesis of the catalyst **5.1***

The retrosynthesis of **5.1** described in Scheme 8 involved the heterogenization of the cationic rhodium complex **5.3** by π-π interaction between the pyrene moiety and a carbon support (carbon nanotube, reduced graphene oxide or carbon beads) in a polar solvent (DCM, EtOAc). The cationic rhodium complex **5.3** could be synthesized by complexation of the chiral phosphite phosphoramidite ligand **5.4** with the rhodium precursor $[Rh(COD)_2]BF_4$. The phosphite phosphoramidite ligand **5.4** would be produced via the reaction of the amino alcohol **5.5** with two equivalents of chlorophosphite generated *in situ* from phosphorus trichloride and 1,1'-Bi-2-naphthol (BINOL). The pyrene-tagged sugar-based amino alcohol **5.5** would be synthesized via nucleophilic substitution from the pyrene tagged cyclohexyl amine

derivative **5.6** and the xylose-based activated tosyl **5.7** easily produced from D-xylose. The pyrene tagged nucleophilic amine **5.6** could be produced from the commercially available 1-pyrenebutyric acid **5.8** and *trans*-1,4-diaminocyclohexane **5.9** by amide coupling.

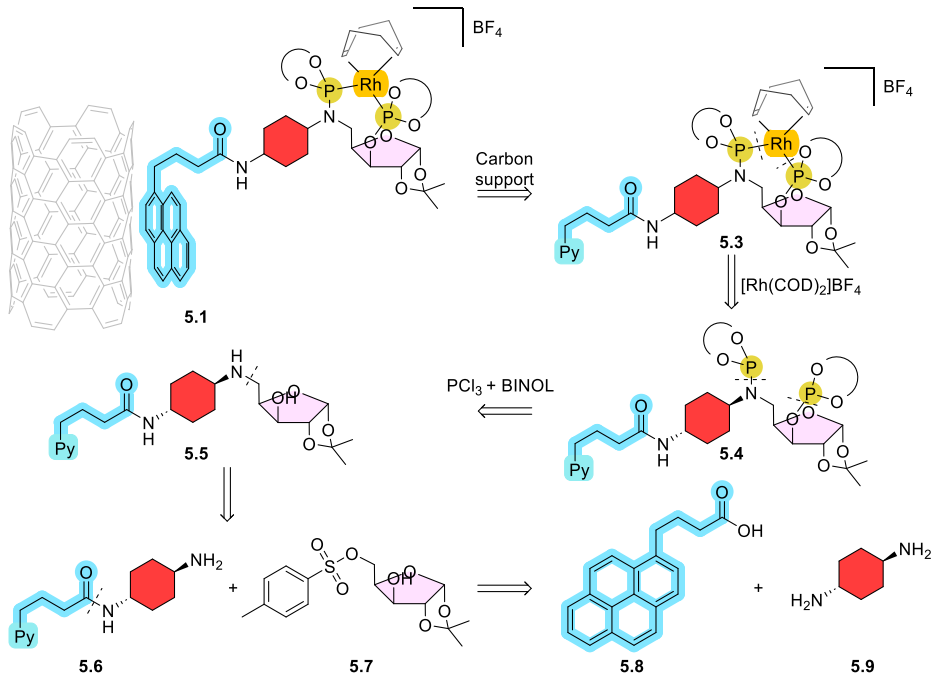

Scheme 8. Retrosynthesis of the heterogenized catalyst 5.1 from 1-pyrenebutyric acid 5.8 and *trans*-1,4-diaminocyclohexane 5.9.

*5.2.1.2. Retrosynthesis of the catalyst **5.2***

The retrosynthesis of **5.2** depicted in Scheme 9 involved the same key steps as for the formation of the heterogenized catalyst **5.1**. Thus, the heterogenization would take place via π-π interaction of the pyrene moiety from the cationic rhodium complex **5.10**. The linear pyrene-tagged sugar-based amino alcohol **5.12** would be synthesized via nucleophilic substitution from the 1-pyrenebutylamine **5.13** and the xylose-based activated tosyl **5.7**. The amine **5.13** can be synthesized via the reduction of 1-pyrenebutanamide **5.14**. The amide **5.14** can be obtained from the commercially available 1-pyrenebutyric acid **5.8** and ammonia.

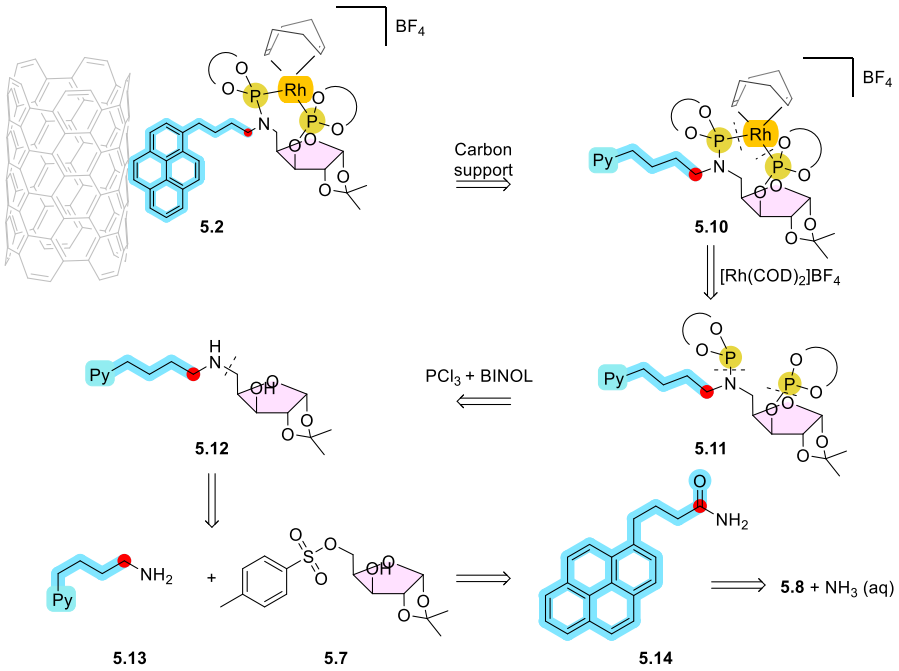

Scheme 9. Retrosynthesis of the heterogenized catalyst 5.2 from 1-pyrenebutyric acid 5.8 and ammonia.

5.2.2. Synthesis of the ligands

*5.2.2.1. Synthesis of the ligand **5.4***

For the synthesis of this ligand, the 1-pyrenebutyric acid **5.8** was initially transformed into its acyl chloride form by reaction with oxalyl chloride in toluene with DMF as a catalyst at 55°C for 2 h. Then, the *trans*-1,4-diaminocyclohexane **5.9** was added portion wise at room temperature to the solution of the acyl chloride intermediate and further stirred for 2 h. The monosubstitution via amide coupling resulted in the formation of the amide containing primary amine **5.6** in 45% yield after column chromatography (Scheme 10). The moderate yield obtained for the amide coupling could be explained by the low solubility of **5.6** during the work-up.

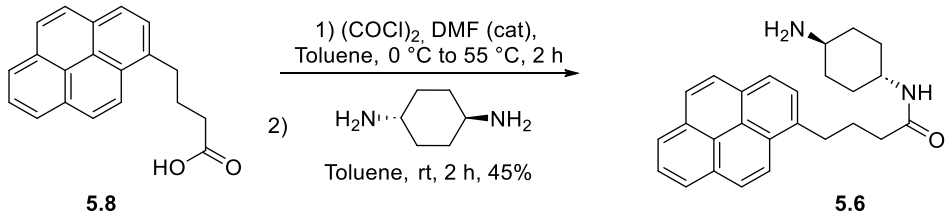

5.8 **5.6**

Scheme 10. Formation of 5.6 via amide coupling of 5.8 and 5.9 by acyl chloride intermediate.

The pyrene tagged amine **5.6** was then reacted in excess with the tosyl intermediate **5.7** in presence of triethylamine in 1-butanol at 110 °C for 38 h (Scheme 11). Tosyl intermediate **5.7** was synthesized from D-xylose in a two-step manner. First D-xylose was treated with concentrated sulfuric acid in acetone to form a monoketal then the primary hydroxyl in position 5 was reacted with tosyl chloride to form **5.7** which detailed formation will be described in chapter 7. Only a slight excess of amine **5.6** was used to prevent the disubstitution of the primary amine. Unfortunately, despite the long reaction time, low conversion and chemoselectivity were observed for this substitution. Indeed, four anomeric peaks were detected by ^{1}H NMR, indicating the formation of 4 species, and the desired product could not be separated via column chromatography. The poor reactivity was thought to be influenced by the poor solubility of the pyrene-tagged amine **5.6** in organic solvents. This methodology of synthesis involving the incorporation of the pyrene directly from the amine **5.6** to further react on the electrophile **5.7** was abandoned because of the difficult synthesis of **5.5** needing an excess of the expensive amine **5.6** for the reaction to pursue.

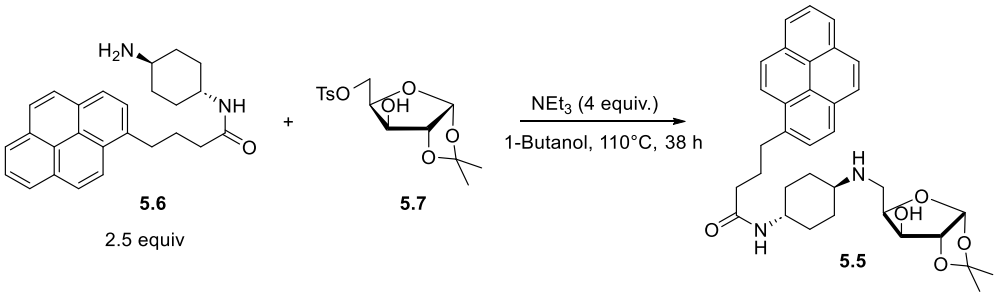

Scheme 11. Synthesis of the pyrene tagged amino alcohol 5.5 via substitution of the tosyl 5.7 with the amine 5.6.

Then, the other strategy was to first incorporate the *trans*-1,4-diaminocyclohexyl moiety in the sugar backbone by reacting *trans*-1,4-diaminocyclohexane **5.9** with the tosyl **5.7** in 1-butanol at 110 °C for 3 h 30 (Scheme 12). In this case again, an excess of amine was necessary in order to avoid the multi-substitution. The chiral amino alcohol backbone **5.15** was obtained in 84% yield without the need of column chromatography. The obtained amino-alcohol presented 3 nucleophilic sites being the primary and secondary amine as well as the hydroxyl group. The challenge was now to selectively introduce the pyrene moiety via an amide bond in the primary amine position.

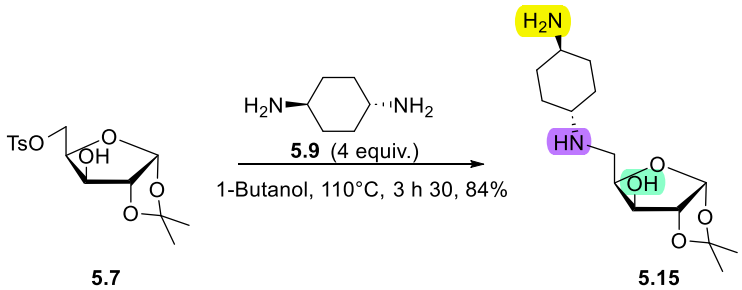

Scheme 12. Synthesis of 5.15 via nucleophilic substitution of the tosyl 5.7 by the amine 5.9.

To do so, the amino-alcohol **5.15** was reacted with 1-pyrenebutyric acid **5.8** in DMF in the presence of various coupling agents. The anomeric proton resonating at 5.94 ppm of the ^{1}H NMR spectra was used to assess the selectivity of the reaction (Figure 4). The results and structure of the coupling agents are described in Scheme 13.

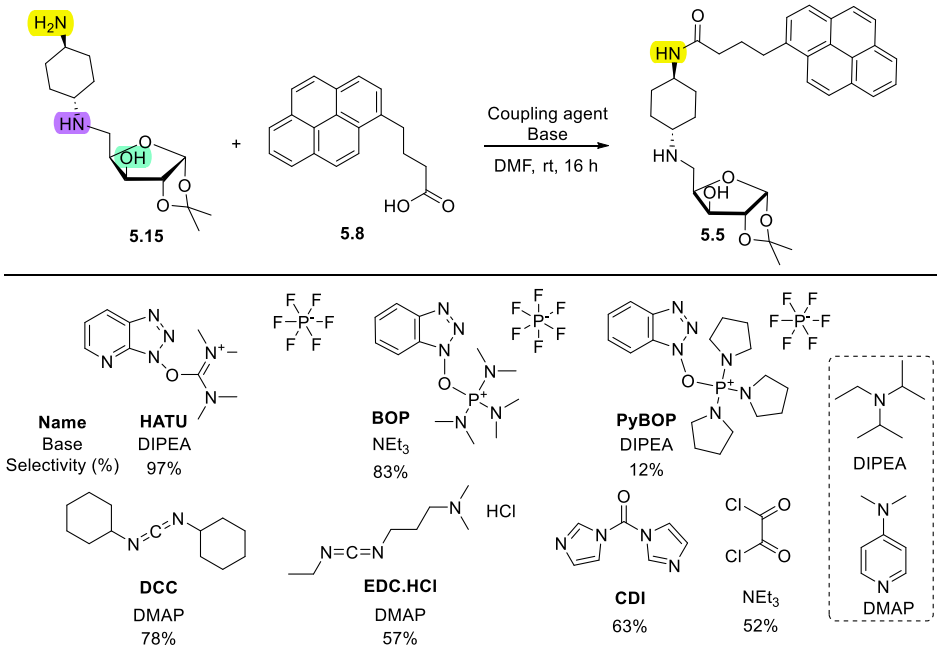

Scheme 13. Screening of coupling agents for the synthesis of 5.5

As expected, the formation of the acyl chloride with oxalyl chloride resulted in the nucleophilic attack of both nitrogens and oxygen. Usually, secondary amines are more nucleophilic than primary amines. Carbonyl diimidazole (CDI) was reported to be a selective coupling agent for primary amines.[31] Unfortunately the selectivity was moderate and the separation of the products was complicated. The use of EDC afforded the product with a poor selectivity. The bulkier DCC provided a higher selectivity for the primary amine. The use of BOP gave the desired product with good selectivity but surprisingly, the use of PyBOP yielded poorer selectivity. Finally, the product was obtained selectively using HATU in stoichiometric amount along with diisopropylethylamine in DMF at rt for 4 h. Tetra methyl urea was removed by column chromatography resulting in the desired product in 73% yield. The chiral pyrene-tagged amino alcohol bulky backbone **5.6** was obtained in a convenient two steps synthesis from the tosyl **5.7** in an overall 64% yield.

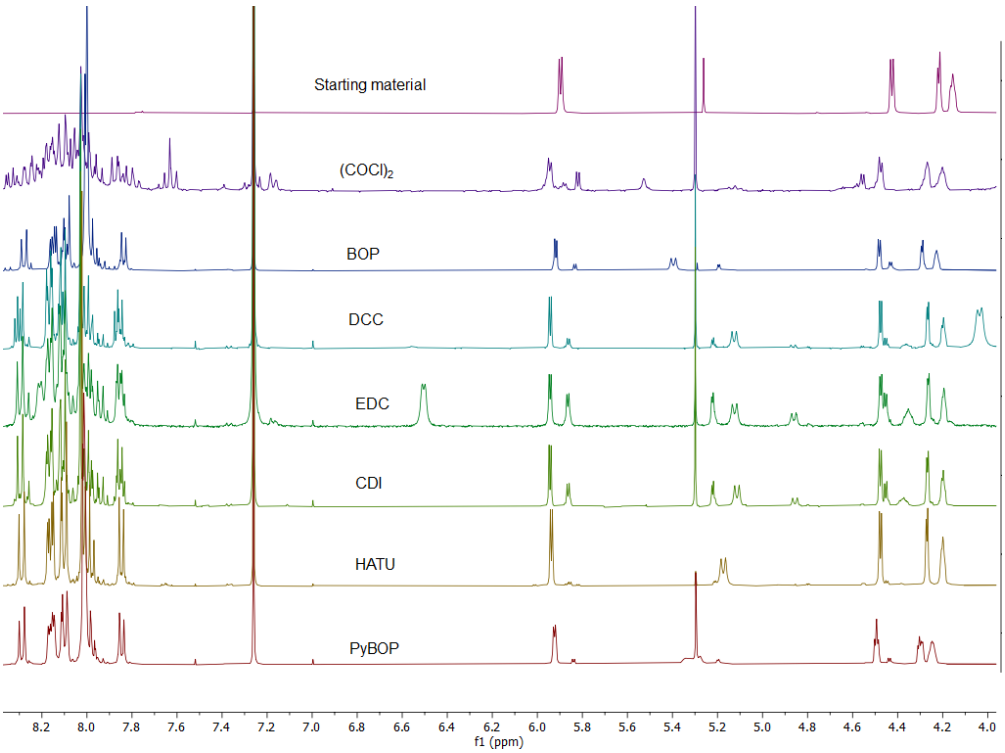

Figure 4. NMR spectra of amide couplings for the synthesis of 5.5.

The phosphite phosphoramidite ligand **5.4** was synthesized using classic procedure.[30] For chlorophosphite preparation, (*S*)-BINOL was reacted with phosphorus trichloride in large excess and in the presence of NMP as catalyst. The chlorophosphite intermediate was formed in 20 min at 75°C (Scheme 14).

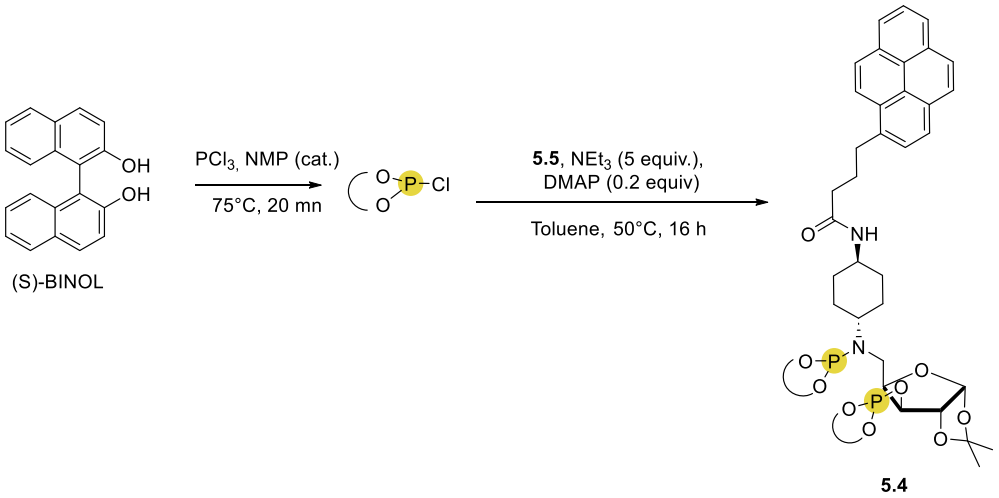

Scheme 14. Attempted synthesis of the phosphite phosphoramidite ligand 5.4

Unluckily, the ligand could not be obtained pure as a decomposition product was always formed and purification by column chromatography was unsuccessful.

Lowering the temperature to rt or changing the solvent to DCM did not improve the selectivity of the reaction.

At this point, complexation with $Rh(acac)(CO)_2$ was attempted to facilitate the purification. Disappointingly decomposition of the products were observed after purification by chromatographic column and the presence of oxides was detected by ^{31}P NMR of the different fractions.

*5.2.2.2. Synthesis of the ligand **5.11***

To synthesize the ligand **5.11**, the linear 1-pyrenebutanamine **5.13** was first synthesized in three steps from 1-pyrenebutyric acid **5.8** wih an overall 83% yield. Initially, the 1-pyrenebutyric acid **5.8** was transformed into the corresponding acyl chloride in the presence of oxalyl chloride. It was then reacted with aqueous ammonia resulting in the 1-pyrenebutanamide **5.14** in 97% yield. The amide was reduced with $LiAlH_4$ in THF at room temperature for several hours yielding the amine in 86% yield (Scheme 15).

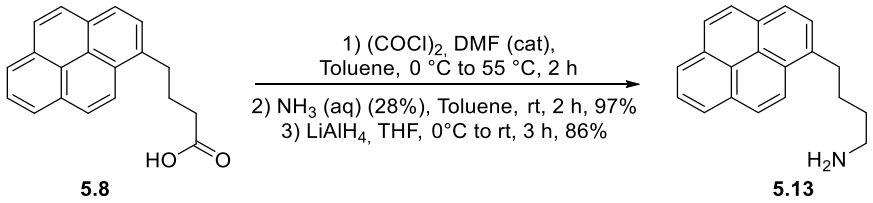

Scheme 15. Synthesis of 1-pyrenebutanamine 5.13 from 1-pyrenebutyric acid 5.8

The pyrene containing amine **5.13** was then reacted in excess with tosyl intermediate **5.7** in the presence of triethylamine in 2-propanol at 90 °C. After 6h30, 50% of the tosyl **5.7** was converted into the amine **5.12**. After 26 hours, the conversion reached a maximum of 81% and another anomeric peak was detected by ^{1}H NMR. Thus the solvent was changed to 1-butanol and the reaction temperature increased to 110°C (Scheme 16). Under these conditions, the conversion was 75% after 18h with an increased selectivity towards the product. However, attempts of purification using column chromatography resulted unsuccessful. Again, the excess of synthesized amine along with the difficulty in purification forced us to change the route to the amino alcohol **5.12**.

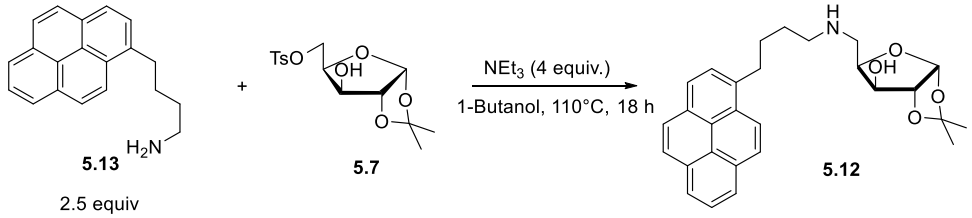

Scheme 16. Synthesis of the pyrene tagged amino alcohol 5.5 via substitution of the tosyl 5.7 with the amine 5.6.

Using the same strategy as described for the synthesis of **5.5**, the amine moiety was introduced first in the xylose backbone followed by the incorporation of the pyrene. For this purpose, the tosyl **5.7** was reacted with sodium azide in dimethylformamide at 90 °C. The azide intermediate **5.16** was reduced with triphenylphosphine in a mixture of water and tetrahydrofuran at room temperature, yielding the water-soluble amino alcohol **5.17** in 64% yield over the two steps, after recrystallization in diethyl ether (Scheme 17).

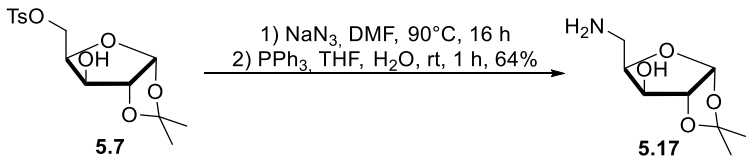

Scheme 17. Synthesis of the amino-alcohol 5.16 from the tosyl 5.7

In parallel, 1-pyrenebutyric acid **5.8** was reduced by $LiAlH_4$ in THF at room temperature for 16 h to 1-pyrenebutanol **5.18** in quantitative yield. The 1-pyrenebutanol **5.18** was further oxidized using pyridinium chlorochromate (PCC) in dichloromethane to the 1-pyrenebutanal **5.19** in 80% yield (Scheme 18).

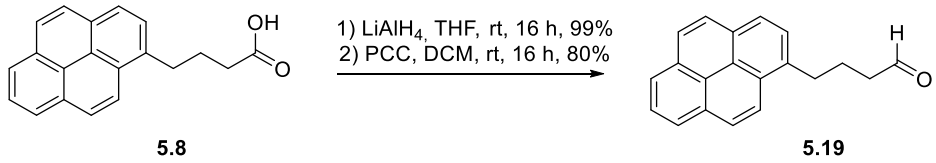

Scheme 18. Reduction and oxidation sequence of 1-pyrenebutyric acid 5.8 to 1-pyrenebutanal 5.19.

The amino-alcohol **5.17** and the aldehyde **5.19** partners were reacted in reductive amination to form the hemiaminal intermediate **5.20** in 90% yield. Surprisingly, neither sodium borohydride or sodium cyanoborohydride could open the 6 members ring intermediate **5.20**.

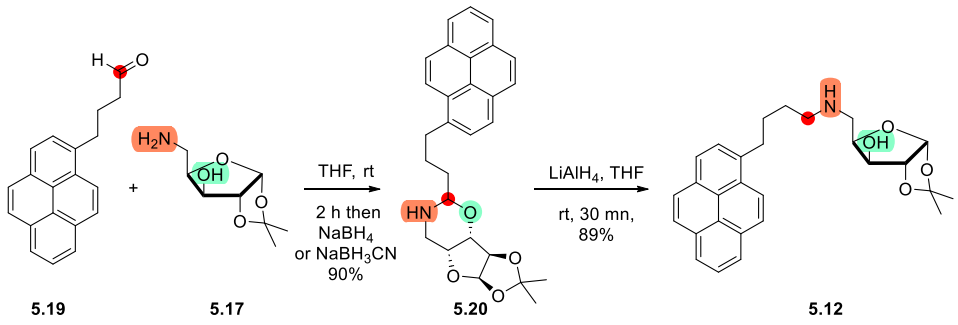

Scheme 19. Synthesis of pyrene-tagged amino alcohol linear backbone 5.12

However, when $LiAlH_4$ was used in THF, the chiral pyrene-tagged amino alcohol linear backbone **5.12** was obtained in 89% yield (Scheme 19). Overall, this product was

obtained in 41% yield from the tosyl intermediate **5.7** and the commercially available pyrene carboxylic acid **5.8**.

The amino-alcohol backbone **5.12** was reacted at rt for 2 h with the (*S*)-binolchlorophosphite formed *in situ* from phosphorus trichloride and (*S*)-BINOL (Scheme 20). The reaction time was critical since impurities that couldn't be separated by chromatography were detected by ^{31}P NMR when the reaction time was increased. The new phosphite phosphoramidite pyrene tagged ligand **5.11** was obtained in a 33% yield after column chromatography.

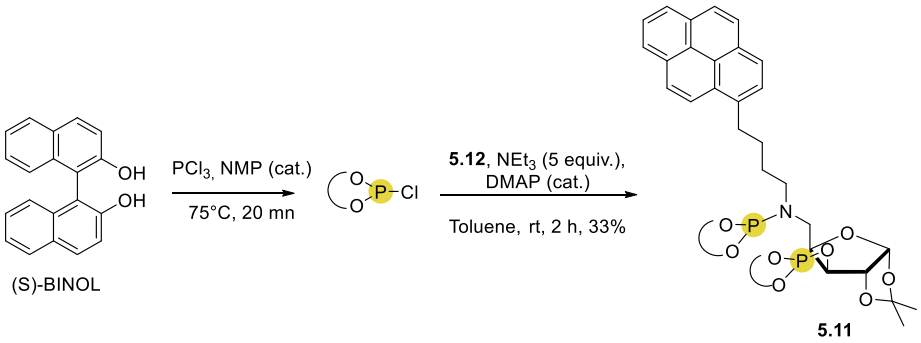

Scheme 20. Synthesis of phosphite phosphoramidite ligand 5.11.

At this point, the successfully obtained pyrene-tagged ligand **5.11** was reacted with rhodium precursors and the results are described in the next section.

5.2.3. Synthesis of Rh complexes bearing the ligand **5.11.**

5.2.3.1. Reaction with the neutral [Rh(acac)(CO)$_2$] precursor.

The phosphite phosphoramidite ligand **5.11** was reacted with an equimolar amount of [Rh(acac)(CO)$_2$] in deuterated toluene at 0°C and stirred at room temperature for 1 h (Scheme 21).

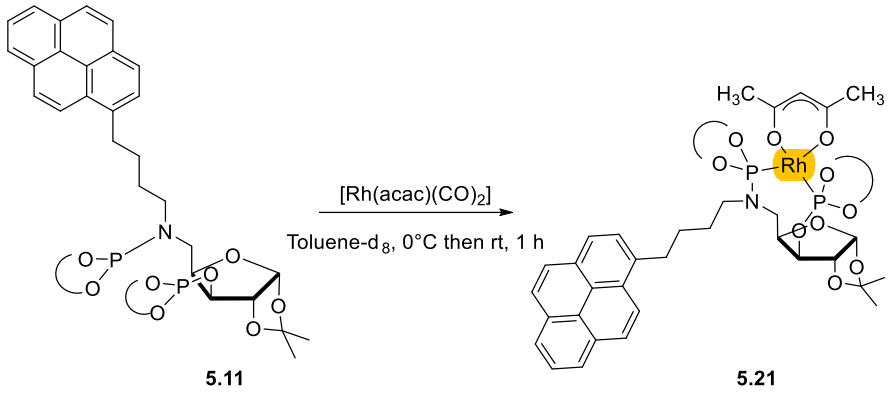

Scheme 21. Expected result from the reaction of 5.11 with [Rh(acac)(CO)$_2$].

The reaction mixture was analyzed by NMR to confirm the structure of the expected complex **5.21**. In the corresponding ^{31}P {^{1}H} NMR spectrum, several sets of signals were detected. The main product presented two doublets at δ 157.74 (d, J_{Rh-P} = 269.0 Hz), 151.25 (d, J_{Rh-P} = 292.8 Hz) that confirmed the coordination of two phosphorus atoms to the rhodium center. The value of this coupling is in agreement with coordination of such a ligand with a Rh(I) center.[32] In this spectrum, 4 other doublet resonances of lower intensity were observed at δ 162.96 (d, J_{Rh-P} = 300.0 Hz), 162.28 (d, J_{Rh-P} = 300.0 Hz), 158.85 (d, J_{Rh-P} = 274.0 Hz), 158.18 (d, J_{Rh-P} = 274.0 Hz). The Rh-P coupling constant again indicated the presence of rhodium in the corresponding species (Figure 5). These signals were tentatively attributed to the formation of [Rh(**5.11**)$_2$][acac] where the C_1-symmetry ligands could be in *cis* or *trans* configuration.

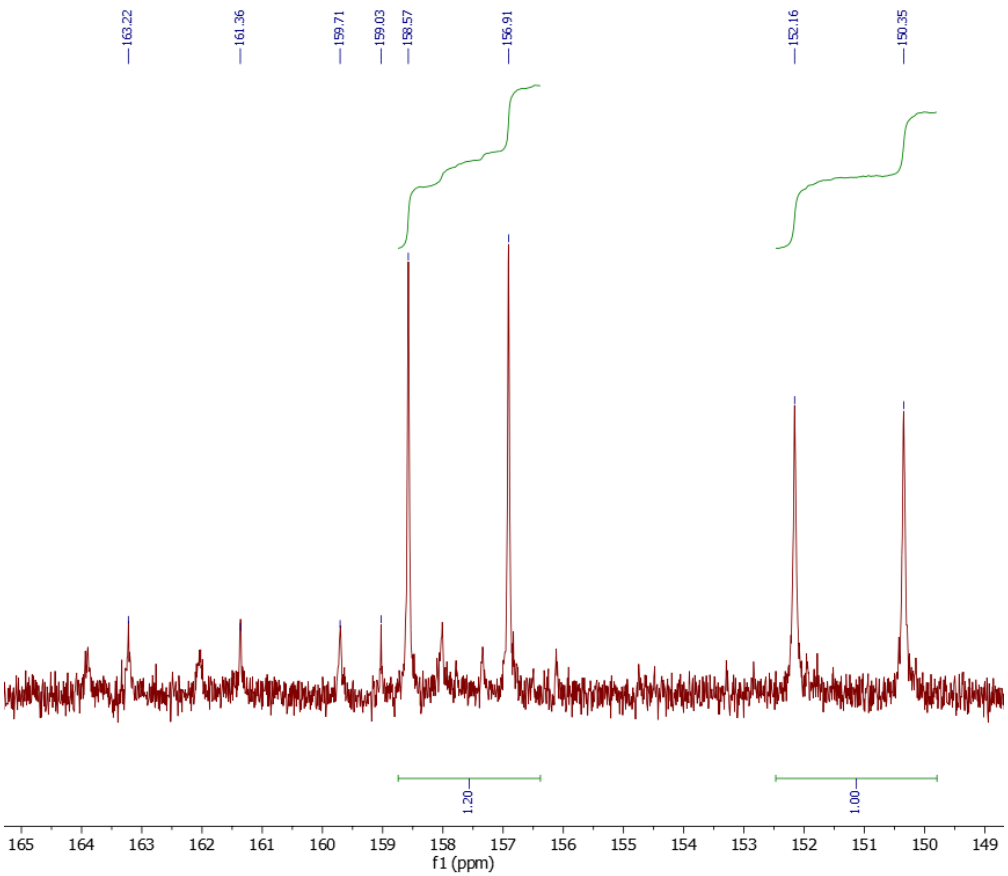

Figure 5. ^{31}P NMR of the complexation of 5.11 with [Rh(acac)(CO)$_2$]

In the ^{1}H NMR spectrum, signals at δ 5.83 (d, *J* = 3.8 Hz, 1H), 5.73 (dd, *J* = 9.7, 2.4 Hz, 1H), 5.29 (br, 1H) and 4.79 (d, *J* = 3.9 Hz, 1H) were observed and attributed to the sugar backbone protons of the ligand (Figure 6). The origin of these signals was confirmed by COSY (^{1}H-^{1}H) and HSQC (^{1}H-^{13}C) analysis with the detection of the corresponding ^{13}C signals at δ 105.55, 82.14, 83.20 and 84.36.

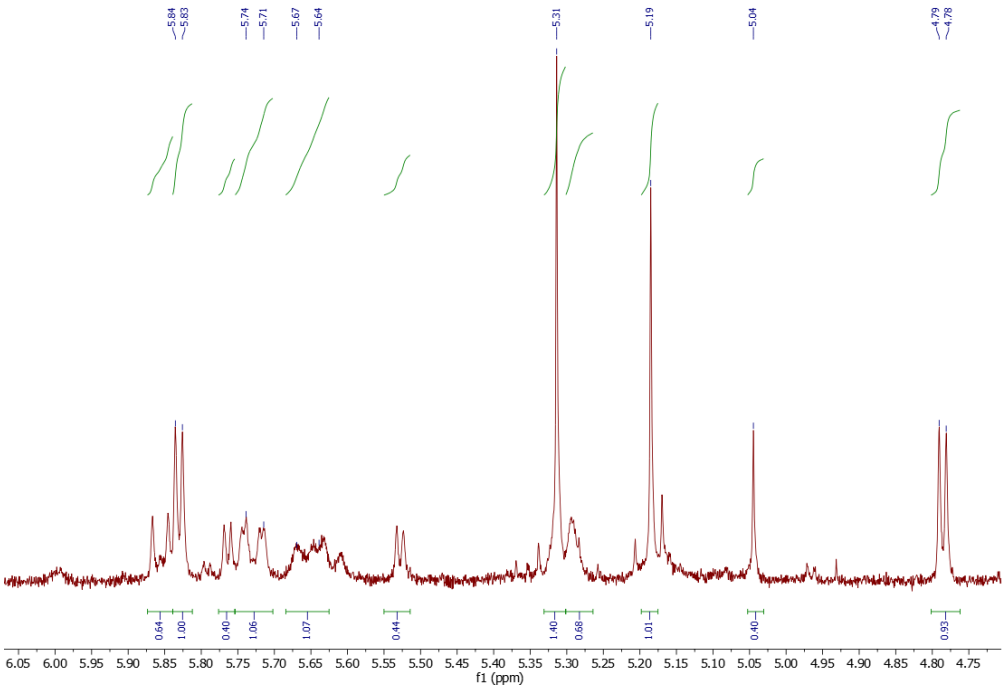

Figure 6. ^{1}H NMR spectrum corresponding to the reaction of 5.11 with [Rh(acac)(CO)$_2$]

V

Two singlet signals at δ 5.31 (s, 1H) and 5.19 (s, 1H) indicated the presence of two acac moieties. This was confirmed by the correlation observed in the corresponding ^{1}H-^{13}C HSQC spectrum between these signals and a ^{13}C signal at 100.97 ppm. As this 2D experiment was run in an EDITED manner, the phase of the correlation indicated that these signals corresponded to C-H moieties with overlapping of the ^{13}C resonances. In the corresponding HMBC ^{1}H-^{13}C spectrum, each of these ^{1}H signals were in correlation with two carbonyl ^{13}C NMR signals at δ 185.51 and 188.16, and 185.41 and 187.75, respectively. These observations thus confirmed that these signals arose from two distinct acac moieties. In the corresponding ^{13}C{^{1}H} NMR spectrum, two other resonances of lower intensity were detected at δ 187.1 and 184.32 that were attributed to an uncoordinated acac moiety acting as counterion in [Rh(**5.11**)$_2$][acac]. No signals corresponding to free or bridging CO ligands were detected in this spectrum (Figure 7).

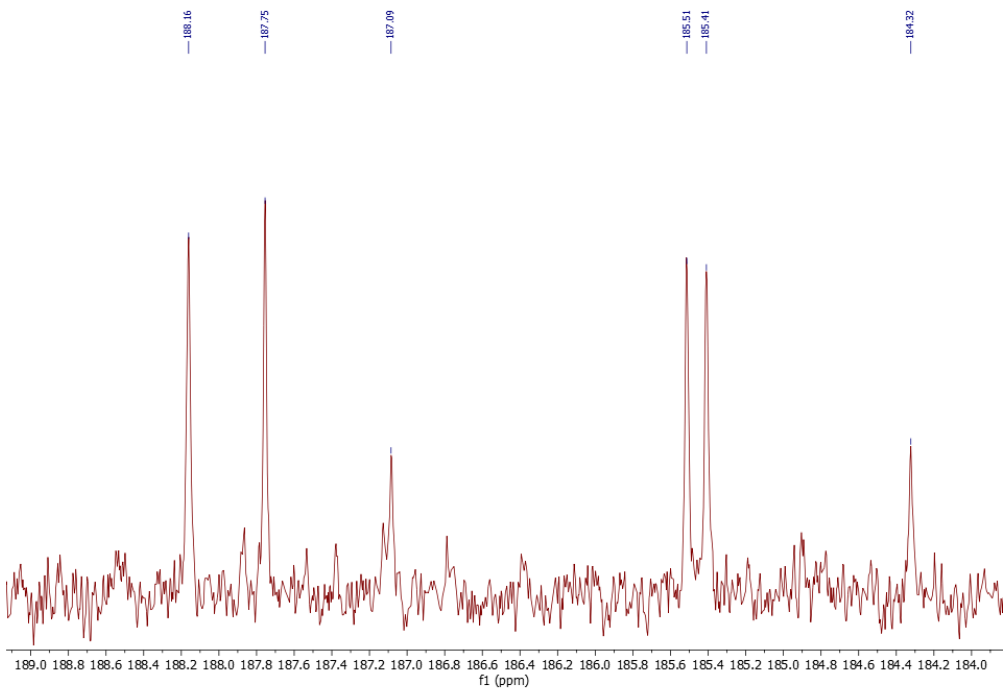

Figure 7. ^{13}C NMR of the complexation of 5.11 with [Rh(acac)(CO)$_2$]

In view of these results, it was concluded that the main product formed contains one ligand **5.11** and two acac moieties. Attempts of purification of this compound by column chromatography resulted unsuccessful. In all cases, the relative intensities of the signals attributed to this compound remain unchanged.

The identity of this compound was tentatively attributed to a Rh dimer bridged by two acac moieties and a P-P ligand (Scheme 22). However, in this structure, each Rh would present a coordination number of 3, which is not appropriate for Rh(I) centers. We therefore deduced that other ligands must be coordinated to the Rh atoms. However, these ligands (written as L in Figure 9) could not be identified during the course of our study. If these ligands would be fluxional CO ligands, for instance, they

could give rise to broad resonances that could explain why they were not detected. Further studies using ^{13}CO labeled $[Rh(acac)(CO)_2]$ are planned in the near future.

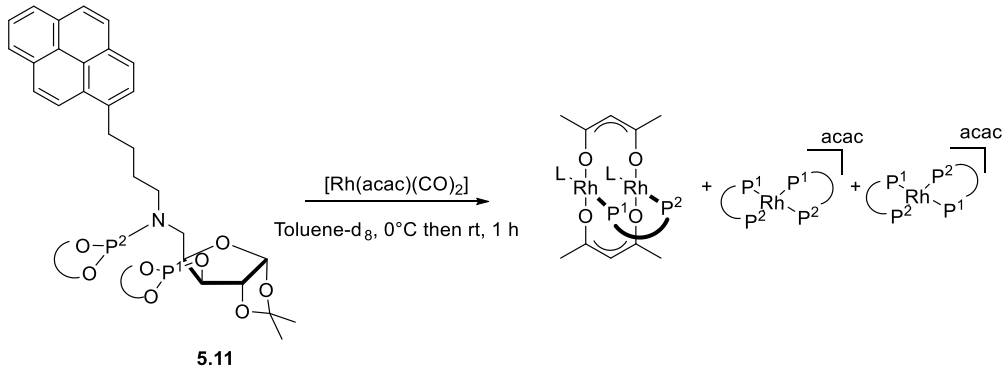

Scheme 22. Proposed structure for the products formed during the reaction between 5.11 with $[Rh(acac)(CO)_2]$

Due to the uncertainty associated to the identity of the main product formed when ligand **5.11** was reacted with $[Rh(acac)(CO)_2]$ in deuterated toluene, the reaction of **5.11** with the cationic $[Rh(COD)_2]BF_4$ precursor was performed.

5.2.3.2. Synthesis with cationic $[Rh(COD)_2]BF_4$ precursor.

The phosphite phosphoramidite ligand **5.11** was reacted in stoichiometric amount with $[Rh(COD)_2]BF_4$ in dichloromethane at 0°C and stirred at room temperature for 1 h (Scheme 23).

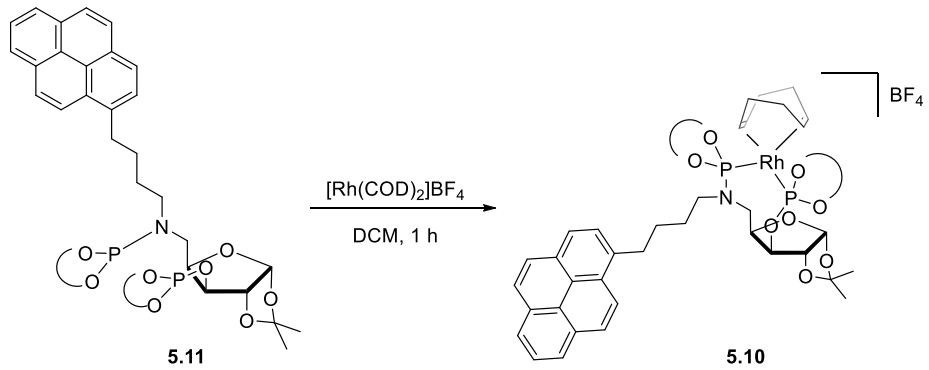

Scheme 23. Expected structure of the product 5.3 from the complexation of 5.11 with $[Rh(COD)_2]BF_4$.

The complex was precipitated with hexane and washed several times to remove the free cyclooctadiene. Then, the complex in deuterated dichloromethane was analyzed by multinuclear NMR spectroscopy. At room temperature, the $^{31}P\{^{1}H\}$ NMR spectrum mainly presented a broad signal δ 135.00 (either two singlets or a doublet with J = 228.9 Hz) suggesting a fluxional system had been formed. When the $^{31}P\{^{1}H\}$ NMR spectrum was repeated at -55°C, the splitting of the signal was observed (Figure 8) and four doublets of doublets were observed at δ 142.74 (dd, J_{RhP} = 228.3 Hz, J_{PP} =44.0 Hz), 138.31 (dd, J_{RhP} = 262.3 Hz, J_{PP} = 42.0 Hz), 135.41 (dd, J_{RhP} = 254.4 Hz, J_{PP} = 44.0 Hz), 131.32 (dd, J_{RhP} = 234.1 Hz, J_{PP} = 42.0 Hz). The intensity of the signal and the J_{PP} coupling values suggested that two systems are present, one including the phosphorus resonances at 142.74 and 135.41 ppm with a coupling constant of 44.0 Hz and other one bearing the phosphorus at 138.31 and 131.32 ppm with a coupling constant of 42.0 Hz.

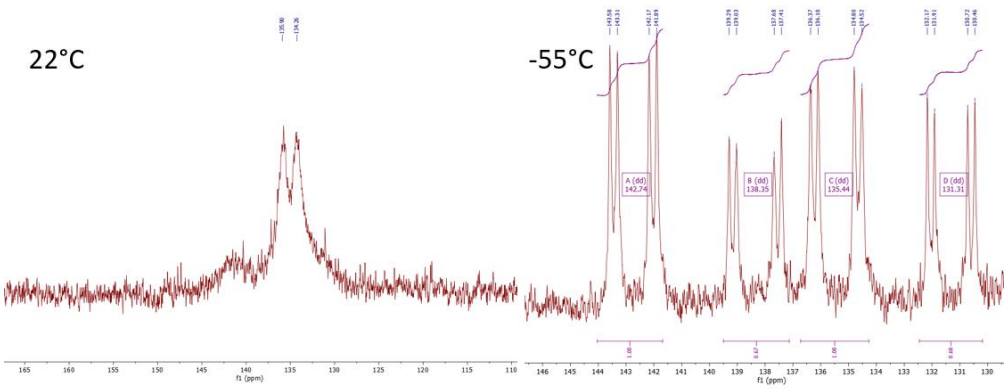

Figure 8. Selected region of the $^{31}P\{^{1}H\}$ NMR spectrum of the product(s) formed by reaction of 5.11 with $[Rh(COD)_2]BF_4$. Spectrum recorded at 22 °C (left) and -55°C (right).

In the corresponding ^{1}H NMR spectra, very broad signals were again detected at room temperature. At -55°C, the signals appeared sharper although no clear multiplicity could be detected. The complexity of the spectra did not allow a precise determination of the product identity although selective NOESY and COSY analyses provided evidence for the presence of two isomeric species involved in a fluxional process (Figure 11).

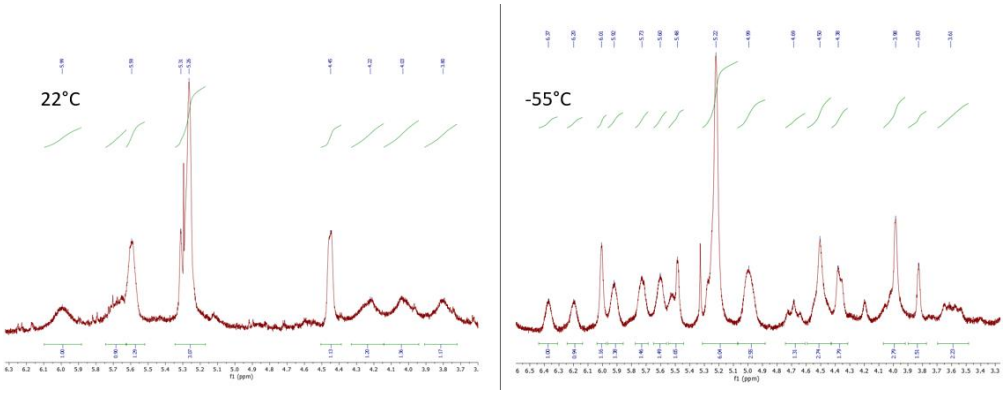

Figure 9. ^{1}H NMR of the complexation of 5.11 with $[Rh(COD)_2]BF_4$ at 22 °C (left) and -55°C (right).

^{1}H- ^{31}P HMBC NMR analysis at -55 °C revealed correlation between some of the proton signals with the ^{31}P signals previously detected, indicating that the two systems contained ligand **5.11** (Table 1).

Table 1. Signals of the ^{31}P-^{1}H NMR of the complexation of 5.11 with $[Rh(COD)_2]BF_4$ at -55°C.

	P1	P2	P3	P4
^{31}P	135.41	142.74	138.31	131.32
^{1}H	5.73	5.60	6.20	5.51
^{1}H	5.27	5.01	5.22	

When the sample was diluted, no changes in the corresponding ^{1}H and ^{31}P{^{1}H} NMR spectra were observed. It was thus concluded that intermolecular $\pi-\pi$ interactions between pyrene moieties were not responsible for the fluxional behaviour observed. Mass analysis indicated a mass of 1176.2299 confirmed the presence of the fragment [Rh(**5.11**)]$^{+}$.

In view of these results, we propose that a mixture of complexes **5.10a** and **5.10b** is formed during the reaction. The fluxional behavior of such species could be explained by the presence of the flexible linker between the phosphoramidite and the pyrene moiety in the ligand structure (Scheme 24). Further characterization at low temperature will be necessary to confirm the origin of this behavior.

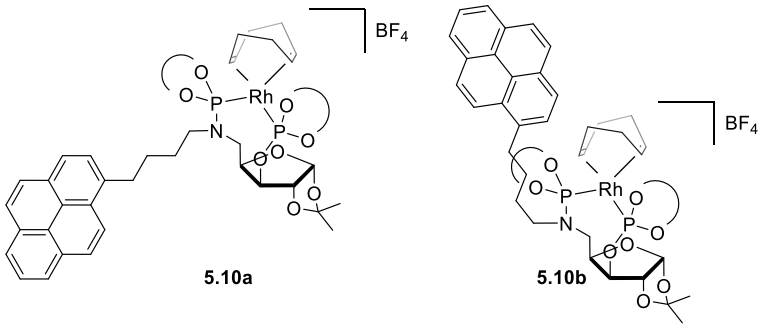

Scheme 24. Structure hypothesis of the rhodium complex 5.10a and 5.10b.

5.2.4. Heterogenization of the complex **5.10** onto carbon materials.

The solvent used for immobilization was ethyl acetate as it was previously reported as an appropriate solvent favoring the π-π interactions between the pyrene moiety and the carbon support.[21]

First, the support was dispersed in dry ethyl acetate by sonification for 30 minutes. At this stage, the complex **5.10** was dissolved in dry ethyl acetate and added at room temperature to the support. The mixture was stirred overnight at room temperature, was filtered via canula and washed three times with ethyl acetate. The complex was then dried under vacuum and the rhodium loading was evaluated by Induced Coupled Plasma (ICP).

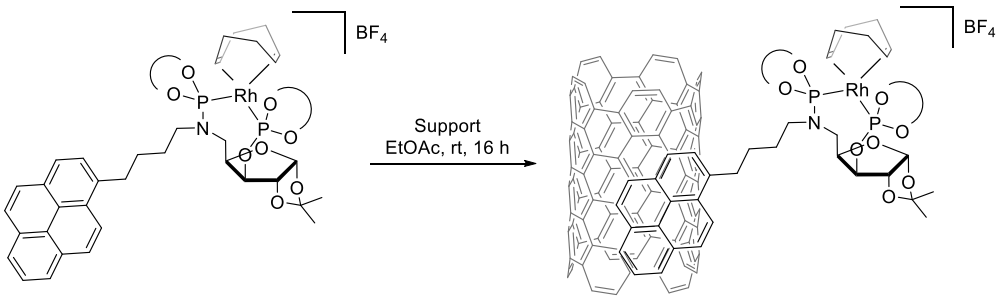

Scheme 25. Immobilization of pyrene tagged complex 5.10 onto carbon materials.

The cationic complex **5.10** was immobilized on multiwall carbon nanotubes (MWCNT), reduced graphene oxide (rGO) and carbon beads (CB) and the corresponding Rh loadings are described in **Table 2**. The highest rhodium loading was on **5.10@MWCNT** with 1.61 wt% followed by **5.10@CB** with 1.44 wt% and finally

5.10@rGO with 1.10 wt%. These results were surprising as the rhodium loadings reported for a cationic rhodium complex with pyrene tagged bisphosphite ligand **5.d** on carbon material was approximately 0.5% (Scheme 4).[21]

Table 2. Immobilization of 5.10 on carbon materials

Catalyst	Rh loading wt%
5.10@MWCNT	1.61
5.10@rGO	1.10
5.10@CB	1.44

The successfully immobilized catalysts were then tested in asymmetric hydroformylation of acrylamide derivatives.

5.2.5. Catalytic tests

5.2.5.1. Homogeneous asymmetric hydroformylation and hydroaminomethylation of N,N-diethylmethacrylamide.

First, the effect of the pyrene unit in the ligand **5.11** was assessed by performing the hydroformylation of **5.22** in MeTHF at 60°C for 16 h under 20 bar of CO/H_2 (1:1) using $[Rh(acac)(CO)_2]$ as precursor (Scheme 26). The acrylamide **5.22** was converted in 39% under these conditions, with 85% chemoselectivity towards the aldehydes **5.23** and **5.24.** In this reaction, 15% of the hydrogenation product **5.25** was also formed. The linear product **5.23** was formed regioselectively in 97% and the branched product **5.24** was only formed in 3%.

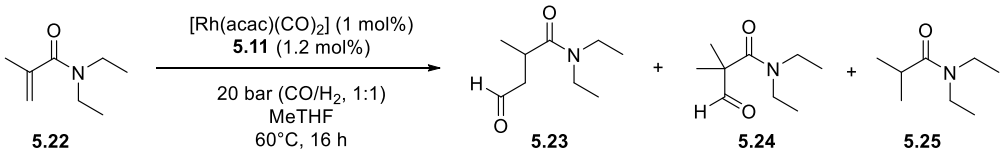

Scheme 26. Homogeneous asymmetric hydroformylation of 5.22 with the catalytic system [Rh/5.11].

The aldehydes were reduced to the alcohols and the enantiomeric excess was measured by chiral GC. The linear alcohol **5.25** (Scheme 27) was obtained in 80% ee. In a previous report from our group, the analogous phosphite phosphoramidite ligand containing a methyl substituent at the nitrogen atom provided 54% conversion and 74% ee in toluene.[30] Thus, the rhodium catalytic system bearing the new ligand **5.11** provided very similar results taking into account that the reactions were performed in different solvents. It was therefore concluded that the introduction of the pyrene moiety did not affect significantly the performance of the catalyst under these conditions.

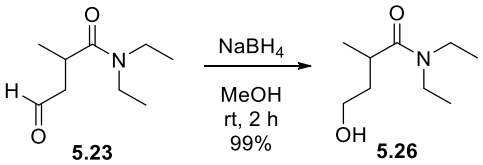

Scheme 27. Reduction of the aldehyde 5.23 with $NaBH_4$.

As the reaction with the heterogenized catalyst **5.2** was to be tested in ethyl acetate, the hydroformylation of **5.22** was repeated in this solvent at 80°C for 38 h under 20 bar of CO/H_2 (1:1). Under these conditions, the conversion was 33% and with a chemoselectivity to aldehydes of 86%. The linear aldehyde was obtained with 95% regioselectivity. The ee was measured after reduction of **5.23** to **5.26** and was 82%. Interestingly, at 110°C for 38 h, the conversion reached 49% and the ee slightly decreased to 79%.

An initial test for the hydroaminomethylation of **5.22** with morpholine catalyzed by the system $[Rh(acac)(CO)_2]$/**5.11** was conducted in MeTHF at 80 °C for 38 h under 20 bar of CO/H_2 (1:1). However, only 3% conversion was measured. When the reaction

was repeated at 110°C, 24% conversion was obtained with the amine **5.27** as the main product (95%) with 67% ee. Moreover, 5% aldehydes were also detected (20% of **5.23** and 80% of **5.24**). The product **5.25** was not observed in the crude mixture.

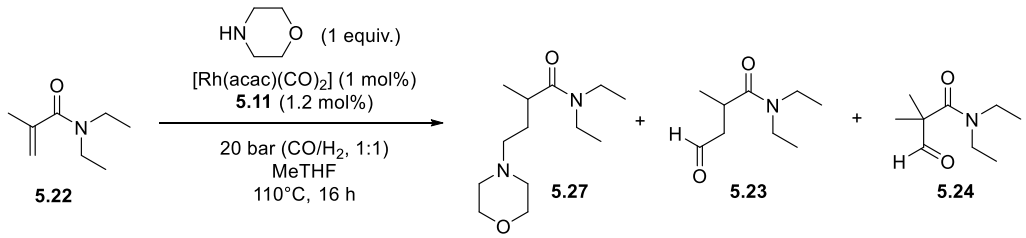

Scheme 28. Homogeneous asymmetric hydroaminomethylation of 5.22 with the catalytic system [Rh/5.11].

The homogeneous catalysis described in this section using [Rh(acac)(CO)$_2$] precursor along with the new pyrene-tagged ligand **5.11** demonstrated a moderate activity as long reaction times and high temperatures are needed to reach higher conversions. However, high enantioselectivity was obtained in the asymmetric hydroformylation of **5.22** in both MeTHF and EtOAc. The reactivity of the new heterogenized catalyst is described in the next section.

V

*5.2.5.2. Asymmetric hydroformylation of N,N-diethylmethacrylamide using the heterogenized catalytic systems **5.10@support**.*

The three catalysts **5.10@MWCNT**, **5.10@rGO** and **5.10@CB** were tested in the hydroformylation of **5.22** in batch as a first step in view of a possible application in continuous flow. The catalyst (1 mol %) was mixed with **5.22** in ethyl acetate and the reaction was stirred at 80°C for 38 h under 20 bar of CO/H$_2$ (1:1, entry 1-3). The results are reported in **Table 3**. Disappointingly, in all cases, the catalysts provided low activity and chemoselectivity as the main product observed was the hydrogenation product **5.25**. The catalyst presenting the higher conversion was **5.10@MWCNT** (14%) with 44% chemoselectivity to the aldehydes (l/b= 38/6). When the temperature was increased to 110°C and the reaction performed for 38 h (entry 4-6), the catalyst **5.10@MWCNT** provided a conversion of 30% (*vs* 49% in homogeneous) with 31% selectivity towards the linear aldehyde **5.23**. The latter was

reduced to **5.26** and an enantiomeric excess of 61% was obtained. Unfortunately, the main product was still the hydrogenation product **5.25** with 67% selectivity (entry 4-6). The catalysts supported on rGO and CB provided low conversions with 70 and 79% selectivity to **5.23**. In view of the low conversions obtained, the ee's were not measured for these samples.

Table 3. Asymmetric hydroformylation of N,N-diethylmethacrylamide using the heterogenized catalytic systems 5.10@support

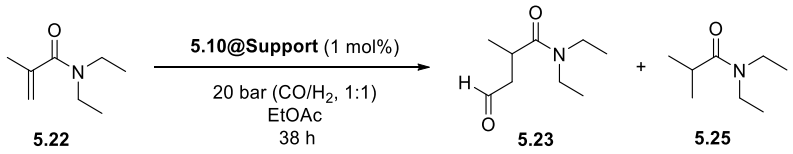

Entry	Catalyst	Temperature	Conv. (%)	**5.23** (%)	**5.25** (%)	ee (%)
1	**5.10@MWCNT**	80	14	38	56	-
2	**5.10@rGO**	80	6	50	50	-
3	**5.10@CB**	80	5	20	80	-
4	**5.10@MWCNT**	110	30	31	67	61
5	**5.10@rGO**	110	9	30	70	-
6	**5.10@CB**	110	12	21	79	-

These results are therefore promising although an optimization of the reaction conditions is needed to enhance the chemoselectivity towards the aldehydes**.** Technical problems with the flow chemistry equipment prevented us to carry out some tests; experiments are planned for a later date.

5.3. Conclusions

- The synthesis of new pyrene-tagged sugar-based amino-alcohol backbone **5.5** and **5.12** was successfully conducted with respectively good yield of 64% over two steps and 41% over three steps.
- The amino-alcohol backbone **5.5** and **5.12** were reacted with the in situ formed (S)-BINOL chlorophosphite to form the pyrene-tagged ligand **5.4** and **5.11**. The bulkier ligand **5.4** couldn't be isolated whereas the ligand **5.11** was successfully synthesized in 33% yield.
- The new pyrene-tagged ligand was reacted with different rhodium precursors and the reaction mixture characterized by NMR. It was concluded that the reaction with $[Rh(acac)(CO)_2]$ didn't afford the product expected but rather a dirhodium complex bearing two bridging acac moieties and the ligand **5.11**. The reaction with $[Rh(COD)_2]BF_4$ provided the complex **5.10**.
- The complex **5.10** was successfully immobilized on multiwall carbon nanotubes, reduced graphene oxide and carbon beads upon reaction with ethyl acetate. The rhodium loading of each catalyst was measured by ICP and was 1.61%, 1.10% and 1.44%, respectively.
- The activity of the [Rh/**5.11**] catalytic system was tested in homogeneous hydroformylation and hydroaminomethylation of **5.22**. The asymmetric hydroformylation of **5.22** resulted in an excellent 80% ee of **5.26** and the asymmetric hydroaminomethylation resulted in a good 67% ee of **5.27**. These results indicated that the introduction of the pyrene moiety in the ligand did not significantly affect the catalytic outcome of the reaction.
- The immobilized catalysts were tested in batch hydroformylation in view of a continuous flow application. The catalysts presented a low activity, but the catalyst **5.10@MWCNT** provided a conversion of 30% at 110°C with a selectivity towards the linear aldehyde of 31% and a good enantioselectivity of 61%.

5.4. Experimental part

General considerations

All the reactions were carried out using Schlenk-line inert atmosphere techniques or glovebox techniques. Anhydrous solvents were collected from the system Braun MB SPS-800. Ethyl acetate was dried with molecular sieves. Commercially available reagents and solvents were purchased at the highest commercial quality from Sigma-Aldrich, Fluka, Alfa Aesar, Fluorochem, Strem and were used as received, without further purification.

^{1}H and $^{13}C\{^{1}H\}$ NMR spectra were recorded using a Varian Mercury VX 400 (400 and 100.6 MHz respectively). Chemical shift values (δ) are reported in ppm relative to TMS (^{1}H and $^{13}C\{^{1}H\}$) and coupling constants are reported in Hertz. The following abbreviations are used to indicate the multiplicity: s, singlet; d, doublet; t, triplet; q, quartet; quint, quintuplet; sext, sextuplet; sept, septet; oct, octet; m, multiplet; bs, broad signal. High-resolution mass spectra (HRMS) were recorded on a Bruker Daltonics Microtof Focus and/or Maxis Impact using ESI-TOF (electrospray ionization-time of flight). Samples were introduced to the mass spectrometer ion source by direct injection using a syringe pump and were externally calibrated using sodium formate. The instrument was operating in the positive ion mode. ICP analysis were performed with Thermo Scientific ICAP 6300 instrument. Enantiomeric excess was measured using GC with ChirasilDex column. Reactions were monitored by TLC carried out on 0.25 mm E. Merck silica gel 60 F_{254} aluminum plates. Developed TLC plates were visualized under a short-wave UV lamp (254 nm) and by heating plates that were dipped in potassium permanganate. Flash column chromatography was carried out using forced flow of the indicated solvent, on Merck silica gel 60 (230-400 mesh). The Rh-catalyzed hydroformylation reaction and Rh-catalyzed hydroaminomethylation reaction were set up in a CAT7 autoclave from HEL Inc. and stirred with a Teflon-coated magnetic stir bar.

4-(pyren-1-yl)butanamide (5.14)[33]

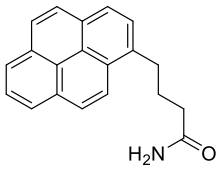

The reaction was carried out following a previously reported procedure. 4-(pyren-1-yl)butanoic acid (4.105 g, 14.24 mmol) was suspended in 35 mL of dry Toluene. Dry DMF (7 drops) was added to this mixture. Next, oxalyl chloride (2.9 eq, 41.3 mmol, 3.6 mL) was added at 0 °C. The temperature was then increased to 55 °C and the reaction was stirred for 2 h. The mixture was cooled down to rt and the volatiles were evaporated. The residue was then solved with dry toluene and aqueous NH_3 (28%) (7.12 mL) was added at 0 °C. The reaction was left 2h at rt. After that, the crude was dried under vacuum. DCM was added and the organic phase was washed with water once. Then it was washed with $NaHCO_3$ and brine. The organic phase was then dried over anhydrous $MgSO_4$ and the solvent removed under vacuum to afford the product as a yellow solid in 97% yield.

^{1}H NMR (300 MHz, $CDCl_3$) δ 8.31 (d, J = 9.3 Hz, 1H), 8.23 – 8.07 (m, 4H), 8.01 (d, J = 11.2 Hz, 3H), 7.87 (d, J = 7.8 Hz, 1H), 5.32 (d, J = 14.9 Hz, 2H), 3.42 (t, J = 7.4 Hz, 2H), 2.42 – 2.14 (m, 4H).

4-(pyren-1-yl)butan-1-amine (5.13)[33]

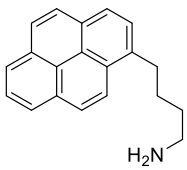

The reaction was carried out following a previously reported procedure. 4-(pyren-1-yl)butanamide (3.38 g, 11.75 mmol) was solved in THF (98 mL). The mixture was placed in an ice bath and $LiAlH_4$ (6 eq., 70.5 mmol, 2.7 g) was added carefully portion wise. After 3h at rt, the reaction was placed again in an ice bath. To quench the reaction, AcOEt was added dropwise carefully followed by water. When most of the unreacted $LiAlH_4$ was quenched, 10 mL of NaOH 1M and 10 mL of H_2O were added. A yellow solution with a white precipitate appeared. A vacuum filtration was carried on and the resulting solution was evaporated. Then, a short flash chromatography was performed (Al_2O_3, 95:5 DCM/MeOH). The desired product was obtained as a dark yellow oil (2.75 g, 86% yield).

^{1}H NMR (401 MHz, $CDCl_3$) δ 8.27 (d, *J* = 9.3 Hz, 1H), 8.19 – 8.13 (m, 2H), 8.10 (dd, *J* = 8.6, 3.1 Hz, 2H), 8.04 – 7.96 (m, 3H), 7.86 (d, *J* = 7.8 Hz, 1H), 3.36 (t, *J* = 7.8 Hz, 2H), 2.76 (t, *J* = 7.1 Hz, 2H), 1.89 (tt, *J* = 9.2, 6.8 Hz, 2H), 1.69 – 1.58 (m, 5H).

N-((1r,4r)-4-aminocyclohexyl)-4-(pyren-1-yl)butanamide (5.6)

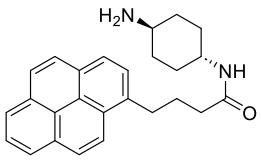

4-(pyren-1-yl)butanoic acid (2.00 g, 6.94 mmol) was suspended in 18 mL of dry Toluene. Dry DMF (7 drops) were added to this mixture. Next, oxalyl chloride (2.9 eq, 1.72 mL) was added at 0 °C. The temperature was then increased to 55 °C and the reaction was stirred for 2 h. The mixture was cooled down to rt and the volatiles were evaporated. The residue was then solved with dry Toluene and *trans*-cyclohexane-1,4-diamine (3 eq., 20.8 mmol, 2.38 g) was added at 0 °C. The reaction was stirred 2h at rt then concentrated under vacuum. The crude mixture was dissolved in DCM and washed with water and $NaHCO_3$ (sat.) to remove the excess of amine. The aqueous phase was extracted with DCM several times. The combined organic phases were dried with $MgSO_4$, filtered, and evaporated to dryness. Purification by flash chromatography (DCM/MeOH, 90/10) afforded the product as a yellow solid (1.2 g, 45% yield).

^{1}H NMR (300 MHz, $CDCl_3$) δ 8.30 (d, J = 9.3 Hz, 1H), 8.21 – 8.06 (m, 4H), 8.01 (d, J = 10.8 Hz, 3H), 7.85 (d, J = 7.8 Hz, 1H), 5.15 (d, J = 8.1 Hz, 1H), 3.82 – 3.66 (m, 1H), 3.39 (t, J = 7.0 Hz, 2H), 2.58 (td, J = 10.8, 5.6 Hz, 1H), 2.26 – 2.14 (m, 3H), 2.01 – 1.91 (m, 2H), 1.89 – 1.78 (m, 2H), 1.41 (s, 5H), 1.33 – 0.99 (m, 4H).

^{13}C NMR (101 MHz, $CDCl_3$) δ 171.80, 135.88, 131.42, 130.91, 129.96, 128.80, 127.47, 127.41, 126.74, 125.88, 125.11, 124.99, 124.94, 124.78, 123.40, 49.94, 47.88, 36.21, 35.33, 32.74, 32.49, 31.93, 31.31, 27.49.

HRMS (ESI) for **$C_{26}H_{28}N_2O$**. Calculated **M:** 384.2201, **$[M+H^+]^+$:** 385.2279, found: 385.2278.

4-(pyren-1-yl)butan-1-ol (5.18)[34]

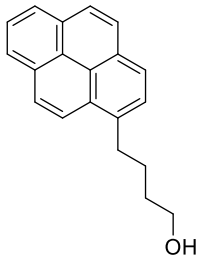

The reaction was carried out following a previously reported procedure. A solution of pyrenebutyric acid in dry THF was added dropwise to a stirring suspension of $LiAlH_4$ in dry THF at 0°C. The reaction mixture was stirred overnight at rt. The reaction was quenched by addition of MeOH (3 mL) and diluted HCl (1N). The aqueous phase was extracted with Et2O (x3) and the combined organic phases were washed with brine. The organic phase was then dried over anhydrous $MgSO_4$, filtered, and dried under vacuum to afford the product as a yellow solid in quantitative yield.

^{1}H NMR (300 MHz, $CDCl_3$) δ 8.27 (d, J = 9.3 Hz, 1H), 8.23 – 7.90 (m, 7H), 7.86 (d, J = 7.8 Hz, 1H), 3.70 (t, J = 6.5 Hz, 2H), 3.43 – 3.32 (m, 2H), 2.01 – 1.88 (m, 2H), 1.80 – 1.69 (m, 2H).

4-(pyren-1-yl)butanal (5.19)[35]

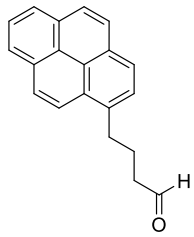

The reaction was carried out following a previously reported procedure. Pyridinium chlorochromate (589 mg, 2.73 mmol, 1.5 equiv.) was suspended in dry DCM (8 mL) and a solution of 1-pyrenebutanol **5.18** (500 mg, 1.82 mmol) in DCM (8 mL) was added at rt. The reaction was stirred overnight at rt under argon atmosphere. The reaction mixture was diluted with Et_2O and washed with water and brine. The organic phase was dried with $MgSO_4$, filtered, and evaporated to dryness to afford the aldehyde as a brown solid (392 mg, 79% yield).

^{1}H NMR (400 MHz, $CDCl_3$) δ 9.84 (t, J = 1.5 Hz, 1H), 8.32 (d, J = 9.3 Hz, 1H), 8.27 – 7.97 (m, 7H), 7.88 (d, J = 7.8 Hz, 1H), 3.47 – 3.34 (m, 2H), 2.61 (td, J = 7.1, 1.5 Hz, 2H), 2.30 – 2.17 (m, 2H).

(3aR,5R,6S,6aR)-5-(azidomethyl)-2,2-dimethyltetrahydrofuro[2,3-d][1,3]dioxol-6-ol (5.16)[36]

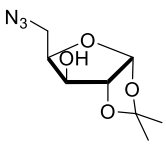

The reaction was carried out following a previously reported procedure. To a stirring solution of tosylate (4.0 g, 12 mmol) in DMF (28 mL) was added NaN_3 (2.3 g, 35 mmol, 3 equiv.). The reaction mixture was stirred at 90°C for 2 h. DMF was evaporated under high vacuum and the resulting syrup was diluted in EtOAc and water. The aqueous layer was extracted with EtOAc and the organic phase was dried over $MgSO_4$ filtered, and dried under vacuum to afford the crude product as a yellow oil that solidified.

^{1}H NMR (400 MHz, $CDCl_3$) δ 5.95 (d, J = 3.7 Hz, 1H), 4.52 (d, J = 3.7 Hz, 1H), 4.30 – 4.22 (m, 2H), 3.70 – 3.55 (m, 2H), 1.50 (s, 3H), 1.32 (s, 3H).

(3aR,5R,6S,6aR)-5-(aminomethyl)-2,2-dimethyltetrahydrofuro[2,3-d][1,3]dioxol-6-ol (5.17) [36]

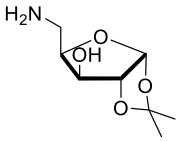

The reaction was carried out following a previously reported procedure. PPh_3 (402 mg, 1.53 mmol, 1.1 equiv.) was added to a solution of the azide **5.16** (300 mg, 1.39 mmol) in a mixture of THF-H2O (4:1, 3 mL) and the mixture was stirred at rt for 1 h. THF was evaporated and the residue was extracted with Et_2O (x2). Aqueous phase was concentrated under vacuum. The 5-aminoxylose was isolated after crystallisation in Et_2O (62% yield).

^{1}H NMR (400 MHz, $CDCl_3$) δ 5.97 (d, J = 3.7 Hz, 1H), 4.49 (d, J = 3.7 Hz, 1H), 4.32 (d, J = 2.8 Hz, 1H), 4.13 (td, J = 3.3, 1.7 Hz, 1H), 3.54 (dd, J = 13.3, 3.6 Hz, 1H), 3.17 (dd, J = 13.3, 1.7 Hz, 1H), 3.04 (br s, 2H), 1.48 (s, 3H), 1.32 (s, 3H).

(3aR,5R,6S,6aR)-5-((((1r,4R)-4-aminocyclohexyl)amino)methyl)-2,2-dimethyltetrahydrofuro[2,3-d][1,3]dioxol-6-ol (5.15)

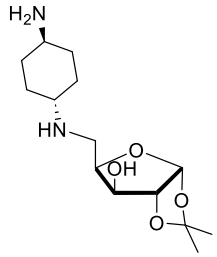

Tosylate **5.7** (3.0 g, 8.7 mmol) and trans-1,4-diaminocyclohexane (4.0g, 35 mmol, 4 equiv.) were dissolved in BuOH (17 mL) and the reaction mixture was stirred at 110°C for 3 h. The mixture was concentrated under vacuum and dissolved in DCM and washed with saturated $NaHCO_3$. The aqueous layer was extracted with DCM and the organic phase was washed with brine, dried over $MgSO_4$ filtered, and dried under vacuum to afford the product as an orange solid in 84%.

^{1}H NMR (300 MHz, $CDCl_3$) δ 5.90 (d, J = 3.7 Hz, 1H), 4.43 (d, J = 3.7 Hz, 1H), 4.25 – 4.11 (m, 2H), 3.35 (dt, J = 13.0, 3.8 Hz, 1H), 2.95 (dd, J = 12.9, 1.6 Hz, 1H), 2.60 (tt, J = 10.6, 4.1 Hz, 1H), 2.45 – 2.26 (m, 1H), 1.98 – 1.72 (m, 4H), 1.43 (s, 3H), 1.27 (s, 3H), 1.17 – 0.95 (m, 5H).

^{13}C NMR (101 MHz, $CDCl_3$) δ 129.13, 125.81, 111.46, 105.08, 86.06, 78.25, 76.93, 56.06, 55.86, 50.15, 45.73, 45.71, 34.21, 34.18, 31.68, 31.52, 31.43, 31.16, 26.85, 26.16.

HRMS (ESI) for **$C_{14}H_{26}N_2O_4$**. Calculated **M:** 286.18925, **$[M+H^+]^+$:** 287.1970, found: 287.1964.

N-((1R,4R)-4-((((3aR,5R,6S,6aR)-6-hydroxy-2,2-dimethyltetrahydrofuro[2,3-d][1,3]dioxol-5-yl)methyl)amino)cyclohexyl)-4-(pyren-1-yl)butanamide (5.5)

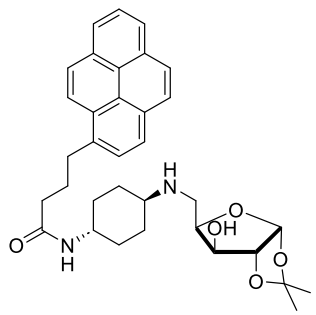

A mixture of pyrenebutyric acid (180 mg, 0.62 mmol), amino alcohol (179 mg, 0.62 mmol), HATU (261 mg, 0.69 mmol, 1.1 equiv.) and DIPEA (216 uL, 1.25 mmol, 2 equiv.) in DMF (3 mL) were stirred at rt for 4 h. The reaction mixture was diluted with DCM and washed with water. The aqueous layer was extracted with DCM and the organic phase was washed with brine, dried over $MgSO_4$ filtered, and dried

under vacuum to afford the crude product as a brown powder. Purification by flash chromatography (AcOEt/NEt_3, 90/10 then DCM/MeOH, 90/10) afforded the product as a brown powder (263 mg, 76% yield).

^{1}H NMR (400 MHz, $CDCl_3$) δ 8.29 (d, J = 9.3 Hz, 1H), 8.20 – 8.07 (m, 4H), 8.05 – 7.95 (m, 3H), 7.85 (d, J = 7.8 Hz, 1H), 5.94 (d, J = 3.7 Hz, 1H), 5.14 (d, J = 8.1 Hz, 1H), 4.48 (d, J = 3.7 Hz, 1H), 4.27 (d, J = 2.8 Hz, 1H), 4.21 (d, J = 3.6 Hz, 1H), 3.72 (ddd, J = 11.5, 7.7, 3.9 Hz, 1H), 3.44 – 3.35 (m, 3H), 2.98 (d, J = 12.8 Hz, 1H), 2.43 – 2.33 (m, 1H), 2.26 – 2.15 (m, 4H), 2.02 – 1.89 (m, 4H), 1.47 (s, 3H), 1.31 (s, 3H), 1.28 – 0.99 (m, 4H).

^{13}C NMR (100 MHz, $CDCl_3$) δ 171.88, 135.82, 131.38, 130.86, 129.93, 128.76, 127.46, 127.41, 126.74, 125.89, 124.94, 124.79, 124.78, 123.38, 111.51, 105.03, 85.94, 78.02, 76.71, 55.91, 47.82, 45.51, 38.61, 36.12, 32.72, 31.45, 31.19, 27.45, 26.84, 26.14.

HRMS (ESI) for **$C_{34}H_{40}N_2O_5$**. Calculated **M:** 556.2937, **$[M+H^+]^+$:** 557.3015, found: 557.3029.

(3aR,3bS,7aR,8aR)-2,2-dimethyl-5-(3-(pyren-1-yl)propyl)hexahydro-5H-[1,3]dioxolo[4',5':4,5]furo[2,3-e][1,3]oxazine (5.20)

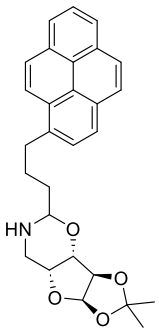

Amino alcohol (104 mg, 0.55 mmol, 1.1 equiv.) and pyrene butanal (136 mg, 0.50 mmol) were dissolved in MeOH and stirred 2 h at rt. $NaBH_4$ (37.8 mg, 1.00 mmol, 2 equiv.) was added in one portion at 0°C and the reaction mixture was stirred overnight at rt. The reaction mixture was diluted with DCM and washed with water. The aqueous layer was extracted with DCM and the organic phase was washed with brine, dried over $MgSO_4$ filtered, and dried under vacuum to afford the product as a brown powder (200 mg, 90% yield).

^{1}H NMR (400 MHz, $CDCl_3$) δ 8.27 (d, J = 9.3 Hz, 1H), 8.19 – 8.14 (m, 2H), 8.14 – 8.08 (m, 2H), 8.07 – 7.95 (m, 3H), 7.86 (d, J = 7.7 Hz, 1H), 5.92 (d, J = 3.6 Hz, 1H), 4.45 (d, J = 3.7 Hz, 1H), 4.12 – 4.05 (m, 2H), 3.89 (q, J = 2.0 Hz, 1H), 3.41 – 3.27 (m, 3H), 3.10

(dd, J = 15.4, 2.4 Hz, 1H), 2.03 – 1.92 (m, 2H), 1.73 – 1.64 (m, 2H), 1.46 (d, J = 3.0 Hz, 3H), 1.30 (s, 3H).

^{13}C NMR (101 MHz, $CDCl_3$) δ 136.51, 131.45, 130.92, 129.84, 128.65, 127.53, 127.29, 127.23, 126.60, 125.81, 125.11, 125.04, 124.86, 124.80, 124.69, 123.42, 111.52, 105.58, 86.57, 84.40, 78.42, 71.62, 44.69, 35.61, 33.23, 26.94, 26.63, 26.12.

(3aR,5R,6S,6aR)-2,2-dimethyl-5-(((4-(pyren-1-yl)butyl)amino)methyl)tetrahydrofuro[2,3-d][1,3]dioxol-6-ol (5.12)

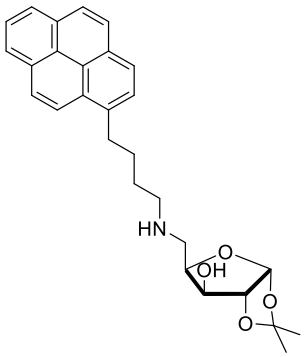

Amino alcohol **5.17** (208 mg, 1.10 mmol, 1.1 equiv.) and pyrene butanal **5.19** (272 mg, 1.00 mmol) were dissolved in THF (4 mL) and stirred 2 h at rt. $LiAlH_4$ (56.9 mg, 1.50 mmol, 1.5 equiv.) was added in one portion at 0°C and the reaction mixture turned immediately red. It was stirred at rt for 30 mn then MeOH was added at 0°C to quench the reaction. The reaction mixture was diluted with DCM and washed with water. The aqueous layer was extracted with DCM and the organic phase was washed with brine, dried over $MgSO_4$ filtered, and dried under vacuum to afford the product as a brown powder (392 mg, 88% yield).

^{1}H NMR (400 MHz, $CDCl_3$) δ 8.29 – 8.07 (m, 5H), 8.07 – 7.95 (m, 3H), 7.85 (d, J = 7.8 Hz, 1H), 5.94 (d, J = 3.7 Hz, 1H), 4.48 (d, J = 3.7 Hz, 1H), 4.28 (d, J = 2.9 Hz, 1H), 4.19 (td, J = 3.3, 1.4 Hz, 1H), 3.43 – 3.31 (m, 3H), 2.95 (dd, J = 13.1, 1.5 Hz, 1H), 2.76 – 2.56 (m, 2H), 1.89 (ddd, J = 15.6, 8.9, 6.5 Hz, 2H), 1.64 (dtd, J = 14.2, 7.0, 2.1 Hz, 2H), 1.48 (s, 3H), 1.31 (d, J = 0.7 Hz, 3H).

^{13}C NMR (101 MHz, $CDCl_3$) δ 136.37, 131.45, 130.91, 129.86, 128.61, 127.52, 127.30, 127.26, 126.63, 125.82, 125.11, 125.04, 124.89, 124.81, 124.72, 123.31, 111.46, 105.08, 86.02, 78.12, 77.23, 76.84, 49.57, 48.45, 33.21, 29.45, 29.21, 26.85, 26.15.

HRMS (ESI) for **$C_{28}H_{31}NO_4$**. Calculated **M:** 445.2253, **$[M+H^+]^+$:** 446.2331, found: 446.2341.

N-(((3aR,5R,6S,6aR)-6-(dinaphtho[2,1-d:1',2'-f][1,3,2]dioxaphosphepin-4-yloxy)-2,2-dimethyltetrahydrofuro[2,3-d][1,3]dioxol-5-yl)methyl)-N-(4-(pyren-1-yl)butyl)dinaphtho[2,1-d:1',2'-f][1,3,2]dioxaphosphepin-4-amine (5.11)

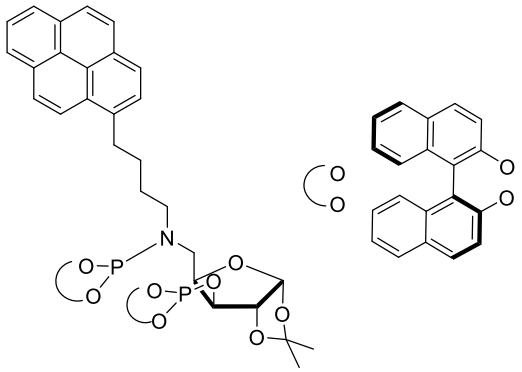

The reaction was carried out following a previously reported procedure.[30] Compound **5.12** (111.4 mg, 0.25 mmol) was azeotropically dried with dry toluene (3x1 mL), and dissolved in dry toluene (3 mL) and dry NEt_3 (174 uL, 1.25 mmol, 5 equiv.). The mixture was added dropwise to a freshly synthesized phosphochloridite in dry toluene (3 mL) and NEt_3 (174 uL, 1.25 mmol, 5 equiv.) at 0°C. The reaction was stirred at this temperature for 5 mn then at rt for 2 h. The reaction mixture was purified by flash chromatography (Toluene, 4% NEt_3) to afford the ligand (98 mg, 36% yield) as a yellow solid.

^{1}H NMR (400 MHz, CD_2Cl_2) δ 8.23 (d, J = 9.3 Hz, 1H), 8.20 – 8.13 (m, 2H), 8.13 – 7.67 (m, 18H), 7.53 – 7.34 (m, 7H), 7.34 – 7.09 (m, 21H), 5.77 (d, J = 3.8 Hz, 1H), 4.49 (dd, J = 9.1, 2.5 Hz, 1H), 4.33 (d, J = 3.8 Hz, 1H), 4.27 (dt, J = 6.5, 3.1 Hz, 1H), 3.39 (ddd, J = 15.1, 8.0, 3.3 Hz, 1H), 3.29 – 3.21 (m, 2H), 3.20 – 3.00 (m, 4H), 1.73 (s, 3H), 1.43 (s, 3H), 1.27 (s, 1H), 1.18 (s, 3H).

^{31}P NMR (162 MHz, CD_2Cl_2) δ 150.24 (d, J = 3.6 Hz), 143.97.

^{13}C NMR (100 MHz, CD_2Cl_2) δ 149.83, 149.41, 147.90, 147.01, 137.03, 132.71, 132.52, 132.42, 131.63, 131.43, 131.41, 131.05, 130.93, 130.78, 130.48, 130.28, 130.19, 129.98, 129.71, 128.96, 128.54, 128.42, 128.31, 128.15, 127.49, 127.40, 127.07, 126.74, 126.62, 126.43, 126.36, 126.28, 126.04, 125.96, 125.80, 125.23, 125.21, 125.04, 124.94, 124.80, 124.78, 124.75, 124.62, 124.45, 124.09, 123.89, 123.54, 122.50, 122.31, 122.04, 121.69, 121.40, 111.71, 104.85, 84.05, 80.81, 77.99, 77.91, 53.97, 53.70, 53.43, 53.16, 52.89, 45.80, 45.63, 44.06, 32.92, 28.80, 28.72, 26.38, 25.83, 21.14.

HRMS (ESI) for **$C_{68}H_{53}NO_8P_2$**. Calculated **M:** 1073.3246, **$[M+H^+]^+$:** 1074.3324, found: 1074.3277.

[Rh(COD)(5.11)]BF_4 (5.10)

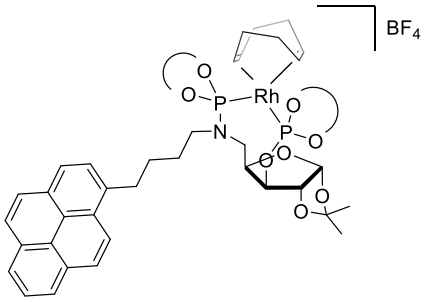

Compound **5.11** (107 mg, 0.1 mmol) in CH_2Cl_2 (1.5 mL) was added to a $[Rh(COD)_2]BF_4$ (40.6 mg, 0.1 mmol) solution in CH_2Cl_2 (1.5 mL) at 0°C, and the reaction was left stirring for 1h at rt.

Then, DCM was partially evaporated and the complex was precipitated with hexane, and washed with hexane three times to afford as an orange solid, which was analyzed by multinuclear NMR spectroscopy.

HRMS (MALDI) for **$C_{76}H_{65}NO_8P_2RhBF_4$**. Calculated **M:** 1371.3269, **$[C_{68}H_{53}NO_8P_2Rh]^+$:** calculated: 1176.2296, found: 1176.2299.

[Rh(COD)(5.11)]BF_4 (5.10@support)

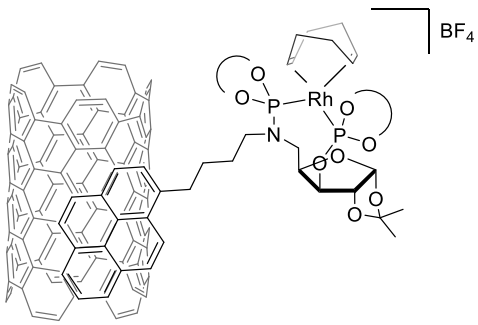

The experimental procedure describes the immobilization of rhodium complexes onto MWCNTs. The same procedure was applied for the other carbon materials. 150 mg of MWCNTs were dispersed in EtOAc (15 mL) and were sonicated in an ultrasound bath for 30 min in order to disperse the MWCNTs. After that, complex **5.10** (50 mg in 10 mL) was added to the previous suspension, and the reaction was left stirring at rt overnight.

Then, the solid was filtered via canula, and washed with EtOAc (3 x 5 mL) and dried under vacuum to yield the heterogenized catalyst (152 mg, Rh content by ICP = 1.61 wt %).

Batch hydroformylation of 5.22 with heterogenized catalysts

A 5 mL glassware reactor tube was charged with **5.10@support** (1 mol%) and **5.22** (35.3 mg, 0.25 mmol) in EtOAc (0.6 mL). The reaction tube was placed in the reactor which was purged with 5 bars of CO (x3) and pressurized at 20 bars ($CO:H_2$ = 1:1). The reactor was stirred at 400 rpm and heated at 110°C for 38 h. The reaction was stopped by cooling the reactor with an ice bath followed by carefully venting of the system in a well-ventilated fumehood. EtOAc was added and the mixture decantated. The liquid layer was concentrated under vacuum and analyzed by NMR.

N,N-diethyl-4-hydroxy-2-methylbutanamide (5.26)[30]

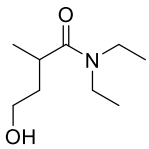

The reaction was carried out following a previously reported procedure. $NaBH_4$ (0.23 mmol) was added at room temperature to a solution of the crude mixture containing aldehyde **5.23** (0.18 mmol) in MeOH (2 mL). The reaction was quenched with water after 2 h and extracted with Et_2O. The combined organic layers were dried over $MgSO_4$ and concentrated under vacuum. Enantiomeric excess was determined by GC analysis on a CP-Chiralsil-Dex column (100 kPa H_2, 130°C for 10 min, 2.5°C/min until 160°C). $t_{r\ minor}$ = 14.26 min, $t_{r\ major}$ = 15.07 min. ^{1}H NMR (400 MHz, $CDCl_3$) δ 3.63 – 3.54 (m, 2H), 3.43 – 3.23 (m, 4H), 2.94 – 2.81 (m, 1H), 1.96 – 1.81 (m, 1H), 1.70 – 1.55 (m, 1H), 1.27 – 1.04 (m, 9H).

N,N-diethyl-2-methyl-4-morpholinobutanamide (5.27)[30]

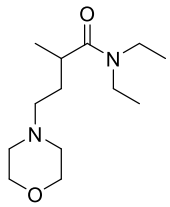

A 5 mL glassware reactor tube was charged with $Rh(acac)(CO)_2$ (1 mol%) in MeTHF (0.2 mL), **5.11** (1.2 mol%) in MeTHF (0.2 mL), **5.22** (35.3 mg, 0.25 mmol) and morpholine (22 µL, 1 equiv.). The reaction tube was placed in the reactor which was purged with 5 bars of CO (x3) and pressurized at 20 bars ($CO:H_2$ = 1:1). The reactor was stirred at 400 rpm and heated at 110°C for 38 h. The reaction was stopped by cooling the reactor with an ice bath followed by carefully venting of the system in a well-

ventilated fumehood. The reaction mixture was purified by column chromatography on silica gel using PE:AcOEt (1:1) then AcOEt:NEt_3 (9:1). The ee of 67 % was determined by HPLC method on a Daicel Chiralpak IF column with a gradient 90:5:5 Hexane/EtOH/DCM, flow rate 0.8 mL/min, = 220 nm: $t_{r\ major}$ = 19.6 min, $t_{r\ minor}$ = 21.8 min. ^{1}H NMR (400 MHz, $CDCl_3$) δ 3.68 (t, J = 4.7 Hz, 4H), 3.54 – 3.19 (m, 4H), 2.75 (h, J = 6.7 Hz, 1H), 2.51 – 2.21 (m, 6H), 1.96 – 1.85 (m, 1H), 1.54 (ddd, J = 13.5, 7.5, 5.6 Hz, 1H), 1.19 (td, J = 7.2, 1.0 Hz, 3H), 1.15 – 1.06 (m, 3H).

5.5. References

[1] Armor, J. N. A History of Industrial Catalysis. *Catal. Today* **2011**, *163* (1), 3–9.

[2] Copéret, C.; Chabanas, M.; Petroff Saint-Arroman, R.; Basset, J. M. Surface Organometallic Chemistry: Homogeneous and Heterogeneous Catalysis: Bridging the Gap through Surface Organometallic Chemistry. *Angew. Chemie - Int. Ed.* **2003**, *42* (2), 156–181.

[3] Bailie, J. E.; Hutchings, G. J.; O'Leary, S. Supported Catalysts. In *Encyclopedia of Materials: Science and Technology*; Elsevier, **2001**; pp 8986–8990.

[4] Cornils, B.; Herrmann, W. A. *Applied Homogeneous Catalysis with Organometallic Compounds*, Vol. 1, Cornils, B.; Herrmann, W. A., Wiley-VCH, Weinheim, Germany, **2002**.

[5] a) McMorn, P.; Hutchings, G. J. Heterogeneous Enantioselective Catalysts: Strategies for the Immobilisation of Homogeneous Catalysts. *Chem. Soc. Rev.* **2004**, *33* (2), 108–122. b) Corma, A.; Garcia, H. Crossing the Borders Between Homogeneous and Heterogeneous Catalysis: Developing Recoverable and Reusable Catalytic Systems. *Top. Catal*. **2008**, *48*, 8-31.

[6] Tournus, F.; Latil, S.; Heggie, M. I.; Charlier, J. C. Π-Stacking Interaction Between Carbon Nanotubes and Organic Molecules. *Phys. Rev. B - Condens. Matter Mater. Phys.* **2005**, *72* (7), 1–5.

[7] Xing, L.; Xie, J. H.; Chen, Y. S.; Wang, L. X.; Zhoua, Q. L. Simply Modified Chiral Diphosphine: Catalyst Recycling via Non-Covalent Absorption on Carbon Nanotubes. *Adv. Synth. Catal.* **2008**, *350* (7–8), 1013–1016.

[8] Moya, J. F.; Rosales, C.; Fernández, I.; Khiar, N. Pyrene-Tagged Carbohydrate-Based Mixed P/S Ligand: Spacer Effect on the Rh(I)-Catalyzed Hydrogenation of Methyl α-Acetamidocinnamate. *Org. Biomol. Chem.* **2017**, *15* (27), 5772–5780.

[9] Hao, E. J.; Li, G. X.; Lv, Z. Z.; Li, F. S.; Chen, Y. Q.; Lin, S. J.; Shi, C. Z.; Shi, L. ": In Situ Immobilization" of a Multicomponent Chiral Catalyst (MCC) via Non-Covalent Interactions for Heterogeneous Asymmetric Hydrogenation Reactions. *Org. Chem. Front.* **2020**, *7* (2), 345–349.

[10] Didier, D.; Schulz, E. π-Stacking Interactions at the Service of [Cu]-Bis(Oxazoline) Recycling. *Tetrahedron Asymmetry* **2013**, *24* (12), 769–775.

[11] Yuan, Y. C.; Abd El Sater, M.; Mellah, M.; Jaber, N.; David, O. R. P.; Schulz, E. Enantiopure Isothiourea@carbon-Based Support: Stacking Interactions for Recycling a Lewis Base in Asymmetric Catalysis. *Org. Chem. Front.* **2021**, *8* (17), 4693–4699.

[12] Abd El Sater, M.; Mellah, M.; Dragoe, D.; Kolodziej, E.; Jaber, N.; Schulz, E. Chiral Chromium Salen@rGO as Multipurpose and Recyclable Heterogeneous Catalyst. *Chem. - A Eur. J.* **2021**, *27* (36), 9454–9460.

[13] (a) Liu, G.; Wu, B.; Zhang, J.; Wang, X.; Shao, M.; Wang, J. Controlled Reversible Immobilization of Ru Carbene on Single-Walled Carbon Nanotubes: A New Strategy for Green Catalytic Systems Based on a

Solvent Effect on π-π Interaction. *Inorg. Chem.* **2009**, *48* (6), 2383–2390. (b) Nasrallah, H.; Germain, S.; Queval, P.; Bouvier, C.; Mauduit, M.; Crévisy, C.; Schulz, E. Non Covalent Immobilization of Pyrene-Tagged Ruthenium Complexes onto Graphene Surfaces for Recycling in Olefin Metathesis Reactions. *J. Mol. Catal. A Chem.* **2016**, *425*, 136–146.

[14] Vriamont, C.; Devillers, M.; Riant, O.; Hermans, S. Catalysis with Gold Complexes Immobilised on Carbon Nanotubes by π-π Stacking Interactions: Heterogeneous Catalysis versus the Boomerang Effect. *Chem. - A Eur. J.* **2013**, *19* (36), 12009–12017.

[15] Keller, M.; Collière, V.; Reiser, O.; Caminade, A. M.; Majoral, J. P.; Ouali, A. Pyrene-Tagged Dendritic Catalysts Noncovalently Grafted onto Magnetic Co/C Nanoparticles: An Efficient and Recyclable System for Drug Synthesis. *Angew. Chemie - Int. Ed.* **2013**, *52* (13), 3626–3629.

[16] (a) Creus, J.; Matheu, R.; Peñafiel, I.; Moonshiram, D.; Blondeau, P.; Benet-Buchholz, J.; García-Antón, J.; Sala, X.; Godard, C.; Llobet, A. A Million Turnover Molecular Anode for Catalytic Water Oxidation. *Angew. Chemie - Int. Ed.* **2016**, *55* (49), 15382–15386. (b) Li, F.; Zhang, B.; Li, X.; Jiang, Y.; Chen, L.; Li, Y.; Sun, L. Highly Efficient Oxidation of Water by a Molecular Catalyst Immobilized on Carbon Nanotubes. *Angew. Chemie - Int. Ed.* **2011**, *50* (51), 12276–12279..

[17] Ballestin, P.; Ventura-Espinosa, D.; Martín, S.; Caballero, A.; Mata, J. A.; Pérez, P. J. Improving Catalyst Activity in Hydrocarbon Functionalization by Remote Pyrene–Graphene Stacking. *Chem. - A Eur. J.* **2019**, *25* (40), 9534–9539.

[18] Souleymanou, M. Y.; El-Ouahabi, F.; Masdeu-Bultó, A. M.; Godard, C. Cooperative NHC-Based Catalytic System Immobilised onto Carbon Materials for the Cycloaddition of CO2 to Epoxides. *ChemCatChem* **2021**, *13* (7), 1706–1710.

[19] Zhang, X.; Wang, B.; Lu, Y.; Xia, C.; Liu, J. Homogeneous and Noncovalent Immobilization of NHC-Cu Catalyzed Azide-Alkyne Cycloaddition Reaction. *Mol. Catal.* **2021**, *504*, 111452–111465.

[20] (a) Sabater, S.; Mata, J. A.; Peris, E. Catalyst Enhancement and Recyclability by Immobilization of Metal Complexes onto Graphene Surface by Noncovalent Interactions. *ACS Catal.* **2014**, *4* (6), 2038–2047. (b) Sabater, S.; Mata, J. A.; Peris, E. Immobilization of Pyrene-Tagged Palladium and Ruthenium Complexes onto Reduced Graphene Oxide: An Efficient and Highly Recyclable Catalyst for Hydrodefluorination. *Organometallics* **2015**, *34* (7), 1186–1190. (c) Ruiz-Botella, S.; Peris, E. Immobilization of Pyrene-Adorned N-Heterocyclic Carbene Complexes of Rhodium(I) on Reduced Graphene Oxide and Study of Their Catalytic Activity. *ChemCatChem* **2018**, *10* (8), 1874–1881.

[21] Cunillera, A.; Blanco, C.; Gual, A.; Marinkovic, J. M.; Garcia-Suarez, E. J.; Riisager, A.; Claver, C.; Ruiz, A.; Godard, C. Highly Efficient Rh-Catalysts Immobilised by π-π Stacking for the Asymmetric Hydroformylation of Norbornene under Continuous Flow Conditions. *ChemCatChem* **2019**, *11* (8), 2195–2205.

[22] (a) Nozaki, K.; Itoi, Y.; Shibahara, F.; Shirakawa, E.; Ohta, T.; Takaya, H.; Hiyama, T. Asymmetric Hydroformylation of Olefins in a Highly Cross-Linked Polymer Matrix. *J. Am. Chem. Soc.* **1998**, *120* (16), 4051–4052. (b) Nozaki, K.; Shibahara, F.; Itoi, Y.; Shirakawa, E.; Ohta, T.; Takaya, H.; Hiyama, T. Asymmetric Hydroformylation of Olefins in Highly Crosslinked Polymer Matrixes. *Bull. Chem. Soc. Jpn.* **1999**, *72* (8), 1911–1918. (c) Shibahara, F.; Nozaki, K.; Matsuo, T.; Hiyama, T. Asymmetric Hydroformylation with Highly Crosslinked Polystyrene-Supported (R,S)-BINAPHOS-Rh(I) Complexes: The Effect of Immobilization Position. *Bioorganic Med. Chem. Lett.* **2002**, *12* (14), 1825–1827.

[23] Shibahara, F.; Nozaki, K.; Hiyama, T. Solvent-Free Asymmetric Olefin Hydroformylation Catalyzed by Highly Cross-Linked Polystyrene-Supported (R,S)-BINAPHOS-Rh(I) Complex. *J. Am. Chem. Soc.* **2003**, *125* (28), 8555–8560.

[24] Adint, T. T.; Landis, C. R. Immobilized Bisdiazaphospholane Catalysts for Asymmetric Hydroformylation. *J. Am. Chem. Soc.* **2014**, *136* (22), 7943–7953.

[25] Künnemann, K. U.; Weber, D.; Becquet, C.; Tilloy, S.; Monflier, E.; Seidensticker, T.; Vogt, D. Aqueous Biphasic Hydroaminomethylation Enabled by Methylated Cyclodextrins: Sensitivity Analysis for Transfer into a Continuous Process. *ACS Sustain. Chem. Eng.* **2021**, *9* (1), 273–283.

[26] Roth, T.; Evertz, R.; Kopplin, N.; Tilloy, S.; Monflier, E.; Vogt, D.; Seidensticker, T. Continuous Production of Amines Directly from Alkenes via Cyclodextrin-Mediated Hydroaminomethylation Using Only Water as the Solvent. *Green Chem.* **2023**, *25* (9), 3680–3691.

[27] Bianga, J.; Künnemann, K. U.; Goclik, L.; Schurm, L.; Vogt, D.; Seidensticker, T. Tandem Catalytic Amine Synthesis from Alkenes in Continuous Flow Enabled by Integrated Catalyst Recycling. *ACS Catal.* **2020**, *10* (11), 6463–6472.

[28] Schlüter, S.; Künnemann, K. U.; Freis, M.; Roth, T.; Vogt, D.; Dreimann, J. M.; Skiborowski, M. Continuous Co-Product Separation by Organic Solvent Nanofiltration for the Hydroaminomethylation in a Thermomorphic Multiphase System. *Chem. Eng. J.* **2021**, *409*, 128219–128231.

[29] Ibrahim, M. Y. S.; Abolhasani, M. Recyclable Cooperative Catalyst for Accelerated Hydroaminomethylation of Hindered Amines in a Continuous Segmented Flow Reactor. *Nat. Commun.* **2022**, *13* (1), 2441–2454.

[30] Miró, R.; Cunillera, A.; Margalef, J.; Lutz, D.; Börner, A.; Pamies, O.; Diéguez, M.; Godard, C. Rh-Catalyzed Asymmetric Hydroaminomethylation of α-Substituted Acrylamides: Application in the Synthesis of RWAY. *Org. Lett.* **2020**, *22* (22), 9036–9040.

[31] Rannard, S. P.; Davis, N. J. The Selective Reaction of Primary Amines with Carbonyl Imidazole Containing Compounds: Selective Amide and Carbamate Synthesis. *Org. Lett.* **2000**, *2* (14), 2117–2120.

[32] Gual, A.; Godard, C.; Claver, C.; Castillón, S. C1-Symmetric Diphosphite Ligands Derived from Carbohydrates: Influence of Structural Modifications on the Rhodium-Catalyzed Asymmetric Hydroformylation of Styrene. *European J. Org. Chem.* **2009**, *8*, 1191–1201.

[33] Dale, T. J.; Rebek, J. Fluorescent Sensors for Organophosphorus Nerve Agent Mimics. *J. Am. Chem. Soc.* **2006**, *128* (14), 4500–4501.

[34] Kang, S.; Zhang, J.; Sang, L.; Shrestha, L. K.; Zhang, Z.; Lu, P.; Li, F.; Li, M.; Ariga, K. Electrochemically Organized Isolated Fullerene-Rich Thin Films with Optical Limiting Properties. *ACS Appl. Mater. Interfaces* **2016**, *8* (37), 24295–24299.

[35] Maurin, A.; Robert, M. Noncovalent Immobilization of a Molecular Iron-Based Electrocatalyst on Carbon Electrodes for Selective, Efficient CO_2-to-CO Conversion in Water. *J. Am. Chem. Soc.* **2016**, *138* (8), 2492–2495.

[36] Raluy, E.; Pàmies, O.; Diéguez, M. Modular Furanoside Phosphite-Phosphoroamidites, a Readily Available Ligand Library for Asymmetric Palladium-Catalyzed Allylic Substitution Reactions. Origin of Enantioselectivity. *Adv. Synth. Catal.* **2009**, *351* (10), 1648–1670.

CHAPTER VI

RHODIUM CATALYZED INTRAMOLECULAR ASYMMETRIC HYDROAMINOMETHYLATION OF ALKENES

6.1. Introduction

As previously described in chapter 1, in the intramolecular asymmetric HAM, the enantioinduction must take place during the imine/enamine hydrogenation step to form a chiral product. For this purpose, this reaction pathway was investigated as it makes possible to overcome the E/Z isomerization of enamines (Cf chapter 1) to enantioselectively form the chiral amine.

6.1.1. Intramolecular hydroaminomethylation

Through intramolecular HAM, compounds such as indoline, tetrahydroisoqunoline or benzazepine derivatives, privileged scaffolds which exhibit interesting and important pharmacological activities, can be accessed in a one step process.[1] As presented in chapter 1 (scheme 19, pathway B), the hydroaminomethylation of monosubstituted alkenes undergoes racemization during the condensation step between the aldehyde formed during the HF step and the amine reagent, and as such, the enantioselectivity must be induced during the hydrogenation of the imine/enamine to produce a chiral amine. In contrast with the intermolecular HAM[2], only one enamine isomer can be formed, making more efficient the asymmetric hydrogenation (Scheme 1).

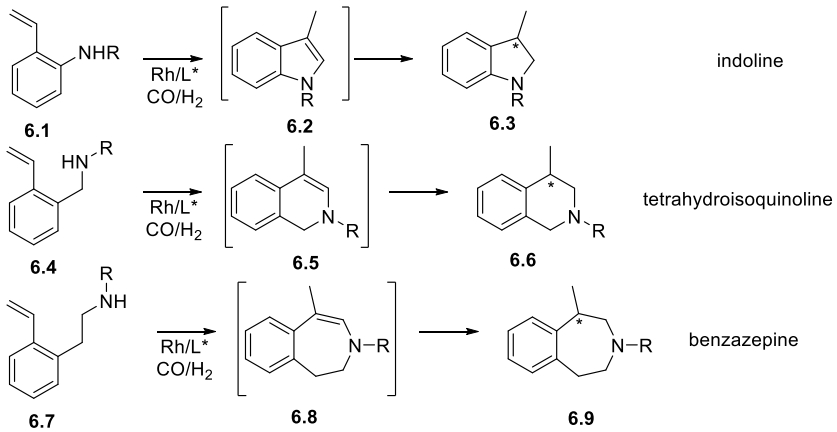

Scheme 1. Intramolecular HAM of different substrates

In the literature, only a few numbers of publications have addressed this intramolecular reaction,[3-6] and to our knowledge, none have dealt with the asymmetric version using a single catalyst.

The intramolecular hydroaminomethylation of derivatives of 2-(prop-1-en-2-yl)aniline, leading to the production of 1, 2, 3, 4-tetrahydroquinolines, was first reported by Alper and co-workers (Scheme 2)**.** Tetrahydroquinolines were synthesized employing 5 mol% of air stable rhodium complexes **6.20** bearing the N,N,N,N-tetramethylethylenediamine (TMEDA) ligand at 120°C and 69 bar of syngas (CO/H_2, 7:3) in toluene for 48 h. [3] Since linear selectivity is usually favored in the rhodium catalyzed hydroformylation of 1,1-disubstituted alkenes, the formation of the 6-membered ring **6.11** was achieved with high selectivity and up to 98% yield.

Benzazepines **6.13** were synthesized in excellent yield (up to 98%) using the same methodology.[4] The substrate **6.12** was used with the same rhodium catalyst **6.20** (7.5 mol%) at 120°C in toluene for 48 h but under 55 bar of pressure (CO/H_2, 7:1). The partial pressure of CO was increased compared to the HAM of **6.10** due to a higher hydrogenation rate of **6.12** when using a mixture of 7:3. Interestingly, the same products were obtained in up to 96% yield via a one-pot route involving as the first step reductive amination of 2-isopropenylbenzaldehyde **6.14** moiety with the aniline derivative, followed by the intramolecular HAM of the isopropenyl moiety.

Later the intramolecular HAM of 2-allylanilines **6.16** was reported using the same catalyst at 100°C and 55 bar of syngas (CO/H_2, 7:1) in toluene for 24 h.[5] A mixture of branched (**6.17**, 48% yield) and linear products (**6.18,** 8% yield) was formed as well as the cyclocarbonylation side product **6.19** in 24% yield. Increasing the partial pressure of hydrogen from CO/H_2=7:1 to CO/H_2=1:7 decreased the formation of **6.19** to traces but increased the hydrogenation rate of the substrate **6.16**. Interestingly, even at high CO partial pressure (CO/H_2=7:1), the hydrogenation of the enamine intermediate was observed. It is worth mentioning that no conjugation with the phenyl ring is present in the enamine formed, which facilitates the hydrogenation of double bond.

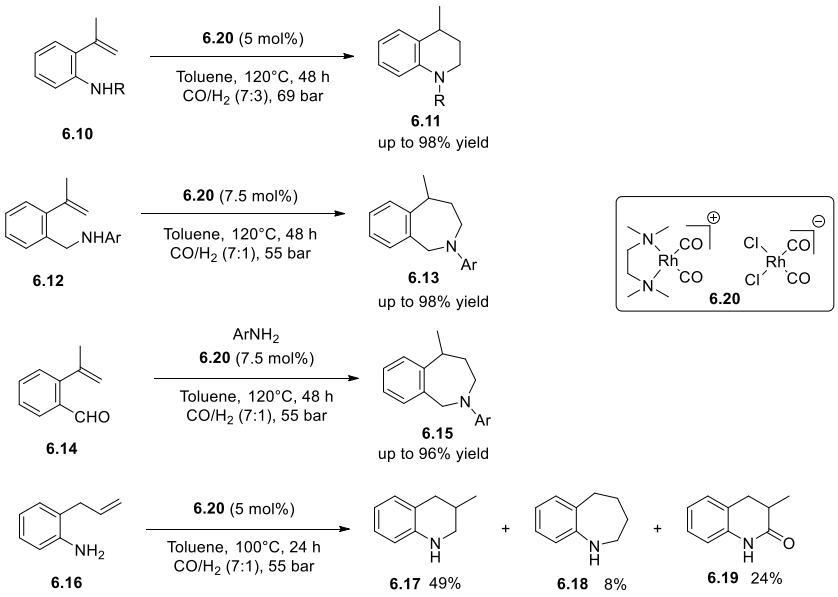

Scheme 2. Rh-catalyzed intramolecular HAM by Alper and co-workers

To access dihydropyrrole derivatives, known as key intermediates in the synthesis of active alkaloids, the interrupted HAM of (*E*)-N-substitutedcinnamylamine **6.21** was described using $Rh(acac)(CO)_2$ (0.1 mol%) and triphenylphosphine (1 mol%) as catalytic system at 80°C and 20 bar of pressure (CO/H_2, 1:1) in toluene (Scheme 3). 4-aryl-2,3-dihydropyrroles **4.22** were obtained in up to 99% yield. An increase of the partial pressure of hydrogen (CO/H_2, 1:2) resulted in a lower yield of **6.22** and no further hydrogenation of dihydropyrrole **6.22** was observed.

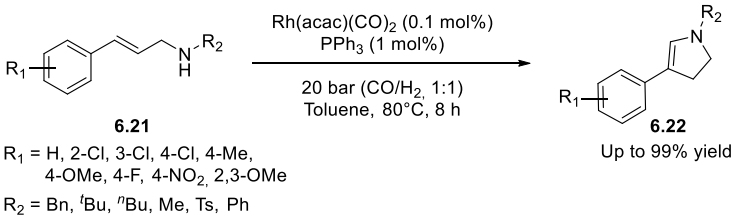

Scheme 3. Interrupted HAM of (E)-N-substitutedcinnamylamine

The interrupted HAM of N-protected-2-vinyl anilines **6.1** was recently reported by Urrutigoïty and co-workers (Scheme 4)[6]. N-protected-2-vinyl anilines **6.1** were tested using $Rh(acac)(CO)_2$ (0.2 mol%) and triphenylphosphine (0.4 mol%) as catalytic system at 60°C and 30 bar of pressure (CO/H_2, 1:1) in toluene. Variations of the R group led to the formation of either 3-substituted indoline-2-ol **6.23** or 3-substituted indole **6.2** scaffolds. When R was an electron-withdrawing group, the dehydration step was prevented, resulting in a preferential formation of **6.23**. This methodology demonstrated the potential to selectively produce either **6.23** or **6.2** in high yields. Additionally, when (*S,S*-Ph-BPE) was employed as ligand for the substrate **6.1** (R=Ts), **6.2** was obtained with a favorable diastereomeric ratio (10:1) and the major *trans* diastereomer was obtained in 43% ee. However, no hydrogenation of the indole **6.2** was observed throughout this study.

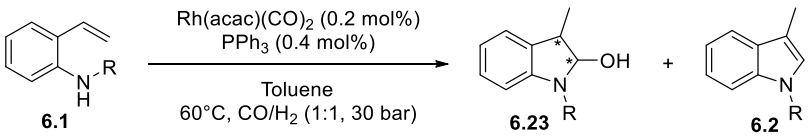

R	**6.23** (d.r)	Yield % **6.2**
H	0	>99
2-ClPh	0	>99
$COCH_3$	77 (5:1)	23
Fmoc	85 (4.5:1)	15
BOC	85 (4.5:1)	15
Ms	>99 (4.5:1)	0
Ts	>99 (5:1)	0

Scheme 4. Interrupted HAM of N-protected-2-vinyl anilines 6.1

To date, the intramolecular hydroaminomethylation thus remains underdeveloped and was often reported as interrupted HAM as the final hydrogenation of the enamine intermediate often revealed very challenging.

In the next sections, reported results on the asymmetric hydrogenation of endocyclic enamines using rhodium catalysts will be presented, as it constitutes the key step in the enantioselective intramolecular hydroaminomethylation reaction.

6.1.2. Rh-catalyzed asymmetric hydrogenation of endocyclic enamines

To date, the asymmetric hydrogenation of enamines using rhodium catalysts was only scarcely reported.[7-8] The application of a Rh-catalyst involving a *trans* chelating ligand based on ferrocene ((*S*,*S*)-(*R*,*R*)-PhTRAP, **L1**) was described by Kuwano and co-workers in the hydrogenation of 2- and 3-substituted indoles (Scheme 5).[7] N-acetyl protected-2-substituted indoles **6.24** were hydrogenated using the catalytic system $[Rh(nbd)_2][SbF_6]$ (1 mol %)/**L1** (1.05 mol%) in the presence of cesium carbonate (10 mol %) at 60°C and 50 bar of H_2 in isopropanol for 2 h. The resulting N-acetyl protected-2-indolines **6.25** were obtained in up to 98% yield and in a range of 79-95% ee. Other Rh-based catalysts containing the diphosphine ligands ((*R*)-BINAP, (2*S*,3*S*)-Chiraphos, (*R*)-(*S*)-BPPFA, (2*R*,3*R*)-DIOP, (*R*,*R*)-Me-DuPHOS, (2*S*,4*S*)-BPPM) were successfully employed to hydrogenate **6.24** but no enantioselectivity was observed.

The N-tosyl protected-3-substituted indoles **6.26** were hydrogenated using the cationic catalytic system bearing the **L1** ligand at 80°C and 50 bar of H_2 in isopropanol for 24 h (Scheme 5). The N-tosyl protected-3-substituted indolines **6.27** were obtained in up to 96% yield and 95-98% ee. Higher temperature and reaction time than those used for the substrate **6.24** were necessary for the hydrogenation of **6.26**. However, no conversion of **6.26** was observed with rhodium complexes bearing triphenylphosphine or BINAP. The system tolerated other solvents like toluene in the hydrogenation of **6.24** but not when **6.26** was the substrate. The role of the base was initially to prevent the N-acetyl group from solvolysis, but it was observed that it also exerted a significant influence on both conversion and enantioselectivity. Indeed, in the absence of a base, the hydrogenation of **6.24** resulted in very low conversion and only 7% ee.[7c] The methodology was also suitable for the hydrogenation of 5-, 6-, and 7- membered 1-aza-2-cycloalkene-2-carboxylates in a range of 11 to 93% ee.[7d] The N-protecting group exerted a pronounced influence on enantioselectivity as N-BOC protected 7-membered ring enamine yielded 87% ee while the N-Cbz analog was obtained in only 11% ee.

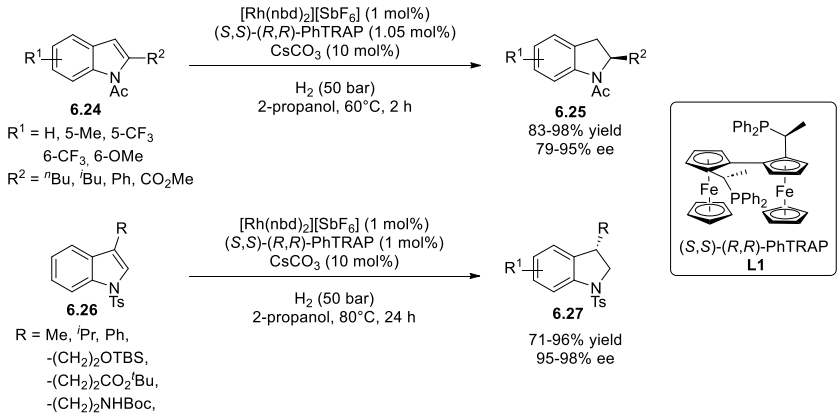

Scheme 5. Rh-catalyzed asymmetric hydrogenation of indoles 6.24 and 6.26 with PhTRAP

More recently, the asymmetric hydrogenation of unprotected indoles **6.28** using HCl as additive was reported by Zhang and co-workers.[8a] The 2-, 3-substituted indoles **6.28** were hydrogenated by the catalytic system $[Rh(COD)Cl]_2$ (0.5 mol %)/(*S*,*R*)-ZhaoPhos **L2** (1.0 mol%) in the presence of HCl (2 equiv.) at 25°C and 40 bar of H_2 in dichloromethane for 48 h. 2-, 3-substituted indolines **6.29** were obtained in up to 98% yield and with 79-95% ee. They demonstrated that hydrogen bonding between the chloride, the substrate and the thiourea moiety of the ligand (*S*,*R*)-ZhaoPhos **L2** in the transition state **6.30** (Scheme 6) was crucial to reach both activity and high enantioselectivity. Indeed, in the absence of a Brønsted acid, no conversion was observed. The proposed mechanism suggests that HCl generates an iminium intermediate, subsequently hydrogenated to yield the indoline products **6.29**. The same catalytic system was employed for the asymmetric hydrogenation of azepine-

type 7-membered iminium hydrochlorides, resulting in yields up to 95% and ee's up to 99%.[8b]

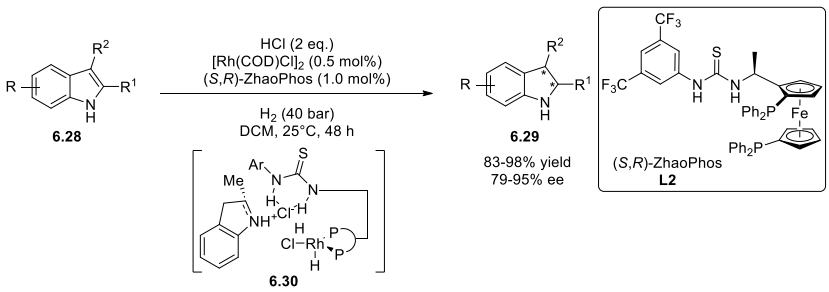

Scheme 6. Rh-catalyzed asymmetric hydrogenation of indoles 6.28 with (S,R)-ZhaoPhos and HCl.

These reports show that there is much progress to be made in the asymmetric hydrogenation of endocyclic enamines which still often requires high hydrogen pressure and long reaction times, and nitrogen protection to efficiently proceed.

6.2. Results and discussion

Based on the previous results obtained in Rh-catalyzed intramolecular HAM of alkenes and Rh-catalyzed asymmetric hydrogenation of endocyclic enamines, we focused our study on the intramolecular HAM of styrene-based substrates **6.1**, **6.3** and **6.5**.

6.2.1. Synthesis of substrates

The different substrates used in our study were synthesized following procedures adapted from the literature. 2-nitrobenzaldehyde **6.31** was converted into 2-vinylnitrobenzene **6.32** via a Wittig reaction using the corresponding ylide formed with $MePPh_3Br$ and nBuLi in dry THF at 45°C. The product **6.32** was obtained in 54% yield after column chromatography. 2-vinylnitrobenzene **6.32** was further transformed to 2-vinylaniline via Béchamp reduction using iron powder and concentrated HCl in refluxing ethanol for 3 h. 2-vinylaniline was obtained in 90% yield without further purification (Scheme 7).

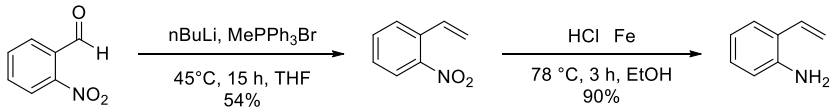

Scheme 7. Formation of 2-vinylaniline 6.33

2-vinylaniline was protected using tosyl chloride in a mixture of pyridine and dichloromethane at room temperature for 16 h. The resulting N-p-tosyl-2-vinyl-aniline **6.34** was obtained in 33% yield after column chromatography.

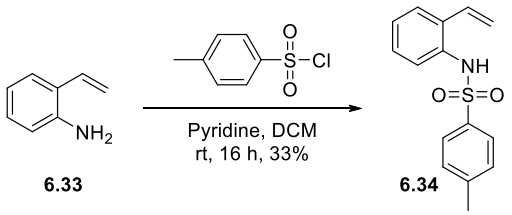

Scheme 8. Formation of N-p-tosyl-2-vinyl-aniline 6.34

N-methyl-2-vinylbenzylamine **6.39** was synthesized in a two-step reaction from 2-bromostyrene **6.35**. First, **6.35** was converted to 2-vinylbenzaldehyde **6.36** via a lithium halogen exchange using nBuLi at -78°C followed by reacting on DMF at the same temperature. The product **6.36** was obtained in 91% yield after slowly allowing the reaction to reach room temperature. The platform aldehyde was converted to 2-vinylbenzaldehyde oxime **6.37** in quantitative yield by reacting with hydroxylamine hydrochloride and sodium acetate in ethanol at 70°C for 16 h. Disappointingly, **6.37** was not reduced to 2-vinylbenzylamine **6.38** using the following reported procedure using glacial acetic acid and zinc powder.[15] The aldehyde **6.36** was transformed into N-methyl-1-(2-vinylphenyl)methanamine **6.39** via reductive amination of

methylamine in presence of sodium borohydride in methanol. The amine product **6.39** was obtained in 77% yield without further purification (Scheme 9).

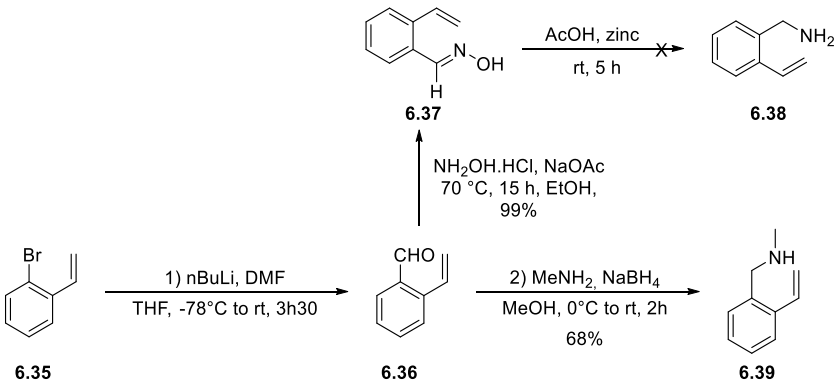

Scheme 9. Formation of N-methyl-1-(2-vinylphenyl)methanamine 6.39

1-Bromo-2-cyanomethylbenzene **6.40** was reduced to 2-(2-bromophenyl)ethan-1-amine **6.41** by a mixture of dry aluminium chloride and lithium aluminium hydride in THF. The pure product **6.41** was obtained in 95% yield after acid/base treatment. 2-(2-bromophenyl)ethan-1-amine **6.41** was tested in a microwave assisted Suzuki-Miyaura cross-coupling with vinylboronic anhydride pyridine complex catalyzed by $Pd(PPh_3)_4$ (0.5 mol%) with potassium carbonate in a mixture of dimethoxyethane and water at 150°C for 30 mn. The alkene product **6.42** was obtained in 33% yield after column chromatography (Scheme 10).

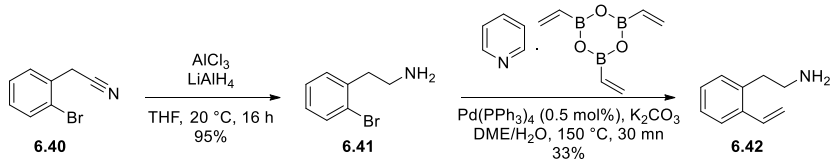

Scheme 10. Formation of 2-(2-vinylphenyl)ethan-1-amine 6.42

6.2.2. Rh-catalyzed hydroaminomethylation of substrates **6.33**, **6.34**, **6.39** and **6.42**

6.2.2.1. Rh-catalyzed hydroaminomethylation of 2-vinylaniline

As reported by Urrutigoïty and co-workers[6], the HAM reaction using 2-vinylaniline or N-protected 2-vinylaniline as substrates yields either indolinol or indole moieties at 60°C using PPh_3 as ligand. [6] In order to convert the indole into indoline, an increase of the temperature to 100°C was first envisaged to favor the hydrogenation (Scheme 11, Table 1).

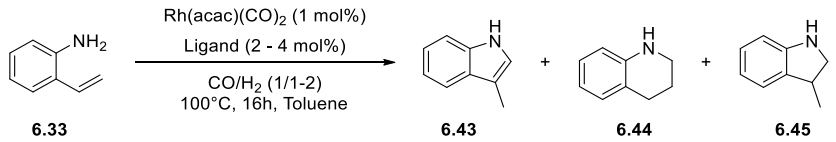

6.33 **6.43** **6.44** **6.45**

Scheme 11. HAM of 2-vinylaniline

$[Rh(acac)(CO)_2]$ was selected as the rhodium precursor and the ligands (PPh_3 or dppf) were selected based on previous reports using these ligands in hydroformylation and hydrogenation reactions. Since dppf contains a ferrocene backbone like the ligands **L1** and **L2**, it was thought to be a good candidate for this reaction. The temperature was thus set to 100°C and the reaction time to 16 h. Full conversion of **6.33** was obtained in all catalytic tests. Initially, a catalytic system containing PPh_3 was tested (entry 1) but only 66% of indole **6.43** was obtained, indicating a poor regioselectivity to the branched aldehyde and that hydrogenation of the enamine group had not taken place. When the ligand was dppf, the regioselectivity increased (entry 2) but the amine produce was not formed. The pressure was increased to 60 bar but no hydrogenation of **6.43** was observed and the regioselectivity decreased (entry 3). When the cationic $[Rh(COD)_2]BF_4$ was used as rhodium precursor, the outcome of the reaction remained similar (entry 4). HBF_4 was added to the reaction mixture to form the iminium intermediate and facilitating the hydrogenation[9] but no indoline was observed and the regioselectivity remained unchanged (entry 5). In view of these results, a test was performed with $CsCO_3$ and a mixture of toluene and isopropanol as solvents in an attempt to mimic the reported hydrogenation of indole

by Kuwano (entry 6).[7] The reaction was carried out in two steps: first, the reaction mixture was reacted with syngas (20 bar, CO/H_2 1/2) at 100°C during 16 h; at this point, the reactor was cooled down and degassed prior to introducing 50 bar of hydrogen and heated again to 100°C. The reaction was left stirring for another 16 h. However, the expected amine product **6.45** was not detected and a mixture of 74% of the indole **6.43** and 26% of the linear amine **6.44** was obtained.

Table 1. Rh-catalyzed hydroaminomethylation of substrate 6.33

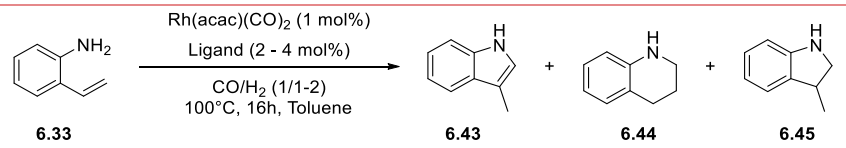

6.33 6.43 6.44 6.45

Entry	Ligand	L/Rh	Pressure	$CO:H_2$	6.43 (%)	6.44 (%)	6.45 (%)
1	PPh_3	4	25	1/1	66	33	0
2	**L3**	2	30	1/2	90	10	0
3	**L3**	2	60	1/2	69	31	0
4[a]	**L3**	2	50	1/2	73	27	0
5[b]	**L3**	2	55	1/2	75	25	0
6[c]	**L3**	2	20	1/2	74	26	0

Reaction conditions: 6.33 *(0.50 mmol), $Rh(acac)(CO)_2$ (1 mol%), toluene (20 mL), 1000 rpm, 100°C for 16 h. Conversion and selectivity measured by ^1H NMR. [a] $[RhCOD_2]BF_4$ (1 mol%). [b] HBF_4(cat) was added. [c] $CsCO_3$ (10 equiv.) was added, solvent = toluene/iPrOH (1:1).*

Based on these results, the reaction was performed using the substrate **6.34** containing a protected nitrogen group by a tosyl (Scheme 12, Table 2).

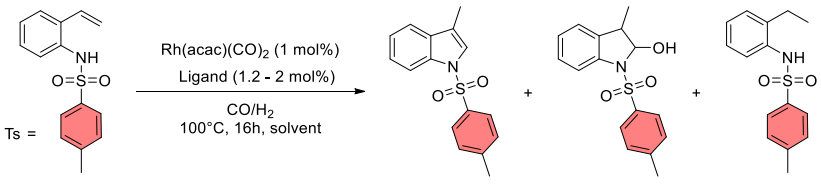

6.34 6.46 6.47 6.48

Scheme 12. HAM of N-p-tosyl-2-vinyl-aniline 6.34

$[Rh(acac)(CO)_2]$ was selected as the rhodium precursor in the presence of dppf in THF at 100°C and 30 bar of CO/H_2 (1:2), giving full conversion in 16 h with total selectivity to the indolinol **6.47** (entry 1, diastereomeric ratio = 66% cis/34% trans).

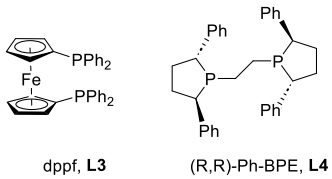

dppf, **L3** (R,R)-Ph-BPE, **L4**

Figure 1. Structure of the ligands used in Rh-catalyzed HAM of 6.34

When the reaction was repeated in the presence of p-toluenesulfonic acid (PTSA) monohydrate, complete selectivity towards **6.46** was achieved (entry 2), demonstrating that the dehydration is favoured in the presence of such acid. When (*R,R*)-Ph-BPE was employed in a mixture of toluene and isopropanol at 30 bar of pressure (CO/H_2, 1:2), the selective formation of **6.47** was observed (entry 3, diastereomeric ratio = 80% cis/20% trans). The introduction of PTSA, along with an increase in pressure to 50 bar and a partial pressure ratio of CO/H_2 = 1:5, resulted in a significant decrease in conversion, with the hydrogenation product **6.48** the major species formed. When the reaction was performed using the cationic [Rh(COD)(1,1-Bis((2S,5S)-2,5-diethylphospholano)ferrocene)]BF_4 in combination with PTSA (entry 5), the formation of the indole **6.46** was observed, along with unidentified side products.

Table 2. Rh-catalyzed hydroaminomethylation of substrate 6.34

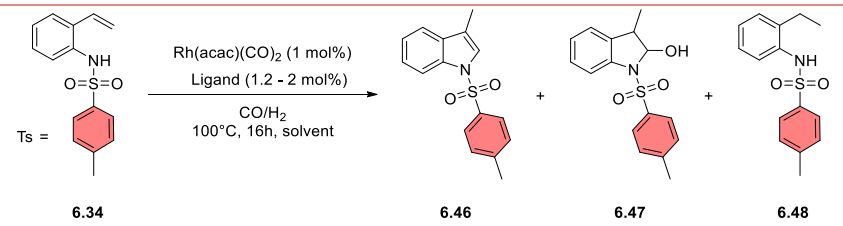

6.34 6.46 6.47 6.48

Entry	Ligand	L/Rh	Pressure	CO:H_2	Solvent	6.46 (%)	6.47 (%)	6.48 (%)
1	**L3**	2	30	1/2	THF	0	100	0
2[a]	**L3**	2	30	1/2	THF	100	0	0
3	**L4**	1.2	30	1/2	Toluene/iPrOH	0	100	0
4[a]	**L4**	1.2	50	1/5	Toluene/iPrOH	5	0	35
5[a,b]	**	1.2	50	1/2	Toluene/iPrOH	50	0	0

Reaction conditions: 6.34 *(0.50 mmol), Rh(acac)(CO)$_2$ (1 mol%), solvent (20 mL), 1000 rpm, 100°C for 16 h. Conversion and selectivity measured by ^{1}H NMR. [a] APTS = p-toluenesulfonic acid monohydrate (0.50 mmol) was added. [b][Rh] = [Rh(COD)(1,1-Bis((2S,5S)-2,5-diethylphospholano)ferrocene)]BF$_4$. Toluene/iPrOH (3:1).*

The Rh-catalyzed hydroaminomethylation of 2-vinylaniline **6.33** and N-protected-vinylaniline **6.34** was tested and afforded mainly the indoles ring **6.43** and **6.46**. The reaction was moderately regioselective but the chemoselectivity of the reaction was not in favor of the formation of the amine **6.45**.

6.2.2.2. Rh-catalyzed hydroaminomethylation of N-methyl-1-(2-vinylphenyl)methanamine

In view of the disappointing results obtained in the HAM of 2-vinylaniline and N-p-tosyl-2-vinyl-aniline, the use of N-methyl-1-(2-vinylphenyl)methanamine as substrate was tested (Scheme 13, Table 3).

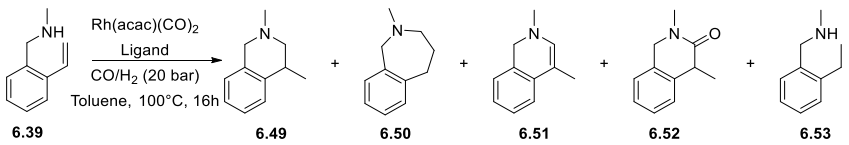

6.39 6.49 6.50 6.51 6.52 6.53

Scheme 13. HAM of N-methyl-1-(2-vinylphenyl)methanamine 6.39

The HAM reaction of **6.39** was performed with Rh(acac)(CO)$_2$ as Rh precursor in toluene at 20 bar and 100°C. When dppf was used as ligand and at a partial pressure

of CO/H_2 (1:2), the hydrogenation product **6.53** was mainly formed. The regioselectivity was 58% to the linear HAM product **6.50** (entry 1). When Xantphos was tested using a CO/H_2 ration (1:1), an equimolar mixture of branched **6.51** and linear **6.50** products was obtained although the main product remained **6.53** (entry 2). The use of the bisphosphite ligand biphephos increased the regioselectivity in favor of the linear amine but the hydrogenation drastically augmented even though the CO partial pressure was increased to CO/H_2 = 2:1 (entry 3).

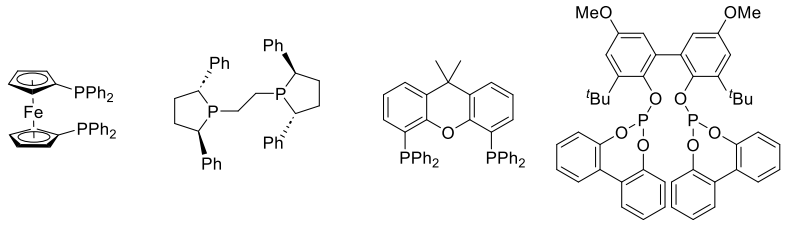

dppf, **L3** (R,R)-Ph-BPE, **L4** Xantphos, **L5** Biphephos, **L6**

Figure 2. Structure of the ligands used in Rh-catalyzed HAM of 6.39

When (R,R)-Ph-BPE was used as ligand (entries 4-9), the hydrogenation of the substrate was decreased and the branched HAM product was detected by GC-MS (entry 4). The chemoselectivity to the amide **6.52** was also increased. As previously described by Alper and co-workers (Scheme 2), the six-membered ring cyclocarbonylation product was formed while the seven membered ring was not observed. To yield this product, the rhodium atom is first coordinated by the nitrogen atom of **6.39**, followed by the insertion of CO, and the reductive elimination of the metal to yield the lactam ring **6.52**.[10]

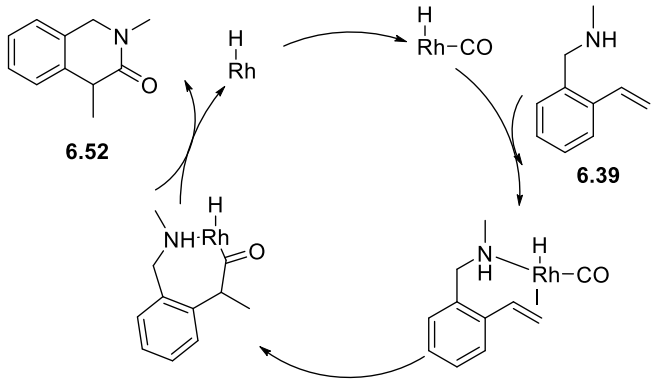

Scheme 14. Mechanism for the Rh-catalyzed hydroaminocarbonylation of 6.39 yielding 6.52.

When the reaction was performed in THF, the formation of **6.52** increased (entry 5). Cationic rhodium precursor $[Rh(COD)_2]BF_4$ was used with PhBPE in THF and a syngas ratio of 1:1 (entry 6). The system showed poor activity as only 34% of **6.39** was converted and no chemoselectivity towards HAM yielding only **6.52** and **6.53**. Increase of the partial pressure of hydrogen to CO/H_2 = 1:2 benefited the hydrogenation of **6.51** but the chemoselectivity remained poor and 39% of the mixture was **6.52** (entry 7). Increasing the partial pressure of carbon monoxide to CO/H_2 = 2:1 and CO/H_2 = 3:1 (entry 8-9) lowered the formation of **6.49** and **6.50** while the unsaturated ring **6.51** and cyclocarbonylation product **6.52** were formed in 24 and 44%, respectively.

Table 3. Catalysis results of HAM of 6.39

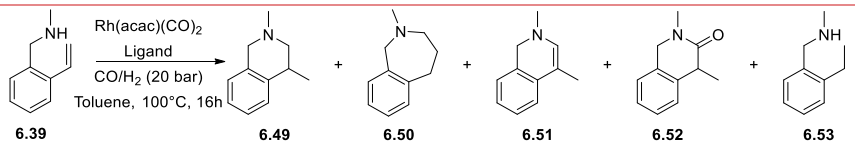

6.39 6.49 6.50 6.51 6.52 6.53

Entry	Ligand	L/Rh	CO:H_2	6.49 (%)	6.50 (%)	6.51 (%)	6.52 (%)	6.53 (%)
1	**L3**	2	1/2	0	14	10	4	37
2	**L5**	2	1/1	0	23	23	7	28
3	**L6**	1.2	2/1	0	26	11	0	62
4	**L4**	2	1/1	14	15	31	16	24
5	**L4** [a]	2	1/1	12	12	19	24	17
6	**L4** [a,b]	2	1/1	0	0	0	15	19
7	**L4**	2	1/2	19	15	2	39	8
8	**L4**	1.5	2/1	0	7	37	24	17
9	**L4**	1.5	3/1	1	4	32	44	7

Reaction conditions: 6.39 *(0.50 mmol), $Rh(acac)(CO)_2$ (1 mol%), toluene (20 mL), 1000 rpm, 100°C, 20 bar, 16 h. Conversion and selectivity measured by ^1H NMR and GCMS. [a] In THF. [b]$[Rh(COD)_2]BF_4$ (1 mol%).*

Although the results of the HAM of **6.39** provided a poor chemo and regioselectivity, the amine **6.49** could be obtained in this reaction. Although the GC yield was low, these results indicated that the hydrogenation of higher membered ring was facilitated in comparison with that of the indole ring **6.46**.

6.2.2.3. Rh-catalyzed hydroaminomethylation of 2-(2-vinylphenyl)ethan-1-amine

In the context of our work, the HAM of the substrate **6.42** was of particular interest as a way to obtain benzazepine derivatives such as the drug Lorcaserin.

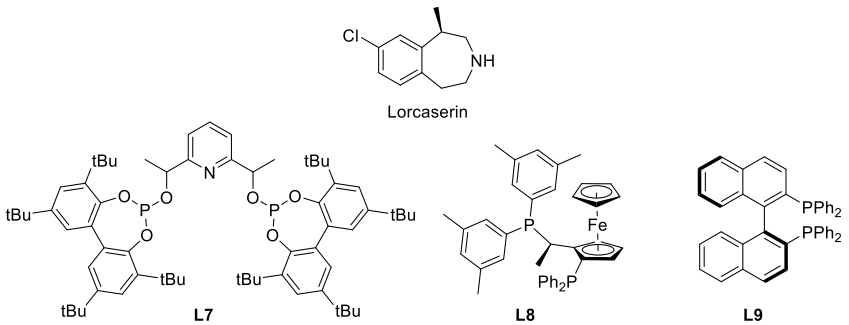

Figure 3. Structure of Lorcaserin and ligands L7-L9

The reaction was performed using $Rh(acac)(CO)_2$ as Rh precursor in a mixture of toluene and MeTHF at 80 bar of $CO:H_2$ (1:1) and 100°C for 16 h. $CsCO_3$ (10 mol%) was also added to the reaction mixture (entry 1-6) in an attempt to favor the hydrogenation of the enamine intermediate.[7] The results were analyzed by GC-MS and the activity of the catalytic systems compared using different ligands. When dppf was used as a ligand, the catalytic system provided full conversion of the starting material with excellent chemoselectivity towards the branched enamine **6.56** (entry 1). However, the desired amine product **6.54** was not detected. Similar results were obtained using PPh_3 as ligand (entry 2). Using the bisphosphite ligand **L7**, full conversion was again obtained with 67% selectivity to the enamine. However, in this case, GC-MS peaks corresponding to the amines **6.54** and **6.55** were observed in 27% and 4%, respectively (entry 3). When the Josiphos ligand **L8** was used, the selectivity was in favor of the enamine **6.56** in 93% and 1% of amine **6.54** was observed. The di*tert*-butylphenylphosphine ligand provided 85% conversion with full selectivity to the enamine **6.56** (entry 5). The (S)-BINAP **L9** also formed the enamine **6.56** in 61% selectivity but with a lower activity (entry 6). When the ligands dppf and PPh^tBu_2 were tested without the additional $CsCO_3$, the chemoselectivity of the reaction was drastically shifted. Indeed, using dppf as ligand, the amine **6.54** and **6.55** were

obtained with 51% and 6% selectivity while the enamine was only present in 35%. Hydrogenation of the substrate into **6.58** was also detected 7% (Entry 7). This result thus indicated that the presence of the base disfavored the enamine hydrogenation when dppf was used. In contrast, when the reaction was repeated using PPh^tBu_2 as ligand, only the hydrogenation of the substrate was observed in 96%. Those results depict the influence of cesium carbonate on the selectivity of the reaction. However, the effect of the base was very different as a function of the ligand used (Entry 1 vs 7 and entry 5 vs 8).

Table 4. Catalysis results of HAM of 6.42

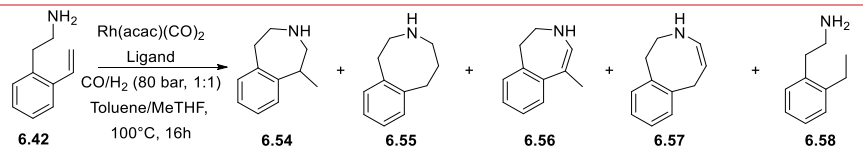

6.42 6.54 6.55 6.56 6.57 6.58

Entry	Ligand	L/Rh	6.42 (%)	6.54 (%)	6.55 (%)	6.56 (%)	6.57 (%)	6.58 (%)
1	**L3**	1.2	0	0	0	100	0	0
2	PPh_3	4	1	0	0	99	0	0
3	**L7**	1.2	1	27	4	67	0	1
4	**L8**	1.2	6	1	0	93	0	0
5	PPh^tBu_2	4	15	0	0	85	0	0
6	**L9**	1.2	38	0	0	61	0	1
7[a]	**L3**	1.2	0	51	6	35	0	7
8[a]	PPh^tBu_2	4	4	0	0	0	0	96

Reaction conditions: 6.42 *(0.20 mmol), $Rh(acac)(CO)_2$ (1 mol%), $CsCO_3$ (10 mol%), toluene (0.2 mL), MeTHF (0.2 mL), 900 rpm, 100°C, 80 bar (1:1), 16 h. Conversion and selectivity measured by ^1H NMR and GCMS. [a] Without $CsCO_3$.*

Due to lack of time, the reaction using chiral ligands in the absence of base could not be carried out. However, the results obtained in the Rh-catalyzed HAM of the substrate **6.42** were very promising since the desired amine could be obtained in up to 51% selectivity, which open the way to the production of benzazepine derivatives such as the drug Lorcaserin via asymmetric hydroaminomethylation.

6.3. Conclusions

- The synthesis of substrates **6.33**, **6.34**, **6.39**, **6.42** were successfully synthesized and tested in intramolecular hydroaminomethylation.
- As a general trend, the hydrogenation of the enamine intermediate is the limiting factor for the reaction to proceed and might require high pressure and temperature.
- Increasing the size of the enamine ring formed from 5 to 7-membered ring resulted in a more efficient hydrogenation under HAM conditions. However, no asymmetric hydroaminomethylation could be tested due to the lack of time.
- As a general conclusion, intramolecular hydroaminomethylation of alkenes remains a challenge and further work will be needed to obtain chiral amines through this pathway.

6.4. Experimental part

General informations

All the reactions were carried out under inert atmosphere using Schlenk-line or glovebox techniques. Anhydrous solvents were collected from the system Braun MB SPS-800. Commercially available reagents and solvents were purchased at the highest commercial quality from Sigma-Aldrich, Fluka, Alfa Aesar, Fluorochem, Strem and were used as received, without further purification.

^{1}H NMR spectra were recorded using a Bruker Avance 300. Chemical shift values (δ) are reported in ppm relative to TMS (^{1}H) and coupling constants are reported in Hertz. The following abbreviations are used to indicate the multiplicity: s, singlet; d, doublet; t, triplet; q, quartet; quint, quintuplet; sext, sextuplet; sept, septet; oct, octet; m, multiplet; bs, broad signal.

GC-MS analyses were performed on a GC Clarus 590 autosystem coupled with MS Clarus SQ 85 from Perkin Elmer equipped with a capillary column ELITE-5MS (30 m, 0.25 mm i.d., 0.25 µm thickness) and using He as the carrier gas. Reactions were monitored by TLC carried out on 0.25 mm E. Merck silica gel 60 F_{254} aluminium plates. Developed TLC plates were visualized under a short-wave UV lamp (254 nm) and by heating plates that were dipped in potassium permanganate. Flash column chromatography was carried out using forced flow of the indicated solvent, on Merck silica gel 60 (230-400 mesh). The Rh-catalyzed hydroaminomethylation reactions of **6.33**, **6.34** and **6.39** were set up in a 90 mL stainless steel autoclave from TOP INDUSTRIES. The autoclave is equipped with a mechanical stirring system and a temperature and pressure control system via a monitor displaying the set and actual temperatures and pressures in the reactor. The reactor is supplied with gas by a ballast containing the CO/H_2 prepared mixture. The Rh-catalyzed hydroaminomethylation reaction of **6.42** was set up in a CAT24 autoclave from HEL Inc. and stirred with a Teflon-coated magnetic stir bar.

Synthesis of 2-nitrostyrene 6.32[6]

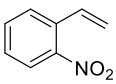

The compound **6.32** was synthesized following a modified literature procedure. $MePPh_3Br$ (5.20 g, 14.6 mmol, 1.1 equiv.) was dried azeotropically with toluene and then dissolved in dry THF (45 mL). nBuLi (9.1 mL, 1.6M in hexane, 14.6 mmol, 1.1 equiv.) was added to the mixture at 0°C and stirred at room temperature forming a yellow solution. Then 2-nitrobenzaldehyde (2.0 g, 13.2 mmol) was added portionwise under argon flow. The media turned black and thicker. The reaction mixture was stirred at 45°C overnight. The reaction was quenched by the addition of saturated aqueous solution of NH_4Cl. The aqueous phase was extracted with DCM. The combined organic layers were dried over $MgSO_4$ and evaporated under reduced pressure. The obtained residue was purified by column chromatography (silica gel, n-hexane/ethyl acetate 95:5) to afford the product (Yellow oil, 1.05 g, 54% yield).

^{1}H NMR (300 MHz, $CDCl_3$) δ 7.93 (dd, J = 8.2, 1.3 Hz, 1H), 7.68 – 7.52 (m, 2H), 7.41 (ddd, J = 8.6, 7.0, 1.8 Hz, 1H), 7.18 (dd, J = 17.3, 11.0 Hz, 1H), 5.75 (dd, J = 17.3, 1.0 Hz, 1H), 5.49 (dd, J = 11.0, 1.0 Hz, 1H).

Synthesis of 2-vinylaniline 6.33[6]

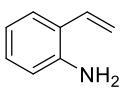

The substrate **6.33** was synthesized following a literature procedure. 2-nitrostyrene **6.32** (2.1 g, 14 mmol) was dissolved in EtOH (30 mL). Iron powder (4.8 g, 87 mmol, 6.2 equiv.) was added followed by concentrated HCl (1.4 mL, 12 M, 17 mmol, 1.2 equiv.). The mixture was refluxed for 3 h and Na_2CO_3 was added by portions at room temperature until no gas evolution was detected. The mixture was filtered over a celite pad and washed with water and brine. The organic layer was dried over $MgSO_4$ and evaporated under reduced pressure to afford the product (brown oil, 1.5 g, 90% yield)

^{1}H NMR (300 MHz, $CDCl_3$) δ 7.29 (dt, J = 7.7, 1.1 Hz, 1H), 7.14 – 7.04 (m, 1H), 6.84 – 6.65 (m, 3H), 5.63 (dd, J = 17.4, 1.5 Hz, 1H), 5.32 (dd, J = 11.0, 1.5 Hz, 1H), 3.76 (br s, 2H).

Synthesis of N-p-tosyl-2-vinyl-aniline 6.34[6]

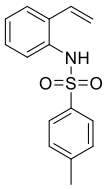

The substrate **6.34** was synthesized following a modified literature procedure. 2-vinylaniline **6.33** (596 mg, 5.00 mmol) was added to a solution of pyridine (566 µL, 7.00 mmol, 1.4 equiv.) in dry DCM (20 mL) at 0°C. Then para toluenesulfonyl chloride (1.14 g, 6.00 mmol, 1.2 equiv.) was added portionwise to the solution and the mixture was stirred overnight at rt. The mixture was concentrated and purified by column chromatography (silica gel, n-hexane/ethyl acetate 95:5 to 80:20) to afford the product (white solid, 450 mg, 33% yield).

^{1}H NMR (300 MHz, $CDCl_3$) δ 7.64 – 7.55 (m, 2H), 7.39 – 7.28 (m, 2H), 7.27 – 7.05 (m, 4H), 6.51 (dd, J = 17.4, 11.0 Hz, 1H), 6.37 (s, 1H), 5.50 (dd, J = 17.4, 1.2 Hz, 1H), 5.27 (dd, J = 11.0, 1.2 Hz, 1H), 2.39 (s, 3H).

Synthesis of 2-vinylbenzaldehyde 6.36[11]

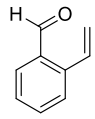

The compound **6.36** was synthesized following a literature procedure. To a solution of 1-bromo-2-vinylbenzene (3.0 g, 16.4 mmol) in THF (20 mL) was added n-BuLi (2.2 M solution in cyclohexane, 8.2 mL, 18.0 mmol, 1.1 equiv.) dropwise at -78° C. The reaction mixture was stirred at -70°C for 1 h, and then DMF (1.9 mL, 24.6 mmol, 1.5 equiv.) was added dropwise. The reaction mixture was slowly warmed up (30 mn at -78°C followed by warming up the cool bath and finally in an ice bucket) up to room temperature (over 3 h)) and stirred for 30 min (conversion checked by TLC 95/5 hexane/EtOAc). The mixture was poured into water (20 mL), and the aqueous layer was extracted with ethyl acetate (20 mLx2). The combined organic layer was dried over $MgSO_4$, filtered and concentrated under vacuum to afford 2-vinylbenzaldehyde as an orange liquid (2.0 g, 91% yield). The product was used without further purification.

^{1}H NMR (300 MHz, $CDCl_3$) δ 10.30 (s, 1H), 7.83 (dt, J = 7.6, 1.1 Hz, 1H), 7.62 – 7.36 (m, 4H), 5.70 (dd, J = 17.4, 1.2 Hz, 1H), 5.52 (dd, J = 11.0, 1.2 Hz, 1H).

Synthesis of 2-vinylbenzaldehyde oxime 6.37[12]

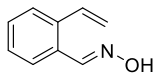

The product **6.37** was synthesized following a modified literature procedure. In a 10 mL sealed monowave tube were dissolved 2-vinylbenzaldehyde **6.36** (132 mg, 1.00 mmol), $NH_2OH{\cdot}HCl$ (104 mg, 1.50 mmol, 1.5 equiv.) and AcONa (123 mg, 1.50 mmol) in EtOH (1 mL) and the mixture was heated at 120°C for 10 mn in MonoWave 50. The reaction mixture was diluted with EtOAc and water. The aqueous layer was extracted with ethyl acetate. The combined organic layer was dried over $MgSO_4$, filtered and concentrated under vacuum to afford 2-vinylbenzaldehyde oxime in quantitative yield.

^{1}H NMR (300 MHz, $CDCl_3$) δ 8.46 (s, 1H), 7.64 (dd, J = 7.7, 1.5 Hz, 1H), 7.51 – 7.44 (m, 1H), 7.40 – 7.26 (m, 2H), 7.06 (dd, J = 17.4, 11.0 Hz, 1H), 5.63 (dd, J = 17.3, 1.2 Hz, 1H), 5.41 (dd, J = 11.0, 1.2 Hz, 1H).

Synthesis of N-methyl-1-(2-vinylphenyl)methanamine 6.39[13]

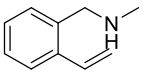

The compound **6.39** was synthesized following a modified literature procedure. 2-vinylbenzaldehyde **6.36** (661 mg, 5.00 mmol) was dissolved in MeOH (5 mL) then methylamine (3.75 mL, 2M in MeOH, 7.5 mmol, 1.5 equiv.) was added at rt via syringe. The reaction was stirred at rt for 1 h and $NaBH_4$ (378 mg, 10.0 mmol, 2 equiv.) was added portionwise at 0°C. The reaction was allowed to warm to rt and stirred for 2 h. Water was added and the aqueous layer was extracted with DCM. The combined organics layers were washed with brine, dried over $MgSO_4$ and concentrated under vacuum to afford **6.39** as a yellow liquid (565 mg, 77% yield). The product was use without further purification.

^{1}H NMR (300 MHz, $CDCl_3$) δ 7.58 – 7.48 (m, 1H), 7.40 – 7.17 (m, 3H), 7.06 (dd, J = 17.4, 11.0 Hz, 1H), 5.76 – 5.62 (m, 1H), 5.41 – 5.27 (m, 1H), 3.79 (s, 2H), 2.47 (s, 3H).

Synthesis of 2-(2-bromophenyl)ethan-1-amine 6.41[14]

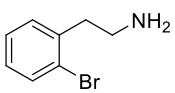

The compound **6.41** was synthesized following a literature procedure. To a solution of $AlCl_3$ (1.733 g, 13.00 mmol, 1.3 equiv.)

in Et_2O (40 mL) was added $LiAlH_4$ (759.0 mg, 20.00 mmol, 2 equiv.) at 0°C and was stirred at this temperature for 10 mn. 1-Bromo-2-cyanomethylbenzene (1.961 g, 1.30 mL, 10.00 mmol) was diluted in Et_2O (5 mL), added to the mixture and was stirred at rt for 16 h. The reaction was quenched with ice water and diluted with water and acidified with fuming H_2SO_4. Layers were separated and the aqueous layer was basified with NaOH (2N) until pH=14. The aqueous layer was extracted three times with Et_2O. The combined organic layers were washed with brine, dried over MgSO4, filtered, and concentrated under reduced pressure to afford the 2-(2-bromophenyl)ethan-1-amine as a yellow oil (1.9 g, 95% yield).

^1H NMR (300 MHz, $CDCl_3$) δ 7.59 – 7.50 (m, 1H), 7.29 – 7.18 (m, 2H), 7.07 (ddd, J = 8.0, 5.5, 3.7 Hz, 1H), 3.03 – 2.94 (m, 2H), 2.94 – 2.83 (m, 2H), 1.38 (s, 2H).

Synthesis of 2-(2-vinylphenyl)ethan-1-amine 6.42[15]

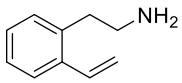

The substrate **6.42** was synthesized following a modified literature procedure. In a 10 mL sealed monowave tube were dissolved 2-(2-bromophenyl)ethan-1-amine **6.41** (400 mg, 2.00 mmol) and $Pd(PPh_3)_4$ (11.6 mg, 10.0 µmol, 0.005 equiv.) in degassed DME (4 mL) and stirred 10 mn at rt under argon. K_2CO_3 (276 mg, 2.00 mmol, 1 equiv.), degassed H_2O (1.5 mL) and vinylboronic anhydride pyridine complex (481 mg, 2.00 mmol, 1 equiv.) were added and the mixture was heated at 150°C for 30 mn in MonoWave 50. Conversion was checked by GCMS. The reaction mixture was cooled to rt and washed with NaOH to remove the boronic acid. Aqueous layer was extracted with Et_2O. The combined organic layers were washed with brine, dried over $MgSO_4$, filtered, and concentrated under reduced pressure. The residue was purified by column chromatography (silica gel, AcOEt/NEt_3 99:1 to 90:10) to afford the product (yellow oil, 97 mg, 33% yield).

2nd procedure: Synthesized following a modified literature procedure. In a 10 mL sealed monowave tube were dissolved 2-(2-bromophenyl)ethan-1-amine **6.41** (1.00 g, 5.00 mmol) and **Pd-PEPPSI** analogue (**6.43**) (28.1 mg, 50.0 µmol, 0.01 equiv.) in

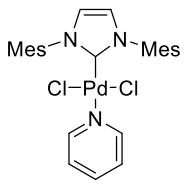

4.43

degassed iPrOH (2 mL) and stirred 10 mn at rt under argon. KOH (337 mg, 6.00 mmol, 1.2 equiv.), degassed H_2O (2 mL) and vinylboronic anhydride pyridine complex (1.20 g, 5.00 mmol, 1 equiv.) were added and the mixture was heated at 110°C for 4 h in MonoWave 50. Conversion was checked by GCMS. The reaction mixture was cooled to rt and washed with NaOH to remove the boronic acid. Aqueous layer was extracted with Et_2O. The combined organic layers were washed with brine, dried over MgSO4, filtered, and concentrated under reduced pressure. The residue was purified by column chromatography (silica gel, AcOEt/NEt_3 99:1 to 90:10) to afford the product (yellow oil, 500 mg, 68% yield).

^{1}H NMR (300 MHz, $CDCl_3$) δ 7.54 – 7.45 (m, 1H), 7.34 – 7.12 (m, 3H), 7.01 (dd, J = 17.4, 10.9 Hz, 1H), 5.65 (dd, J = 17.3, 1.4 Hz, 1H), 5.30 (dd, J = 11.0, 1.4 Hz, 1H), 2.96 – 2.79 (m, 4H), 1.38 – 1.25 (m, 3H).

General Procedure for Hydroaminomethylation Experiments with substrates 6.33, **6.34** and **6.39**.

Most experiments were performed following the same procedure in a 90 mL stainless-steel autoclave purchased from TOP Industrie. The gas mixture was previously prepared in the desired CO/H_2 ratio. The alkene (0.50 mmol) solubilized in 10 mL of solvent was introduced in the reactor, followed by the rhodium complex and the ligand solubilized in 10 mL of solvent. The closed reactor was then purged three times with the CO/H_2 gas mixture. The reaction mixture was placed under the desired pressure and temperature with a 1000 rpm stirring rate. The experiment was running under a continuous feed of gas mixture. The autoclave was cooled to room temperature and then slowly depressurized. The crude mixture was analyzed by gas chromatography and NMR spectroscopy.

General Procedure for Hydroaminomethylation Experiment with substrate 6.42.

The Rh-catalyzed hydroaminomethylation reaction of **6.42** was set up in a CAT24 autoclave from HEL Inc. and stirred with a Teflon-coated magnetic stir bar.

A 2 mL glassware reactor tube was charged with **6.42** (0.20 mmol), [Rh(acac)$(CO)_2$] (1 mol%) and **L** (1.2-4 mol%) in a mixture of toluene (0.2 mL) and MeTHF (0.2 mL). $CsCO_3$ (10 mol%) was added in tests 1-6. The reaction tube was placed in the reactor, which was pressurized at 80 bar ($CO:H_2$=1) heated to 100°C and left stirring at 900 rpm for 16 h. The reaction was stopped after the desired time by cooling the reactor in an ice bath for 20 min followed by venting of the system.

6.5. References

[1] (a) Kouznetsov, V.; Palma, A.; Ewert, C. Synthesis and Applicability of Partially Reduced 2-Benzazepines. *Curr. Org. Chem.* **2001**, *5*, 519-551. (b) Ansari A., Satalkar S., Patil V., Shete A. S., Kaur S.,Gupta A., Singh S., Raja M.,. Severance D. L, Bernales S., Chakravarty S., Hung D. T., Pham S. M., Herrera F. J., Rai R. Novel 3-methylindoline inhibitors of EZH2: Design, synthesis and SAR. *Bioorganic & Medicinal Chemistry Letters* **2017**, *27*, 217–222. (c) The chemistry and biology of isoquinoline alkaloids, Ed: Philipson J. D., Roberts M. F., Zenk M. H. Springer, Verlag Berlin Heilberg **1985**.

[2] Crozet, D.; Kefalidis, C. E.; Urrutigoïty, M.; Maron, L.; Kalck, P. Hydroaminomethylation of Styrene Catalyzed by Rhodium Complexes Containing Chiral Diphosphine Ligands and Mechanistic Studies: Why Is There a Lack of Asymmetric Induction? *ACS Catal.* **2014**, *4* (2), 435–447.

[3] Vieira, T. O.; Alper, H. Rhodium(I)-Catalyzed Hydroaminomethylation of 2-Isopropenylanilines as a Novel Route to 1,2,3,4-Tetrahydroquinolines. *Chem. Commun.* **2007**, 26, 2710–2711.

[4] Vieira, T. O.; Alper, H. An Efficient Three-Component One-Pot Approach to the Synthesis of 2,3,4,5-Tetrahydro-1H-2-Benzazepines by Means of Rhodium-Catalyzed Hydroaminomethylation. *Org. Lett.* **2008**, *10* (3), 485–487.

[5] Okuro, K.; Alper, H. Ionic Diamine Rhodium Complex Catalyzed Hydroaminomethylation of 2-Allylanilines. *Tetrahedron Lett.* **2010**, *51* (38), 4959–4961.

[6] Hochberger-Roa, F.; García-Ríos, P. H.; López-Cortés, J. G.; Ortega-Alfaro, M. C.; Daran, J.-C.; Gouygou, M.; Urrutigoïty, M. Interrupted Intramolecular Hydroaminomethylation of N-Protected-2-Vinyl Anilines: Novel Access to 3-Substitued Indoles or Indoline-2-Ols. *Molecules* **2022**, *27* (3), 1074.

[7] (a) Kuwano, R.; Kaneda, K.; Ito, T.; Sato, K.; Kurokawa, T.; Ito, Y. Highly Enantioselective Synthesis of Chiral 3-Substituted Indolines by Catalytic Asymmetric Hydrogenation of Indoles. *Org. Lett.* **2004**, *6* (13), 2213–2215. (b) Kuwano, R.; Kashiwabara, M.; Sato, K.; Ito, T.; Kaneda, K.; Ito, Y. Catalytic Asymmetric Hydrogenation of Indoles Using a Rhodium Complex with a Chiral Bisphosphine Ligand PhTRAP. *Tetrahedron Asymmetry* **2006**, *17* (4), 521–535. (c) Kuwano, R.; Sato, K.; Kurokawa, T.; Karube, D.; Ito, Y. Catalytic Asymmetric Hydrogenation of Heteroaromatic Compounds, Indoles. *J. Am. Chem. Soc.* **2000**, *122* (31), 7614–7615. (d) Kuwano, R.; Karube, D.; Ito, Y. Catalytic Asymmetric Hydrogenation of 1-Aza-2-Cycloalkene-2-Carboxylates Catalyzed by a Trans-Chelating Chiral Diphosphine PhTRAP-Rhodium Complex. *Tetrahedron Lett.* **1999**, *40*, 9045–9049.

[8] Wen, J.; Fan, X.; Tan, R.; Chien, H. C.; Zhou, Q.; Chung, L. W.; Zhang, X. Brønsted-Acid-Promoted Rh-Catalyzed Asymmetric Hydrogenation of N-Unprotected Indoles: A Cocatalysis of Transition Metal and Anion Binding. *Org. Lett.* **2018**, *20* (8), 2143–2147. (b) Li, P.; Huang, Y.; Hu, X.; Dong, X. Q.; Zhang, X.

Access to Chiral Seven-Member Cyclic Amines via Rh-Catalyzed Asymmetric Hydrogenation. *Org. Lett.* **2017**, *19* (14), 3855–3858.

[9] Routaboul, L.; Buch, C.; Klein, H.; Jackstell, R.; Beller, M. An Improved Protocol for the Selective Hydroaminomethylation of Arylethylenes. *Tetrahedron Lett.* **2005**, *46* (43), 7401–7405.

[10] Omae, I. Transition Metal-Catalyzed Cyclocarbonylation in Organic Synthesis. *Coord. Chem. Rev.* **2011**, *255* (1–2), 139–160.

[11] Kleine, T.; Bergander, K.; Fröhlich, R.; Wibbeling, B.; Würthwein, E.-U. Ring-Closure Reactions of 1,2-Diaza-4,5-Benzoheptatrienyl Metal Compounds: Experiment and Theory. *J. Org. Chem.* **2011**, *76* (7), 1979–1991.

[12] Kubo, T.; Katoh, C.; Yamada, K.; Okano, K.; Tokuyama, H.; Fukuyama, T. A Mild Inter- and Intramolecular Amination of Aryl Halides with a Combination of CuI and CsOAc. *Tetrahedron* **2008**, *64* (49), 11230–11236.

[13] Tomioka, K.; Ogata, T.; Kimachi, T.; Yamada, K.; Yamamoto, Y. Catalytic Asymmetric Synthesis of (S)-Laudanosine by Hydroamination. *Heterocycles* **2012**, *86* (1), 469-485.

[14] Kubo, T.; Katoh, C.; Yamada, K.; Okano, K.; Tokuyama, H.; Fukuyama, T. A Mild Inter- and Intramolecular Amination of Aryl Halides with a Combination of CuI and CsOAc. *Tetrahedron* **2008**, *64* (49), 11230–11236.

[15] Bennasar, M. L.; Roca, T.; Monerris, M.; García-Díaz, D. Sequential N-Acylamide Methylenation-Enamide Ring-Closing Metathesis: Construction of Benzo-Fused Nitrogen Heterocycles. *J. Org. Chem.* **2006**, *71* (18), 7028–7034.

CHAPTER VII

ITALMATCH STAY: LIGAND SCALE-UP

Italmatch Chemicals

7.1. Introduction

Italmatch Chemicals is a leading global chemical group, specializing in performance additives and solutions for water treatment & lubricants, oil & gas and plastics, flame retardants and produces a wide product range able to fulfill the requirements of the most demanding applications, including personal care.

The group operates through 19 manufacturing plants and seven state-of-the-art innovation centers. It employs approximately 1,100 workers and generates around ~862 million euros of sales. My stay was carried out at the Arese technical and R&D Center of excellence whose team is part of the advanced water solutions business unit, which deals with the additives for industrial water treatment & process, desalination, geothermal, mining, personal care and HI&I markets. The main focuses of Arese laboratory are critical elements recovery, energy reduction, near zero waste industrial processes, catalytic processes, and sustainable chemical specialties products. The laboratory was hosting 3 PhD students from the EU project CCIMC for a 3 month secondment.

7.1.1. Phosphorus compound synthesis in continuous flow

PCl_3 and $POCl_3$ are affordable and easily accessible, enhancing their practicality as primary raw materials for various phosphorus-containing compounds. However, their high electrophilicity leads to exceedingly exothermic reactions and a tendency for overreactions. Furthermore, there is a notable operational risk associated with these reactions.

Micro-flow processes exhibit several advantages over conventional batch processes: 1) the ability to precisely regulate reaction times through efficient solution mixing; 2) precise control of reaction temperatures facilitated by efficient heat exchange due to reactors' substantial surface-to-volume ratio 3) safe utilization of explosive and toxic substances, as micro-reactors confine small amounts of hazardous compounds; and 4) a numbering-up strategy or straightforward extension of pumping time

enabling a reproducible process scale-up.[1] In the substitution reaction involving PCl_3 and $POCl_3$ with a nucleophile, a stoichiometric amount of HCl is formed. Its trapping by a base usually forms an insoluble salt that is not suitable for implementation in microflow processes. To overcome this issue, the strategy developed is to use a base that would form an ionic liquid upon protonation (Figure 1).[2] Typically, N-methylimidazole can be used for the deprotonation of oxoniums generated in the substitutions with alcohols. More potent bases like tributylamine and DBU can be used for deprotonation of ammoniums to replace the classic triethylamine.

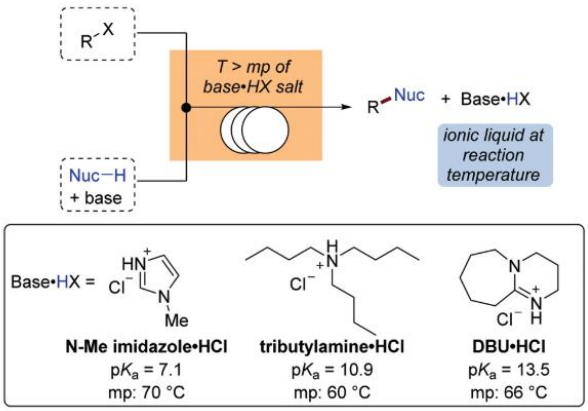

Figure 1. Ionic liquid syntheses under flow conditions[2]

The synthesis of binaphthylphosphoric acid **7.1** was reported using syringe pumps by Nagaki and co-workers (Figure 2).[3] A solution of $POCl_3$ in acetone (4 mL/mn) was tested in a T mixer with DMAP (1 equiv.) in acetone (4 mL/mn) at 20°C for only 2.9 seconds to activate the phosphoryl chloride. The resulting mixture was reacted with a solution of BINOL (1 equiv.) and tributylamine (2 equiv.) in acetone (2mL/mn) at 20°C for 2.4 seconds resulting the product **7.1** in 74% yield. Triarylphosphites were also synthesized in a range of 89-91% yield using the same methodology.

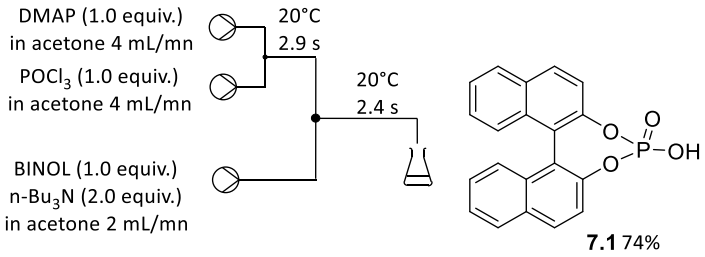

Figure 2. Continuous flow synthesis of binaphthylphosphoric acid

Continuous flow synthesis of triphenylphosphites was reported using syringe pumps by reacting a solution of phenol (3 equiv.) and triethylamine (3.3 equiv.) in chloroform with a solution of PCl_3 (1 equiv.) in chloroform.[4] The two fluids were mixed in a T mixer before entering a 5.0 mL microreactor at 70°C for 20 seconds. After aqueous work-up and purification, the triphenylphosphites were obtained in up to 92% yield. Indeed, chloroform was able to solubilize the hydrochloride salts of NEt_3, DMAP, pyridine, DIPEA, imidazole or NMI enabling the reaction in continuous flow.

Recently, the continuous flow preparation of cyclic phosphate was reported by Monbaliu and co-workers (Figure 3).[5] Along the synthesis, the formation of cyclic chlorophosphite was of major interest. The reaction conditions were optimized using neat ethylene glycol and a solution of PCl_3 in MeTHF (3M). Online ^{31}P monitoring confirmed the full conversion of PCl_3 in one minute at room temperature. 8 different ethylene glycol based chlorophosphite were produced without the use of a base in 44-85% yield. However, when the substrate was more congested, the formation rate was diminished thus a base was added. Thus, the substrates were dissolved in a mixture of dry acetonitrile (1-2M) and a base (NMI or DBU, 2-2.2 equiv.) and reacted with a solution of PCl_3 in dry acetonitrile (1-2M, 1 equiv.) for 1 min at room temperature. The methodology afforded the products **7.2**-**7.6** in up to 83% yield after purification.

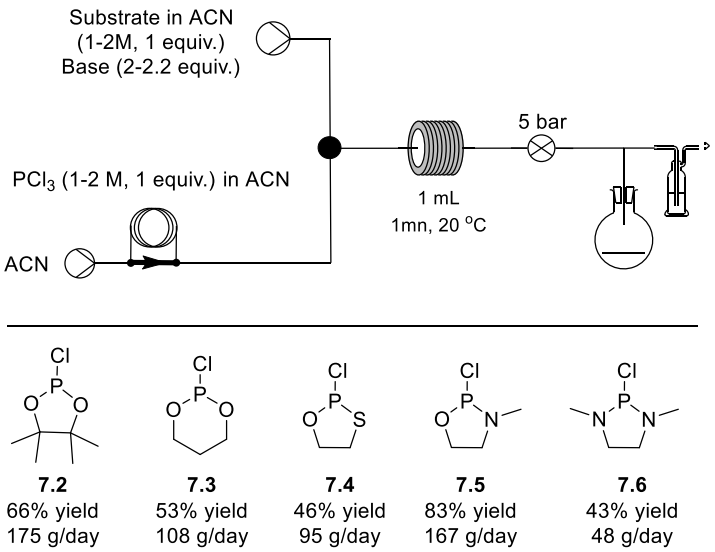

Figure 3. Continuous flow synthesis of chlorophosphite

Phosphorus compounds synthesis using $POCl_3$ or PCl_3 in continuous flow remains recent and scarcely studied. However, the results reported so far are promising and online ^{31}P monitoring make it an efficient process to study in continuous flow. Chlorophosphites are not end-products and often further react with alcohols or amines to yield phosphite or phosphoramidite ligands. In the next sections, the synthesis of chiral amino-alcohols is described.

7.1.2. Betti based scaffold synthesis

As 1,3 amino alcohols were recently reported as efficient ligand backbones for AHF and asymmetric HAM, a suitable synthesis of those chiral scaffolds would be of interest. Among the synthesis of 1,3 amino alcohols, the so-called Betti bases were vastly studied. These amino alcohols can be easily synthesized in a one-pot manner from 2-naphthol **7.7**, amines **7.8** and arylaldehydes **7.9** (Scheme 1).[6] The reaction proceeded via the *in-situ* formation of an imine by the condensation of the amine and the aldehyde. The imine further reacted with 2-naphthol yielding the Betti bases **7.10**. The variety of aldehydes and amines that can be used make it a good candidate for a ligand family.

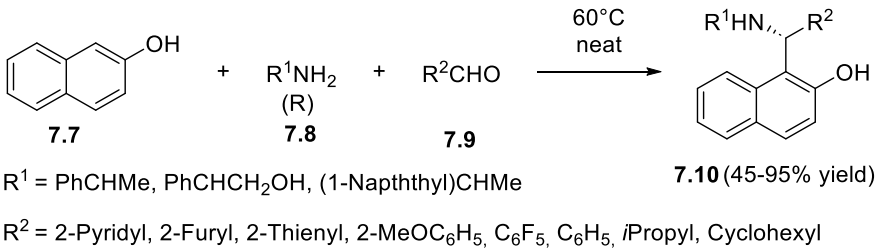

Scheme 1. Synthesis of chiral Betti base

Phosphorus based ligands derived from Betti bases (Figure 4), were applied in asymmetric transformations such as Pd-catalyzed asymmetric hydrosilylation[7] (**7.11**) and asymmetric allylic substitution[8] (**7.14**) as well as Rh-catalyzed asymmetric hydrogenation[8,9] (**7.13**, **7.14**) and asymmetric hydroformylation[10] (**7.12**).

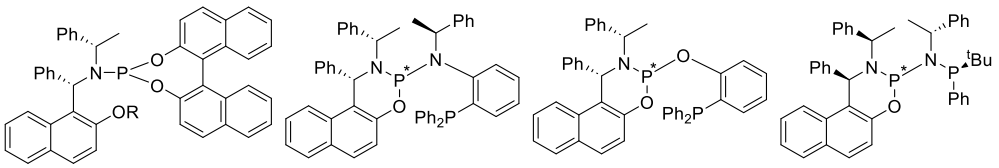

Figure 4. Betti base ligands

Based on previous results from our group[11], the synthesis of sugar-based 1,3 amino alcohol backbone as well as Betti base syntheses were carried out. Attempts to convert these molecules into phosphorus-based ligands were also studied under batch and continuous flow conditions.

7.2. Results and discussion

The first objective of the stay was to study the scale-up of the sugar-based 1,3 amino alcohol backbone **7.19** since the corresponding phosphite phosphoramidite ligand was previously used for Rh-catalyzed asymmetric HAM.

7.2.1. Scale-up of amino-alcohol backbone

The lab scale synthetic route[11] (Scheme 2) of the target amino alcohol **7.19** was reported in four steps with an overall yield of 33%. It was synthesized from the commercially available *D*-xylose **7.15** by first protecting the 4 hydroxyls groups into

2 ketals with acetone and catalyzed by iodine at room temperature for 16 h. The diketal **7.16** was formed in 96% yield. Then, the selective deprotection of the 6-membered ring ketal was realized by reacting **7.16** with diluted H_2SO_4 (0.8%) in methanol for 16 h at room temperature followed by a basic treatment with barium carbonate affording the diol **7.17** in 92% yield. The primary hydroxyl of **7.17** was selectively reacted with 4-toluenesulfonyl chloride in pyridine and dichloromethane at room temperature for 16 h. The activated hydroxyl was obtained in 60% yield. The last step of the backbone formation consisted in the substitution of the tosyl by cyclohexylamine. The electrophile **7.18** was reacted with an excess of cyclohexylamine in refluxing isopropanol for 24 h to produce **7.19** in 63% yielding after column chromatography. Although the process afforded **7.19** in a good overall yield, it was not suitable for industrial scale-up because of the use of expensive (iodine, $BaCO_3$), toxic (pyridine, dichloromethane) chemicals and the last costly purification step.

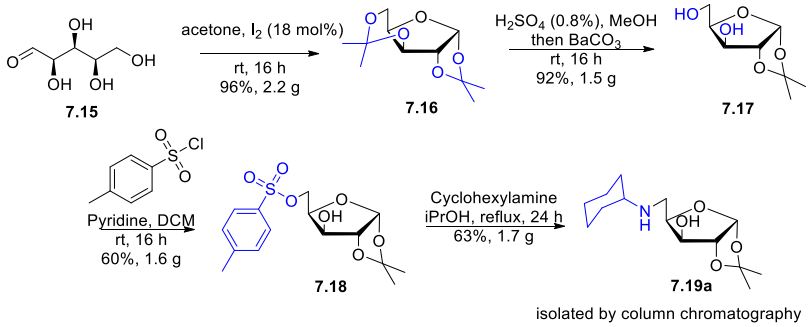

Scheme 2. Original synthetic route for 7.19

The lab scale-up was realized in three steps with an overall yield of 26%. The first step was the synthesis of the selective monoprotected ketal **7.17** (Scheme 3). *D*-xylose **7.15** was reacted with concentrated sulfuric acid in acetone for 1 h at room temperature. Then, the selective monodeprotection of the ketal was realized *in situ* by adding potassium carbonate and stirred for 3 h. Then, K_2CO_3 was added until

neutral pH was reached, yielding **7.17** in 90% after work-up and evaporation of the aqueous phase.

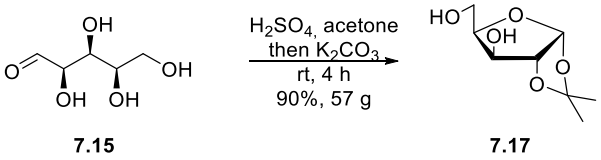

7.15 **7.17**

Scheme 3. Synthesis of the diol 7.17 in one step

Activation of the primary alcohol was achieved with a slightly modified procedure. The diol **7.17** was reacted with 4-toluenesulfonyl chloride in triethylamine and tetrahydrofuran at room temperature for 16 h (Scheme 4). The product **7.18** was obtained in a similar 57% yield after precipitation in cold diethyl ether. The system NEt_3/THF was preferred to the pyridine/DCM system due to safety hazard and waste management.

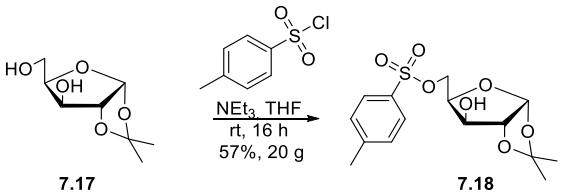

7.17 **7.18**

Scheme 4. Synthesis of tosylated product 7.18

Finally, the amino alcohol **7.19a** was synthesized by reacting **7.18** with an excess of cyclohexylamine (4 equiv.) in 1-butanol at 110°C for 3 h 30 (Scheme 5). The product was obtained in 50% yield after acid base work up. Changing isopropanol to 1-butanol drastically reduced the reaction time as further heating was possible. The final aqueous treatment avoided the purification by column chromatography.

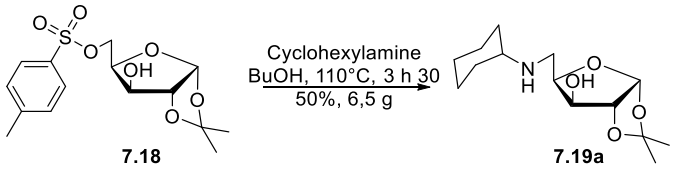

7.18 **7.19a**

Scheme 5. Synthesis of the amino alcohol 7.19a

This methodology was also employed for the synthesis of new amino alcohol backbones bearing an extra coordinating group (**7.19b**, **7.19c** or a bulky substituent

7.19d). These backbones will be applied in the synthesis of new chiral ligands in near future.

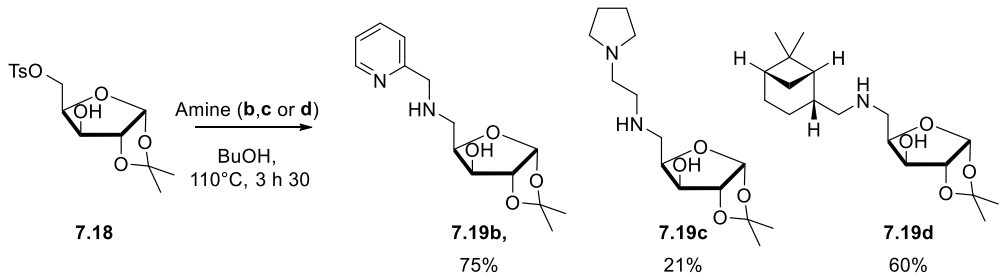

Scheme 6. Synthesis of new chiral amino alcohol backbones 7.19b-d from tosyl 7.18

The last step to synthesize the ligand was realized via the *in-situ* N-methylpyrrolidone catalyzed formation of the phosphochloridite **7.21** from (*S*)-BINOL **7.20** in refluxing PCl_3 for 15 min. A solution of the amino alcohol **7.19** in triethylamine and toluene was added onto a solution of **7.21** in triethylamine and toluene and was stirred for 16 h at 50 °C. The ligand **7.22** was isolated after filtration of the tryethylamine hydrochloride salt and column chromatography on silica gel. The main problems for the scale-up of the ligand synthesis are the use of PCl_3 as solvent and the purification step by column chromatography.

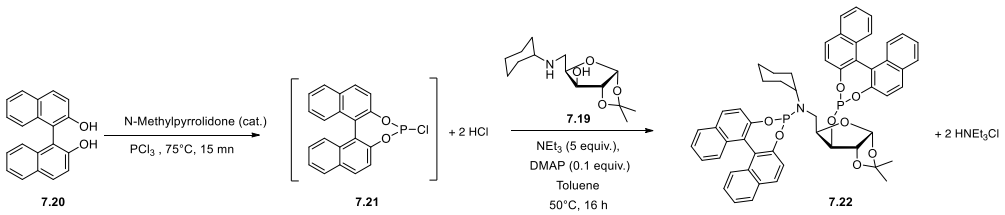

Scheme 7. Batch synthesis of chiral ligand 7.22

The scale-up synthesis of the backbone was achieved by decreasing the overall reaction time by 3 and removing the most hazardous chemicals from the process. Moreover, the three step synthesis yielded the product without the need for column chromatography. In the next section, attempts to form chlorophosphite intermediates without the need for an excess of PCl_3 are described.

7.2.2. Synthesis of chlorophosphite in continuous flow

To study the synthesis of the chlorophosphite intermediate, the use of flow chemistry was considered as a safe and industrially viable pathway. Unfortunately, the batch procedure could not be directly applied in flow due to the formation of triethylamine hydrochloride salt in the media. Chloroform could have been considered to solubilize the salt but was not ideal from an industrial point of view. The second option was to substitute triethylamine with a base that can form ionic liquids. Since Monbaliu and co-workers reported that acetonitrile can solubilize ionic liquids such as N-methylimidazole (NMI) hydrochloride or 1,8-diazabicyclo[5,4,0]undec-7-ene (DBU) hydrochloride, [5] our system was tested using this methodology. Pinacol and NMI were dissolved in acetonitrile (2M) and reacted with PCl_3 in acetonitrile (2M) in a T-mixer. After 1 min residence time, 96% of the phosphorus trichloride was converted into the chlorophosphite (**7.24**, 44%) and the corresponding oxide (**7.25**, 56%).

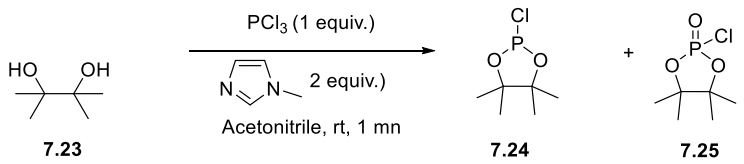

7.23 **7.24** **7.25**

Scheme 8. Synthesis of pinacol chlorophosphite 7.24 under flow conditions.

Then, the conditions were adapted for the synthesis of **7.28** using 1M solution of PCl_3, 2M solution of the **7.26** and NMI in acetonitrile. Complete conversion of PCl_3 was observed in one minute with 79% selectivity towards the monosubstituted product **7.27**. An increase of the residence time to 2.5 min reduced the selectivity to 75% of **7.27**. It was concluded that **7.28** was more difficult to synthesize than **7.24** due to the increased steric hindrance in ortho positions. We then focused on the synthesis of the biphenol based chlorophosphite **7.30**.

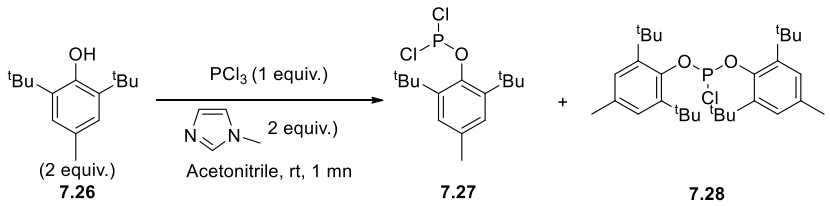

Scheme 9. Synthesis of 7.27 and 7.28 in flow.

Due to the higher cost of (S) or (R)-BINOL, initial experiments were conducted with biphenol **7.29** as a model. The reaction was set in syringe pumps, carried out with acetonitrile and a base and samples were rapidly analyzed by ^{31}P NMR. Initially, two equivalents of NMI were engaged with high molarity (2M). In one minute of residence time, 73% of the PCl_3 was converted with only 14% selectivity towards the chlorophosphite **7.30** (entry 1). Under these conditions, the bisphosphite **7.31** was obtained in 81% selectivity. Then, the concentration was divided by 10 (entry 2) to avoid the formation of the bisphosphite **7.31**. This resulted in the formation of a large amount of the oxidation product **7.32** along with the bisphosphite **7.31**. The base was then removed while maintaining the same concentration (entry 3). In this case the formation of **7.31** was not observed but a large amount of **7.32** was detected. Interestingly, increasing the concentration to 1M or 2M without the use of a base (entry 4 and 5) led to a higher selectivity towards **7.30**. However, increasing the residence time to 2.5 min did not increase the conversion or selectivity (entry 6). In contrast, when NMI was used in substoichiometric amount with 1M concentration, an increase of the conversion to 92% and selectivity to 64% of **7.30** was observed. The only side product formed the oxidized form **7.32** (entry 7). With 0.2 equiv. of NMI, full conversion of phosphorus trichloride was observed (entry 8). When DBU (0.3 equiv.) was used as the base, 93% conversion was reached along with 74% selectivity towards the chlorophosphite **7.30**. The presence of a base therefore had a clear influence on the conversion and selectivity of this reaction. NMI was preferred due to its lower cost but an essay with DBU gave slightly improved result.

Table 1. Flow synthesis of chlorophosphite 7.30

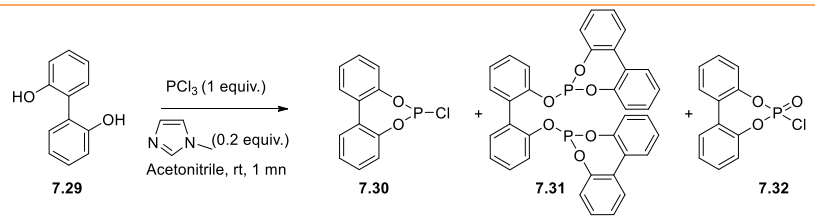

Entry	Conv. (%)	Selectivity	Base	Equivalent	Molarity
1	73	14	NMI	2	2M
2	100	0	NMI	2	0.2M
3	100	11	no		0.2M
4	75	30	no		1M
5	73	28	no		2M
6[a]	73	30	no		1M
7	92	64	NMI	0,1	1M
8	100	58	NMI	0,2	1M
9	93	74	DBU	0,3	1M

[a] residence time 2.5 min

The promising results obtained in the synthesis of **7.30** prompted us to test the system using BINOL as reagent. Full conversion of PCl_3 was observed in one minute but the selectivity towards **7.21** was only 17%. The main product observed was **7.33** (60%) and the hydrolyzed form (24%). This decrease in selectivity can be possibly explained by the increased water content of acetonitrile along the time of the stay, degrading the formed chlorophosphite.

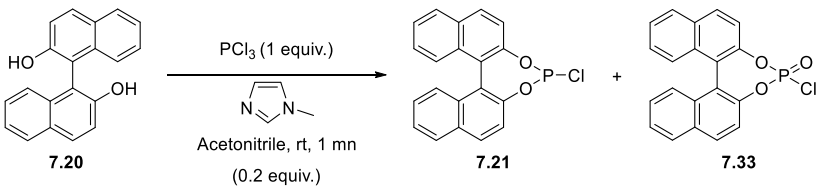

Scheme 10. Flow synthesis of binaphtholchlorophosphite 7.34

While these results were promising to reduce the amount of PCl_3 engaged in the reaction, the chlorophosphite intermediate must react immediately to prevent hydrolysis and oxidation. In the following section, the formation of Betti-base and further attempts for their transformations into ligands are described.

7.2.3. Synthesis and reactions with the Betti-base **7.36**

The Betti base **7.36** was synthesized according to a reported procedure.[12] Benzaldehyde **7.34** was mixed with the chiral amine **7.35** (R) or (S) along with the 2-naphthol **7.7** and stirred overnight at 60°C. The product was obtained after precipitation in ethanol and recrystallisation from AcOEt/Heptane yielding (R,R)-**7.36** in 82% and (S,S)-**7.36** in 54%.

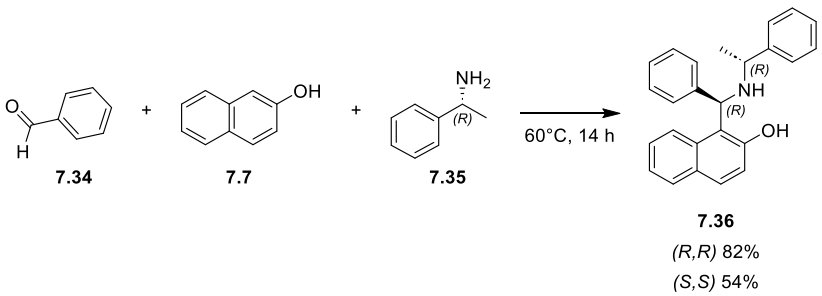

7.34 **7.7** **7.35**

7.36
(R,R) 82%
(S,S) 54%

Scheme 11. Betti base 7.36 synthesis.

It was then attempted to substitute both O and N atoms of the Betti-base using preformed phosphochloridites intermediates. The biphenol chlorophosphites **7.30** solution in acetonitrile (0.5 M) was synthesized using the syringe pumps and reintroduced in another syringe to react with a solution of Betti-base **7.36** and NMI (2 equiv.) in acetonitrile (0.25 M) for 1 min at room temperature. Full conversion of the chlorophosphite was observed but the only products detected by ^{31}P NMR were corresponding to hydrolyzed and oxidized products. The system suffered from exposure to air and moisture upon the second reaction with the amino alcohol backbone.

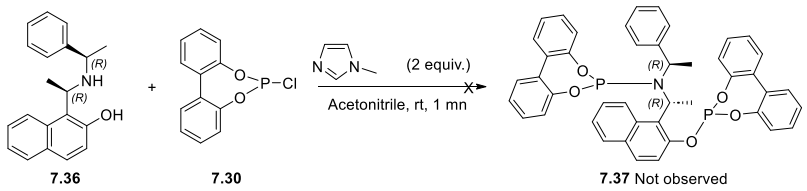

Scheme 12. Ateempt of ligand formation in flow

At this stage, batch procedure was envisaged to avoid any contamination for the conversion of Betti base into a phosphite phosphoramidite ligand. Biphenol chlorophosphite **7.30** was synthesized according to reported procedure. Biphenol was dissolved in an excess of PCl_3 (10 equiv.) and NMP (cat.) and stirred at reflux for 5 min. The **7.30** solution was concentrated under vacuum and redissolved in toluene and triethylamine. The Betti base solution in a mixture of toluene and triethylamine was added at 0°C and stirred at room temperature overnight. The mixture was analyzed by ^{31}P NMR. A broad peak at 145 ppm was formed and the **7.30** peak at 178 ppm was still observed in lower quantity. After column chromatography (dry silica, dry toluene, 2% dry NEt_3), it was observed that a monosubstitution occurred on the O atom since the NH peak was detected by ^{1}H NMR leading to product **7.38**. The free amino-alcohol **7.36** form was observed as the major product (65% vs 35% of phosphite **7.38**).

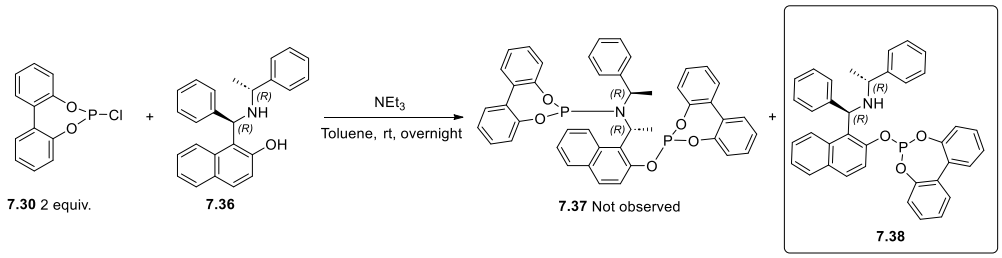

Scheme 13. Batch synthesis of biphenol Betti ligand 7.38

When the Betti base **7.36** was tested with BINOL chlorophosphite **7.20** under the same conditions, the phosphite was obtained after column chromatography. No phenol peak was detected by ^{1}H NMR in the crude sample whereas it appeared after

column chromatography (39% **7.36** vs 61% phosphite **7.39**) demonstrating partial decomposition upon purification.

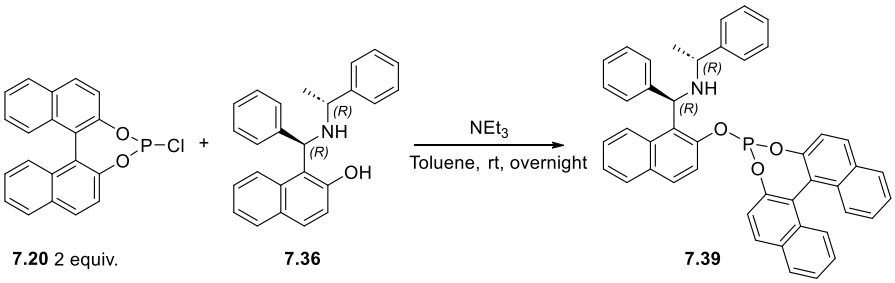

Scheme 14. Batch synthesis of binaphthol Betti ligand 7.39

Finally, the Betti base was reacted with the bulkier chlorophosphite **7.40** under the same conditions. The phosphite was obtained in 98% yield after column chromatography. No decomposition was observed demonstrating the higher stability of the substituted phenol. However, no substitution on N atom was observed in any stage, even when nBuLi was used as a base.

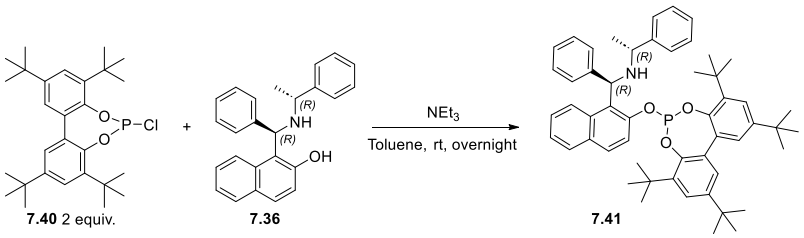

Scheme 15. Batch synthesis of congested biphenol Betti ligand 7.41

When the phosphite **7.41** was reacted with PPh_2Cl, the desired product was not detected and only the decomposition of **7.41** was observed (Scheme 16).

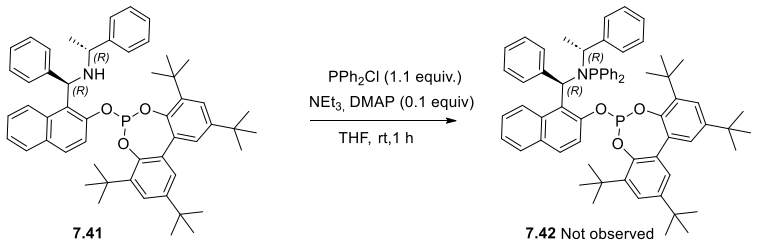

Scheme 16. Attempt of N substitution of 7.41 with PPh_2Cl

7.3. Conclusion

From the study described in this chapter, the following conclusions can be extracted:

- The synthesis of amino-alcohol backbone **7.19** was successfully scaled-up.
- A series of amino-alcohol backbones were synthesized using the intermediate **7.18**.
- Study on the continuous flow synthesis of chlorophosphites, notably **7.30** and **7.20**, was performed using syringe pumps. The optimal conditions included the use of diol solution with NMI (0.2 equiv.) in acetonitrile (1 M) and PCl_3 in acetonitrile (1 M) for 1 min at room temperature.
- The synthesis of the Betti base **7.36** was performed as well as attempts in functionalizing O and N atoms. However, only the O atom could be substituted, probably due to steric issues.

7.4. Experimental part

General considerations

All the reactions were carried out using Schlenk-line inert atmosphere techniques when necessary. Solvents were dried with activated molecular sieves. Commercially available reagents and solvents were purchased at the highest commercial quality from Sigma-Aldrich, Fluka, Alfa Aesar, Fluorochem, Strem and were used as received, without further purification.

^{1}H and $^{13}C\{^{1}H\}$ NMR spectra were recorded using a Bruker 300 MHz (300 and 100.6 MHz respectively). Chemical shift values (δ) are reported in ppm relative to TMS (^{1}H and $^{13}C\{^{1}H\}$) and coupling constants are reported in Hertz. The following abbreviations are used to indicate the multiplicity: s, singlet; d, doublet; t, triplet; q, quartet; quint, quintuplet; sext, sextuplet; sept, septet; oct, octet; m, multiplet; bs, broad signal. High-resolution mass spectra (HRMS) were recorded on a Bruker Daltonics Microtof Focus and/or Maxis Impact using ESI-TOF (electrospray ionization-time of flight). Samples were introduced to the mass spectrometer ion source by direct injection using a syringe pump and were externally calibrated using sodium formate. The instrument was operating in the positive ion mode. Reactions were monitored by TLC carried out on 0.25 mm E. Merck silica gel 60 F_{254} aluminum plates. Developed TLC plates were visualized under a short-wave UV lamp (254 nm) and by heating plates that were dipped in potassium permanganate. Flash column chromatography was carried out using forced flow of the indicated solvent, on Merck silica gel 60 (230-400 mesh).

Syringe pumps from Razel were calibrated before use.

(3aR,5R,6S,6aR)-5-(hydroxymethyl)-2,2-dimethyltetrahydrofuro[2,3-d][1,3]dioxol-6-ol (7.17)[13]

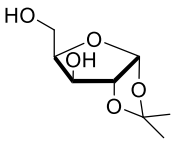

A three neck round bottom flask equipped with a mechanical stirrer was charged with D-xylose (50 g, 0.33 mol), acetone (1.2 L, 16 mol, 49 equiv.) and concentrated H_2SO_4 (95%, 52 mL, 0.96 mol, 2.8 equiv.). The media turned yellow and the suspension was stirred at rt for 1 h to reach full dissolution. The reaction mixture was cooled with an ice bath and an aqueous solution of K_2CO_3 (570 mL, 1.1 M, 0.63 mol, 1.89 equiv.) was slowly added. The white suspension was stirred at rt for 3 h then solid K_2CO_3 (44.5 g, 0.34 mol, 1.04 equiv.) was added portion wise at rt. The pH was adjusted to 7-8 with additional water. The suspension was filtered over Büchner and the liquid phase concentrated under vacuum to evaporate the excess of acetone. The residue was washed with EtOAc (x3) and the organic phase back extracted with water. The aqueous phases were concentrated under vacuum. The oil was then diluted with EtOAc and dried with $MgSO_4$, filtered and concentrated under vacuum to afford the product as a viscous oil (57 g, 90% yield).

^{1}H NMR (400 MHz, $CDCl_3$) δ 5.96 (d, *J* = 3.7 Hz, 1H), 4.50 (d, *J* = 3.7 Hz, 1H), 4.27 (d, *J* = 2.8 Hz, 1H), 4.18 – 4.10 (m, 1H), 3.97 (qd, *J* = 12.2, 4.2 Hz, 2H), 1.46 (s, 3H), 1.29 (s, 3H).

((3aR,5R,6S,6aR)-6-hydroxy-2,2-dimethyltetrahydrofuro[2,3-d][1,3]dioxol-5-yl)methyl 4-methylbenzenesulfonate (7.18)[14]

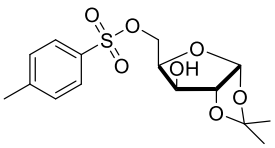

Protected xylose **7.17** (20 g, 105 mmol) was dissolved in THF (120 mL) and NEt_3 (29.3 mL, 210 mmol, 2 equiv.). Tosyl chloride (22.1 g, 116 mmol, 1.1 equiv.) in THF (26 mL) was slowly added at 0°C. The reaction mixture was stirred overnight at rt. EtOAc was added and the organic phase was washed with water, $NaHCO_3$ and brine. The organic phase was dried with $MgSO_4$, filtered and concentrated under vacuum to afford the crude product which was further dissolved

in Et_2O and stored at -20°C for 1 h. The precipitate was filtered to afford the product as a white solid (20.5 g, 57% yield).

^{1}H NMR (400 MHz, $CDCl_3$) δ 7.84 – 7.76 (m, 2H), 7.40 – 7.31 (m, 2H), 5.88 (d, *J* = 3.6 Hz, 1H), 4.51 (d, *J* = 3.6 Hz, 1H), 4.39 – 4.28 (m, 3H), 4.19 – 4.08 (m, 1H), 2.45 (s, 3H), 1.46 (s, 3H), 1.30 (s, 3H).

General procedure A: Nucleophilic substitution of 7.18 with amines a-d leading to amino alcohols 7.19a-d.

Tosyl **7.18** (1 equiv.) and amine a-d (4 equiv.) were dissolved in 1-butanol (2 mL/mmol). The reaction mixture was stirred at 110°C for 3h30 then it was concentrated under high vacuum.

(3aR,5R,6S,6aR)-5-((cyclohexylamino)methyl)-2,2-dimethyltetrahydrofuro[2,3-d][1,3]dioxol-6-ol (7.19a)

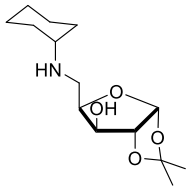

Tosyl **7.18** (16.6 g, 48.2 mmol) and cyclohexylamine (22.1 mL, 193 mmol, 4 equiv.) were dissolved in 1-butanol (96 mL). The reaction mixture was stirred at 110°C for 3h30 then it was concentrated under high vacuum. The residue was washed with $NaHCO_3$ and extracted with EtOAc. Organic phase was washed with water and brine then dried with Na_2SO_4 and concentrated to dryness. The residue was taken in EtOAc and filtered to recover a salt of amine and tosyl. The liquid phase was washed with HCl (1M, 90 mL) and basified to pH=12 with NaOH (5%) and a white precipitate formed. It was extracted with EtOAc, washed with brine and dry with Na_2SO_4 and concentrated to dryness to afford a yellow oil, that solidified at rt to give the pure product (6.5 g, 50 % yield) as a white solid.

^{1}H NMR (400 MHz, $CDCl_3$) δ 5.95 (d, *J* = 3.6 Hz, 1H), 4.47 (d, *J* = 3.7 Hz, 1H), 4.27 (d, *J* = 2.9 Hz, 1H), 4.20 (dt, *J* = 4.5, 2.3 Hz, 1H), 3.41 (dd, *J* = 12.9, 3.5 Hz, 1H), 2.99 (dd, *J* = 13.0, 1.5 Hz, 1H), 2.39 (tt, *J* = 10.2, 3.7 Hz, 1H), 1.93 – 1.80 (m, 2H), 1.70 (dt, *J* = 12.7, 4.1 Hz, 2H), 1.58 (dt, *J* = 12.1, 4.1 Hz, 1H), 1.47 (s, 3H), 1.31 (s, 3H), 1.26 – 0.98 (m, 5H).

(3aR,5R,6S,6aR)-2,2-dimethyl-5-(((pyridin-2-ylmethyl)amino)methyl)tetrahydrofuro[2,3-d][1,3]dioxol-6-ol (7.19b)

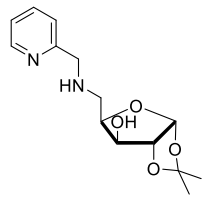

Synthesized according to general procedure A. Purification by flash chromatography (DCM/MeOH, 90/10) afforded the product as an orange oil (1.04 g, 75% yield).

^{1}H NMR (300 MHz, $CDCl_3$) δ 8.60 – 8.50 (m, 1H), 7.64 (td, J = 7.7, 1.8 Hz, 1H), 7.32 – 7.10 (m, 2H), 5.97 (d, J = 3.7 Hz, 1H), 4.50 (d, J = 3.6 Hz, 1H), 4.31 (d, J = 2.9 Hz, 1H), 4.25 – 4.16 (m, 1H), 3.92 (s, 2H), 3.38 (dd, J = 13.0, 4.0 Hz, 1H), 3.04 (dd, J = 13.0, 1.8 Hz, 1H), 1.47 (s, 3H), 1.31 (s, 3H).

^{13}C NMR (101 MHz, $CDCl_3$) δ 157.49, 149.40, 136.80, 122.48, 122.46, 111.49, 105.05, 85.89, 77.81, 77.10, 54.42, 47.81, 26.85, 26.16.

HRMS (ESI) for **$C_{14}H_{21}N_2O_4$**. Calculated **M:** 281.1501, **$[M+H^+]^+$:** 281.1496, found: 281.1490.

(3aR,5R,6S,6aR)-2,2-dimethyl-5-(((2-(pyrrolidin-1-yl)ethyl)amino)methyl)tetrahydrofuro[2,3-d][1,3]dioxol-6-ol (7.19c)

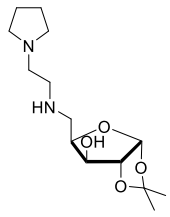

Synthesized according to general procedure A. Purification by flash chromatography (DCM/MeOH, 90/10) afforded the product as an orange oil (150 mg, 21% yield).

^{1}H NMR (401 MHz, $CDCl_3$) δ 6.02 – 5.92 (m, 1H), 4.52 (d, *J* = 3.7 Hz, 1H), 4.31 (d, *J* = 2.8 Hz, 1H), 4.21 (dt, *J* = 5.0, 2.5 Hz, 1H), 3.28 (dd, *J* = 12.9, 5.0 Hz, 1H), 3.11 (dd, *J* = 12.8, 2.3 Hz, 1H), 3.05 – 2.95 (m, 6H), 2.07 (s, 2H), 2.02 (s, 4H), 1.48 (s, 3H), 1.35 – 1.29 (m, 3H).

^{13}C NMR (101 MHz, $CDCl_3$) δ 111.56, 105.10, 85.93, 77.41, 54.87, 54.09, 48.02, 47.43, 26.94, 26.26, 23.47.

HRMS (ESI) for **$C_{14}H_{26}N_2O_4$**. Calculated **M:** 286.1892, **$[M+H^+]^+$:** 287.1970, found: 287.1955.

(3aR,5R,6S,6aR)-5-(((((1S,2R,5S)-6,6-dimethylbicyclo[3.1.1]heptan-2-yl)methyl)amino)methyl)-2,2-dimethyltetrahydrofuro[2,3-d][1,3]dioxol-6-ol (7.19d)

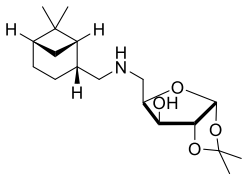

Synthesized according to general procedure A. Purification by flash chromatography (DCM/MeOH, 90/10) afforded the product as an orange oil (173 mg, 60% yield).

^{1}H NMR (300 MHz, $CDCl_3$) δ 5.95 (d, *J* = 3.7 Hz, 1H), 4.48 (d, *J* = 3.7 Hz, 1H), 4.28 (d, *J* = 2.9 Hz, 1H), 4.18 (td, *J* = 3.5, 1.3 Hz, 1H), 3.40 (dd, *J* = 13.0, 3.5 Hz, 1H), 2.92 (dd, *J* = 13.0, 1.5 Hz, 1H), 2.65 (dd, *J* = 11.3, 6.3 Hz, 1H), 2.56 – 2.45 (m, 1H), 2.39 – 2.27 (m, 2H), 2.00 – 1.77 (m, 7H), 1.47 (s, 3H), 1.31 (s, 3H), 1.16 (s, 3H), 0.95 (d, *J* = 1.1 Hz, 3H).

^{13}C NMR (101 MHz, $CDCl_3$) δ 111.84, 104.91, 85.57, 76.24, 76.06, 55.54, 47.22, 43.87, 41.06, 39.23, 38.57, 32.87, 27.83, 26.91, 26.22, 25.83, 23.15, 20.03.

HRMS (ESI) for **$C_{18}H_{31}NO_4$**. Calculated **M:** 325.2253, **$[M+H^+]^+$:** 326.2331, found: 326.2325.

Phosphite phosphoramidite ligand 7.22[11]

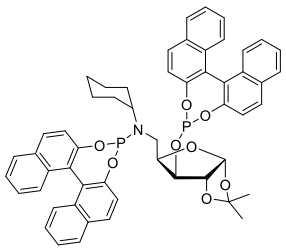

The product was synthesized according to a reported procedure.[11] PCl_3 (1.6 mL) was placed in an oven dried, argon purged, Schlenk tube followed by (S)-BINOL **7.20** (315 mg, 1.10 mmol) and NMP (3 drops). The reaction mixture was heated to 80°C for 15 min then it was concentrated under vacuum and dried azeotropically with toluene (3 x 1 mL) to remove any residual PCl_3 and give the chlorophosphite intermediate **7.21** as a white solid which was used in the next step without further purification. To a Schlenk flask containing a solution of chlorophosphite **7.21** in toluene (4 mL) and NEt_3 (0.35 mL, 2.5 mmol) was added a solution of **7.19** (136 mg, 0.50 mmol) and NEt_3 (0.35 mL, 2.5 mmol) in toluene (4 mL). DMAP The reaction mixture was then allowed to stir at room temperature overnight. The salts were filtered via a filtrating plate under an

inert atmosphere, and the filtrate was evaporated under vacuum yielding the crude product. The latter was purified by column chromatography on silica gel (previously dried at 130°C overnight in an oven) under an inert atmosphere, using dry toluene + 2% dry NEt_3. The product **7.22** was obtained as a white foamy solid (180 mg, 40% yield).

^{1}H NMR (401 MHz, CD_2Cl_2) δ 8.02 – 7.85 (m, 7H), 7.71 (dd, *J* = 8.2, 1.3 Hz, 1H), 7.56 – 7.38 (m, 6H), 7.35 – 7.03 (m, 10H), 5.59 (d, *J* = 3.7 Hz, 1H), 4.32 (dd, *J* = 8.6, 2.4 Hz, 1H), 4.15 – 4.07 (m, 2H), 3.27 (ddd, *J* = 15.2, 6.6, 4.1 Hz, 1H), 3.18 – 2.97 (m, 2H), 2.89 (ddd, *J* = 14.8, 8.2, 6.2 Hz, 1H), 2.07 (d, *J* = 12.5 Hz, 1H), 1.96 (d, *J* = 11.8 Hz, 1H), 1.79 (d, *J* = 14.1 Hz, 2H), 1.59 (d, *J* = 12.0 Hz, 5H), 1.36 (s, 3H), 1.11 (t, *J* = 10.4 Hz, 2H), 1.06 (s, 3H).

^{31}P NMR (162 MHz, CD_2Cl_2) δ 150.71 (d, *J* = 4.2 Hz), 147.95 (d, *J* = 4.2 Hz).

1-((S)-phenyl(((S)-1-phenylethyl)amino)methyl)naphthalen-2-ol (7.36)[15]

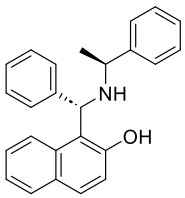

The product was synthesized according to a reported procedure. 2-naphthol (14.46 g, 100.3 mmol) was dissolved in benzaldehyde (12.2 mL, 120 mmol, 1.2 equiv.) and (R)-phenylethylamine (13.5 mL, 105 mmol, 1.05 equiv.). The mixture was stirred overnight at 60°C, leading to a solid material. EtOH was added and the mixture was grounded in a mortar. The resulting white solid was filtered and washed with EtOH. It was recrystallized from EtOAc (120 mL) and heptane (200 mL) to yield the pure enantiomer as colorless crystals (16.6 g, 47% yield).

(R,R) enantiomer was synthesized using (R)-phenylethylamine.

^{1}H NMR (300 MHz, $CDCl_3$) δ 13.71 (s, 1H), 7.76 (dd, J = 9.1, 3.3 Hz, 2H), 7.49 – 7.34 (m, 4H), 7.22 (tq, J = 6.3, 1.8 Hz, 10H), 5.48 (s, 1H), 3.92 (s, 1H), 2.31 (s, 1H), 1.53 (d, J = 6.8 Hz, 3H).

(R)-1-phenyl-N-((R)-phenyl(2-((2,4,8,10-tetra-tert-butyldibenzo[d,f][1,3,2]dioxaphosphepin-6-yl)oxy)naphthalen-1-yl)methyl)ethan-1-amine (7.41)

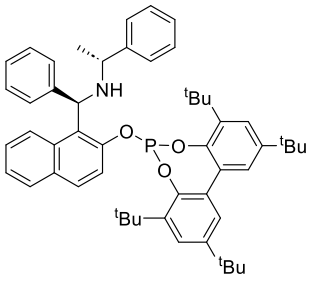

3,3',5,5'-tetra-tert-butyl-[1,1'-biphenyl]-2,2'-diol (903 mg, 2.20 mmol) was placed in an oven dried, argon purged, Schlenk tube and dissolved in 8 mL of toluene. NEt_3 (0.914 mL, 6.56 mmol) was added and the resulting solution was cooled in an ice bath. PCl_3 (0.239 mL, 2.73 mmol) was added dropwise to the reaction mixture which was then removed from the ice bath and was stirred at 80 °C overnight. The suspension was filtered via a filtrating plate under an inert atmosphere, and the filtrate was evaporated under vacuum to remove any residual PCl_3 and give the chlorophosphite intermediate **7.40** as a white solid which was used in the next step without further purification. To a Schlenk flask containing a solution of chlorophosphite **7.40** in toluene (8 mL) and NEt_3 (0.7 mL, 5.00 mmol) was added a solution of **7.36** (353 mg, 1.00 mmol) and NEt_3 (0.7 mL, 5.00 mmol) in toluene (8 mL). The reaction mixture was then allowed to stir at room temperature overnight. The salts were filtered via a filtrating plate under an inert atmosphere, and the filtrate was evaporated under vacuum yielding the crude product. The latter was purified by column chromatography on silica gel (previously dried at 130°C overnight in an oven) under an inert atmosphere, using dry toluene + 2% dry NEt_3. The resulting solution was evaporated in vacuo to afford a white foamy solid. The product **7.41** was obtained as a white powder (777 mg, 98% yield).

^{1}H NMR (400 MHz, CD_2Cl_2) δ 7.81 (dd, J = 8.1, 1.4 Hz, 1H), 7.68 (d, J = 9.0 Hz, 1H), 7.45 (dd, J = 17.2, 2.5 Hz, 2H), 7.35 (ddd, J = 8.0, 6.8, 1.1 Hz, 1H), 7.30 – 7.04 (m, 18H), 5.61 (s, 1H), 3.64 (d, J = 6.7 Hz, 1H), 2.56 (s, 1H), 2.50 (s, 0H), 2.34 (s, 3H), 1.49 (s, 3H), 1.42 (s, 9H), 1.39 – 1.23 (m, 32H), 1.05 (d, J = 6.4 Hz, 3H).

^{13}C NMR (101 MHz, $CDCl_3$) δ 147.33, 145.90, 145.70, 145.02, 144.23, 143.24, 142.09, 139.61, 139.34, 139.07, 136.84, 132.01, 131.73, 128.70, 128.03, 128.01, 127.93,

127.72, 127.47, 127.33, 127.20, 127.09, 126.93, 126.90, 126.87, 126.65, 126.16, 125.85, 125.68, 125.60, 125.57, 125.34, 125.23, 124.84, 124.27, 124.02, 123.41, 123.31, 121.35, 120.07, 119.97, 119.03, 76.30, 76.18, 75.98, 75.67, 59.27, 55.63, 55.02, 54.50, 34.41, 34.26, 34.22, 33.77, 33.71, 33.66, 30.55, 30.50, 30.47, 30.40, 30.05, 30.02, 29.92, 29.90, 29.87, 24.28, 21.95, 20.43.

^{31}P NMR (162 MHz, CD_2Cl_2) δ 136.88.

HRMS (ESI) for **$C_{53}H_{62}NO_3P$**. **Exact: (M:** 791.4467, **$[M+H^+]^+$:** calculated: 792.4545, found: 792.4557.

Flow synthesis of chlorophosphite

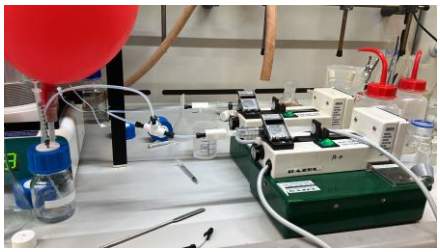

In a 10 mL syringe (A) is taken a solution of diol + base in dry acetonitrile (1M) while syringe (B) contains a solution of PCl_3 in dry acetonitrile (1M). Both pumps are set at 0.5 mL/min (setting 77.4 for green pump). (A) and (B) react in a T mixer followed by a 1 mL loop giving a residence stay of 1 min and a total flow of 1mL/min. First 4 min are discarded to reach a steady state in the loops. Collecting vessel should be under a nitrogen atmosphere, using a balloon.

Using this conditions, HCl (g) is formed and released upon opening of the flask. Product (C) is air and moisture sensitive; it should react directly with another reactant. Concentration of (C) is now 0.5M.

7.5. References

[1] Kitamura, H.; Fuse, S. Continuous-/Micro-Flow Reactions Using Highly Electrophilic PCl_3 and $POCl_3$. *Chempluschem* **2023**, *88* (6).

[2] Kashani, S.; Sullivan, R. J.; Andersen, M.; Newman, S. G. Overcoming Solid Handling Issues in Continuous Flow Substitution Reactions through Ionic Liquid Formation. *Green Chem.* **2018**, *20* (8), 1748–1753.

[3] Tamaki, T.; Nagaki, A. Flash Production of Organophosphorus Compounds in Flow. *Tetrahedron Lett.* **2021**, *81*, 153364–153368.

[4] Mao, M.; Zhang, L.; Yao, H.; Wan, L.; Xin, Z. Development and Scale-up of the Rapid Synthesis of Triphenyl Phosphites in Continuous Flow. *ACS Omega* **2020**, *5* (16), 9503–9509.

[5] Morodo, R.; Riva, R.; van den Akker, N. M. S.; Molin, D. G. M.; Jérôme, C.; Monbaliu, J.-C. M. Accelerating the End-to-End Production of Cyclic Phosphate Monomers with Modular Flow Chemistry. *Chem. Sci.* **2022**, *13* (36), 10699–10706.

[6] Olyaei, A.; Sadeghpour, M. Recent Advances in the Synthesis and Synthetic Applications of Betti Base (Aminoalkylnaphthol) and Bis-Betti Base Derivatives. *RSC Adv.* **2019**, *9* (32), 18467–18497.

[7] Li, X.; Song, J.; Xu, D.; Kong, L. Asymmetric Hydrosilylation of Styrenes by Use of New Chiral Phosphoramidites. *Synthesis,* **2008**, *6*, 925–931.

[8] Chakrabortty, S.; Konieczny, K.; Müller, B. H.; Spannenberg, A.; Kamer, P. C. J.; de Vries, J. G. Betti Base Derived P -Stereogenic Phosphine-Diamidophosphite Ligands with a Single Atom Spacer and Their Application in Asymmetric Catalysis . *Catal. Sci. Technol.* **2022**, *12* (5), 1392–1399.

[9] Schmitz, C.; Holthusen, K.; Leitner, W.; Franciò, G. Bidentate Phosphine–Phosphoramidite Ligands of the BettiPhos Family for Rh-Catalyzed Asymmetric Hydrogenation. *European J. Org. Chem.* **2017**, *28*, 4111–4116.

[10] Schmitz, C.; Holthusen, K.; Leitner, W.; Franciò, G. Highly Regio- and Enantioselective Hydroformylation of Vinyl Esters Using Bidentate Phosphine,P-Chiral Phosphorodiamidite Ligands. *ACS Catal.* **2016**, *6* (3), 1584–1589.

[11] Miró, R.; Cunillera, A.; Margalef, J.; Lutz, D.; Börner, A.; Pamies, O.; Diéguez, M.; Godard, C. Rh-Catalyzed Asymmetric Hydroaminomethylation of α-Substituted Acrylamides: Application in the Synthesis of RWAY. *Org. Lett.* **2020**, *22* (22), 9036–9040.

[12] Cimarelli, C.; Mazzanti, A.; Palmieri, G.; Volpini, E. Solvent-Free Asymmetric Aminoalkylation of Electron-Rich Aromatic Compounds: Stereoselective Synthesis of Aminoalkylnaphthols by Crystallization-Induced Asymmetric Transformation. *J. Org. Chem.* **2001**, *66* (14), 4759–4765.

[13] Daniels, E. L.; Runge, J. R.; Oshinowo, M.; Leese, H. S.; Buchard, A. Cross-Linking of Sugar-Derived Polyethers and Boronic Acids for Renewable, Self-Healing, and Single-Ion Conducting Organogel Polymer Electrolytes. *ACS Appl. Energy Mater.* **2023**, *6* (5), 2924–2935.

[14] Tran, D. K.; Rashad, A. Z.; Darensbourg, D. J.; Wooley, K. L. Sustainable Synthesis of CO_2-Derived Polycarbonates from d -Xylose. *Polym. Chem.* **2021**, *12* (37), 5271–5278.

[15] Cimarelli, C.; Mazzanti, A.; Palmieri, G.; Volpini, E. Solvent-Free Asymmetric Aminoalkylation of Electron-Rich Aromatic Compounds: Stereoselective Synthesis of Aminoalkylnaphthols by Crystallization-Induced Asymmetric Transformation. *J. Org. Chem.* **2001**, *66* (14), 4759–4765.

CHAPTER VIII

GENERAL CONCLUSIONS

In this manuscript, the work performed on the homogeneous asymmetric intermolecular hydroaminomethylation of 1,1-diarylethenes and cyclopropylmethacrylamides, the intramolecular hydroaminomethylation of amine-containing styrene derivatives, and our preliminary results for the development of heterogenized chiral catalysts for the hydroaminomethylation reaction under flow condition are described.

The results in the asymmetric hydroformylation and hydroaminomethylation of 1,1-diarylethenes are described in Chapter III and the conclusions that were drawn were:

- The straightforward synthesis of 1,1-diarylethenes **3.2a-i** was performed using a modified reported procedure involving the use of a microwave.
- The racemic hydroaminomethylation of substrates **3.2a-g**, **3.20** and **3.21** was performed using the phosphine ligand **L8** and providing the racemic amines in moderate to good yield.
- The racemic hydroformylation of substrates **3.2a-g** was performed providing the racemic chromanols **3.8a-g** in moderate yield. The racemic products were oxidized to the corresponding chromanones **3.6a-g** for subsequent HPLC analysis.
- From a screening of chiral ligands for the asymmetric hydroaminomethylation of **3.2a**, two classes of ligands stood out: the sugar-based phosphite phosphoramidite **L14** and sugar-based bisphosphite **L15**.
- The ligand **L14e** was selected to evaluate the scope of substrates **3.2** in the asymmetric hydroaminomethylation reaction. Chiral amines were obtained in 30-47% yield with ee's between 23% and 36%.
- When the asymmetric hydroaminomethylation of the protected phenol **3.20** was performed, the chemoselectivity and

enantioselectivity were slightly enhanced compared to the hydroaminomethylation of **3.2a**.

- The ligand **L14e** was selected for the asymmetric hydroformylation of **3.2**. The chiral chromanols **3.8a-g** were obtained in 45-90% yield with enantiomeric excesses from 14% to 44%.

These results constitute the first direct synthesis of Tolterodine and its derivatives via asymmetric hydroaminomethylation of 1,1-diarylethenes.

The work outlined in Chapter IV focused on the synthesis of a series of 2-cyclopropylmethacrylamides and the evaluation of their reactivity in Rh-catalyzed hydroformylation and hydroaminomethylation. The following conclusions were drawn:

- The synthesis of the α-cyclopropyl acrylamides containing primary, secondary and tertiary amides was explored via three synthetic routes, among which the most appropriate pathway was based on the Pd-catalyzed hydroaminocarbonylation of cyclopropylacetylene **4.13.** Using this methodology, the new 2-cyclopropylacrylamides **4.2**, **4.23-4.27** were successfully produced with yields ranging from 40% to 60%.
- The synthesized cyclopropylacrylamides were tested in the Rh-catalyzed hydroformylation and hydroaminomethylation reactions using various ligands.
    - The reactivity of tertiary amides revealed to be substrate dependent since using the same catalytic system**,** high conversion was measured in the case of substrate **4.26**, whereas the conversion of **4.22** was much lower.
    - 2-cyclopropylacrylamides undergo a ring opening reaction under hydroformylation and hydroaminomethylation conditions.

- Hydroformylation of secondary 2-cyclopropylacrylamides provided new dihydropyridinone products which were isolated and fully characterized. Moreover, reduction of the catalysis crude revealed that the hydroformylation product **4.45** was also formed as the main linear aldehyde.

In the hydroaminomethylation of secondary 2-cyclopropylacrylamides, no hydroaminomethylation products could be detected. However, the new amine **4.54** coming from a cascade reaction involving the ring opening of the cyclopropyl unit of the substrate was evidenced.

Regarding the development of heterogenized catalysts for the asymmetric hydroformylation and hydroaminomethylation of 1,1-disubstituted alkenes that is described in Chapter V, the following conclusions could be extracted:

- The synthesis of the two new pyrene-tagged sugar-based amino-alcohol backbone **5.5** and **5.12** was successfully conducted in two and three steps, respectively.
- The ligand **5.11** was successfully synthesized in 33% yield by reaction of the amino-alcohol backbone with the (S)-BINOL chlorophosphite while the bulkier ligand **5.4** could not be isolated.
- The new pyrene-tagged ligand was reacted with different rhodium precursors and the reaction mixture characterized by NMR. It was concluded that the reaction with $[Rh(acac)(CO)_2]$ did not afford the product expected but rather a dirhodium complex bearing two bridging acac moieties and a ligand **5.11**. provided the complex **5.10**.
- The complex **5.10,** formed by reaction with $[Rh(COD)_2]BF_4$, was successfully immobilized on multiwall carbon nanotubes, reduced graphene oxide and carbon beads.
- The activity of the Rh/**5.11** catalytic system was tested in homogeneous hydroformylation and hydroaminomethylation of the

substrate **5.22**. The asymmetric hydroformylation of **5.22** resulted in an excellent 80% ee of **5.26**, indicating that the introduction of the pyrene moiety did not significantly affect the properties of the ligand.

- The immobilized catalysts were tested in batch hydroformylation and presented a low activity, but the catalyst **5.10@MWCNT** provided a conversion of 30% at 110°C with a selectivity towards the linear aldehyde of 31% and an enantioselectivity of 61%.

The reactivity of *ortho* substituted styrene derivatives containing an amine moiety was evaluated in the Rh-catalyzed intramolecular hydroaminomethylation and is detailed in Chapter VI. The following conclusions were drawn:

- In the Rh-catalyzed intramolecular hydroaminomethylation of the substrates **6.33**, **6.34**, **6.39**, **6.42**, the hydrogenation of the enamine intermediate is the limiting factor for the reaction to proceed.
- Increasing the size of the enamine ring formed from a 5 to a 7-membered ring resulted in a more efficient hydrogenation under HAM conditions.

As a general conclusion, intramolecular hydroaminomethylation of alkenes remains a challenge and further work will be needed to obtain chiral amines through this pathway.

Chapter VII describes the work performed during a 3-month secondment in Italmatch Chemicals, Arese, Italy. From the results obtained, the following conclusions were extracted:

- The synthesis of the amino-alcohol backbone **7.19** was successfully scaled-up.
- A series of amino-alcohol backbones were synthesized using the intermediate **7.18**.

- The continuous flow synthesis of chlorophosphites, notably **7.30** and **7.20**, was successfully performed.
- The synthesis of the Betti base **7.36** was performed as well as attempts in functionalizing O and N atoms. However, only the O atom could be substituted, probably due to steric issues.

APPENDIX

SCIENTIFIC CONTRIBUTIONS

Publications

J. Langlois, M. Urrutigoïty, C. Godard, Chapter 00072. Olefins hydrofunctionnalization; hydroformylation and hydrocarboxyamination. In: O. Riant and E. Schultz (eds.), *Comprehensive Chirality*, **2023**, 2nd edition. https://doi.org/10.1016/B978-0-32-390644-9.00019-6.

Margalef, J.; Langlois, J.; Garcia, G.; Godard, C.; Diéguez, M. Evolution in the Metal-Catalyzed Asymmetric Hydroformylation of 1,1'-Disubstituted Alkenes. In *Advances in Catalysis*; **2021**; Vol. 69, pp 181–215. https://doi.org/10.1016/bs.acat.2021.11.004.

J. Langlois, M. Urrutigoïty, C. Godard, Rhodium-catalyzed asymmetric hydroaminomethylation of 1,1-diphenylethenes towards Tolterodine derivatives. *Manuscript under preparation*.

Conferences and Scientific Meetings

J. Langlois, M. Urrutigoïty, C. Godard, "Synthesis of pharmaceuticals via rhodium-catalyzed asymmetric hydroaminomethylation of alkenes." 3rd Trans Pyrenean Meeting in Catalysis, Toulouse, France, November **2023**. Oral communication.

J. Langlois, M. Urrutigoïty, C. Godard, "Rh-catalyzed asymmetric hydroaminomethylation of 1,1-diarylethenes towards Tolterodine." Congress from Société Chimique de France, Nantes, France, June **2023**. Oral communication.

J. Langlois, M. Urrutigoïty, C. Godard, "Rh-catalyzed asymmetric hydroaminomethylation of 1,1-diarylethenes towards Tolterodine." 2nd Cutting-Edge Homogeneous Catalysis, Leipzig, Germany, Mars **2022**. Flash communication and poster. Organizing committee.

J. Langlois, M. Urrutigoïty, C. Godard, “Rh-catalyzed asymmetric hydroaminomethylation of 1,1-diarylethenes towards Tolterodine.” 5th HC3A, Barcelona, Spain, January **2022**. Poster.

J. Langlois, M. Urrutigoïty, C. Godard, “Design of efficient catalytic tools for a direct access to chiral amines.” 1st Cutting-Edge Homogeneous Catalysis, Toulouse, France, May **2021**. Poster.

Workshops

J. Langlois, M. Urrutigoïty, C. Godard, “On the way to chiral heterogeneous catalysts for Rh-catalyzed asymmetric hydroaminomethylation.”5th network workshop. Bucharest, Romania. 24/04/2023.

International School on Innovations in Homogeneous and Supported Homogeneous (ISI-HSC). Bucharest, Romania. 25th-28th April 2023

J. Langlois, M. Urrutigoïty, C. Godard, “Rh-catalyzed intramolecular hydroaminomethylation and Italmatch Chemicals project” 4th network workshop. Lyon, France. 25/10/2022.

J. Langlois, M. Urrutigoïty, C. Godard, “Rh-catalyzed intramolecular hydroaminomethylation.” 3rd network workshop. Leipzig, Germany. 28/03/2022.

J. Langlois, M. Urrutigoïty, C. Godard, “Rh-catalyzed asymmetric hydroaminomethylation of 1,1-disubstituted alkenes.”2nd network workshop. York, United Kingdom. 06/10/2021

J. Langlois, M. Urrutigoïty, C. Godard, “Design of efficient catalytic tools for a direct access to chiral amines.”1st network workshop. Toulouse, France, 03/05/2021

International stays

12-month stay in Laboratoire de Chimie de Coordination, INP-Ensiacet, University of Toulouse, France. The work was focused on Rh-catalyzed intramolecular hydroaminomethylation (Chapter VI). The other focus was the synthesis and application of Rh single atom catalysts on carbon materials for hydroformylation and hydroaminomethylation reactions. November 2021-February 2023.

3-month secondment in Italmatch Chemicals, Arese, Italy, under the supervision of Dr. Frédéric Bruyneel. The purpose of the stay was to study the laboratory scale-up of a ligand synthesis. 1/09/2022-1/12/2022.